2019

Characterization of immunity transcription factor NF-kappaB in a symbiotic Cnidarian model organism, the sea anemone Exaiptasia pallida

BOSTON UNIVERSITY

GRADUATE SCHOOL OF ARTS AND SCIENCES

Dissertation

CHARACTERIZATION OF IMMUNITY TRANSCRIPTION FACTOR NF-kappaB IN A SYMBIOTIC CNIDARIAN MODEL ORGANISM, THE SEA ANEMONE *EXAIPTASIA PALLIDA*

by

KATELYN M. MANSFIELD

B.S., West Chester University of Pennsylvania, 2013

Submitted in partial fulfillment of the

requirements for the degree of

Doctor of Philosophy

2019

Approved by

First Reader _____

Thomas D. Gilmore, Ph.D.
Professor of Biology

Second Reader _____

Trevor W. Siggers, Ph.D.
Assistant Professor of Biology

ACKNOWLEDGMENTS

I owe many people thanks for my time spent at BU. Firstly I would like to thank my advisor, Dr. Thomas Gilmore, for his support of my Ph.D research, for his guidance, knowledge, and writing expertise. I would like to thank my thesis committee members: Dr. Ulla Hansen, Dr. Trevor Siggers, Dr. Sean Mullen, Dr. Sarah Davies, and Dr. John (Chip) Celenza, for their encouragement, insight, and support. I thank my fellow labmates for stimulating discussions and their willingness to work together and thank you to all the undergraduates and collaborators who have contributed to this work. A very special thanks goes to my parents, my biggest fans, who never once in my life doubted my ability to succeed. Thank you to my sister, whose remarkable example I live by, for teaching me how to make dreams become reality. Thank you to my MomMom, my guardian angel, for helping me through my Ph.D. Words cannot express how grateful I am to my partner Dr. Greg Dillon for his unwavering support and ability to fill any room with laughter and love. To my best friend Dr. Leila Haery, thank you for your steadfast guidance and for the many years of friendship still to come. A special thank you goes to my lifelong friends Alyssa Timoteo and Chelsea Petre. And finally, I am grateful for all the friendships BU has blessed me with. Thank you for making Boston feel like home: Dr. Sanda Zolj, Dr. Albert Mondragon, Dr. Natasha Khatri & Carl Facer, Dr. Michaela Smith, Dr. JP Gilbert, and future doctors Johnny Elguero, Nick Ray, and Quinn Ho.

CHARACTERIZATION OF IMMUNITY TRANSCRIPTION FACTOR NF-kappaB IN A SYMBIOTIC CNIDARIAN MODEL ORGANISM, THE SEA ANEMONE *EXAIPTASIA PALLIDA*

KATELYN M. MANSFIELD

Boston University Graduate School of Arts and Sciences, 2019

Major Professor: Thomas D. Gilmore, Professor of Biology

ABSTRACT

Many organisms form mutually beneficial, symbiotic partnerships with other organisms. Corals and sea anemones undergo mutualistic symbioses with photosynthetic algae of the family Symbiodiniaceae, and these partnerships are key for the viability of coral reef ecosystems. Cnidarian-Symbiodiniaceae symbioses are sensitive to climate change-induced ocean warming, which causes the disruption of symbiosis, commonly referred to as bleaching, and can lead to coral mortality. Cellular and molecular aspects of how this symbiosis is established and disrupted by heat stress are not well understood. The research presented herein characterizes immunity transcription factor NF-kappaB in the cnidarian model organism *Exaiptasia pallida* (Aiptasia). It is shown that the DNA-binding site specificity of Aiptasia NF-kappaB is similar to mammalian NF-kappaB subunit p50 and that this binding specificity is conserved across a broad expanse of metazoans. Moreover, Aiptasia and human IkappaB kinases can phosphorylate serine residues in the Cterminus of NF-kappaB, signaling the protein for proteasomal processing to allow for nuclear localization, DNA binding, and transactivation. In Aiptasia, NF-kappaB expression is downregulated by symbiosis onset in larvae, and NF-kappaB total

expression, DNA-binding activity, and tissue-specific expression are increased following laboratory-induced loss of symbiosis in adult Aiptasia. NF-kappaB downregulation during the onset of symbiosis occurs only with the compatible symbiont *Breviolum minutum* and data suggest that host TGFbeta plays a role in NF-kappaB downregulation. Results demonstrate that aposymbiotic Aiptasia (with high NF-kappaB levels) have increased survival following bacterial infection as compared to symbiotic anemones. A bioinformatic analysis shows that potential NF-kappaB binding sites are enriched in promoter regions of immune-related genes that are upregulated in aposymbiotic Aiptasia. Increased levels of NF-kappaB are also found in a genet of the coral *Pocillopora damicornis* that exhibits resilience to heat-induced bleaching. Overall, the results in this thesis suggest a role for NF-kappaB-directed immunity in symbiosis onset, bleaching, and resistance to biological stressors in cnidarians. It is proposed that NF-kappaB downregulation in Aiptasia is a mechanism to lower host immunity and promote the establishment of symbiosis, but that this process compromises host immunity to pathogen infection. Nevertheless, constitutively high basal levels of NF-kappaB may be protective against bleaching in cnidarians.

TABLE OF CONTENTS

LIST OF TABLES

LIST OF FIGURES

LIST OF ABBREVIATIONS

°C .....degrees Celsius

aa .....amino acid(s)

Ab.....antibody

Ac-DEVD-CHO..... Ac-Asp-Glu-Val-Asp-CHO

Am.....*Acropora millepora*

ANK..... ankyrin

Ap..... Aiptasia

APS .....ammonium persulfate

Aq..... *Amphimedon queenslandica*

ATG ..... autophagy-related protein 12

Av..... *Anemonia viridis*

bp..... base pair(s)

Bf.....factor B

BLAST ..... basic local alignment search tool

BMP ..... bone morphogenic protein

BSA.....bovine serum albumin

BU ..... Boston University

cDNA ..... complementary DNA

ChIP .....chromatin immunoprecipitation

Co..... *Capsaspora owczarzaki*

cPTIO 2-4-carboxyphenyl-4,4,5,5-tetramethylimidazoline-1-oxyl-3-oxide

CST ..... Cell Signaling Technology

CTCF.....corrected total cell fluorescence

DAMP.....danger associated molecular patterns

DBD ..... DNA-binding domain

dH_2O ..... deionized water

Dm.....*Drosophila melanogaster*

DMEM ..... Dulbecco's Modified Eagle's medium

DMSO..... dimethyl sulfoxide

DNA..... deoxyribonucleic acid

dNTPs .....deoxyribonucleotide triphosphate

DTT.....dithiothreitol

E. coli ..... *Escherichia coli*

EDTA ..... ethylenediaminetetraacetic acid ethylene glycol tetraacetic acid

Elk ..... E26 transformation-specific domain-containing protein

eNOS.....endothelial nitric oxide synthase

FBS .....fetal bovine serum

g..... gram(s)

Gbp.....giga basepairs

GRR ..... glycine rich region

GTP .....guanosine triphosphate

GST ..... glutathione-S-transferase

GSNO..... S-Nitrosoglutathione

h.....hour(s)

HRP.....horseradish peroxidase

Hu.....human

IF.....immunofluorescence

Ig.....immunoglobulin

IHC.....immunohistochemistry

IKK.....IκB kinase

IPTG.....isopropyl-β-D-1-thiogalactopyranoside

IRF.....interferon regulatory factor 1

IκB.....inhibitor of NF-κB

KD.....kinase domain

kDa.....kilodalton(s)

LAG.....L-aminoguanidine

L.....liter(s)

LB.....Luria broth

LPS.....lipopolysaccharide

Luc.....luciferase

M.....molar

mA.....milliamps(s)

MAMP.....microbial-associated molecular pattern

MASP.....MBL-associated serine protease

MBL.....mannose binding lectin

MCS ..... multiple cloning site

MEME ..... multiple EM for motif elicitation

min ..... minute(s)

ml ..... milliliter(s)

mM ..... millimolar

Mo ..... mouse

mRNA ..... messenger RNA

MyD ..... myeloid differentiation primary response

NADPH ..... nicotinamide adenine dinucleotide phosphate

NCBI ..... National Center for Biotechnology Information

NEB ..... New England Biolabs

NF-κB ..... nuclear factor-κB

NIK ..... NF-κB inducing kinase

NLS ..... nuclear localization sequence

NO ..... nitric oxide

NOD ..... nucleotide oligomerization domain (NOD)

NOS ..... nitric oxide synthase

NOSIP ..... nitric oxide synthase interacting protein

Nv ..... *Nematostella vectensis*

OCT ..... optimal cutting temperature

OD ..... optical density

p ..... phospho

PBM ..... protein binding microarray

PBS ..... phosphate-buffered saline

PCR .....polymerase chain reaction

PdC-lectin .....*Pocillopora damicornis* C-type lectin

PEI.....polyethylenimine

PO ..... phenoloxidase

PI3K .....phosphoinositide-3 kinase

PMSF .....phenylmethylsulfonyl fluoride

ppt ..... parts per thousand

PRR ..... pattern recognition receptor

REL .....Reticuloendotheliosis

RHD .....Rel homology domain

RNA .....ribonucleic acid

RNAi .....ribonucleic acid interference

RNase ..... ribonuclease

ROS.....reactive oxygen species

rRNA.....ribosomal ribonucleic acid

RT ..... reverse transcription PCR

RT-PCR..... reverse transcription PCR

SR..... scavenger receptor(s)

SDS ..... sodium dodecyl sulfate

SDS-PAGE .....SDS-polyacrylamide gel electrophoresis

sec ..... second(s)

SLL ..... *Sinularia lochmodes* lectin

SS ..... supershift

TAD ..... transactivation domain

TB ..... terrific broth

TBK ..... TANK-binding kiase

TBS ..... Tris-buffered saline

TBS-Tween ..... TBS with Tween 20

TE ..... Tris buffer with EDTA

TEMED ..... N, N, N', N'-tetramethylethylenediamine

TF ..... transcription factor

TGFβ ..... transforming growth factor β

TIR ..... Toll/interleukin-1 receptor

TLR ..... Toll-like receptor(s)

TNF ..... tumor necrosis factor

TNFR ..... tumor necrosis factor receptor

TRAF ..... tumor necrosis factor receptor-associated factor

Tris ..... Tris[hydroxymethyl]amino-methane

TSR ..... thrombospondin-type-1 repeat

Tween-20 ..... polyxyethelene sorbitan monolaurate

UV ..... ultraviolet

v ..... volume

V.....volts

w.....weight

WT ..... wild-type

βgal.....β-galactosidase

Δ.....deletion

µg .....microgram(s)

µl .....microliter(s)

µM.....micromolar

CHAPTER ONE[1]

INTRODUCTION

1.1 Cnidarian-Symbiodiniaceae mutualism and bleaching

Many corals and anemones (phylum Cnidaria) undergo mutualistic symbiotic partnerships with photosynthetic algae (dinoflagellates) in the family Symbiodiniaceae (formerly *Symbiodinium*; Lajeunesse et al. 2018). These symbioses form the trophic and structural foundation of coral reef ecosystems, supporting much of the biodiversity of marine life (Weis et al. 2008). In the cnidarian-Symbiodiniaceae mutualism, photosynthetically fixed carbon produced by algal symbionts is transported to the cnidarian host tissue, providing up to 90% of the energy requirement for the cnidarian host (Yellowlees et al. 2008). In turn, the algae are housed and protected within host cells located in the gastroderm. Within these gastrodermal cells, the symbiotic algae reside in specialized, host-derived membrane vesicles called symbiosomes, which arise during the process of symbiont uptake that occurs early in the life cycle of the cnidarian host (Hong et al. 2009).

Cnidarian-Symbiodiniaceae partnerships are sensitive to environmental disturbances such as increased ocean temperature, pH changes, and pollution, all of which can cause the symbionts to be expelled from host tissue (Weis 2008). Loss of algal symbionts ("bleaching") increases coral mortality and can lead to the collapse of reef ecosystems (Hoegh-Guldberg et al. 2007, Hughes et al. 2018, Weis 2010). Although coral bleaching events have been well documented, the molecular basis of bleaching is

[1]Large parts of Chapter One are taken from Mansfield and Gilmore 2019.

not well-understood. With global temperatures predicted to continue to rise over the next century, bleaching events are projected to increase in number, severely endangering corals and their ecosystems (Hughes et al. 2018).). For example, an October 2018 report prepared by the United Nations-sponsored Intergovernmental Panel on Climate Change predicts a massive die-off of coral reefs by 2040 (Intergovernmental Panel on Climate Change SR15, 2018). Thus, there has been great interest in understanding the environmental, ecological, and more recently, molecular bases of these important symbioses.

1.2 *Exaiptasia pallida* is a model organism for studying coral bleaching

Understanding how cnidarian-Symbiodiniaceae symbioses are affected by increased ocean temperature and the cellular mechanisms by which environmental change leads to loss of symbiosis is an important goal. Compared to more traditionally used laboratory organisms, such as worms, flies, and mice, cnidarian biology is not well-characterized (Weis et al. 2008). Therefore, efforts aimed at understanding cellular and molecular aspects of cnidarian-Symbiodiniaceae biology and dysbiosis are in their relatively early stages.

One hurdle in the cellular and molecular characterization of bleaching is the difficulty of maintaining coral in a laboratory setting (Weis et al. 2008). Coral colonies grow slowly and their hard, calcareous skeletons make molecular manipulation challenging. To facilitate cnidarian research, investigators have developed the sea

anemone *Exaiptasia pallida* (Aiptasia herein) as a model organism for studying cnidarian biology and symbiosis. Both corals and Aiptasia undergo mutualism with Symbiodiniaceae. However, unlike obligate symbiotic corals, Aiptasia are facultatively symbiotic, therefore they can be bleached in the lab by various methods, but can still be maintained completely without symbionts (i.e., in an aposymbiotic state). In addition, Aiptasia's small size, ease of culture, and the ability to create strains of genetically identical polyps have made it a useful lab model for studying symbiosis and loss of symbiosis. The advancement of Aiptasia as a model system has led to substantial progress in understanding cnidarian biology (Weis et al. 2008). Nevertheless, it is important to bear in mind that one key difference in studying symbiosis/dysbiosis in Aiptasia versus threatened corals is that corals generally die upon loss of symbionts, whereas Aiptasia can live indefinitely in the aposymbiotic state.

1.3 The algal family Symbiodiniaceae

Symbiodiniaceae is a family of endosymbiotic dinoflagellate symbionts. These dinoflagellates are single-celled, flagellate eukaryotic organisms that are commonly found in marine environments. Symbiodiniaceae cells range from 6-12 μm in size (LaJeunesse et al. 2018) with a genome of ~1.5 Gbp (Shoguchi et al 2013). Symbiodiniaceae engage in mutualistic symbioses with tropical cnidarians such as corals and anemones wherein the algae provide carbon produced from photosynthesis to their cnidarian host (Muscatine 1990). Symbiodiniaceae are horizontally transferred. Juvenile cnidarians ingest Symbiodiniaceae from the environment and the algae are then

incorporated into gastrodermal cells (Weis et al. 2008). The family Symbiodiniaceae now refers to seven formally defined genera of algae that were previously classified as specific clades of *Symbiodinium* sp. (LaJeunesse et al. 2018). The genera of Symbiodiniaceae (and the former names of their *Symbiodinium* clades) that are mentioned or used in experiments in this thesis are listed in Table 1.1.

1.4 Cnidarian immunity and the establishment and maintenance of symbiosis

The innate immune system has been implicated as playing a key role in many animal and plant symbiotic partnerships, including the following: plant-rhizobium (Cao et al. 2017), carpenter ant-Blochmannia (Zientz et al. 2005), marine invertebrates-symbionts (Nyholm and Graf 2012), Drosophila-gut microbiota (Chu and Mazmanian 2013), salamander-algae (Burns et al. 2017), and cnidarian-Symbiodiniaceae (Davy et al. 2012). As with other organisms, the cnidarian innate immune system must distinguish between harmful pathogens that need to be cleared versus beneficial microbes that are symbiotic (McFall-Ngai et al. 2013). Therefore, it is perhaps no surprise that innate immunity has also been implicated in several aspects of the cnidarian-Symbiodiniaceae mutualism, based on studies using a variety of reef-building corals that undergo obligate symbiosis with Symbiodiniaceae, as well as the facultatively symbiotic sea anemone model Aiptasia (Table 1.2).

Even though cnidarians and mammals are distantly related metazoans, cnidarians utilize many of the same immune strategies and pathways found in mammals to interact with microbial organisms. Moreover, cnidarian immune-related processes have been

implicated in loss of symbiosis and coral bleaching (Weis 2008 Palmer 2018). Therefore, understanding what immune components and pathways are involved in the cnidarian response to environmental stress and how these pathways may impact loss of symbiosis is of importance for comparative immunology and coral reef conservation efforts.

As with other symbiotic mutualisms (McFall-Ngai et al. 2013), the cnidarian immune system must manage the host's response to both beneficial and pathogenic microbes. Symbiotic cnidarians have the ability to take up and tolerate beneficial Symbiodiniaceae of specific genera, and can block the establishment of symbiosis with non-optimal genera within this algal family. For example, the sea anemone Aiptasia, the coral *Fungia scutaria*, and some species of the coral genus *Acropora* can take up and tolerate only certain members of the family Symbiodiniaceae (Hambleton et al. 2014, Rodriguez-Lanetty et al. 2004, Rodriguez-Lanetty et al. 2006b, Weis et al. 2001, Wolfowicz et al. 2016). However, the mechanisms underlying this selectivity are not well-understood. As with other symbiotic mutualisms (Burns et al. 2017, Chu and Mazmanian, 2013, McFall-Ngai et al. 2013, Nyholm and Graf 2012, Zientz et al. 2005), host innate immunity is hypothesized to be involved in the selective uptake of Symbiodiniaceae by corals and anemones.

As in most metazoans, the detection of microbes in cnidarians begins with a class of cellular receptors called pattern recognition receptors (PRRs), which bind a wide array of microbial ligands (Rosenstiel et al. 2009). That being said, the onset of symbiosis and the subsequent maintenance of symbiosis appear to be generally associated with an overall downregulation of host immune pathways in Aiptasia as indicated by

transcriptomic and functional data showing the downregulation of seven putative immune-related genes across three studies using either Aiptasia adults or larvae (Table 1.3). In the sections below, we describe cells, receptors, and downstream signaling pathways that have been shown or suggested to be involved in cnidarian immunity as well as the establishment and maintenance of symbiosis.

1.5 Immune cells in cnidarians

Most animals rely on circulating immune cells for the identification and removal of pathogens via phagocytosis (Rosales and Uribe-Querol 2017, Uribe-Querol and Rosales 2017). However, in the absence of a contained circulatory system, the identification of immune-related cells capable of phagocytosis in cnidarians has been challenging. Cells that have phagocytic capabilities and express enzymes that are involved in phagocytosis have been observed in symbiotic cnidarians (Menzel and Bigger 2015, Rosental et al., 2017); however, the identity of these cells is not well-characterized, making their involvement in either pathogen or symbiont uptake only a hypothesis. For example, in the coral *Swiftia exserta* certain cells in the mesoglea were identified as potential immune cells because they express enzymes similar to those used by mammalian immunocytes to phagocytose and degrade pathogens (Menzel and Bigger 2015). Additionally, in Aiptasia, possible phagocytic cell types were identified by FACS of cells that stained positively for LysoTracker (Rosental et al. 2017). The LysoTracker-positive cells in Aiptasia had four-fold higher phagocytic activity for inert plastic beads than did control cells, suggesting that acidic organelles (i.e., LysoTracker-positive) are markers for phagocytic, immune-

related cells in symbiotic cnidarians (Rosental et al. 2017). Although phagocytic cells have been identified in symbiotic cnidarians, the cell types responsible for phagocytosis of pathogens vs the uptake of symbionts have not yet been identified. Thus, it is unclear whether the recognition of pathogens and symbionts are common or distinct processes in symbiotic cnidarians. The identification and characterization of cell types in cnidarians that specifically take up Symbiodiniaceae remain an important goal. The field would benefit from the characterization of cell types in symbiotic cnidarians, perhaps using new technologies such as whole organism single cell RNA-seq, as has been performed in the non-symbiotic cnidarian model *Nematostella vectensis* (Sebé-Pedrós et al. 2018).

1.6 Pattern recognition receptors (PRRs)

1.6.1 PRRs in symbiosis onset

Animals have a variety of secreted and cell-surface PRRs that can recognize and bind microbial-associated molecular patterns (MAMPS) to modulate downstream cellular signaling pathways to initiate the correct response to a particular class of microbe (Rosenstiel et al. 2009). The following subsections summarize the PRR homologues identified in symbiotic cnidarians and their potential roles in symbiont recognition and uptake.

1.6.2 Lectins

One of the best-studied mechanisms of host-symbiont recognition involves lectin-glycan interactions (Hirsch 1999, Meints and Pardy 1980, Nyholm and McFall-Ngai 2004). In this pathway, host lectin receptors bind glycans on symbiotic microbes, and this interaction initiates innate immune signaling cascades such as the complement pathway, which has been shown to be involved in symbiont uptake in corals and anemones (Poole et al. 2016). Genomic and transcriptomic searches have revealed lectins in cnidarian hosts (Ocampo et al. 2015), and numerous cell-surface glycans have been identified in Symbiodiniaceae (Logan et al. 2010, Parkinson et al. 2018). Different genera of Symbiodiniaceae express slightly different cell-surface glycan profiles (Logan et al. 2010, Parkinson et al. 2018); however, the role of glycans in symbiont uptake in cnidarians is controversial. The enzymatic digestion of cell-surface molecules of *Breviolum* sp. and the saturation of cell-surface glycans of *Cladocopium* sp. with exogenous lectins have both been reported to cause a decrease in the abilities of these symbionts to colonize host tissue in adult Aiptasia and in larval *Fungia scutaria* (Lin et al. 2000, Wood-Charlson et al. 2006). In addition, the cell surface of *Cladocopium* sp. contains α-Man/α-Glc and α-Gal residues, and blocking of these glycans reduces symbiont colonization in *F. scutaria* (Wood-Charlson et al. 2006). In contrast, a recent study reported that adult Aiptasia show no difference in the uptake of *B. minutum* with their cell-surface glycans masked by two different lectins as compared to non-masked *B. minutum* (Parkinson et al. 2018); however, that study does not rule out the possibility that other glycan-lectin interactions are important for symbiont recognition and uptake.

Overall, the role of glycan-lectin interactions in cnidarian-Symbiodiniaceae uptake is not clear, and may differ between cnidarian hosts and the different algae within Symbiodiniaceae that can populate permissive cnidarians.

In addition to studying the glycans of Symbiodiniaceae, several studies (Jimbo et al. 2000; Koike et al. 2004, Kvennefors et al. 2008, 2010, Vidal-Dupiol et al. 2009, Zhou et al. 2018) have sought to characterize microbial interactions specified by cnidarian lectins. In the coral *Acropora millepora*, millectin can bind both Symbiodiniaceae (*Cladocopium* sp. and *Symbiodinium* sp) and exogenous mannose *in vitro*, and millectin is expressed around intracellular Symbiodiniaceae cells *in vivo* (Kvennefors et al. 2008). The expression of millectin was also shown to be upregulated by bacterial lipopolysaccharide (LPS), suggesting that millectin plays a role in both symbiont recognition and an innate immune response to bacteria (Kvennefors et al. 2010). Although the overall protein structure of millectin is unique, certain domains bear striking resemblance to known innate immunity proteins such as the vertebrate mannose binding lectin (MBL), an important protein in the vertebrate complement system (Kvennefors et al. 2008).

Other cnidarian lectins may also play a role in recognition of both Symbiodiniaceae and pathogens (Jimbo et al. 2000, Koike et al. 2004, Vidal-Dupiol et al. 2009, Zhou et al. 2018). The stony coral *Pocillopora damicornis* has a C-type lectin, PdC-lectin, which can bind both Symbiodiniaceae (isolated from *P. damicornis*) and LPS *in vitro* (Zhou et al. 2018). In addition, PdC-lectin expression (Vidal-Dupiol et al. 2009) and the overall binding of Symbiodiniaceae to PdC-lectin (Zhou et al. 2018) are both

reduced during heat stress, suggesting that ocean warming can affect lectin-mediated host-Symbiodiniaceae interactions. Aiptasia also express the C-type lectin MBL and the expression of this lectin is higher in naïve aposymbiotic larvae than in symbiotic larvae (Wolfowicz et al. 2016). In the coral *Sinularia lochmodes* SLL-2 (*S. lochmodes* lectin-2) localizes around the cell surface of intracellular Symbiodiniaceae (Jimbo et al. 2000), and the addition of exogenous SLL-2 to cultures of symbiotic Symbiodiniaceae isolated from *S. lochmodes* promotes the physiological transition of Symbiodiniaceae to a non-motile sessile stage known to be important for symbiosis establishment (Koike et al. 2004).

1.6.3 Scavenger receptors

A second group of PRRs that is important for the onset of symbiosis comprises the scavenger receptors (SRs) (Lehnert et al. 2014, Neubauer et al. 2016, Rodriguez-Lanetty et al. 2006a). In vertebrates, SRs help clear microbial pathogens via phagocytosis (Areschoug and Gordon 2009). The SR superfamily includes multiple classes of molecules, named SR-A through SR-I, which are categorized by specific protein domains. SR superfamily members can recognize many microbial ligands (Areschoug and Gordon 2009). In seven cnidarian species, multiple genes that resemble mammalian SR-A, SR-B, SR-E, and SR-I have been identified (Neubauer et al. 2016, Ocampo et al. 2015). Functional experiments have suggested that Aiptasia SRs play a role in symbiosis establishment in that treatment with the SR inhibitor fucoidan (shown to block vertebrate SR-A and SR-B [Li et al. 2008]) causes a decrease in colonization by *B. minutum* (Neubauer et al. 2016). In addition, the Aiptasia SR-B1 homologue was shown to be

upregulated by 28-fold in symbiotic anemones as compared to aposymbiotic anemones, suggesting a role for SR-B1 in the maintenance of symbiosis (Lehnert et al. 2014, Rodriguez-Lanetty et al. 2006a). In humans, SR-B1 is a lipoprotein receptor that is used by the Hepatitis C virus and the parasite Plasmodium falciparum (Catanese et al. 2007, Rodrigues et al. 2008) to gain entry into host cells. Therefore, by analogy, the upregulation of SR-B1 during symbiosis in Aiptasia suggests that Symbiodiniaceae use SR-B1 to colonize host cells in cnidarians. In humans, SR-B1 also plays a role in binding thrombospondins to activate the tolerogenic TGFβ pathway (Adams and Lawler 2004, Crawford et al. 1998), and TGFβ signaling is conserved in symbiotic corals and anemones (Berthelier et al. 2017, Detournay et al. 2012).

1.6.4 Other putative PRRs identified in symbiotic cnidarians

Through phylogenetic and transcriptomic searches two additional classes of PRRs—Toll-like receptors (TLRs) and nucleotide oligomerization domain (NOD)-like receptors—have been identified in many symbiotic cnidarians. Nevertheless, it is not known whether these PRRs play a role in symbiont recognition or uptake.

Toll-like receptors (TLRs) are one of the best characterized innate immune receptors in flies and vertebrates (Gerdol et al. 2017). TLRs have extracellular MAMP recognition domains and intracellular TIR domains that engage proteins to activate downstream signaling pathways, including NF-κB (see below) (Beutler and Moresco 2008, Brennan and Gilmore 2018). In symbiotic corals and anemones, both complete TLR-like and TIR domain-only proteins are present (Brennan and Gilmore 2018,

Ocampo et al. 2015, Poole and Weis 2014, Shinzato et al. 2011), although the number of proteins from each class varies greatly among species (Poole and Weis 2014, Williams et al. 2018).

NOD-like receptors are cytosolic PRRs that are involved in microbial recognition and host defense in the innate immune response of vertebrates (Franchi et al. 2009). An array of NOD-like receptor proteins have been identified in the corals *Acropora digitifera* and *Pseudodiploria strigosa* (Hamada et al. 2013, Ocampo et al. 2015, Shinzato et al. 2011).

1.7 Thrombospondin-type-1 repeat (TSR) domain-containing proteins

Thrombodpondin-type-1 repeat (TSR) domain-containing proteins are a diverse family of membrane-bound and secreted proteins involved in cell-cell interactions and pathogen recognition in mammals (Tucker 2004). Bioinformatic searches have revealed a variety of TSR domain-containing proteins that are greatly expanded in symbiotic cnidarians as compared to mammals (Neubauer et al. 2017, Ocampo et al. 2015, Schwarz et al. 2007). These cnidarian TSR domain-containing proteins are generally similar in sequence to mammalian properdin, which can act as a PRR to initiate phagocytosis of microbes via the alternative complement system pathway (Kemper et al. 2010, Neubauer et al. 2017). In addition, these searches have identified many cnidarian TSR domain-containing ADAMT metalloprotease-like proteins, which in mammals are involved in immunity and inflammation (Porter et al. 2005).

In cnidarians, TSR domain-containing proteins have been hypothesized to bind to secondary proteins to help initiate a signaling cascade that leads to engulfment of symbionts by host cells and tolerance of symbionts (Neubauer et al. 2017). In Aiptasia, the blocking of TSR domain-containing proteins reduces symbiont colonization, and conversely, the addition of exogenous TSR peptides increases *B. minutum* colonization as compared to untreated anemones (Neubauer et al. 2017). RNA-seq analysis of Aiptasia larvae colonized with *B. minutum* showed that many TSR domain-containing genes are downregulated once symbiosis is established (Wolfowicz et al. 2016), suggesting that TSR-domain containing proteins are important for the establishment, but not the maintenance, of symbiosis in Aiptasia.

1.8 The complement system

In vertebrates, the complement pathway is important for recognition and phagocytosis of pathogens (Dunkelberger and Song 2010). Complement is activated by the association of PRRs and MAMPs, which leads to the recognition and "tagging" of pathogens so that they can be identified for subsequent phagocytosis (Dunkelberger and Song 2010). This molecular tagging of pathogens is called opsonization (Dunkelberger and Song 2010). Although the complement pathway is well known for its role in pathogen recognition in vertebrates, in symbiotic cnidarians this pathway also appears to be involved in the recognition and establishment of symbiosis (Ganot et al. 2011, Kvennefors et al. 2010, Poole et al. 2016).

The vertebrate complement system has three main pathways: the classical, the lectin, and the alternative pathways. All of these vertebrate pathways lead to the cleavage of the C3 complement protein into C3a, which is important for the recruitment of macrophages, and C3b which is a molecular tag used to coat pathogens and label them for phagocytosis (Dunkelberger and Song 2010). In symbiotic cnidarians, only components of the lectin and alternative complement pathways have been identified, including mannose binding lectins (MBLs), MBL-associated serine proteases (MASPs), Factor B, and C3 (Baumgarten et al. 2015, Ganot et al. 2011, Kvennefors et al. 2008, Ocampo et al. 2015, Poole and Weis 2014).

In Aiptasia, there are three homologues of the mammalian alternative pathway Factor B gene (Ap-Bf-1, Ap-Bf-2a, and Ap-Bf-2b), and one homologue of the lectin pathway MASP gene (Ap-MASP) (Poole et al. 2016). Based on transcript modulation, these complement genes have been proposed to have distinct roles in different aspects of symbiosis/loss of symbiosis (Poole et al. 2016). The transcript levels of Ap-Bf-1 and Ap-MASP were upregulated by the onset of symbiosis in light conditions or when anemones were challenged with the pathogenic bacteria *Serratia marcescens* (Poole et al. 2016), suggesting a role for these genes in symbiosis onset and pathogen response. However, Ap-Bf-2b was downregulated during both of these events (Poole et al. 2016), highlighting that Aiptasia's two factor B genes are functionally distinct. In addition, Ap-Bf-2b and Ap-MASP were downregulated in symbiotic anemones as compared to aposymbiotic anemones (Poole et al. 2016). On the other hand, expression of Ap-Bf-1 was upregulated in symbiotic Aiptasia (Poole et al. 2016).

Similar to Aiptasia, two studies (Ganot et al. 2011, Kvennefors et al. 2010) have implicated complement genes as having a role in the onset of symbiosis in the coral *Acropora millepora* and the anemone *Anemonia viridis*. In *A. millepora*, expression of the C3 gene (C3-Am) is not significantly altered by immune challenge (Kvennefors et al. 2010). Nevertheless, the expression of C3-Am RNA in close proximity to intracellular Symbiodiniaceae within gastrodermal tissue suggests a role for C3-Am in the maintenance of symbiosis (Kvennefors et al. 2010). In the symbiotic anemone *Anemonia viridis*, the AvC3-2 isoform is expressed in both the ectodermal and gastrodermal tissue layers of adult anemones and is downregulated in the presence of symbionts; in contrast, AvC3-1 is only expressed in the gastroderm and its expression is unchanged between symbiotic and aposymbiotic anemones (Ganot et al. 2011). Overall these studies suggest that the downregulation of the complement pathway is important for symbiosis establishment; however, direct roles for different members of the complement pathway in symbiotic cnidarians have not yet been demonstrated.

1.9 Transforming Growth Factor beta (TGFβ)

TGFβ designates a superfamily of related cytokines that are involved in cell proliferation, cell differentiation, and immunity (Chen and Ten Dijke 2016). In mammals, TGFβ family members include TGFβ itself, as well as activins and bone morphogenic proteins (BMPs), which bind various TGFβ receptors to activate downstream signaling that can lead to transcriptional programs that impact apoptosis, cell cycle arrest, differentiation, immunity, and inflammatory responses (Chen and Ten Dijke 2016). In many cases, TGFβ

induces anti-inflammatory or anti-immunity responses. For example, in *Drosophila*, TGFβ superfamily members have an anti-inflammatory role in the response to infection and physical injury (Clark et al. 2011). Moreover, in many vertebrate-pathogen associations the TGFβ pathway is activated to induce tolerance that helps some bacterial pathogens, parasites, and viruses evade host immunity (Denney et al. 2017, Ndungu et al. 2005, Simmons et al. 2006).

TGFβ-like proteins, and TGFβ homologs have been suggested to have roles in promoting symbiosis and inhibiting immunity in Aiptasia and the coral *F. scutaria* (Berthelier et al. 2017, Detournay et al. 2012). Treatment of aposymbiotic Aiptasia with an anti-human TGFβ antibody caused them to take up fewer *Breviolum* sp. as compared to control, untreated anemones (Detournay et al. 2012). In *F. scutaria* larvae, the anti-human TGFβ antibody reduced uptake of symbionts and also increased NO synthesis, which is often an indication of increased innate immunity (Coleman 2001). Together, these results suggest that TGFβ plays a role in dampening the immune response and thus promoting symbiont uptake in cnidarians (Berthelier et al. 2017, Detournay et al. 2012). Further experiments investigating a role for TGFβ in the establishment of symbiosis in Aiptasia are described in Chapter Four.

1.10 Immunity transcription factor NF-κB

NF-κB is an evolutionarily conserved transcription factor that promotes many immune and inflammatory processes (Dev et al. 2011, Gilmore and Wolenski 2012, Lawrence 2009). In flies and mammals, the activation of NF-κB is associated with increased

inflammation, cytokine release, and the production of antimicrobial peptides. The NF-κB transcription factor family has been widely studied for its roles in a variety of immune-related processes, as well as diseases, in Metazoans. Based primarily on genomic and transcriptomic sequencing, it is clear that NF-κB-like transcription factors are present in some of the earliest emerging animal phyla (e.g., Porifera, Cnidaria) and some closely related outgroups to Metazoa (e.g., Filasterea) (Degnan et al. 2009, Mansfield et al. 2017, Gilmore and Wolenski 2012).

All NF-κB proteins have an N-terminal DNA-binding/dimerization domain called the Rel Homology Domain (RHD) (Gilmore 2006). In mammals, the NF-κB superfamily comprises five related transcription factors that fall into two subgroups: the NF-κB proteins (p52/p100; p50/p105) and the Rel proteins (c-Rel, p65/RelA, RelB). By comparison of protein sequences (Finnerty and Gilmore 2015) and DNA-binding site preferences (Siggers at al. 2011), the RHDs of human NF-κB proteins are more similar to one another than they are to the Rel proteins. *Drosophila* has a single NF-κB-like protein (Relish) and two Rel-like proteins (Dorsal, Dif). Sponges, cnidarians, and *Capsaspora owczarzaki* (Sebé-Pedrós et al. 2008), a unicellular holozoan, have single NF-κB-like proteins that are more similar by amino acid sequence and DNA-binding specificity to vertebrate NF-κB proteins than to Rel proteins (Finnerty and Gilmore 2015, Gauthier and Degnan 2008, Mansfield et al. 2017).

There are also differences between the NF-κB and Rel subclasses in sequences outside of the RHD (Gilmore 2006). The NF-κB proteins have a C-terminal inhibitory domain, which consists of a series of ankyrin (ANK) repeats that must be removed by

proteolysis to activate the DNA-binding activity of the transcription factor. For example, vertebrate p100 and p105 proteins are processed by the proteasome to their active forms, p52 and p50, respectively. In contrast, Rel-like proteins do not have ANK repeats, do not require processing for activation, and contain C-terminal transactivation domains.

In vertebrates, Rel/NF-κB dimers are generally held in the cytoplasm in an inactive state by interaction with NF-κB inhibitor proteins called IκBs. In mammals, there are two distinct NF-κB activation pathways: the canonical and the non-canonical pathways (Hayden and Ghosh, 2008). In the canonical pathway, a dimer such as p50/65 is bound to a separate IκB inhibitor, and this complex is activated to enter the nucleus when the IκB protein is phosphorylated by an IκB kinase (IKKβ), which promotes IκB ubiquitination and proteasomal degradation (Hayden and Ghosh 2008). In the non-canonical pathway, the RelB/p100 dimer is activated by IKKα-dependent phosphorylation of p100 at a cluster of serine residues C-terminal to the ANK repeats (Sun 2012). This phosphorylation event marks p100 for ubiquitination and proteasome-mediated proteolysis of the C-terminal ANK domain, allowing the p52/RelB dimer to enter the nucleus (Sun 2012). In *Drosophila*, the single NF-κB protein (Relish) is activated by caspase-mediated proteolytic cleavage at a specific site C-terminal to the RHD, which then removes the C-terminal ANK repeats (Kim et al. 2014). Although activation of NF-κB is generally considered to be an induced process, in some normal resting cell types, such as mammalian B cells, NF-κB proteins are constitutively found in the nucleus (Doerre and Corley 1999).

Even though NF-κB proteins from most early animal phyla have an overall structure that is similar to the mammalian RHD-ANK repeat bipartite configuration, there is considerable variation in the overall structures of NF-κB protein among cnidarians (Mansfield et al. 2017, Wolenski et al. 2011). For example, the single NF-κB-like protein in *Nematostella vectensis* contains an intact RHD, but lacks the C-terminal ANK repeat domain. Instead, *Nematostella* has an IκB-like ANK repeat domain protein encoded by a separate, unlinked gene (Wolenski et al. 2011), but the Nv-IκB protein is, by certain phylogenetic criteria, most similar to the C-terminal sequences of mammalian NF-κB proteins (Sullivan et al. 2009). However, the Nv-IκB protein has no discernible C-terminal sites of IKK phosphorylation (like NF-κB p100) (Wolenski et al. 2011). Thus far, single NF-κB homologues with linear structures resembling the mammalian RHD-ANK repeat bipartite configuration have been identified in symbiotic cnidarians such as Aiptasia (Mansfield et al. 2017) and the corals *Orbicella faveolata* (Williams et al. 2017) and *Pocillopora damicornis* (Traylor-Knowles et al. 2011). Due to reports of a correlation between immune gene expression and bleaching in certain corals, NF-κB has become a gene of interest in cnidarian symbiosis and dysbiosis. Three studies (DeSalvo et al. 2010, Mansfield et al. 2017, Wolfowicz et al. 2016) have indicated that NF-κB is downregulated by the establishment of symbiosis and upregulated following loss of symbiosis in cnidarians.

1.11 Downregulation of immunity and inflammation as shown by transcriptional changes

Many transcriptomic studies have found that homologs of genes involved in the innate immune response and inflammation are downregulated in symbiotic cnidarians as compared to aposymbiotic animals (Table 1.3). For example, RNA expression of immune genes involved in mediating oxidative stress (catalase, dual oxidase 1) and inflammation (serine protease 6) have been shown to be downregulated in symbiotic adult Aiptasia as compared to bleached anemones (Lehnert et al. 2014). In laboratory spawned Aiptasia, symbiotic larvae colonized with *B. minutum* have reduced expression of the immune-related genes encoding NF-κB, calnexin, thrombospondin, and C-type lectins as compared to naïve, aposymbiotic larvae (Wolfowicz et al. 2016). These studies suggest that downregulation of these immune-related genes in symbiotic Aiptasia is required for host tolerance of Symbiodiniaceae.

Furthermore, the ability to modulate the cnidarian immune system may, at least in part, distinguish colonizing vs non-colonizing Symbiodiniaceae. Indeed, when certain cnidarians are exposed to non-preferred genera of Symbiodiniaceae, such as *Durusdinium trenchii*, some immune genes are upregulated, whereas immune genes are downregulated by the preferred Symbiodiniaceae member *B. minutum* (Matthews et al. 2017). The immunity genes that are upregulated by non-preferred *D. trenchii* include homologs of tumor necrosis factor (TNF), caspase-8, and Malt (a protease involved in innate immunity and inflammation) (Yu et al. 2015). Similarily, ROS attenuators such as NADPH reductases are downregulated, which may result in ROS accumulation in host tissue that

perhaps triggers increased immunity to non-preferred *D. trenchii* (Matthews et al. 2017). These results suggest that preferred algae within Symbiodiniaceae suppress immunity to enable colonization, whereas non-preferred algae within Symbiodiniaceae upregulate innate immunity, which may inhibit their ability to establish symbiosis.

As a result of the suppression of immune genes and proteins (e.g., NF-κB) in symbiotic cnidarians, the ability of symbiotic cnidarians to withstand pathogen infection via immune activity may be suppressed as well. Consistent with that hypothesis, one recent field study found higher rates of pathogen-induced disease in *Acropora cervicornis* harboring symbionts than in their naturally bleached counterparts (Merselis et al. 2018). Thus, the observed positive correlation between pathogen-induced disease and symbiotic status suggests that downregulation of immune effector genes in response to Symbiodiniaceae leads to a reduced ability to tolerate pathogen infection. Therefore, symbiotic mutualism in cnidarians may represent a trade-off of decreased immunity for increased nutrition, which is a hypothesis that will be explored further by research described in this thesis.

1.12 Cnidarian immunity and the breakdown of symbiosis

Many cellular processes have been implicated in cnidarian loss of symbiosis/bleaching, however, there is still not a clear understanding at the molecular level of the series of events that leads from alteration of an environmental condition to loss of symbiosis.

Elevated ocean temperature and sunlight are major causes of cnidarian bleaching. Nevertheless, other environmental perturbations, including increased salinity, pollution,

and sedimentation, have also been implicated in bleaching (Coles and Brown 2003). Increases in ocean temperature and UV light cause Symbiodiniaceae to increase photosynthetic activity, which often leads to damaged photosystems as well as a buildup of reactive oxygen species (ROS) in both symbionts and the host tissue that houses them (Weis 2008). Thus, it has been proposed that environmentally induced increases in ROS overwhelm anti-oxidant systems, leading to cellular damage and loss of symbiosis (Weis 2008). However, others have argued that increased stress leads to the production of molecules used to indicate potentially damaging conditions such as heat shock proteins and uric acid and that these danger-associated molecular patterns (DAMPS) affect host-microbe immune interactions, and that this altered immunity may be more relevant to loss of symbiosis than the stress itself (Palmer 2018).

During bleaching, symbiont cells are expelled from the host and this event has been reported to involve many processes, including the digestion of symbionts, symbiont exocytosis from host cells, and host cell apoptosis and necrosis (Bieri et al. 2016, Dunn et al. 2007, Dunn and Weis 2009, Fujise et al. 2014, Kvitt et al. 2011, Pernice et al. 2011, Tchernov et al. 2011). To understand the cellular genes and pathways involved in bleaching, RNA-seq experiments have sought to identify genes and clustered gene pathways that are upregulated or downregulated at various times during or after bleaching in a variety of cnidarians (Table 1.4 and 1.5). The experimental conditions of these studies are listed in Table 1.6. Although the results of these RNA-seq experiments vary greatly in terms of the differentially expressed genes identified, immunity is one of the most common host cellular processes that has been reported as altered during bleaching

(Table 1.4 and 1.5, Figure 1.1). This section describes immune-related pathways that have been associated with loss of symbiosis, as well as proposed models for how immunity is involved in cnidarian bleaching.

1.13 Immune-related pathways involved in cnidarian bleaching

1.13.1 Nitric oxide

In vertebrates, nitric oxide (NO) is an effector molecule used by many immune and inflammatory cell types including macrophages and neutrophils (Coleman 2001). NO is synthesized by a class of nitric oxide synthase (NOS) enzymes. In innate immunity, NO production is a defense mechanism used by host cells to target pathogens. In cnidarians, NO has also been proposed to be an important signaling molecule for initiating an immune-like response, which can lead to loss of symbiosis during environmental stress (Weis 2008).

In Aiptasia, treatments such as heat stress of symbiotic anemones at 33ºC for 24 h and induction of oxidative stress by chemical treatment lead to increases in NO production (Perez and Weis 2006). The NO produced following heat treatment was found primarily in the gastroderm, where host cells containing Symbiodiniaceae are also located (Perez and Weis 2006). However, heat stress did not cause increased NO production in aposymbiotic anemones or in cultured Symbiodiniaceae (Perez and Weis 2006), suggesting that NO production in Aiptasia requires the presence of symbionts within host tissue during heat stress. A NOS-specific inhibitor, LAG, was used to demonstrate that most of the NO produced during heat stress was due to induced NOS activity (Perez and

Weis 2006). NO production has also been associated with heat stress in corals in that NOS expression was shown to be increased by heat treatment in *Montipora aequituberculata* (van de Water et al. 2018) and expression of a putative homologue of a negative regulator of eNOS activity (NOSIP) was found to be downregulated in *Acropora palmata* (DeSalvo et al. 2010). Although increased NO production is known to be involved in innate immunity (Coleman 2001), NO is a signaling molecule utilized in many other biological processes (Thomas et al. 2008), and therefore, the production of NO in cniadrian heat stress and its potential link to immunity need further characterization.

Although the above studies provide a correlation between NO production and bleaching in cnidarians, two studies have investigated whether heat-induced NO actually has an active a role in the bleaching process. In Aiptasia, the addition of an NO donor (SNP) caused an increase in the release of Symbiodiniaceae from host tissue at control temperatures (Perez and Weis 2006). In addition, reduction of NO levels during heat stress by the use of an NO scavenger (cPTIO) decreased bleaching (Perez and Weis 2006). Hawkins et al. (2013) sought to understand how NO leads to the induction of bleaching in Aiptasia. They found that an increase in host-derived NO levels is associated with increased caspase-like activity, suggesting that caspase-dependent apoptosis has a role in loss of symbiosis. Specifically, increased NO production caused by either an increase in temperature or by application of an NO donor (GSNO) led to an increase in both caspase activity and symbiont loss (Hawkins et al. 2013). Additionally, inhibition of caspase activity led to a reduction in bleaching (Hawkins et al. 2013).

While the effects of NO on cnidarian loss of symbiosis are beginning to be understood, the source of NO during bleaching is not known, i.e., whether NO is of cnidarian origin, Symbiodiniaceae origin, or both. The production of host NO in response to heat stress has been observed in symbiotic corals (DeSalvo et al. 2010, Safavi-Hemami et al. 2010 van de Water et al. 2018) and anemones (Hawkins et al. 2013, Perez and Weis 2006, Trapido-Rosenthal et al. 2005). NO production has also been reported in Symbiodiniaceae that were freshly isolated from either the coral *Madracis mirabilis* (Trapido-Rosenthal et al. 2005) or Aiptasia (Hawkins et al. 2013, Trapido-Rosenthal et al. 2001) and by axenic *Symbiodinium microadriaticum* that were cultured in the lab (Bouchard and Yamasaki 2008). However, other studies have failed to detect NO production in heat-stressed Symbiodiniaceae isolated from Aiptasia or corals, or in Symbiodiniaceae cultured in the lab (Perez and Weis 2006, Safavi-Hemami et al. 2010). One reason for these discrepancies may be the intensity and duration of the heat treatment used to induce NO production. For example, Symbiodiniaceae isolated from Aiptasia were found to produce NO in response to heat treatment, however, the timing of induced NO production in these Symbiodiniaceae (i.e., 10 days of heat treatment) did not correlate with the timing of increased NO levels in symbiotic hosts (i.e., 4 and 6 days of heat treatment) (Hawkins et al. 2013). Overall, the above studies suggest that the NO production that causes bleaching in Aiptasia is mostly generated by the anemone host (Hawkins et al. 2013, Perez and Weis 2006).

Future studies aimed at determining how NO levels induce cnidarian bleaching, and the source of NO produced during heat stress will greatly increase our knowledge of

the mechanism underlying loss of symbiosis and may lead to the identification of cellular pathways affected by NO signaling.

1.13.2 Prophenoloxidase activating system

The prophenoloxidase system is an innate immune process widely used by invertebrates, whereby the enzymatic cleavage of prophenoloxidase (ProPO) into the enzyme phenoloxidase (PO) leads to the production of melanin, a toxic molecule used to coat invading pathogens and inactivate them (Cerenius and Soderhall 2004). PO and melanization have been shown to have an important role in the cnidarian immune response to pathogens (Palmer et al. 2011, van de Water et al. 2018), and this system may also have a role in loss of symbiosis. For example, the levels of PO activity were shown to significantly increase when the coral *Montipora aequituberculata* was subjected to heat stress under laboratory conditions (van de Water et al. 2018). Similarly, naturally bleached *Orbicella faveolata* had higher ProPO activity as compared to both healthy and diseased (yellow band disease) symbiotic corals (Mydlarz et al. 2009). Furthermore, high basal PO activity and melanin-containing granular size (i.e., increased immunity) was inversely correlated with susceptibility to bleaching among several individual *Acropora millepora* coral colonies (Palmer et al. 2011). Taken together, such studies suggest although that the ProPO->melanin system plays a role in bleaching, there are differences among individual cnidarians in terms of whether the PO/melanin activity is induced or constitutive.

1.13.3 Tumor necrosis factor (TNF)

The soluble cytokine TNF plays a major role in vertebrate antimicrobial immunity and inflammation (Sedger and McDermott 2014). TNF molecules bind TNF-receptors (TNFR) to initiate immune cell signaling events such as cytokine release, inflammation, and cell death (Sedger and McDermott 2014). The cnidarian genome has 40 putative TNFR genes with high diversity (Quistad et al. 2016), and heat treatment has been shown to increase expression of TNFR in symbiotic cnidarians (Barshis et al. 2013, Palumbi et al. 2014, Seneca and Palumbi 2015, Traylor-Knowles et al. 2017). In addition, the *in vitro* activation of the TNF pathway in coral cells using human TNFα as a ligand is associated with an increase in caspase activity, apoptosis, and loss of symbiosis, suggesting that the TNF pathway plays a role in cell death pathways associated with loss of symbiosis (Quistad et al. 2016).

1.14 Immunity and the elimination of symbionts from host tissue

1.14.1 In situ *degradation of* Symbiodiniaceae

In the vertebrate innate immune response, professional phagocytic cells such as macrophages engulf pathogens and degrade them. Similarly, virus- and pathogen-infected cells can be removed by inducing cellular degradation via lysosome-mediated autophagy (Kuballa et al. 2012). To determine if a similar mechanism of lysosome-mediated degradation is used by cnidarian host cells during loss of symbiosis, studies in Aiptasia have characterized the localization of Rab proteins, which are an important class of GTPases used to regulate membrane trafficking during events of the innate immune

response such as endocytosis and phagocytosis (Hutagalung and Novick 2011, Prashar et al. 2017). A Rab7 homologue in Aiptasia, Ap-Rab7, was predicted to be involved in late phagosomal-lysosomal processing of damaged Symbiodiniaceae (Chen et al. 2003). Ap-Rab7 is excluded from Aiptasia phagosomes containing healthy, photosynthetically active Symbiodiniaceae (Chen et al. 2003). However symbiotic Aiptasia incubated for 1 h with DCMU, an inhibitor of photosynthesis used to mimic the negative effects of increased temperature, showed increased Ap-Rab7 expression, suggesting that Ap-Rab7 is involved in heat stress-induced loss of symbiosis (Chen et al. 2003). Thus, Chen et al. (2003) proposed that the upregulation of Ap-Rab7 during heat stress aids in inducing phagosomal-lysosomal fusion of Symbiodiniaceae-containing vacuoles, leading to the degradation of symbionts and loss of symbiosis.

Treatment of symbiotic Aiptasia with rapamycin, an inducer of autophagy, increased bleaching 43-fold in treated anemones as compared to non-treated anemones (Dunn et al. 2007). However, rapamycin did not increase bleaching under heat stress conditions (Dunn et al. 2007). Similarly, the induction or blockage of apoptosis did not affect symbiont loss during heat stress-induced bleaching (Dunn et al. 2007). However, when autophagy and apoptosis were simultaneously inhibited during heat stress, there was a four-fold decrease in loss of symbiosis in Aiptasia, suggesting that autophagy and apoptosis work together to induce loss of symbiosis during heat stress-induced bleaching (Dunn et al. 2007). Future investigations are needed to determine how lysosomal-mediated degradation of Symbiodiniaceae may contribute to loss of symbiosis.

1.14.2 Cell death

Apoptosis is an important process of the immune response because it can lead to removal of pathogen-infected cells (Nagata and Tanaka 2017). Apoptosis has been shown to play a role in the cnidarian immune response to pathogens (Ainsworth et al. 2007) as well as in cnidarian bleaching in that apoptosis of host cells containing symbionts contributes to loss of symbiosis (Dunn et al. 2007, Paxton et al. 2013).

In Aiptasia, Dunn et al. (2007) used hallmarks of apoptosis, such as condensation of organelles, cytoplasm, and nuclear chromatin and membrane blebbing, to measure cell death rates during heat stress-induced bleaching. They found that signs of apoptosis were visible as early as 2 min after exposure to high temperature, and that these signs of apoptosis increased as loss of symbiosis ensued. Interestingly, more cell death occurred in gastrodermal tissue where Symbiodiniaceae are housed, than in ectodermal tissue, suggesting that the presence of symbionts makes gastrodermal cells more sensitive to heat stress-induced apoptosis (Dunn et al. 2007). As heat stress continued, host tissue necrosis increased (Dunn et al. 2007). Together, these results suggest that apoptosis and necrosis have roles in heat stress-induced bleaching in Aiptasia.

Because it is difficult to determine by microscopy when host cells and the symbionts they contain undergo cell death, apoptosis was measured in isolated Aiptasia cells using SYTOX green, a fluorescent probe that can selectively label nucleic acids in dying cells. After 8 h of temperature stress at 33ºC, 100% of heat-treated host cells showed evidence of cell death, whereas only 28% of control (25ºC) cells showed evidence of cell death (Paxton et al. 2013). Of the host cells that died in control

conditions, the majority of the symbionts they housed remained alive and did not stain with SYTOX green, whereas during heat stress the majority of host cells that died also had dead symbionts, suggesting that heat stress induces host cell death that leads to loss of symbiosis via the death of symbionts (Paxton et al. 2013). However, because heat stress was shown to cause cell death of cultured *B. minutum*, Paxton et al. (2013) measured the levels of Symbiodiniaceae cell death *in hospite* by treating symbiotic Aiptasia with a cell death inducer (colchicine) that causes the death of host cells but not the death of Symbiodiniaceae. Treatment of Aiptasia with colchicine induced apoptosis in host cells, which also led to Symbiodiniaceae cell death, suggesting that host cell death can then lead to symbiont cell death and loss of symbiosis (Paxton et al. 2013).

Four studies (Bieri et al. 2016, Dunn et al. 2007, Paxton et al. 2013, Richier et al. 2008) have sought to identify specific proteins involved in cnidarian apoptosis such as caspases and pro-apoptotic molecules. Using the caspase substrate fluoroprobe Rhodamine 110 aspartic acid, Paxton et al. (2013) showed that caspase activity increased when cell death was induced in Aiptasia using the inducer of host apoptosis colchicine. Additionally, after colchicine treatment, Aiptasia showed a greater increase in caspase activity in the gastroderm, where symbionts are located, than in the ectoderm (Paxton et al. 2013). Taken together, these studies suggest that caspase-induced apoptosis in specific cells housing Symbiodiniaceae is involved in loss of symbiosis.

Caspase activity has also been correlated with loss of symbiosis caused by heat stress. In the sea anemone *Anemonia viridis*, heat stress increased caspase activity specifically in cells of the gastroderm (Richier et al. 2008). In Aiptasia, Bieri et al. (2016)

measured caspase activity over time during high temperature treatments and saw that caspase activity increased early on during the treatment and then decreased back to baseline levels. Nevertheless, the levels of bleaching in Aiptasia were reported to be unchanged in the presence of the caspase inhibitor Ac-DEVD-CHO or when caspase was knocked down by RNAi (Dunn et al. 2007). Together, these results suggest either that caspases do not significantly contribute to bleaching or that when caspases are blocked, other cellular processes compensate for the loss of caspase activity during bleaching (Bieri et al. 2016). In support of the latter hypothesis, Dunn et al. (2007) showed that the inhibition of autophagy or apoptosis separately did not affect rates of bleaching, whereas the simultaneous inhibition of both processes greatly decreased loss of symbiosis. Overall, although the precise contribution of caspases to loss of symbiosis in cnidarians is unclear, the increased activity of this class of enzymes during loss of symbiosis has been repeatedly reported.

1.14.3 Host cell exocytosis

Exocytosis is an important aspect of the immune response, which occurs in many immune cells such as eosinophils, neutrophils, and macrophages, whereby these cells release proteins and cellular effector molecules such as antimicrobial peptides and proinflammatory cytokines, to aid in the immune response (Logan et al. 2003). As such, one hypothesis to explain symbiont loss in cnidarians is that heat stress-induced immune pathways initiate host cell exocytosis of intracellular Symbiodiniaceae out of the host gastrodermal tissue and into the gastric cavity (Weis 2008). Consistent with this

hypothesis, Bieri et al. (2016) found that greater than 90% of expelled *Symbiodinium* sp. following heat stress in Aiptasia were not surrounded by host cell material, suggesting that host cell exocytosis, as opposed to host cell detachment, is the major contributor to symbiont loss. Furthermore, the expelled *Symbiodinium* sp. appeared to be healthy and undamaged as compared to *in hospite*, unperturbed *Symbiodinium* sp., suggesting that *in situ* degradation of symbionts does not play a significant role in heat-induced bleaching in Aiptasia (Bieri et al. 2016).

1.15 Modulation of immunity and inflammation in bleached cnidarians as shown by transcriptional changes

In an effort to identify genes and pathways important for cnidarian loss of symbiosis, transcriptional profiles have been characterized during heat stress-induced bleaching. Such transcriptomic studies have found that homologs of many genes involved in innate immunity and inflammation are upregulated in bleached cnidarians as compared to control animals (Table 1.3 and 1.6). For example, mRNAs encoding immunity and inflammation activating proteins (e.g., Elk-1, Irf, Kruppel-like factors, MyD88, NF-κB, TRAF3) and proteins involved in cell death and mitigating cell stress (e.g., Rab, NOS, caspase, catalase) have been shown to be upregulated in bleached corals and anemones as compared to control, non-treated animals (Table 1.4). Conversely, mRNAs encoding other innate immune and cell stress proteins (TRAF2, ATG12, MBL) have been found to be downregulated by heat-induced bleaching (Table 1.5). Moreover, Pinzón et al. (2015) noted discordant changes in 17 immunity genes over the course of a year in a natural *O.*

faveolata bleaching event. Thus, such conflicting results make the exact role of immunity in loss of symbiosis unclear.

Furthermore, RNA-seq datasets from different studies have not always identified the same genes as being modulated and are sometimes conflicting. Moreover, because these studies have been based on whole animal RNA-seq experiments, it is not clear whether these changes in immune effector genes occur in cells harboring Symbiodiniaceae or, for example, the changes occur in immune-like cells that then affect cells containing algal symbionts. Therefore, it has been difficult to glean from the disparate RNA-seq experiments what are the contributions of RNA-seq-defined biological pathways, such as immunity, to the overall process of bleaching/loss of symbiosis. Thus, experiments in this thesis have sought to look at protein expression and activity of an immune-related master regulator, NF-κB, in order to gain a better understanding of how changes in gene and protein expression may lead to physiological changes in cnidarian-symbiont biology.

1.16 Conclusions and prospects

The studies above have contributed to what we know about the possible role of immune modulation in cnidarians for the establishment and maintenance of symbiosis, as well as to the loss of symbiosis. A model for the role of immune-related processes in cnidarian symbiosis and loss of symbiosis is presented in Figure 1.1. For the onset of symbiosis, many host pattern recognition receptors are likely required for symbiont detection and entry, and immune signaling pathways, such as complement, TGFβ, and NF-κB, are

modulated by Symbiodiniaceae for immune suppression. In contrast, many immune-related genes and processes are upregulated during loss of symbiosis. However, many additional functional experiments will be required to determine precisely how these immune processes are involved in symbiosis/dysbiosis.

The preponderance of experimental evidence indicates that both the onset and maintenance of symbiosis in host cnidarians are associated with the downregulation of immune-related pathways, suggesting that Symbiodiniaceae downregulates host immunity to allow its survival in the host, similar to what occurs in other symbiotic mutualisms (Burns et al. 2017 Detournay et al. 2012, Mansfield et al. 2017, McFall-Ngai et al. 2013, Nyholm and Graf 2012, Ryu et al. 2010, Weis et al. 2008). Of note, one field study indicated that recently bleached corals are less susceptible to pathogen-induced diseases than are symbiotic corals (Merselis et al. 2018), supporting that reduced immunity is part of the bargain for cnidarians that take part in obligate symbioses with Symbiodiniaceae. Nevertheless, another field-based study of long-term bleached corals suggested that some immunity genes are downregulated (Pinzón et al. 2015). Thus, future studies, along the lines of those carried out in this thesis, will be required to define the cellular and molecular mechanisms by which Symbiodiniaceae alters cnidarian host immunity, and whether host immunity to pathogens changes in different symbiotic states and over time.

Alterations in marine environments such as increased ocean temperature and light are well documented causes of cnidarian bleaching. In addition, transcriptomic information on the genes and pathways altered by temperature stress and loss of

symbiosis (such as NO signaling, immunity, and cell death) are abundant. Many mechanisms of symbiont expulsion have been characterized such as exocytosis, apoptosis, autophagy, necrosis, etc. Nevertheless, we currently lack information on the host pathways that lead from the exposure to and detection of heat stress to the ejection of symbionts.

1.17 Thesis rationale

Immunity plays a role in regulating symbiosis in many organisms. In symbiotic cnidarians such as corals and anemones, the dysregulation of many immune-related genes has been noted during symbiosis establishment and bleaching, but rarely have any of these genes and the proteins that they encode been further characterized molecularly. One such gene, encoding transcription factor NF-κB, has been shown to be upregulated by bleaching (DeSalvo et al. 2010, Traylor-Knowles et al. 2017) and downregulated by the onset of symbiosis (Wolfowicz et al. 2016). These data suggest that the well-known mammalian immune regulator NF-κB also plays a role in cnidarian symbiosis and dysbiosis.

Based on such studies, the primary goals of this thesis are to characterize transcription factor NF-κB in the symbiotic model organism Aiptasia and to determine whether it has a role in the regulation of immunity and/or during the onset of symbiosis as well as the loss of symbiosis. The results of this study in Aiptasia may elucidate the role of NF-κB-directed immunity in the regulation of symbiosis and provide insights into the molecular mechanism of the ecologically devastating phenomenon of coral bleaching.

Table 1.1 Symbiodiniaceae discussed in this thesis

Symbiodiniaceae family member	***Symbiodinium* clade**
Breviolum minutum	B
Cladocopium sp.	C
Durusdinium trenchii	D
Symbiodinium microadriaticum	A

New nomenclature is based on LaJeunesse et al. 2018.

The abbreviaton “sp.” is used when the species is not known.

Table 1.2 Cnidarians discussed in Chapter One

Genus species	**Common name**	**Habitat**	**Status[1]**	**References**
Acropora digitifera	Staghorn coral	Indo-Pacific	near threatened	Hamada et al. 2013
Acropora hyacinthus	brush coral tabletop coral	Western Pacific	near threatened	Barshis et al. 2013, Seneca and Palumbi 2015
Acropora millepora	branching, stony coral	Indo-pacific	near threatened	Kvennefors et al. 2008
Acropora palmata	elkhorn coral	Western Atlantic, Caribbean	critically endangered	DeSalvo et al. 2010
Fungia scutaria	mushroom coral	Indo-pacific	least concern	Berthelier et al. 2017, Lin et al. 2000, Wood-Charlson et al. 2006
Madracis mirabilis	yellow finger coral	Western Atlantic, Caribbean	na	Trapido-Rosenthal et al. 2005
Montipora aequituberculata	stony coral	Indo-Pacific	least concern	van de Water et al. 2018
Orbicella faveolata	mountainous star coral	Western Atlantic, Caribbean	endangered	DeSalvo et al. 2008, Mydlarz et al. 2009, Williams et al. 2018
Pocillopora damicornis	cauliflower coral	Indo-Pacific	least concern	Zhou et al. 2018, Vidal-Dupiol et al. 2009
Pseudodiploria strigosa	stony, brain coral	Caribbean	least concern	Ocampo et al. 2015
Sinularia lochmodes	octocoral (soft coral)	Indo-Pacific	na	Jimbo et al. 2000
Swiftia exserta	Octocoral, Orange tree coral	Eastern Atlantic	na	Menzel and Bigger 2015

[1]Status indicates the organism's endangered level as defined by IUCN Red List of Threatened Species. na: taxon has not yet been assessed for IUCN Red List.

Table 1.3 Immune-related genes downregulated in symbiotic vs aposymbiotic *Aiptasia*

Protein	**Protein class**	**Putative function**	**Aiptasia life stage**	**References**
Calnexin	type I membrane protein	protein folding chaperone	larva	Wolfowicz et al. 2016
Catalase	enzyme	hydrogen peroxide reduction	adult	Lehnert et al. 2014
Dual Oxidase 2 (DUOX2)	enzyme	ROS production, antimicrobial activity	adult	Lehnert et al. 2014
Mannose binding C-type lectin (MBL)	receptor	microbial pattern recognition	larva	Wolfowicz et al. 2016
NF-κB	transcription factor	inducer of innate immunity and inflammation	adult and larva	Mansfield et al. 2017, Wolfowicz et al. 2016
Thrombospondin	cell surface glycoprotein	mediator of cell-to-cell interactions	larva	Wolfowicz et al. 2016
Transmembrane serine protease 6	transmembrane protease	cell surface proteolysis	adult	Lehnert et al., 2014

Immune-related genes downregulated in symbiotic vs aposymbiotic anemones were characterized by RNA-seq and, in the case of NF-κB, protein assays.

Table 1.4 Immune-related genes upregulated by bleaching identified by transcriptomic analysis

Upregulated gene	Protein function	Putative biological function	Cnidarian host	References
AP-1	transcription factor	apoptosis	*Acropora hyacinthus*	Traylor-Knowles et al. 2017
Caspase 3	cysteine-aspartic protease	apoptosis	*Acropora millepora*	Kaniewska et al. 2012
Rab	GTPase	autophagy	*Acropora millepora, Acropora hyacinthus*	Barshis et al. 2013, Kaniewska et al. 2012
C-type lectin	carbohydrate binding protein	microbial pattern recognition	*Montipora aequituberculata*	van de Water et al. 2018
Ficolin	oligomeric lectin	microbial pattern recognition	*Montipora aequituberculata*	van de Water et al. 2018
Toll-like receptor 4 (TLR4)	cell-surface receptor	microbial pattern recognition	*Montipora aequituberculata*	van de Water et al. 2018
TNF receptor-associated factor 3	TNF receptor binding protein	immune activation	*Acropora millepora, hyacinthus, palmata*	Barshis et al. 2013, DeSalvo et al. 2010, Kaniewska et al. 2012, Seneca and Palumbi 2015
TNF receptor-associated factor 6	TNF receptor binding protein	immune activation	*Acropora hyacinthus, Montipora aequituberculata*	Barshis et al. 2013, van de Water et al. 2018
Kruppel-like factors 5 and 7	transcription factor	immune activation	*Acropora hyacinthus*	Traylor-Knowles et al. 2017

Upregulated gene	**Protein function**	**Putative biological function**	**Cnidarian host**	**References**
NF-κB	transcription factor	immune activation and inflammation	*Aiptasia, Acropora hyacinthus, palmata*	DeSalvo et al. 2010, Mansfield et al. 2017, Traylor-Knowles et al. 2017
C/EBPβ	transcription factor	innate immunity	*Anthopleura elegantissima*	Richier et al. 2008
Interferon regulatory factor	transcription factor	innate immunity, pathogen recognition	*Montipora aequituberculata*	van de Water et al. 2018
Myd88	cytosolic adapter protein	innate immunity	*Montipora aequituberculata*	van de Water et al, 2018
Nitric oxidase synthase (NOS)	enzyme	nitric oxide production	*Montipora aequituberculata*	van de Water et al. 2018
Elk-1	transcription factor	inducer of inflammation	*Acropora hyacinthus, Montipora aequituberculata Montipora aequituberculata*	Barshis et al. 2013, van de Water et al. 2018
Elk-3	transcription factor	macrophage activity	*Acropora hyacinthus*	Traylor-Knowles et al. 2017

Table 1.5 Immune-related genes downregulated by bleaching identified by transcriptomic analysis

Downregulated gene	**Protein class**	**Putative biological function**	***Genus species***	**References**
TNF receptor-associated factor 2	TNF receptor binding protein	apoptosis	*Acropora hyacinthus*	Barshis et al. 2013
AP-2	transcription factor	Apoptosis	*Acropora hyacinthus*	Barshis et al. 2013
Mannose binding lectin (MBL)	carbohydrate binding receptor	microbial pattern recognition	*Acropora hyacinthus*, *A. millepora, Pocillopora damicornis,*	Barshis et al. 2013, Rodriguez-Lanetty et al. 2009, Vidal-Dupiol et al. 2009
C-type mannose receptor 2	carbohydrate binding receptor	microbial pattern recognition	*Acropora hyacinthus*	Traylor-Knowles et al. 2017
Autophagy related protein 12 (ATG12)	E3-like enzyme	autophagosome formation	*Acropora palmata*	DeSalvo et al. 2010
C/EBPα	transcription factor	immune cell differentiation	*Anthopleura elegantissima*	Richier et al. 2008
C/EBPβ	transcription factor	macrophage function	*Orbicella faveolata*	DeSalvo et al. 2008
eNOS interacting protein (NOSIP)	E3 ubiquitin-protein ligase	negative regulator of NO production	*Acropora palmata*	DeSalvo et al. 2010

Table 1.6 Experimental conditions of bleaching RNA-seq experiments

Reference	*Genus species*	Treatment conditions	Length of treatment	Genes upregulated	Genes downregulated	Measure of bleaching	Signs of bleaching
van de Water et al. 2018	*Montipora aequituberculata*	Control 27°C, heated to or 29.5°C or 32°C, reached by increasing 0.5°C per day	22 days	C-type lectin, TRAF6, TNF converting enzyme, Rab21, TLR4, MyD88, Ficolin, Nitric oxide synthase, mannose Receptor C type, TNFR	na	Visually	no
DeSalvo et al. 2010	*Acropora palmata*	Control 29.7°C, heated to 32.7°C over 3 h and collected at 1 day and 2 day	2 days	TRAF3, NF-κB	ATG12, NOSIP	Hemocytometer counts	yes
Richier et al. 2008	*Anthopleura elegantissima*	Control 12°C, heated to 20°C	24 h	C/EBPβ	C/EBPα	No	no
DeSalvo et al. 2008	*Orbicella faveolata*	Control 29°C, heated 32°C increased over 3 h	10 days, 17 h	na	C/EBPβ	Hemocytometer counts	yes
Seneca and Palumbi 2015	*Acropora hyacinthus*	Control 29°C, heated 35°C. Ramped from 29°C to 35°C over 3 h, held at 35°C 1 h, then returned to 29°C for 2 h. Samples collected at 5 and 20 h after start of experiment	5 h and 20 h	TRAF3	na	Visual	yes before 20 h timepoint

Experimental conditions of studies that characterized the dysregulation of immune-related genes in cnidarians.

Reference	*Genus species*	Treatment conditions	Length of treatment	Genes upregulated	Genes downregulated	Measure of bleaching	Signs of bleaching
Kaniewska et al. 2012	*Acropora millepora*	28 days high CO2 (pH 7.6-7.7)	28 days	Caspase, Rab, TRAF3	na	Symbiont cell counts and pigment quantification	yes
Vidal-Dupiol et al. 2009	*Pocillopora damicornis*	Control 28°C, 1°C increase every 3 days until reached 32°C	15 days	na	MBL	Symbiont cell counts	yes
Rodriguez-Lanetty et al. 2009	*Acropora millepora*	Control 24°C, heated 28°C and 31°C	0, 3, 10 h	na	MBL	na (naïve lab spawned larvae)	na
Barshis et al. 2013	*Acropora hyacinthus*	Control 29.2°C, heated 31.9°C	72 h	Elk-1, TRAF3, TRAF6, Rab	MBL, TRAF2, Ap-2	no	yes, after 72h
Traylor-Knowles et al. 2017	*Acropora hyacinthus*	Control 29°C, heated from 29-35°C over course of 5 h	5 h	Ap-1, Kruppel-like factors 5 and 7	C-type mannose receptor 2	no	no
Mansfield et al. 2017	*Exaiptasia pallida*	Control 25°C, heated 32°C	7 d	NF-κB	na	qPCR of symbionts	yes

Figure 1.1 Immune molecules implicated in cnidarian symbiosis and loss of symbiosis

(a) In the establishment of symbiosis (1), it is proposed that pattern recognition molecules (PRRs) on the surface of gastrodermal cells recognize Symbiodiniaceae. For the establishment of symbiosis (2), preferred genera of Symbiodiniaceae suppress immunity by decreasing levels of the indicated immunity factors and increasing levels of TGFβ, which is an immunosuppressive molecule. (b) During the early stages of bleaching, environmental perturbations induce the production of immune molecules such as NO and ROS (1), followed by differential expression of immune-related genes/proteins that are known to lead to upregulation of immunity (2). Changes in host cell signaling processes (3) lead to the loss of symbionts by mechanisms such as cell death, autophagy, and exocytosis. Note: in (a) and (b) it is depicted that the immune-regulated transcripts are increased or decreased in the host cells harboring Symbiodiniaceae, but in many cases, these changes may occur in non-colonized immune-like cells which then affect the Symbiodiniaceae-containing cells. Figure taken from Mansfield and Gilmore (2019).

Figure 1.1 Immune molecules implicated in cnidarian symbiosis and loss of symbiosis

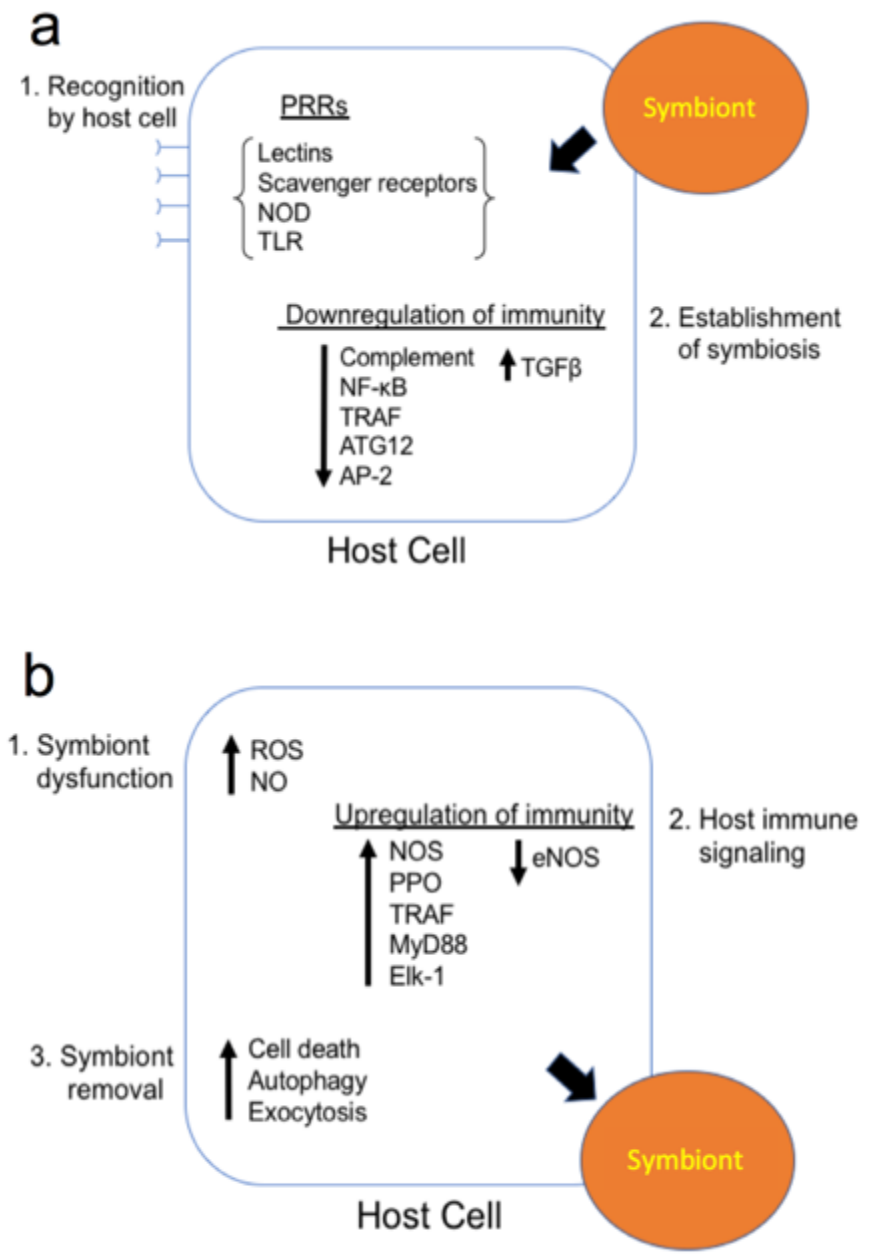

CHAPTER TWO

MATERIALS AND METHODS

2.1 Recombinant DNA techniques and plasmid constructions

Details about plasmids and plasmid constructions are described in Table 2.1. Restriction digestions were performed with approximately 1 μg of plasmid DNA and 1 ul of restriction enzyme (New England Biolabs [NEB], Ipswich, MA) in 1x reaction buffer for 1 h at 37°C (or at the temperature recommended by the manufacturer). Plasmids were verified by restriction enzyme mapping and/or DNA sequence analysis.

2.2 DNA ligation and transformation

The DNA fragment used for subcloning was isolated using gel electrophoresis in 1% low-melt agarose (FMC Bio Products, Rockland MA) and the appropriate DNA band was extracted from the gel using UV light to identify the band. Gel fragments were melted at 72°C and used in ligation reaction as follows: insert:vector DNA ratio of approximately 10:1 in T4 ligase buffer (50 mM Tris-HCl [pH 8.0], 10 mM $MgCl_2$, 10 mM dithiothreitol [DTT], 1 mM ATP, 25 mg/ml bovine serum albumin [BSA]), supplemented with 1 mM ATP and 500 units of T4 DNA ligase (NEB) in a total volume of 40 μl, and incubated overnight at 18°C.

The resulting ligation was used to transform competent DH5α *E. coli* cells or, if using vectors for bacterial expression, BL21 *E. coli* cells. Before transforming, the ligation reaction was heated to 72°C for 10 min to melt any solidified agarose and kept at 42°C while the reaction was assembled. The re-heated ligation reaction or an already

assembled plasmid DNA was then mixed with 60 µl of competent *E. coli* cells and 170 µl of TCM buffer (10 mM Tris [pH 7.5], 10 mM $CaCl_2$, 10 mM $MgCl_2$) and incubated on ice for 60 min. The reaction was then heat shocked at 42°C for 2 min and then added to 1 ml of LB. The LB/cell mixture was incubated at 37°C for 40-60 min with shaking. Then the bacterial cells were pelleted, resuspended in about 100 µl of residual LB, and plated on an LB plate with the appropriate antibiotic for selection of the plasmid.

2.3 Small-scale plasmid preparations

Small-scale preparations of plasmid DNA were performed using the TENS method (Zhou et al., 1990).

2.4 Large-scale plasmid preparations

Large-scale preparations of plasmid DNA were performed using the cesium chloride gradient/ultracentrifugation method as described previously (Thompson 2013).

2.5 PCR and PCR-based site-directed mutagenesis

Primers used to perform PCR are listed in Table 2.2. PCR-based site-directed mutagenesis was performed with a primer containing a point mutation to amplify the appropriate gene. PCRs were performed with 10-50 ng of DNA template, 1.25 µM forward primer, 1.25 µM reverse primer, 0.2 µM dNTPs and 1 unit Vent polymerase (NEB) in 50 µl 1x Thermopol buffer (NEB). PCR cycling conditions used: 94°C for 5 min, 25 cycles of 94°C denaturation (30 sec), 50-65°C annealing (temperature optimized

for each primer pair, 30 sec), and 72°C extension (1 min / 500 bp of the product sequence), followed by a final elongation step of 72°C for 10 min with a final hold at 4°C. PCR products were purified by phenol/chloroform extraction and ethanol precipitation.

2.6 cDNA synthesis

cDNAs were synthesized by GenScript. In some cases, where indicated, the DNA sequences were subjected to codon optimization to enhance protein expression in mammalian cells. The purchased plasmids were purified by large-scale plasmid preparation and the cDNA sequences were subcloned into the appropriate vector for expression and functional studies.

2.7 Cell culture

Vertebrate cell lines used in this study are listed in Table 2.3. Cells were grown in Dulbecco's modified Eagle's Medium (DMEM; Invitrogen) supplemented with 10% fetal bovine serum (FBS; Biologos, Montgomery, IL), 50 U/ml penicillin, and 50 µg/ml streptomycin. Cells were maintained in a tissue culture incubator at 37°C and 5% CO_2. Cells were passaged, frozen, and thawed as described previously (Thompson 2013).

2.8 Polyethylenimine-based cell transfection

Transfection of cells with expression plasmids was performed using polyethylenimine (Polysciences, Inc.) as described previously (Haery 2016). Cells were seeded to be ~60%

confluent on the day of transfection at which time cells were incubated with DNA/PEI at a ratio of 1:6 in serum-free media (300 µl for a 60 mm plate) for 15 min at room temperature. Following incubation, this mixture was added to cells with 3 ml DMEM/10% FBS. Twenty-four hours later, the medium was replaced with 3 ml of fresh DMEM/10% FBS. The following day, cells were harvested for the appropriate assay.

2.9 Whole cell extract preparation

Whole cell extracts were prepared under non-denaturing conditions using mechanical lysis in AT buffer (20 mM HEPES (pH 7.0), 150 mM NaCl, 1 mM EDTA, 1 mM EGTA, 20% v/v glycerol, 1% v/v Triton X-100, 20 mM NaF, 1 mM Na4P2O7-10H_2O, 1 mM DTT, 1 mM Na_3VO_4, 10 µl/ml aprotinin,1 mM phenylmethylsulfolnyl fluoride (PMSF), 1 µg/ml pepstatin A, 1 µg/ml leupeptin). Cells in culture were washed twice with 5 ml PBS before being collected by scraping and transferred to a 1.5-ml microcentrifuge tube. Approximately 120 µl ice-cold AT buffer was added for every 2 million cells in the cell pellet and the cells were resuspended. The cell solution was homogenized by passage through a 27.5-gauge needle at least five times. NaCl was then added to each sample to a final concentration of 150 mM and debris was removed by centrifugation in a microcentrifuge for 30 min at top speed and 4°C. The supernatant was collected and samples were maintained on ice during use or were stored at -80°C.

2.10 SDS-polyacrylamide gel electrophoresis

SDS-polyacrylamide gel electrophoresis (SDS-PAGE) was used to separate proteins under denaturing conditions, and was performed using standard methods described previously (Thompson 2013).

2.11 Western blotting

Western blotting was performed to detect the relative expression levels of proteins using antibodies directed against the proteins of interest. Proteins were separated by SDS-PAGE as described above. Proteins in the gel were then transferred to a nitrocellulose membrane (Bio-Rad) using a wet transfer apparatus in transfer buffer (20 mM Tris, 150 mM glycine, 10% methanol). Transfers were performed at 4°C and 250 mA for 1 h followed by 160 mA overnight, a procedure that was required for nearly complete transfer of high molecular weight proteins to the nitrocellulose filter. After transfer, the membrane was blocked with a solution of 5% milk (Lab Scientific, Livingston, NJ) in TBS-T (10 mM Tris-HCl [pH 7.4], 150 mM NaCl, 0.1% v/v Tween 20) for 1 h at room temperature with gentle rocking. The membrane was then incubated with a solution of primary antibody in TBS-T for 1 h at room temperature or overnight at 4°C with gentle rocking. After incubation with primary antibody, membranes were washed with approximately 50 ml TBS-T for three rounds of 10 min with gentle shaking and then incubated with a solution of secondary antibody conjugated to horseradish peroxidase in TBS-T for 1 h at room temperature with gentle shaking. After incubation with secondary antibody, membranes were washed (same as above) followed by two additional 5 min

washes with 50 ml TBS (10 mM Tris-HCl [pH 7.4], 150 mM NaCl). After the final wash, 1 ml of a solution of SuperSignal West Dura Extended Duration Substrate (Thermo Scientific, Rockford, IL) was added to the membrane and the filters were incubated for 5 min at room temperature with gentle rocking. Luminescence on the membranes was then visualized by exposure to Blue Basic Autorad Film (Bioexpress, Kaysville, UT), which was developed on the Kodak M35 X-OMAT Processor (Kodak Diagnostic Imaging, Rochester, NY). The identities of protein bands were assessed in relation to either known protein molecular weight standards or internal control proteins on the Western blots. Quantification of bands on Western blots was performed using ImageJ on scans of the original film images. Target protein expression was normalized to a loading control protein.

2.12 Antibodies

Antibodies used in this study are listed in Table 2.4.

2.13 Electrophoretic mobility shift assay (EMSA)

A double-stranded κB-site oligonucleotide (5'-TCGAGAGGTCGGGGAATTCCCCCCCCG-3') (Table 2.2) was end labeled with T4 polynucleotide kinase (NEB) in 15 µl reaction with 1x T4 polynucleotide kinase buffer, 1 µg double-stranded probe, and 20 µCi [γ-^{32}P]-dATP (Perkin Elmer) at 37° for 2 h. The reaction volume was then brought up to 100 µl with TE and excess label was removed by filtration through a Bio-Spin 6 Chromatography Column (Bio-Rad). Approximately 10-

30 μg total protein and 200,000 cpm of the κB-site probe were used. Reactions were carried out in either animal lysate binding buffer (10 mM Hepes pH 7.8, 50 mM KCl, 1 mM DTT, 1 mM EDTA, 4% w/v glycerol) or cell lysate binding buffer (10 mM Tris pH 7.4, 50 mM NaCl, 1 mM DTT, 1 mM EDTA, 4% w/v glycerol) for 30 min at 30°C.

2.14 GST-tagged protein purification

BL21 cells were transformed pDEST bacterial expression vectors. A single colony was used to inoculate 5 ml LB supplemented with chloramphenicol (50 μg/ml) and ampicillin (100 μg/ml) and the culture was grown at 37 °C overnight with shaking. The 5 ml culture was used to inoculate 1 L LB supplemented with 100 μg/ml Amp, which was then incubated for 1 h at 37°C. After 1 h, IPTG was added to a final concentration of 1 mM to induce protein expression and the culture was incubated for an additional 2-3 h at 37 °C with shaking. The bacteria were then collected by centrifugation in an HB-4 rotor of a Sorvall RC-5 centrifuge for 10 min at 5,000 rpm at 4 °C. Cells were washed twice with 10ml PBS and then resuspended in 10 ml PBS supplemented with protease inhibitors (1% aprotinin, 2 μg/ml leupeptin, and 1 mM PMSF). Cells were mechanically lysed using a French press. Genomic DNA was lysed with 1 μg/ml Benzonase (Sigma) at 4 °C for 20 min. Debris was then removed by centrifugation in an Eppendorf 5810 R centrifuge for 10 min at 4 °C. The supernatant was then collected and combined with 100 μl of a 50% slurry of glutathione agarose beads and the samples were incubated on a nutator overnight at 4°C. The next day, the beads were washed five times with 1 ml cold PBS

and were then eluted. Purified protein was flash frozen and stored at -80°C in 10% glycerol.

2.15 Protein-binding microarray

PBM experiments were carried out using custom NF-κB oligonucleotide arrays designed as part of this study (Agilent Technologies, AMADID 045485), based on a previously published "10-mer" κB microarray used to assay human and mouse NF-κB proteins (Siggers et al. 2011). DNA probe sequences synthesized on the custom-designed arrays are listed in Mansfield et al. (2017). Proteins used for PBM analysis were expressed in BL21 cells from Gateway pDEST15 GST-tagged vectors. Probes on PBMs were made double-stranded by incubating the array with dNTP annealing mix at 85°C for 10 min, 75°C 10 min, 65°C 10 min, then 60°C for 90 min. The array was blocked at room temperature in filtered PBS with 2% milk for 1 h followed by washing in 0.1% PBS, Tween-20 (5 min) and 0.01% PBS, Triton X-100 (2 min). Arrays were incubated in the dark for 1 h at room temperature with ~300 nM protein and protein binding buffer (6 mM HEPES pH 7.8, 80 mM KCl, 0.5 mM EDTA, 0.5 mM EGTA, 6% glycerol, 35 ng/µl poly-dIdC, 1% milk,). Arrays were then washed with 0.05% PBS Tween-20 (3 min) and 0.01% PBS TX-100 (2 min). An A488-conjugated anti-GST (Invitrogen) antibody was used at 1:40 dilution in PBS containing 2% milk and incubated in the dark for 20 min at room temperature. Arrays were then washed as above followed by an additional wash in PBS (2 min) and then scanned on a GenePix 4400A Scanner (Molecular Devices) and fluorescence was quantified with GenePix Pro 7.2 (Molecular Devices). PBM probe

fluorescence values were spatially averaged and normalized using MicroArray LINEar Regression (Dudley et al. 2002) as described (Berger et al. 2006). Replicate experiments were combined using quantile normalization of probe fluorescence values using the *normalize.quantiles* method in the 'R' statistical package (www.r-project.org). For each unique DNA binding sequence, median fluorescence values were determined over eight replicate probe measurements. Log median fluorescence values (i.e., log(F)) were transformed into a 'z-score' using the mean (μ) and variance (σ) of the log median fluorescence values for the 1195 random background DNA sequences: $z = (\log(F) - \mu)/ \sigma)$.

2.16 Indirect immunofluorescence of DF1 chicken fibroblasts

Indirect immunofluorescence was performed on transfected DF1 cells as described previously (Wolenski et al. 2011). Two days after transfection, DF1cells were passaged onto glass coverslips in 35-mm tissue culture plates. The next day, coverslips were washed 3x with PBS, and then fixed in 100% methanol at -20ºC for 10 min. Fixed cells were blocked in PBS containing 3% calf serum for 1 h and were then incubated with anti-FLAG antiserum (Cell Signaling) at a 1:50 dilution in PBS for 1 h at 37C. Cells were washed as above and incubated with A488-conjugated anti-rabbit secondary antiserum (ThermoFisher) at 1:80 dilution for 1.5 h and then washed again. Coverslips were mounted onto slides using Vectashield (Vector Laboratories), and samples were visualized by confocal microscopy.

2.17 Luciferase reporter assays

Luciferase reporter assays were performed using the Luciferase Assay System (Promega, Madison, WI) as described previously (Wolenski et al. 2011). 293 cells in 35-mm plates were transfected with 0.5 μg of 3X κB-site luciferase reporter plasmid pGL2-3x-κB-luciferase and 0.5 μg of normalization plasmid pRSV-βgal. Cells were co-transfected with 1 μg of pcDNA-FLAG expression vectors or pcDNA3.1 vector alone. For all luciferase reporter assay experiments, total DNA per transfection was kept constant by including varying amounts of pcDNA3.1 vector. Two days after transfection lysates were prepared and then luciferase and β-galactosidase activities were measured. Values were normalized to the relevant vector control (1.0). Statistical analyses were performed using a paired one-tailed t-test and $p < 0.05$ was considered significant.

2.18 *In vitro* kinase assay

In vitro kinase assays were performed essentially as described previously (Wolenski et al. 2011). Human 293 cells were transfected with pcDNA-FLAG-IKK constructs and the kinases were immunoprecipitated with anti-FLAG beads (Sigma). Immunoprecipitates were incubated with 4 μg of GST-tagged peptides and 5 μCi [γ-^{32}P]ATP (Perkin Elmer) in kinase reaction buffer (25 mM Tris-HCl, pH 7.5, 20 mM β-glycerophosphate, 10 mM NaF, 10 mM $MgCl_2$, 2 mM DTT, 500 μM Na_3VO_4, 50 μM ATP) for 30 min at 30°C. Samples were then electrophoresed on a 10% SDS-polyacrylamide gel, and ^{32}P-labeled GST-peptides were detected by phosphorimaging. In parallel, 4 μg samples of GST and

the GST-peptides were electrophoresed on a 10% SDS-polyacrylamide gel, and proteins were detected by staining with Coomassie blue (Bio-Rad).

2.19 NF-κB processing assays

Human 293 cells were transfected with full-length wild-type or 3X Ser-Ala mutant Ap-NF-κB in the absence (-) or presence (+) of IKK expression vectors. Extracts were analyzed by anti-Ap-NF-κB Western blotting, and the full-length and processed forms of Ap-NF-κB were detected. Western blotting was used to demonstrate IKK kinase expression as determined by its migration against molecular weight standards.

2.20 Cell treatments with MG132

Human 293 cells were transfected with full-length Ap-NF-κB and Ap-IKK in the absence (-) or presence (+) of proteasome inhibitor MG132 (Sigma, M7449) at 40 μM in DMEM for 16 h. Lysates were analyzed by Western blotting.

2.21 Anemone maintenance

Aiptasia strain H2 (originally from Kaneohe Bay, Oahu, HI) animals, symbiotic with *Breviolum minutum*, were maintained in 150 ml of 32 ppt artificial sea water (ASW) in glass dishes at 22°C with light provided by Sylvania Gro-Lux (GRO/Aq/RP) fluorescent bulbs at approximately 20 μmol photons/m^2/sec with a 12h:12h light:dark cycle. Aposymbioic anemones were incubated at 22°C in the dark. Anemones were fed *Artemia* brine shrimp 3x a week.

2.22 Generation of anti-Ap-NF-κB antibody

A GST-Ap-NF-κB RHD fusion protein (containing amino 2-422 of Ap-NF-κB), encoded by plasmid pDEST15-Ap-NF-κB-RHD, was expressed in BL21 bacterial cells. The GST-Ap-NF-κB protein was then purified using glutathione beads (ThermoFisher) packed in a column following methods described in section 2.14 using 12 L of culture. Seven mg of purified GST-Ap-NF-κB protein was sent to ThermoFisher Pierce for custom antibody production in rabbits, followed by purification of the resulting antiserum by passage through a GST-Ap-NF-κB column and then a GST column to obtain antibodies to only Ap-NF-κB. 50 ml of purified antiserum was obtained at 0.1µg/µl. Antiserum was aliquoted and stored at -80°C.

2.23 Preparation of Aiptasia for Western blotting

Single anemones were homogenized in 20-40 µl of 2x SDS sample buffer (0.125 M Tris-HCl pH 8.0, 4.6% w/v SDS, 20% w/v glycerol, 10% v/v β-mercaptoethanol) followed by boiling for 10 min and a 10-min centrifugation to remove cell debris.

2.24 Menthol-induced loss of symbiosis of Aiptasia

Menthol-induced loss of symbiosis was achieved by treatment of symbiotic anemones in a glass dish with 150 ml of 0.58 mM menthol (Sigma, M2772) in ASW (that had been aerated for 4 h prior to use). Animals were incubated in the dark with the menthol/ASW solution with fresh menthol changes daily for three 24 h treatment periods (Matthews et

al. 2016). After the last treatment, anemones were placed into fresh, aerated ASW until collected for assaying.

2.25 Heat-induced loss of symbiosis of Aiptasia

Heat treatments were performed by placing symbiotic anemones into 150 ml of ASW in a glass bowl placed in a 25°C water bath. The water bath temperature was raised from 25°C to 32°C by increasing the temperature 1°C every hour for 7 h. Then anemones were kept in the water bath at 32°C for 6 days (with daily water changes to maintain salinity levels at 32 ppt) to induce bleaching, after which they were collected for assaying.

2.26 RNA isolation, cDNA generation, and real-time qualitative PCR

Total cellular RNA was extracted using TRIzol Reagent (Invitrogen, Grand Island, NY) according to the manufacturer's protocol. The mRNA was reverse transcribed into cDNA from 500 ng RNA. RNA was combined with 1.68 µl of 15.4 µM random primers (Promega) and nuclease-free water to 16 µl. Samples were incubated at 65°C in a heating block for 5 min and then incubated on ice for 5 min. cDNA synthesis was initiated by the addition of 6 µl 2.5 mM dNTPs, 1 µl RNasin (Promega), 6 µl 5X M-MLV buffer (Promega), and 1 µl M-MLV reverse transcriptase (Promega), and samples were incubated at 37°C for 1 h. cDNA samples were diluted 10-fold and used as the template for qPCR. 10 µl reactions were prepared (5 µl 2X-PowerUp SYBR Green Master Mix (ThermoFisher), 1 µl each forward and reverse primer (at 1 µM), 2 µl cDNA (1:10), and 1 µl nuclease-free water. All experiments included at least three biological replicates of

each condition and each biological replicate was run in triplicate. No-template controls were included for each primer pair. Reactions were run in standard mode on a 7900-HT Real Time PCR System (Applied Biosystems) using the following thermocycling conditions: 2 min UDG activation at 50°C, 2 min Dual-Lock DNA polymerase activation at 95°C, and 40 cycles of denaturation and annealing/extension at 95°C for 15 sec and 60°C for 60 sec, respectively. Dissociation curves were generated by 15 sec incubation at 95°C, 15 sec incubation at 60°C, and then ramping from 60°C to 95°C at a 2% ramp rate. mRNA expression data were analyzed following the ΔΔCt method (Livak and Schmittgen 2001). For each sample run in triplicate, the average Ct value for the target gene and the average Ct value for the reference gene (L10) was calculated. The Ct value for the reference gene was then subtracted from the value for the target gene to obtain ΔCt (i.e., $Ct_{target} - Ct_{L10}$). The average and standard deviation of ΔCt for each set of biological replicates were calculated. The average ΔCt for bleached samples was then subtracted from the average ΔCt for the symbiotic samples to obtain the ΔΔCt. The fold change in target mRNA relative to the control samples was determined to be $2^{-\Delta\Delta Ct}$. Statistical analysis was performed with an unpaired two-tailed t-test using the GraphPad QuickCalcs online software. Differences in gene expression were considered statistically significant if $p < 0.05$.

2.27 Relative symbiont quantification using qPCR

qPCR using primers against *Breviolum minutum* 28S rRNA was performed on Aiptasia anemones. 28S rRNA levels are relative to the amount in symbiotic control anemones. Statistical significance was determined using an unpaired t-test.

2.28 Preparation of whole cell extracts of Aiptasia for EMSA

Aiptasia anemones used for EMSA were lysed by homogenizing anemones in 100 µl of AT lysis buffer supplemented with protease inhibitors (20 mM HEPES, pH 7.9, 150 mM NaCl, 1 mM EDTA, 1 mM EGTA, 20% w/v glycerol, 1% w/v Triton X-100, 20 mM NaF, 1 mM $Na_4P_2O_7 \cdot 10H_2O$, 1 mM dithiothreitol, 1 mM Na_3VO_4, 1 mM phenylmethylsulfonyl fluoride, 1 µg/ml leupeptin, 1 µg/ml pepstatin A, 10 µg/ml aprotinin) and incubated for 20 min on ice. Lysates were then put through a 27.5 gauge needle to break up cell clumps, and samples were then supplemented with NaCl to a final concentration of 150 mM. Lysates were spun at 13,000 rpm for 30 min at 4 °C to remove cell debris. Protein concentration in the lysates was measured using Nanodrop.

2.29 Supershift assay

Supershifts were performed by incubating EMSA DNA-binding reactions with 2 µl of antiserum for 2 h on ice after completion of the EMSA binding reaction. Samples were analyzed on 5% polyacrylamide gels, and bands were visualized on dried gels by autoradiography or phosphorimaging.

2.30 Cold-induced loss of symbiosis of Aiptasia

Cold treatments were performed by placing symbiotic anemones in ASW in a glass bowl at 4°C for 6 h twice a week for six weeks with animals kept in the dark for the entire period.

2.31 Aiptasia cryosectioning

Adult anemones were relaxed in ASW with 10% w/v $MgCl_2$ and fixed in 4% paraformaldehyde at 4°C for 5 h. Anemones were dehydrated in 30% sucrose in ASW at 4°C overnight. Samples were frozen in 5 ml OCT formula (Tissue-Tek) in plastic cube trays using dry ice and ethanol. Trays were stored for at least 2 h at -20°C before sectioning. Whole-body sections were cut on a cryostat at 10-20 µm, adhered to SuperFrost plus slides (ThermoFisher), and incubated at room temperature for 30 min before staining or freezing at -20°C for later use.

2.32 Immunohistochemistry of Aiptasia cryosections

Slides of frozen cryosections were hydrated in PBS for 2 h at room temperature in a glass slide holder. Tissue sections were outline with a PAP-pen (Sigma) to allow liquid to stay on the slide. Slides were incubated with 400 µl blocking/permeabilization buffer (PBS, 0.3% Triton X-100, 5% goat serum, and 1% BSA) at room temperature for for 4-5 h. Slides were incubated overnight at room temperature in a humidity chamber with 400 µl blocking/permeabilization buffer with NF-κB antiserum or pre-immune serum at a 1:50,000 dilution. Slides were then washed three times for 10 min with 10 ml PBS and

0.05% Tween 20 in glass slide holders at room temperature. Alexa Flour 488-conjugated goat anti-rabbit secondary antiserum (Invitrogen) was added at 1:500 with 5 µM Hoechst in blocking/permeabilization buffer for 1.5 h at room temperature, and then slides were washed as above. Slides were fixed with 40 µl prolong gold, and 170 µm coverslips were applied. Slides were imaged with confocal microscopy. Slides were imaged with Zeiss LSM 700 laser scanning confocal microscope and the ZEN software package (Black Edition) using A488, DAPI, and mCherry. NF-κB puncta were quantified with ImageJ and statistical significance was determined using an unpaired t-test.

2.33 Anemone spawning and infection of larvae with Symbiodiniaceae

Aiptasia adults were spawned in the laboratory to generate larvae using a method similar to that described by Grawunder et al. (2015). Anemones from the clonal male line (CC7), clonal female line (PLF3), or wild-collected anemones from Florida were used for spawning. Larvae were reared in glass finger bowls in ASW until 3-4 days post-fertilization under a 25 µmol photons m^{-2} s^{-1} on a 12:12 h light:dark schedule at 27°C. Prior to infection, Symbiodiniaceae cells were rinsed three times by centrifugation at 3000 x g in ASW and were counted using a Guava Flow Cytometer (Millipore) (Hambleton et al. 2014). Infections were performed at 50,000 cells/ml for 5-6 days in 50 ml of ASW.

2.34 Immunohistochemistry of Aiptasia larvae

Larvae were fixed 4% formaldehyde in ASW for 4 h at room temperature with gentle rocking. Fixed larvae were incubated in 500 µl blocking/permeabilization buffer (PBS, 0.3% Triton X-100, 5% goat serum, and 1% BSA) at room temperature for 1 h. Larvae were then incubated overnight at room temperature with primary antibody of Ap-NF-κB (1:10,000) and α-tubulin (Sigma; 1:500) diluted in blocking/permeabilization buffer. Larvae were then washed three times in 1ml of PBS-T (PBS, 0.05% Tween 20) for 10 min. Larvae were incubated with fluorescent conjugated goat anti-rabbit secondary antiserum (Invitrogen; 1:500) and Alexa fluor-649-conjugated mouse anti-goat secondary antiserum (Invitrogen; 1:500) in blocking/permeabilization buffer for 1 h at room temperature. Nuclei were stained with Hoechst (Sigma; 5 µM) for 5 min followed by three washes in PBS-T as above. Larvae were then pipetted onto 10 µl of Prolong Gold on SuperFrost Plus slides and mounted with a 170 µm coverslip. Larvae were imaged by confocal microscopy. Symbiont cells were counted by manually scanning through the Z-plane to detect Symbiodiniaceae autofluorescence with mCherry. Corrected Total Cell Fluorescence (CTCF) of NF-κB was quantified using ImageJ. For each image, larvae were outlined using the circle tool and area, integrated density, and mean gray value were measured as well as the mean gray value for background fluorescence. CTCF was calculated by the formula (CTCF = Integrated Density - (Area x Mean gray value of background)). Statistical significance was determined using an unpaired, two-tailed t-test.

2.35 Transforming Growth Factor beta (TGFβ) treatment

Aposymbiotic larvae were treated with 200 ng/ml of human TGFβ1 (Sigma, T7039) in ASW at room temperature overnight. Larvae were then either fixed for IHC staining or 200 larvae per treatment group were pooled and processed for mRNA extraction (for qPCR analysis).

2.36 *Serratia marcescens* infections and assessing anemone viability

Aiptasia, adult anemones of four different strains (H2, VW9, CC7, and wild [purchased from Carolina Biologicals]) were incubated with 10 ml of ~1.90 x10^8 *S. marcescens* cells/ml in 32 ppt artificial seawater (ASW) for seven days in 6-well plates. Anemones were then switched to fresh ASW (i.e., in the absence of bacteria) to allow recovery for two weeks. Anemone survival at the end of two weeks in fresh ASW was assessed visually, by observing the presence of extended tentacles and anemone movement when touched using a plastic Pasteur pipette. All infected anemones were compared to non-infected Aiptasia controls.

2.37 Heat treatment of *P. damicornis*

Three independent and genetically distinct *Pocillopora damicornis* colonies were maintained long-term in common garden conditions at Boston University for many years at 26°C with a 12 h: 12 h light/dark schedule under fluorescent lighting. From these common garden conditions, six fragments were obtained from each of three genotypes for a total of 18 fragments (n=9 per treatment). Upon collection, fragments were

immediately affixed to petri dishes with ethyl cyanoacrylate adhesive and were randomly assigned to treatment tanks such that every genotype was represented once in each of three replicate tanks per treatment. For the duration of the experiment, fragments were maintained in 30 gallon aquaria with ASW (Instant Ocean) at 35 psu. Light was standardized at 200 μmol photons m^{-2} s^{-1} using AquaIllumination Hydra TwentySix HD LED aquarium lights. Temperature and salinity were measured daily using a glass thermometer and a YSI Pro30 handheld conductivity meter, respectively. After fragmentation, coral fragments were acclimated to tank conditions for two days at 28 °C. The target temperature for thermal stress (32 °C) was achieved after two days of ramping at 2 °C per day. Heat treatment of this first trial lasted for five-seven days until fragments in heat stress treatments started to present bleached phenotypes. Samples collected for bleaching measurements and genotyping were flash frozen, while samples collected for Western blotting were collected in 1 ml of AT lysis buffer (see section 2.39).

2.38 Measuring bleaching in *P. damicornis*

Measurements of coral tissue color intensity were obtained and analyzed according to Winters et al. (2009). Each photograph contained a color standard chart using the Coral Health Chart (CoralWatch). Photographs were analyzed as described in Winters et al. (2009). Briefly, a white color standard in each photograph was assigned as the maximum white saturation value using Adobe Photoshop. After white standardization, red, green, and blue color channel values were obtained at 10 randomly placed points on each coral fragment. These 10 points were summed and averaged for each coral fragment, and

values were then plotted in R statistical environment as 'final color intensity (au)', which was then compared among the three coral colonies.

2.39 Genotyping of *P. damicornis* colonies and symbiont composition

Coral species and algal symbiont lineage identification were confirmed via sequencing of the 18S and ITS2 DNA, and were assigned to their most likely taxonomic order based on BLAST matches (Altschul et al., 1997) against nonredundant (nr) NCBI database sequences. Algal symbionts were genotyped via metabarcoding of ITS2 following Green et al. (2014) to fully characterize the broad algal communities present.

2.40 Preparation of whole cell extracts of *P. damicornis* for Western blotting

To prepare coral branches for anti-NF-κB Western blotting, branches were incubated in 1 ml of AT lysis buffer supplemented with protease inhibitors (20 mM HEPES, pH 7.9, 150 mM NaCl, 1 mM EDTA, 1 mM EGTA, 20% v/v glycerol, 1% w/v Triton X-100, 20 mM NaF, 1 mM $Na_4P_2O_7 \cdot 10H_2O$, 1 mM dithiothreitol, 1 mM Na_3VO_4, 1 mM phenylmethylsulfonyl fluoride, 1 μg/ml leupeptin, 1 μg/ml pepstatin A, 10 μg/ml aprotinin) for 1 h at 4 °C on a rotator. Lysates were then put through a 27.5 gauge needle to break up cell clumps, and samples were then supplemented with NaCl to a final concentration of 150 mM. Lysates were spun at 13,000 rpm for 30 min at 4 °C to remove cells debris. Protein concentration in the lysates was measured using Nanodrop. Lysates were supplemented with 1x SDS sample buffer (0.125 M Tris-HCl

pH 8.0, 4.6% w/v SDS, 20% w/v glycerol, 10% v/v β-mercaptoethanol) and boiled for 10 min followed by a 10-min centrifugation at 13,000 rpm.

2.41 Promoter analysis

Putative promoter regions of genes dysregulated in aposymbiotic Aiptasia anemones and predicted to be involved in oxidative stress response, inflammation, and apoptosis by Lehnert et al. (2014) were compiled from the Aiptasia genome (Baumgarten et al. 2013). Although Aiptasia promoters have not been experimentally defined, we estimated the promoter regions by using sequences 1 kb upstream of the predicted transcription start site in Aiptasia. The genomic sequences were scanned for predicted NF-κB binding sites using Aiptasia NF-κB's DNA-binding site preference data assayed by protein binding microarray (PBM) analyses in Mansfield et al. (2017). The top 950 sites above a Z-score of 5 were used for the scan (sequences listed in Appendix I). Promoters with predicted NF-κB sites were defined by the presence of at least one site. The promoter regions used and the NF-κB DNA-binding site sequences (and associated PBM z-score) identified in these regions are listed in Appendix II. Fisher's exact test was used to determine statistical significance of the proportion of promoter sequences with and without predicted NF-κB sites in the assayed promoter regions of upregulated and downregulated genes in each category.

Table 2.1 Plasmids used in this study

Mammalian Expression Vectors

pPacPL-FLAG-Relish	N-terminal FLAG-tagged Relish gene. From Neal Silverman (University of Massachusetts Medical School)
pMD5-Aq-NF-κB	From Bernard Degnan (University of Queensland).
pUCIDT-Co-NF-κB	pUCIDT-with Capsaspora-NF-κB codons 200-346 that were codon optimized for expression in *E. coli*, synthesized by IDT.
pUC57-Ap-NF-κB	pUC57 with Ap-NF-κB cDNA synthesized by GenScript with a 5' EcoRI restriction site and a 3' BamHI restriction site.
pUC57-Ap-IKK	pUC57-Simple with Ap-IKK cDNA codon optimized for expression in human cells. Synthesized by GenScript with 5' EcoRI site and 3' XhoI site.
pcDNA-FLAG	pcDNA with a 5' FLAG Tag (Wolenski et al. 2011b).
pcDNA-FLAG-Nv-NF-κB	Wolenski et al. (2011b).
pcDNA-FLAG-Ap-NF-κB	EcoRI-BamHI fragment containing Ap-NF-κB was excised from pUC57-Ap-NF-κB and subcloned into EcoRI-BamHI digested pcDNA-FLAG.
pcDNA-FLAG-Ap-NF-κB-SSS/AAA	EcoRI-Ap-NF-κB-1-2421-3X-Ser-Ala and Ap-NF-κB-2395-2547-3x-Ser-Ala-BamHI PCR fragments were used as a template for assembly PCR of an EcoRI-BamhI fragment containing Ap-NF-κB-3x-Ser-Ala. Primers used for amplification were pcDNA-Flag-Ap-NF-κB-F, Ap-NF-κB-3x-Ser-Ala-F, pcDNA-Flag-Ap-NF-κB-R-Full, Ap-NF-κB-3x-Ser-Ala-R.
pcDNA-FLAG-Ap-NF-κBΔ427	EcoRI-BamHI digested Ap-NF-κB-Δ427 PCR product containing codons 2-422 was subcloned into EcoRI-BamHI digested pcDNA-FLAG. Primers: pcDNA-FLAG-Ap-NF-κB-F and pcDNA-FLAG-Ap-NF-κB-R-427. PCR-amplified from pUC57-Ap-NF-κB.
pcDNA-FLAG-IKKα	Starczynowski et al. (2007).
pcDNA-FLAG-IKKβ	Starczynowski et al. (2007).
pcDNA-FLAG-Ap-IKK	EcoR-XhoI fragment containing Ap-IKK (codons 2-674) was excised from pUC57-Ap-IKK and subcloned into EcoRI-XhoI digested pcDNA-FLAG.

pcDNA-FLAG-Aq-NF-κB	BamHI-BamHI fragment containing codons 2-1193 of Sponge NF-κB was subcloned into BamHI-digested pcDNA-FLAG. Primers: pcDNA-Flag-Sponge-NF-κB-F and pcDNA-Flag-Sponge-NF-κB-R. PCR-amplified from pMD5-Sponge-NF-κB.
pcDNA3.1-Ap-NF-κB	BamHI-EcoRI fragment containing Ap-NF-κB codons 1-849 was subcloned into BamHI-EcoRI digested pcDNA3.1. Primers: pcDNA-ATG-Ap-NF-κB-F and pcDNA-Ap-NF-κB-R. PCR-amplified from pcDNA-FLAG-Ap-NF-κB.
pcDNA3.1-Ap-NF-κB-SSS/AAA	BamHI-EcoRI Ap-NF-κB-SSS/AAA fragment was subcloned into BamHI-EcoRI digested pcDNA3.1. Primers: pcDNA-ATG-Ap-NF-κB-F and pcDNA-Ap-NF-κB-R were used to PCR-amplify the fragment from pcDNAFLAG-Ap-NF-κB-SSS/AAA.
HA-NIK	From Shao-Cong Sun (MD Anderson)

Bacterial Expression Vectors

pGEX-KG	Expression plasmid containing a 5' GST tag.
pGEX-KG-Ap-NF-κB-C-term	EcoRI-HinDIIII fragment containing Ap-NF-κB codons 782-812 was subcloned into EcoRI-HinDIII digested pGEX-KG. Primers- pGEX-KG-Ap-C-term-F and pGEX-KG-Ap-C-term-R were used to PCR-amplify the fragment from pcDNA-FLAG-Ap-NF-κB.
pGEX-KG-Ap-NF-κB-C-term-SSS/AAA	EcoRI-HinDIII fragment containing Ap-NF-κB-SSS/AAA codons 782-812 was subcloned into EcoRI-HindIII digested pGEX-KG. Primers- pGEX-KG-Ap-C-term-F and pGEX-KG-Ap-C-term-R. PCR-amplified from pcDNA-FLAG-Ap-NF-κB-SSS/AAA.
pDEST15	Gateway destination expression plasmid containing a 5' GST tag
pDEST15-Ap-NF-κB-RHD	PCR amplified from pUC57-Ap-NF-κB using Gateway primers to insert codons 2-422 into pDEST-15. Primers: Ap-Gateway-F and Ap-Gateway-R
pDEST15-Aq-NF-κB	PCR amplified from pMD5-Sponge-NF-κB using Gateway primers to insert codons 2-389 into pDEST15. Primers: Sponge-Gateway-F and Sponge-Gateway-R
pDEST15-Co-NF-κB	PCR amplified from pUCIDT-Capsa-NF-κB using Gateway primers to insert codons 200-546 into pDEST15. Primers Capsa-Gateway-F and Capsa-Gateway-R.

pDEST15-Relish	PCR amplified from pPacPL-FLAG-Relish using Gateway primers to insert codons 265-649 into pDEST15. Primers: Relish-Gateway-F and Relish-Gateway-R
pDEST15-Hu-p50	Siggers et al. 2011.
pDEST15-Nv-NF-κB-S	PCR amplified from pcDNA3.1(-)-Nv-NF-κB-Ser67 using Gateway primers to insert codons 2-411 into pDEST15. Primers Nv-NF-κB-F and Nv-NF-κB-R
pDEST15-NV-NF-κB-C	PCR amplified from pcDNA3.1(-)-Nv-NF-κB-Cys67 using Gateway primers to insert codons 2-411 into pDEST15. Primers Nv-NF-κB-F and Nv-NF-κB-R

Table 2.2 Primers used in this study

Primers used for subcloning.

pcDNA-FLAG-Aq-NF-κB-For	5'- CGAAGGATCCCTGCTTTTAATGGTATTGATCCC
pcDNA- FLAG -Aq-NF-κB-Rev	5'- CGAGGGATCCCTAAACTTGACTAGAAGG
pcDNA- FLAG -Ap-NF-κB -For	5'- CGGACGAATTCAACACATTCAGAACAGCAAGTC
pcDNA- FLAG -Ap-NF-κB-R-427-Rev	5'- CAAGGATCCCTAATCAAACAGGAAACCACTGCC
pcDNA- FLAG -Ap-NF-κB-R-Full-length-Rev	5'- CGAGGATCCTCAGTTCGTTCTTCCCATTGG
Ap-NF-κB-3x-Ser-Ala-For	5'- GACGCAGGCTTTGGGGCCCAGGCTGCA
Ap-NF-κB-3x-Ser-Ala-Rev	5'- TGCAGCCTGGGCCCCAAAGCCTGCGTC
pcDNA-ATG-Ap-NF-κB-For	5'- CGCGGATCCATGACACATTCAGAACAGCAA
pcDNA-Ap-NF-κB-Rev	5'- GCGCGGAATTCTCAGTTCGTTCTTCCCAT
pGEX-KG-Ap-NF-κB-C-term-For	5'- GCGCGCGAATTCTAAACTATGGCGACTAT
pGEX-KG-Ap-NF-κB-C-term-Rev	5'- GCGCGAAGCTTCTAATCATTGTCTCTTTCTGA
Ap-Gateway-For	5'-GGGGACAAGTTTGTACAAAAAAGCACGCTTCACACATTCAGAACAGCAA
Ap-Gateway-Rev	5'- GGGGACCACTTTGTACAAGAAAGCTGGGTCCTAATCAAACAGGAAACCACTG
Aq-Gateway-For	5'- GGGGACAAGTTTGTACAAAGCAGGCTTCGCTTTTAATGGTATTGATCCC
Aq-Gateway-Rev	5'- GGGGACCACTTTGTACAAGAAAGCTGGGTCCTAACCCCCTCCACCGGGACCTTC

Aq-Gateway-For	5'- GGGGACAAGTTTGTACAAAAAAGCAGGC TTCGGCGTTAGTTTCGGCGTTGCT
Relish-Gateway-Rev	5'- GGGGACCACTTTGTACAAGAAAGCTGGG TCCTAATTAGAGCTTTCTGTTCCCGAA
Co-Gateway-For	5'- GGGGACAAGTTTGTACAAAAAAGCAGGC TTCTCCCCATCCGTTTCAACC
Co-Gateway-Rev	5'- GGGGACCACTTTGTACAAGAAAGCTGGG TCCTAACCGTCGCTGCCGTCGAAG
Nv-NF-κB-For	5'- GGGGACAAGTTTGTACAAAAAAGCAGGC TTCGCACAGTCTGAACAGCAAG
Nv-NF-κB-Rev	5'- GGGGACCACTTTGTACAAGAAAGCTGGG TCTAACCTGTAGCTCCAGATGAG

Restriction enzyme sites used are underlined.

Primers for EMSA

Consensus NF-κB-site double-stranded oligonucleotide	5'- TCGAGAGGTCGGGGAATTCCCCCCCCG CTCCAGCCCCTTAAGGGGGGGGCAGTT -5'

Canonical NF-κB DNA-binding site underlined.

Primers for qPCR

Ap-NF-κB	5'- CGACCCCACCAGAATCTGAAAG 5'- ACGAATCATTGTCTCTTTCTGCAG
B. minutum 28S rRNA (from Poole et al. 2016)	5'- GTCTTTGTGAGCCTTGAGC 5'- GGCACACTAACAAGTGTACCATG
L10 (from Poole et al. 2016)	5'- ACGTTTCTGCCGTGGTGTCCC 5'- CGGGCAGCTTCAAGGGCTTCA

Table 2.3 Vertebrate cell lines used in this study

293	Human embryonic kidney cell line
293T	Human embryonic kidney cell line expressing the SV40 large T-antigen
DF1	Chicken fibroblast cell line

Table 2.4 Antibodies used in this study

Protein	Catalog #	Type/Antigen	Dilution (Application)	Host	Source
Aiptasia NF-κB	custom	pAb/RHD	1:10,000 (WB); 1:50,000 (IHC)	Rabbit	Thermo Fisher
FLAG	D6W5B	mAb	1:1000 (WB); 1:50 (IF)	Rabbit	CST
Mouse IgG	7076	pAb/HRP-conjugated	1:4000 (WB)	Horse	CST
Mouse IgG	A21235	pAb/A647 conjugated	1:500 (IHC)	Goat	Thermo Fisher
Rabbit IgG	7074	pAb/HRP-conjugated	1:4000 (WB)	Goat	CST
Rabbit IgG	A27034	pAb/A488 conjugated	1:500 (IHC); 1:80 (IF)	Goat	Thermo Fisher
α-tubulin	3837	p/Ab	1:5000 (WB); 1:500 (IHC)	Mouse	CST

CST, Cell Signaling Technology; IF, indirect immunofluorescence; IHC, immunohistochemistry; mAb, monoclonal antibody; pAb, polyclonal antibody; WB, Western blotting

CHAPTER THREE

TRANSCRIPTION FACTOR NFKB IS MODULATED BY SYMBIOTIC STATUS IN AIPTASIA, A SEA ANEMONE MODEL OF CNIDARIAN BLEACHING

3.1 Introduction

Due to reports of a correlation between immune gene expression and bleaching in certain corals (Anderson et al. 2016, Pinzon et al. 2015), as well as the pervasive role of NF-κB in immunity and disease across a broad evolutionary expanse (Gilmore and Wolenski 2012) we have now characterized NF-κB signaling in the sea anemone Aiptasia. In this chapter, we have performed a series of in vitro and cell-based assays to characterize the structure and activity of the Aiptasia NF-κB (Ap-NF-κB) protein, and have determined the expression, activity, and tissue distribution of NF-κB in Aiptasia following modulation of symbiosis in larvae and adult anemones. Overall, these results suggest that the structure and function of Ap-NF-κB is similar to that of human NF-κB p100 and that downregulation of an NF-κB-dependent pathway is important for the establishment of symbiosis in Aiptasia.

3.2 The Aiptasia NF-κB protein has similarities in structure, activity, and regulation to mammalian non-canonical NF-κB

The analysis of transcriptomic and genomic databases of Aiptasia revealed a single gene encoding an NF-κB-related protein. The Aiptasia NF-κB protein (Ap-NF-κB) has a structural organization that is analogous to mammalian NF-κB p100: an N-terminal RHD,

followed by a glycine-rich region (GRR), a series of ANK repeats, and putative regulatory sites of serine phosphorylation by IKK (Figure 3.1a) that closely resemble IKK phosphorylation sites in human p100 (Figure 3.1b).

To analyze the biological regulation and molecular properties of Ap-NF-κB, we first created pcDNA-FLAG mammalian expression vectors for full-length Ap-NF-κB and a C-terminally truncated mutant (Δ427) that approximates the structure of a processed form of Ap-NF-κB. These two vectors expressed appropriately sized proteins in human 293 cells (Figure 3.1c). The Ap-NF-κBΔ427 protein migrated similarly to the *Nematostella* NF-κB protein (Nv-NF-κB), which lacks a C-terminal IκB-like domain (Sullivan et al. 2004, Wolenski et al. 2011a-b). In an electrophoretic mobility shift assay (EMSA), extracts from 293 cells transfected with the Δ427 mutant, but not full-length Ap-NF-κB, showed a high level of DNA-binding activity, which was comparable to that seen with Nv-NF-κB (Figure 3.1d) (Wolenski et al. 2011a).

To determine the overall DNA binding site specificity of Ap-NF-κB, we assessed the DNA-binding profile of bacterially expressed, affinity purified Ap-NF-κB in a protein-binding microarray (PBM) consisting of 2592 κB-type sites and 1195 random background sequences (sequences listed in Mansfield et al. 2017). We have previously used similar PBM analyses to compare the DNA binding site preferences of mammalian NF-κB family proteins (Siggers et al. 2011). By comparing z-scores for binding to specific sites on the PBM, we found that the DNA-binding profile of Ap-NF-κB is similar to human NF-κB p50 and Nv-NF-κB, but is distinct from human c-Rel and RelA (Figure 3.1e). Furthermore, a comparison of the DNA-binding profile of a variety of

other Rel/NF-κB proteins across a broad evolutionary expanse clearly places Ap-NF-κB among the subfamily of NF-κB proteins (Figure 3.2). In addition, a comparison of the general structure of the Ap-NF-κB protein shows that it is most similar to NF-κB subfamily proteins (Figure 3.3).

NF-κB p100 protein activation requires phosphorylation by an upstream IKK, which is followed by C-terminal proteolytic processing and nuclear localization of the mature NF-κB p52 protein. In the mammalian non-canonical pathway, activated IKKα initiates processing of NF-κB p100 by phosphorylating three serine residues downstream of the p100 C-terminal ANK repeats, which then promotes processing of p100 to p52 by the proteasome (Kim et al. 2014). Ap-NF-κB contains three serine residues in a similar arrangement and location as the serine residues in human p100 that are phosphorylated by IKKα (Figure 3.1b). A BLAST analysis identified a single IKK-like protein in Aiptasia, which, by MEME and phylogenetic analyses, was indicated to be an IKKα/β-like protein homolog (Figure 3.4) (sequences used for analysis listed in Mansfield et al. 2017). Therefore, we analyzed Ap-NF-κB for these central properties of NF-κB signaling and regulation.

First, by immunofluorescent staining of transfected chicken fibroblasts, we found that the full-length Ap-NF-κB localized exclusively to the cytoplasm, whereas the C-terminally truncated Ap-NF-κBΔ427 mutant was exclusively in the nucleus (Figure 3.5a). As a control, we show that Nv-NF-κB, which has a structure that is similar to the Ap-NF-κBΔ427 mutant, was also exclusively in the nucleus of transfected cells (Figure 3.5a), consistent with our previous results (Wolenski et al. 2011). Secondly, we found that Ap-

NF-κBΔ427 transactivated a multimeric NF-κB site reporter in 293 cells to approximately the same extent as Nv-NF-κB (Figure 3.5b) (Wolenski et al. 2011b). In contrast, full-length Ap-NF-κB showed little ability to activate the reporter above vector control levels (Figure 3.5b). Thus, our results show that the C-terminally truncated Ap-NF-κBΔ427 protein has increased DNA-binding activity, nuclear localization, and transactivation ability as compared to full-length Ap-NF-κB. Ap-NF-κBΔ427 shares these three properties with the processed p52 form of the mammalian NF-κB p100 protein, suggesting that the removal of the C-terminal ANK repeat of Ap-NF-κB is necessary for activation of the protein.

In an *in vitro* kinase assay, Aiptasia IKK (sequence in Mansfield et al. 2017) can phosphorylate a peptide containing C-terminal sequences (aa 783-812) of Ap-NF-κB, but cannot phosphorylate the same peptide in which the three Ser residues are converted to Ala (Figure 3.5c). Moreover, co-transfection of 293 cells with an expression vector for Ap-IKK induces processing of wild-type Ap-NF-κB to a protein of approximately 52 kDa, but Ap-IKK did not induce processing of the SSS/AAA mutant of Ap-NF-κB under the same conditions (Figure 3.5d). Ap-IKK-induced processing of Ap-NF-κB in 293 cells is reduced in the presence of the proteasome inhibitor MG132 (Figure 3.5e).

Additionally, in an *in vitro* kinase assay human IKKα and β can all phosphorylate a peptide containing C-terminal sequences (aa 783-812) of Ap-NF-κB, but cannot phosphorylate the same peptide in which the three Ser residues are converted to Ala (Figure 3.6a).Co-transfection of Ap-NF-κB with human NIK (to activate endogenous

IKKα) or a constitutively active human IKKβ also induced processing of Ap-NF-κB in 293 cells (Figure 3.6b).

Finally, we show that lysates from Aiptasia contain forms of Ap-NF-κB that co-migrate with both full-length and processed forms of Ap-NF-κB that were detected upon expression in 293 cells (Figure 3.7). These results identify phosphorylation sites and conditions that are necessary for Ap-IKK induced processing of Ap-NF-κB, and suggest that similar processing events occur in Aiptasia.

Taken together, these results show that Ap-NF-κB has structural, functional and regulatory similarities to the non-canonical mammalian NF-κB protein p100, and that these properties are conserved even upon expression of Ap-NF-κB in human cells. Furthermore, the co-migration of full-length and processed forms of Ap-NF-κB expressed in 293 cells with two forms of Ap-NF-κB detected in extracts from anemones suggests that a similar processing event occurs in Aiptasia.

3.3 NF-κB mRNA, protein, and activity increase with loss of symbiosis in Aiptasia

To determine whether Ap-NF-κB is affected by the symbiotic status of Aiptasia, we induced loss of symbiosis in anemones by two commonly used methods, namely elevated water temperature and menthol treatment. Elevated temperature has been used to mimic climate change-induced bleaching, and in the laboratory, symbiotic anemones can be bleached by gradually increasing the water temperature from 25°C to 32°C for 6 days. Menthol treatment produces bleached anemones after just three days of treatment

(Matthews et al, 2016). With either treatment, the anemones take on a strikingly bleached appearance (Figure 3.8a, top right), and they show greatly reduced numbers of symbionts by fluorescence (Figure 3.8a, bottom right) and by qPCR of symbiont 28S RNA (Figure 3.8b). In this thesis, we will refer to our heat- and menthol-treated anemones as aposymbiotic, based on the greatly reduced numbers of symbionts present after either treatment.

To determine whether NF-κB expression is altered by symbiotic status in Aiptasia, we compared the protein and mRNA levels of Ap-NF-κB between symbiotic and aposymbiotic animals. The levels of processed Ap-NF-κB protein were increased approximately three-fold in heat- and menthol-induced aposymbiotic anemones as compared to symbiotic anemones (Figure 3.8c) and similarly, the level of Ap-NF-κB mRNA was increased by approximately three-fold in menthol-induced aposymbiotic anemones as compared to symbiotic anemones (Figure 3.8d). There was also an approximately six-fold increase in κB-site DNA-binding activity in extracts from menthol- and heat-induced aposymbiotic Aiptasia (Figure 3.8e and 3.8f). That the increased DNA-binding activity in aposymbiotic anemone extracts is due to Ap-NF-κB is suggested by the similar migration of the DNA-protein complex with the complex generated by the Δ427 protein expressed in 293 cells and by the ability of Ap-NF-κB antiserum (but not preimmune serum) to supershift the complex from aposymbiotic animals (Figure 3.8e and 3.8f). Additionally, anemones made aposymbiotic by cold shocking (Poole et al. 2016) showed increased κB site DNA-binding activity as compared to symbiotic anemones. (Figure 3.8g).

To compare the whole organism pattern of Ap-NF-κB expression, we performed anti-Ap-NF-κB immunofluorescence on cryosections of symbiotic and heat- and menthol-induced aposymbiotic Aiptasia (Figure 3.8h). At low magnification imaging of tentacle cross-sections (Figure 3.8h, top), Ap-NF-κB staining was noticeably brighter in aposymbiotic anemones. At higher magnification (Figure 3.8h, middle), NF-κB was detected in symbiotic animals in a few cells primarily in the epidermis and away from cells containing intracellular symbionts located in the gastrodermis. After heat- or menthol-induced bleaching, there was an approximately three- to four-fold increase in NF-κB-positive cells, which are mostly in the gastrodermis where symbionts were greatly reduced in number. The three- to four-fold increase in Ap-NF-κB-positive cells seen in aposymbiotic Aiptasia tissue sections is consistent with the increased levels of Ap-NF-κB protein seen by Western blotting of whole animal extracts (Figure 3.8c). The staining of Ap-NF-κB in tissue sections from both symbiotic and bleached anemones coincides with nuclear DAPI staining (Figure 3.8h, bottom). Overall, these results show that loss of symbionts from Aiptasia is correlated with increased NF-κB protein levels and DNA-binding activity as well as expanded tissue expression of nuclear NF-κB.

3.4 Increased NF-κB protein expression follows loss of symbiosis

To investigate the kinetics of increased NF-κB expression during loss of symbiosis, Ap-NF-κB expression and symbiont levels were quantified at multiple time-points during the process of menthol-induced loss of symbiosis. In these experiments, symbiotic anemones were treated for three days with menthol and were then given regular seawater for the

remainder of the experiment. Aiptasia were collected during the first two menthol treatments (Days 1 and 2, i.e., D1 and D2) and at three time-points after menthol treatment when the anemones were in seawater (D4, D7 and D14). As shown by qPCR, menthol treatment induced a rapid and progressive loss of symbionts, with an ~80% loss of symbionts at D1 as compared to control anemones, and an approximately 99% decrease in symbionts by D4 (Figure 3.9a). After D4, the symbiont densities remained at this low level through D14 (Figure 3.9a), indicating that the symbionts were not repopulating the animal after removal of the menthol. By Western blotting, Ap-NF-κB protein levels in anemones at D1 and D2 of menthol treatment were similar to those seen in control, untreated animals (Figure 3.9b). However, by D4 Ap-NF-κB protein levels were statistically increased (i.e., 3.8-fold) as compared to control anemones, and the levels of Ap-NF-κB protein remained statistically higher than in control animals even at D14 (Figure 3.9b). In addition, anemones that have been kept aposymbiotic for a longer period of time, i.e. 73 days, had significantly higher NF-κB expression as compared to symbiotic anemones (Figure 3.9c). These results show that increased levels of NF-κB occur only after there has been a substantial loss of symbionts and that the increase in NF-κB protein levels is maintained in aposymbiotic animals for over two months after bleaching is initially induced.

3.5 Introduction of Symbiodiniaceae species *Breviolum minutum* into naïve Aiptasia larvae leads to reduced NF-κB expression

Given that loss of symbionts was correlated with increased Ap-NF-κB expression, we hypothesized that introduction of *Breviolum minutum* (formerly clade B01) into aposymbiotic Aiptasia would decrease NF-κB expression. For these experiments, naturally and completely aposymbiotic Aiptasia larvae were inoculated with *B. minutum*, and Ap-NF-κB expression was then assessed using indirect immunofluorescence of whole-mount specimens. This approach was used for two reasons: 1) we could ensure that the larvae were aposymbiotic and had never seen *B. minutum*; and 2) the population of anemones with *B. minutum* could be done within a much shorter period (i.e., about 11 days) than the lengthy period (months) required for repopulating aposymbiotic adults. In these experiments, larvae at 4-5 days post-fertilization (dpf) were inoculated with *B. minutum*, and then 5-6 days after infection the larvae were fixed and stained with Ap-NF-κB antiserum. In larvae that were successfully infected, the numbers of symbionts present ranged from 2-15 cells (mean of 7.8 *B. minutum*/larva) (Figure 3.10a). Larvae infected with *B. minutum* showed a 92% decrease in Corrected Total Cell Fluorescence (CTCF) for Ap-NF-κB as compared to control uninfected larvae (Figure 3.10b and 3.10c). This result demonstrates that Ap-NF-κB protein expression is down-regulated in Aiptasia upon infection with *B. minutum*.

3.6 Chapter 3 summary

Overall, the results presented in this Chapter show that there is a correlation between NF-κB transcription factor expression and activity with symbiotic status in Aiptasia, demonstrating that NF-κB expression is suppressed by the establishment of symbiosis and is increased by loss of symbiosis. Our results also suggest that a form of non-canonical NF-κB processing is constitutively present in the sea anemone Aiptasia. Using protein binding microarrays and amino acid sequence analysis, we show that basal NF-κB proteins have DNA-binding site specificities and overall structures, respectively, that are more similar to human NF-κB proteins than to human Rel proteins. Moreover, the Aiptasia NF-κB protein undergoes processing in human cells when human or Aiptasia IKK proteins are overexpressed. Furthermore, PBM analyses demonstrate that there is little difference between the DNA-binding site profiles of human NF-κB p50 and either sponge or anemone NF-κB proteins. We show that laboratory-induced bleaching of Aiptasia is associated with increased expression and activity of NF-κB and that infection of naïve aposymbiotic Aiptasia larvae with *B. minutum* reduces NF-κB expression

Figure 3.1 Conserved DNA-binding activity of Ap-NF-κB

(a) Shown are the generalized structures of Ap-NF-κB, a C-terminal truncation mutant of Ap-NF-κB (Δ427), and the naturally shortened Nv-NF-κB protein. White: Rel homology domain (RHD). Dark grey: Glycine-rich region. Red: Ankyrin repeats. Ap-NF-κB putative IKK-phosphorylation sites shown. (b) Alignment of the serine residues that are phosphorylated by IKKα in human p100 with the phosphorylation sites of Ap-NF-κB. (c) Western blot of extracts from human 293 cells transfected with FLAG-tagged versions of the indicated proteins. The relevant section of the scanned film is shown; no other bands were detected on the gel. (d) An NF-κB-site EMSA of extracts from 293 cells transfected with the indicated proteins. The arrow indicates the position of the DNA-protein complex. The free probe is seen as a black band across the bottom of the image. (e) Comparison of the PBM-based DNA-binding profile of Aiptasia NF-κB to human p50, c-Rel, Rel-A, and *Nematostella vectensis* (Nv) NF-κB to 2592 κB sites (black dots) and 1195 random background sites (blue dots). (Analysis of PBMs done by Dr. Trevor Siggers.)

Figure 3.1 Conserved DNA-binding activity of Ap-NF-κB

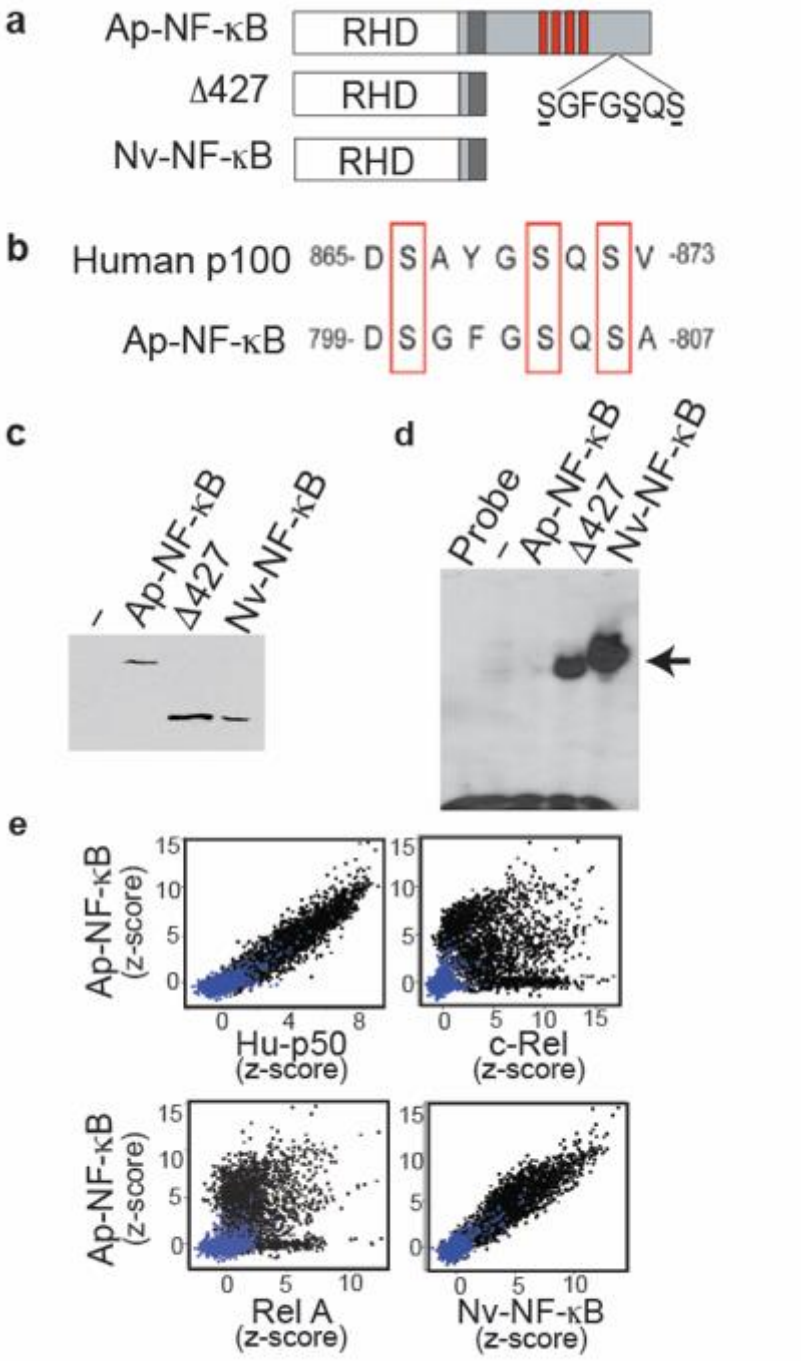

Figure 3.2 Comparison of DNA-binding site preferences of NF-κB orthologs

Pairwise comparisons of the DNA-binding specificity of bacterially expressed NF-κB family proteins from multiple species. Pairwise binding similarity was assessed by Pearson correlation of PBM-determined z-score values to 2592 NF-κB binding sites. Hierarchical clustering was carried out on the comparison matrix as described previously (Siggers et al. 2011). * indicates previously published PBM binding data[7], and in some cases (e.g., Hu-cRel and Hu-p50 were repeated in our lab to verify the reproducibility of our PBM analyses. (Abbreviations: Ap, *Aiptasia pallida*; Aq, *Amphimedon queenslandica*; Co, *Capsaspora owczarzaki*; Dm, *Drosophila melanogaster*; Mo, mouse; Hu, human; Nv, *Nematostella vectensis*. C and S indicate the polymorphic NF-κB proteins from *Nematostella* (Ryzhakov et al. 2013, Sullivan et al., 2009, Wolenski et al. 2001). (This analysis was performed by Dr. Trevor Siggers.)

Figure 3.2 Comparison of DNA-binding site preferences of NF-κB orthologs

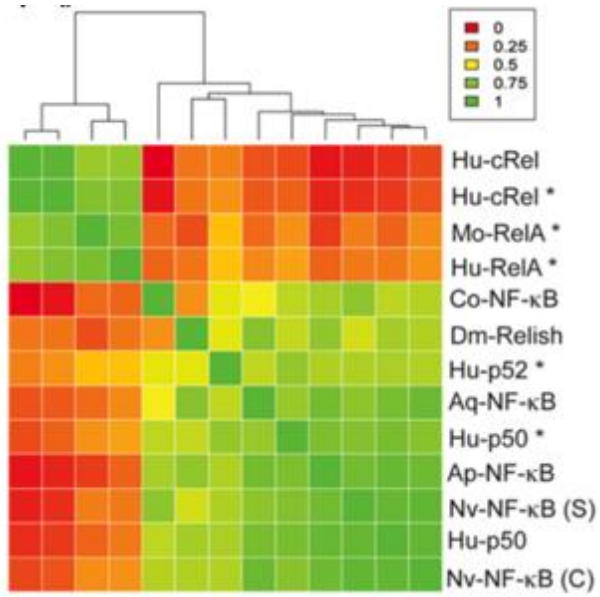

Figure 3.3 Comparison of the structures of NF-κB proteins

Conserved motifs in the NF-κB protein were identified by MEME analysis. Motifs within the Rel Homology domain (RHD) and Ankyrin repeats (ANK) were encapsulated into single motifs and boxed (grey shading). Clustal Omega was used to align the protein sequences, and the relevant regions were then visually inspected to identify glycine-rich regions (green inverted triangles) and predicted IKK phosphorylation sites (red inverted triangles) were inferred by sequence homology to known phosphorylation sites in human NF-κB proteins. (This phylogeny was generated by Linda Nguyen.)

Figure 3.3 Comparison of the structures of NF-κB proteins

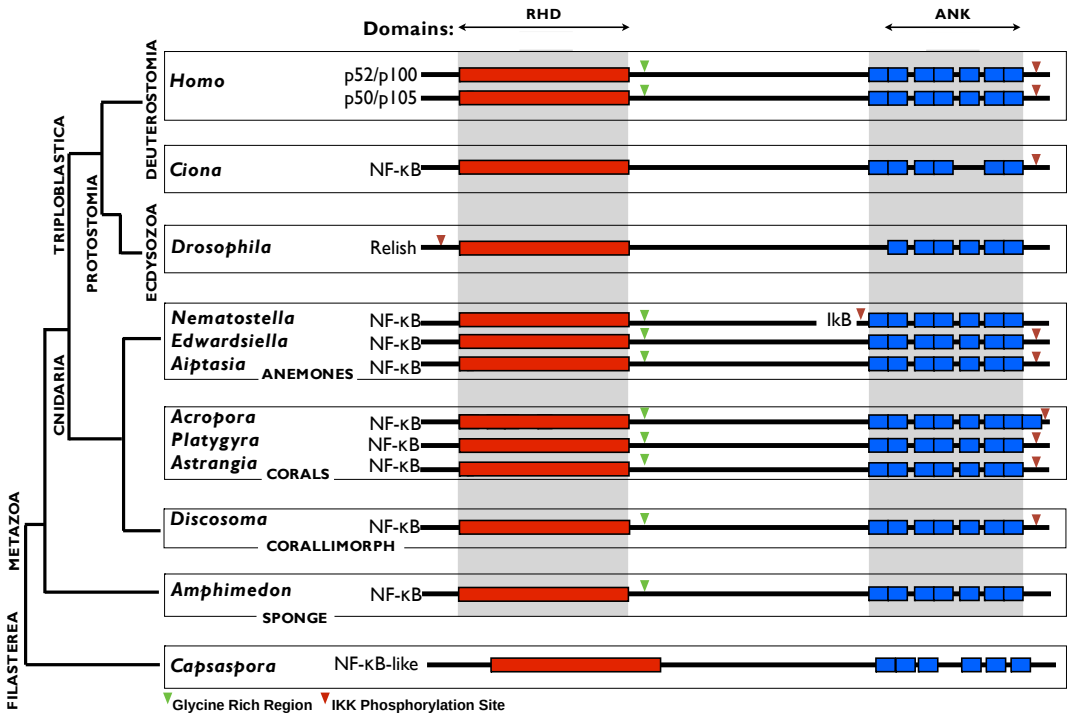

Figure 3.4 MEME analysis and phylogenetic comparison of IKK-like proteins.
(a) MEME analysis of IKK proteins from different taxa. Colored boxes indicate conserved protein motifs among the indicated IKK proteins. The shaded region indicates the serine/threonine kinase domain. IKKα/β and TBK/IKKε single orthologs are named as such because they had extensive shared motifs with their vertebrate counterparts, had at least 33% similarity to the human counterparts by reciprocal BLAST analysis, and were in the same clades by phylogenetic analysis. (b) Phylogenetic analysis of IKK evolution using maximum likelihood tree that was bootstrapped 1000 times. The phylogeny was rooted with the TBK/IKKε of *Amphimedon* and branches indicate bootstrap support values. The IKKα/β and TBK/ε clades are clearly distinguished and mostly recapitulate evolution with Homo and sea anemone proteins sequences clustering. Proteins were named according to at least 33% sequence similarity for reciprocal BLASTs against the human genome using tBLASTn on NCBI. (This analysis was performed by Linda Nguyen.)

Figure 3.4 MEME analysis and phylogenetic comparison of IKK-like proteins.

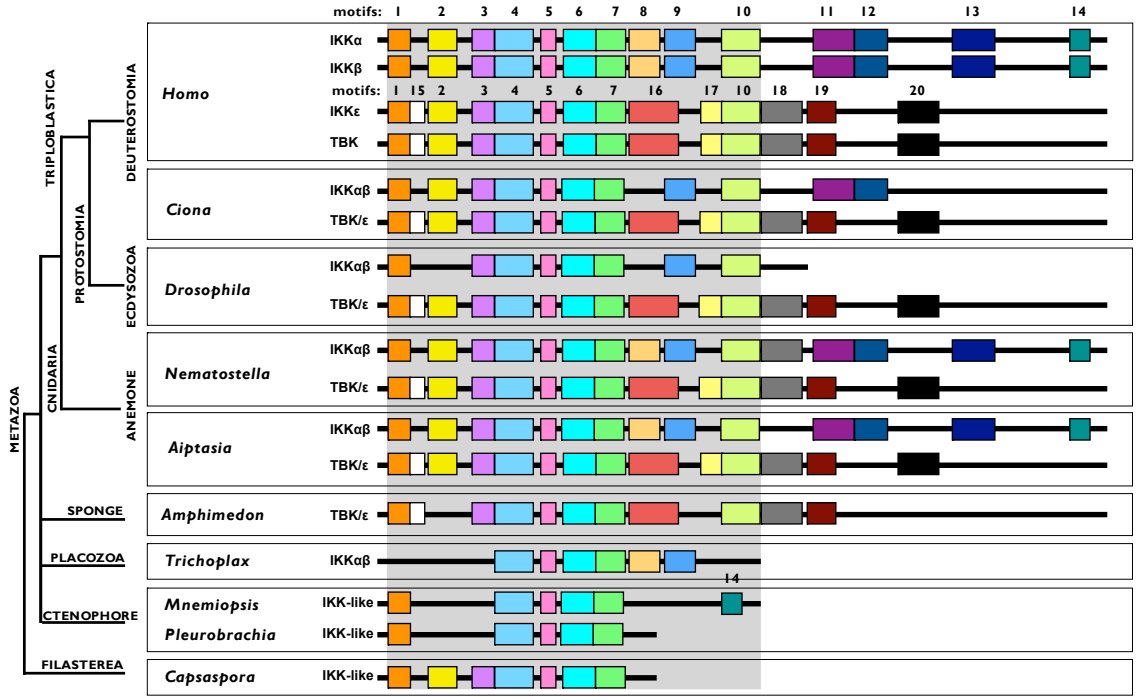

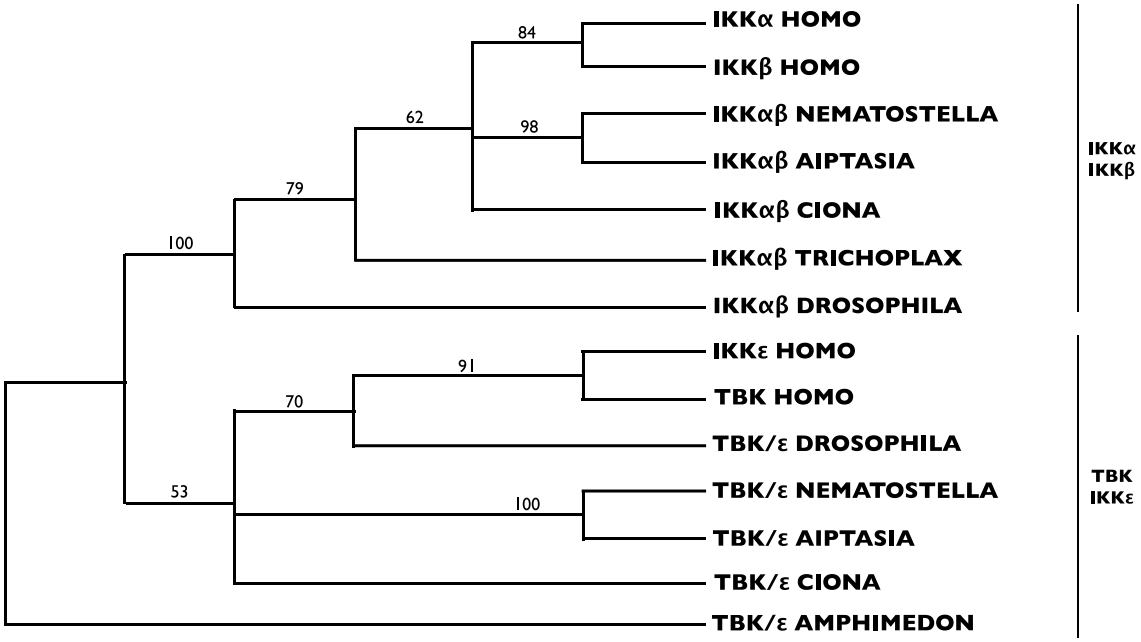

Figure 3.5 Processing of Ap-NF-κB by Ap-IKK in human cells

(a) Indirect immunofluorescence (green) using anti-FLAG primary antiserum of DF-1 chicken fibroblasts transfected with the indicated FLAG-tagged proteins. Nuclear staining with DAPI is shown in blue. (Experiment performed by Dr. Thomas Gilmore.) (b) An NF-κB site luciferase reporter gene assay was performed in 293 cells with the indicated proteins. Luciferase activity is relative to that seen with the vector control (1.0), and is the average of three experiments done in triplicate. Standard error is indicated. (Experiment performed by Anara Alshanbayeva.) (c) An *in vitro* kinase assay using FLAG-Ap-IKK and GST-fusion proteins containing C-terminal sequences (amino acids 783-812) of wild-type and 3X Ser-Ala mutant Ap-NF-κB. The top image is a phosphorimage of ^{32}P-labelled proteins, showing the relevant portion of the image; the free ATP images at the bottom on the gel are not shown. The bottom image shows a Coomassie blue-stained gel of GST proteins used in the kinase assay. An anti-FLAG blot of the 293 cell extract was also performed to confirm Ap-IKK expression (not shown). (d) 293 cells were transfected with full-length wild-type or 3X Ser-Ala mutant Ap-NF-κB in the absence (-) or presence (+) of an Ap-IKK expression vector. Extracts were analyzed by anti-Ap-NF-κB Western blotting, and the full-length and processed forms of Ap-NF-κB are indicated. At the bottom is an anti-FLAG Western blot showing expression of Ap-IKK, as determined by its migration against molecular weight standards. (e) 293 cells were transfected with full-length Ap-NF-κB and Ap-IKK in the absence (-) or presence (+) of proteasome inhibitor MG132.

Figure 3.5 Processing of Ap-NF-κB by Ap-IKK in human cells

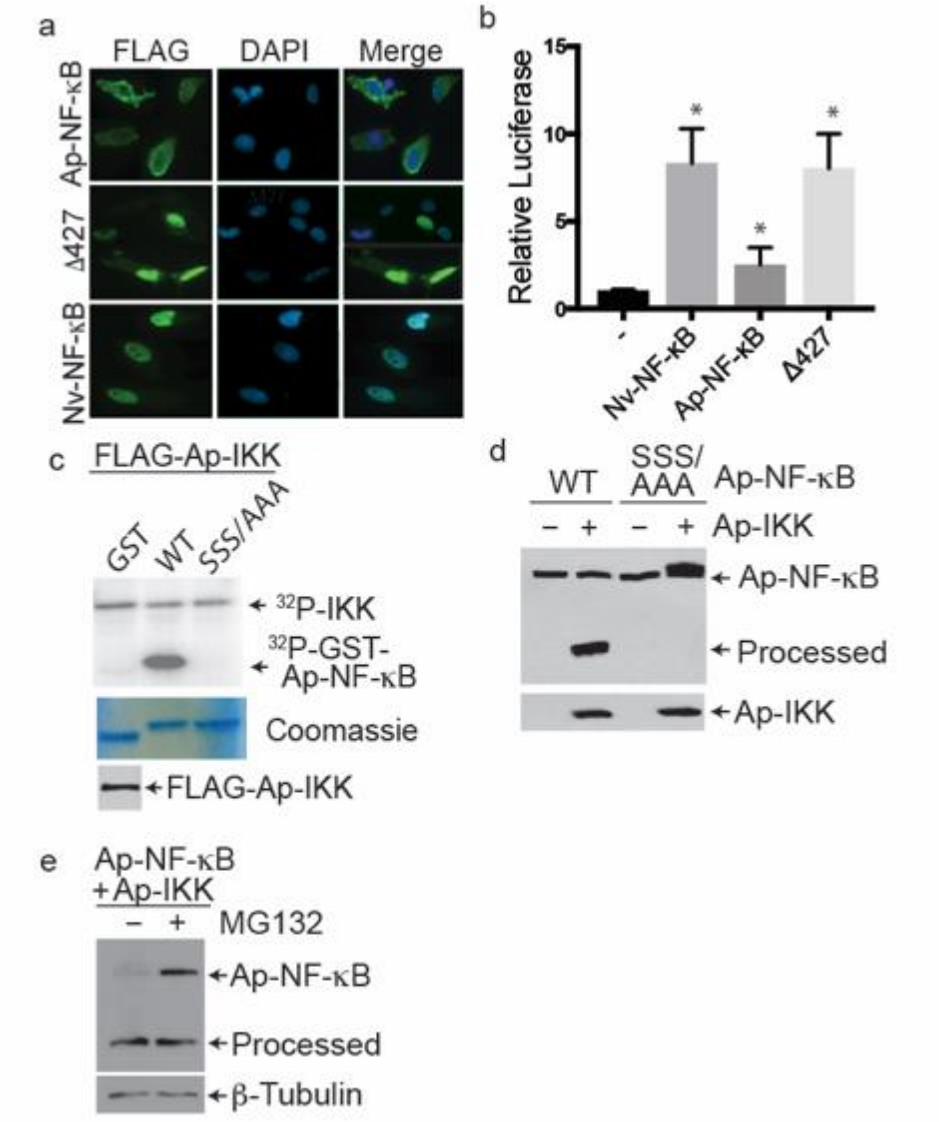

Figure 3.6 Phosphorylation and induced processing of Ap-NF-κB by human IKK's

(a) Human IKKα and IKKβ can phosphorylate Ap-NF-κB but not Ap-NF-κB-SSS/AAA in vitro. GST-tagged peptides were incubated with FLAG-tagged IKKα or IKKβ in kinase reaction buffer (25 mM Tris HCl, pH 7.5, 20 mM β-glycerophosphate, 10 mM NaF, 10 mM $MgCl_2$, 2 mM DTT, 500 μM Na_3VO_4, 50 μM ATP) in the presence of gamma-[32P]-ATP (free ATP is the large band shown at the bottom of the gel). Samples were then electrophoresed on a 12.5% SDS-polyacrylamide gel. The gel was dried and radioactivity was detected by phosphorimaging. The middle panel shows the GST peptides used in the assay. The bottom panel shows the relevant portion of an anti-FLAG Western blot of the kinases expressed in 293 cells that were used in the kinase assay. (b) Human NIK and constitutively active IKKβ can induce processing of Ap-NF-κB but not the Ap-NF-κB-SSS/AAA mutant. Plasmids were co-transfected into 293 cells and lysates were analyzed by Western blotting for Ap-NF-κB. The blot was stripped and reprobed for the HA-tagged kinases. The relevant portions of the images are shown and the relevant immunoreactive bands are shown.

Figure 3.6 Processing of Ap-NF-κB by human IKK's

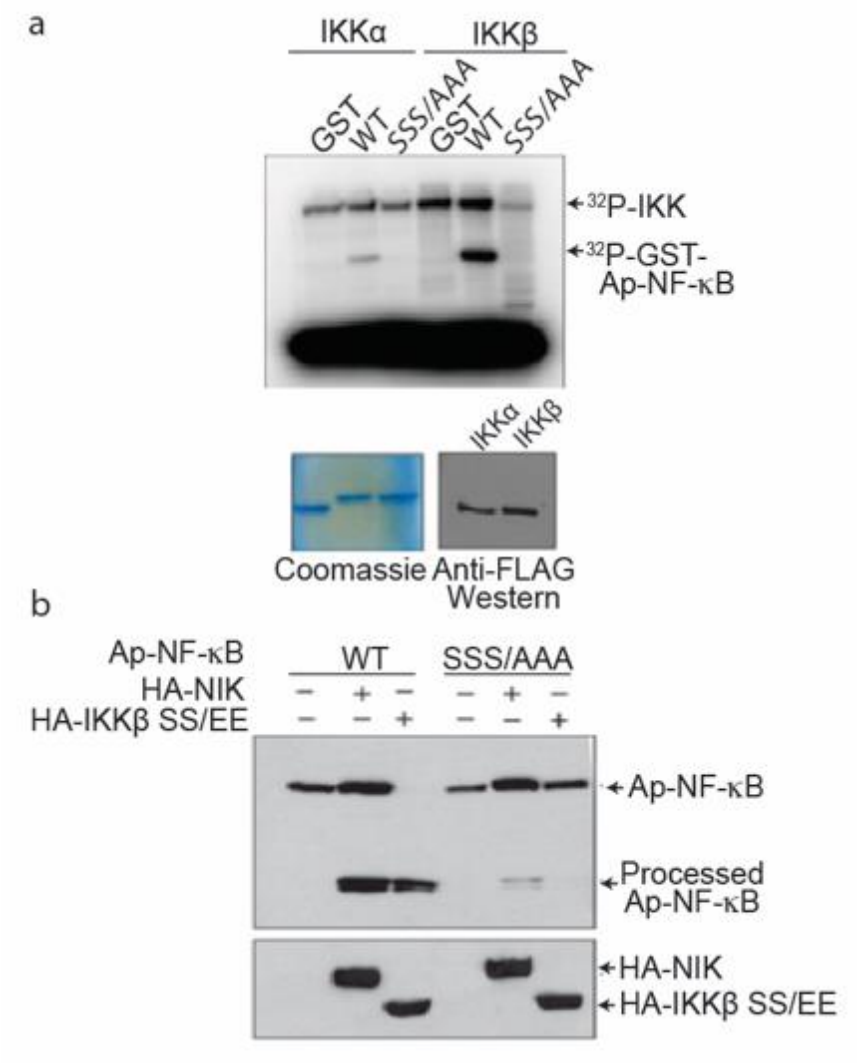

Figure 3.7 Expression of Ap-NF-κB in Aiptasia

Anti-Ap-NF-κB Western blotting was performed on lysates of 293 cells transfected with vector alone (-) or pcDNA-Ap-NF-κB or with lysates from symbiotic Aiptasia anemones (Aiptasia). The full-length (Ap-NF-κB) and processed forms of Ap-NF-κB are indicated to the right. The only bands seen on the film are shown. ns, non-specific band.

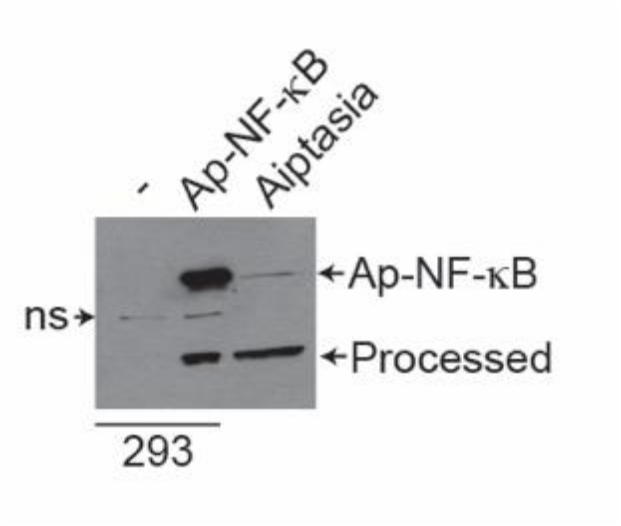

Figure 3.8 Increased levels and activity of Ap-NF-κB in bleached anemones

(a) Aiptasia were maintained in the symbiotic state or rendered aposymbiotic by treatment with menthol, and were then imaged by light microscopy (top) or fluorescence microscopy. In the bottom image, symbionts fluoresce red due to chlorophyll autofluorescence. (b) qPCR using primers against *B. minutum* 28S rRNA was performed on Aiptasia treated as indicated. *B. minutum* 28S rRNA levels are relative to the amount in symbiotic control anemones (100). n=3. Statistical significance compared to sym determined using an unpaired t-test: *** p<_0.001. (Experiment performed by Nicole Carter.) (c) Aiptasia extracts (symbiotic, heat-bleached or menthol-bleached) were analyzed by anti-Ap-NF-κB Western blotting. The relative amount of Ap-NF-κB protein was determined by band quantitation using ImageJ on Western blots of three biological replicates per group, and values were normalized to the amount of β-tubulin in each sample. Statistical significance of the increases in Ap-NF-κB in aposymbiotic animals as compared to those in symbiotic anemones was determined using an unpaired t-test: * $p<0.05$. The Ap-NF-κB bands were detected by anti-Ap-NF-κB Western blotting. β-tubulin was detected following stripping of the primary anti-Ap-NF-κB Western blot. (d) Relative amounts of Ap-NF-κB mRNA were determined by qPCR of RNA from symbiotic and menthol-bleached Aiptasia. Values are relative to the amount of NF-κB mRNA in control symbiotic anemones (1.0). Sym n=6, apo n=3. Statistical significance compared to sym was determined using an unpaired t-test: * $p<0.05$. (Experiment performed by Nicole Carter.) (e) An NF-κB-site EMSA was performed using extracts from symbiotic (SYM) and menthol-bleached (APO) Aiptasia. Δ427 indicates that

extracts from 293 cells transfected with pcDNA-FLAG-Ap-NF-κBΔ427 were used. Supershifts were performed with Ap-NF-κB antiserum (Ab) preimmune serum or no antiserum (-). The relevant portion of the image containing the NF-κB-DNA complex (NF-κB) or the supershifted (SS) complex is shown. (f) Aiptasia made aposymbiotic by heat stress have increased NF-κB DNA-binding activity as compared to symbiotic Aiptasia. Symbiotic anemones were heat shocked (at 32°C) for 6 days. Animal lysates were made and used in an EMSA. Two animals were used for each condition. The position of the Ap-NFκB-DNA complex was determined by co-migration with a complex generated from 293 cells transfected with a pcDNA-FLAG-Ap-NF-κBΔ427 expression plasmid. Where indicated, supershifts (SS) were performed with Ap-NF-κB antiserum (Ab) or pre-immune serum. The free-probe is shown at the bottom of the image. (g) Aiptasia made aposymbiotic by cold stress have increased NF-κB DNA-binding activity as compared to symbiotic Aiptasia**.** Symbiotic anemones were cold shocked (at 4ºC) for 6 h twice a week for six weeks with animals kept in the dark for the entire period. Animal lysates were made and used in an EMSA and two animals were used for each condition. The position of the Ap-NF-κB-DNA complex was determined by co-migration with an Nv-NF-κB-DINA complex generated from 293 cells transfected with a pcDNA-Nv-NF-κB expression plasmid. (Cold shocking of anemones was done by Camerron Crowder.) (h) Immunohistochemistry analysis of whole-body sections from symbiotic and aposymbiotic (heat- and menthol-threated) anemones. 20 μm frozen sections were stained with Ap-NF-κB primary antiserum and Alex Fluor 488-conjugated secondary antiserum. Ap-NF-κB staining (green); DAPI staining (blue); *B. minutum* cells (red,

autofluorescence). Top images were taken at 4X, middle images at 40X (scale bar: 20 μm). e, epidermis; g, gastrodermis. The graph (bottom, left) shows quantitation using ImageJ of relative NF-κB puncta in three different sections of tentacles for each type of anemone. Statistical significance compared to Sym was determined using an unpaired t-test: * $p<0.05$. The bottom right panels are high magnification images showing that NF-κB staining (A488) coincides with nuclear DAPI staining in anemone sections. Scale bar: 2 μm.

Figure 3.8 Increased levels and activity of Ap-NF-κB in bleached anemones

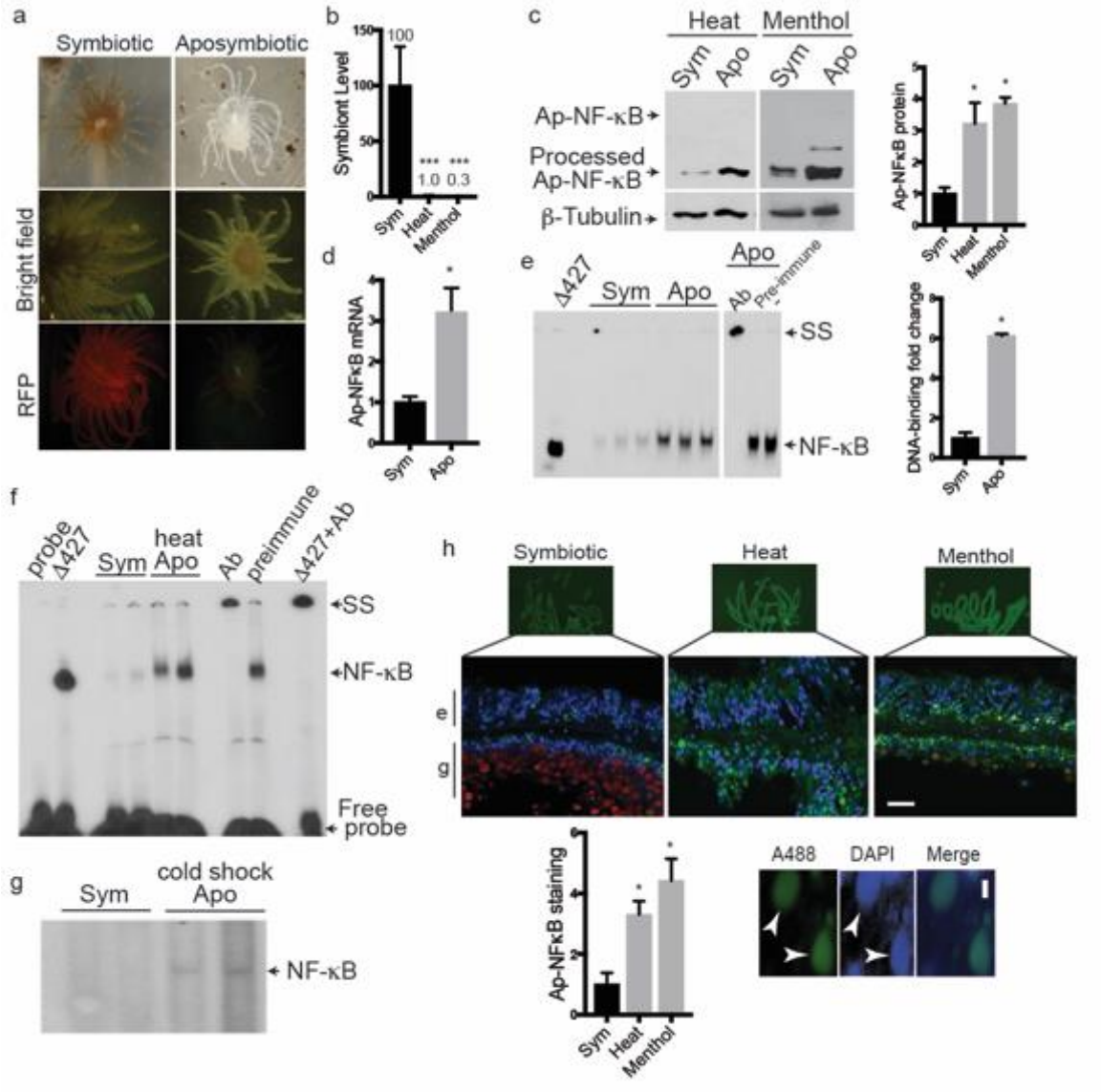

Figure 3.9 Increased expression of NF-κB protein following loss of symbiosis in adult Aiptasia

(a) qPCR of *B. minutum* 28S rRNA was performed on RNA from anemones collected at the indicated time-points during or after menthol treatment. Anemones were incubated with menthol on D1-D3 and were placed in fresh ASW from D4-D14. *B. minutum* 28S rRNA levels are relative to the amount of 28S rRNA in symbiotic animals (100). Sym n=6, all other groups n=3. Statistical significance for each group compared to symbiotic was determined using an unpaired t-test: **p<.01, **** p<.0001. (Experiment performed by Nicole Carter.) (b) Representative anti-Ap-NF-κB Western blot of extracts from symbiotic and menthol-treated Aiptasia extracts prepared from animals treated as in (a). Shown is the portion of the gel containing the processed form of Ap-NF-κB. At this exposure, the much weaker full-length form of Ap-NF-κB was not seen (e.g., see Figure 3.7). The filter was then stripped and reprobed for β-tubulin. Quantitation (bottom) is based on the relative amount of Ap-NF-κB protein from band quantitation using ImageJ of all biological replicates for each group. In each case, Ap-NF-κB values normalized to the amount of β-tubulin in each sample, and values are relative to the amount of NF-κB in the Sym animals (1.0). Statistical significance was determined using an unpaired t-test for each group as compared to the symbiotic control group. * p<0.05. (c) Quantitation of relative Ap-NF-κB protein from symbiotic anemones (1.0) compared to anemones that were maintained in the aposymbiotic for 73 days. NF-κB was quantified from Western blots as described for panel b. Sym n=5, Apo n=3. Statistical significance was determined using an unpaired t-test as above: * p<0.05.

Figure 3.9 Increased expression of NF-κB protein following loss of symbiosis

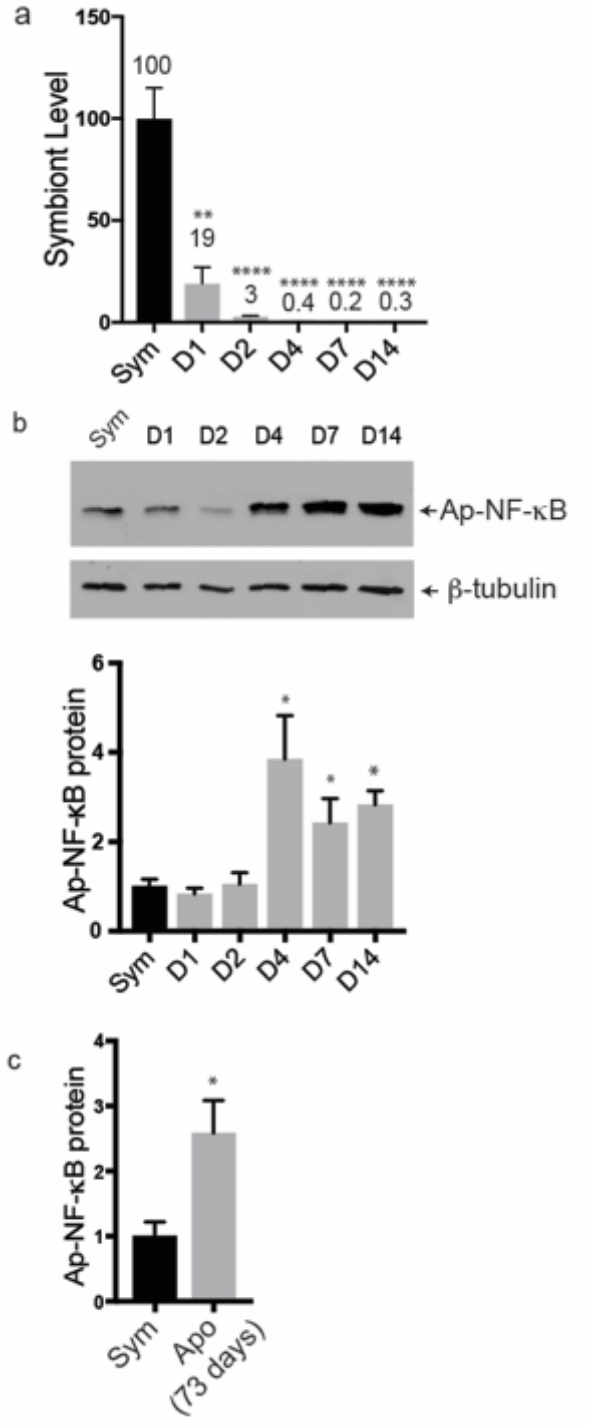

Figure 3.10 Infection with *B. minutum* reduces NF-κB expression in Aiptasia larvae (a) NF-κB protein levels were measured by indirect immunofluorescence of aposymbiotic larvae and larvae infected with *B. minutum* for 5 days. The number of symbiont cells in individual larvae were counted by manually scanning through the z-plane in confocal images. Apo, n=8; Sym, n=6. No symbionts were seen in Apo larvae. (Larval infections with symbionts were performed by Phillip Cleves.) (b) Ap-NF-κB fluorescence in Apo and Sym Aiptasia larvae was quantified using Corrected Total Cell Fluorescence (CTCF) of confocal images measured using ImageJ. Values are relative to the CTCF value of Apo larvae (100). Five larvae were quantified for each group. ***= p<.0001. (c) Representative immunofluorescence images of naïve aposymbiotic larvae and larvae infected with *B. minutum*. NF-κB panels, NF-κB staining alone. Merged panels: Green, NF-κB; Blue, nuclei; Red, *B. minutum* (e.g., white arrows); Magenta, α-tubulin.

Figure 3.10 Infection with *B. minutum* reduces NF-κB expression in Aiptasia larvae

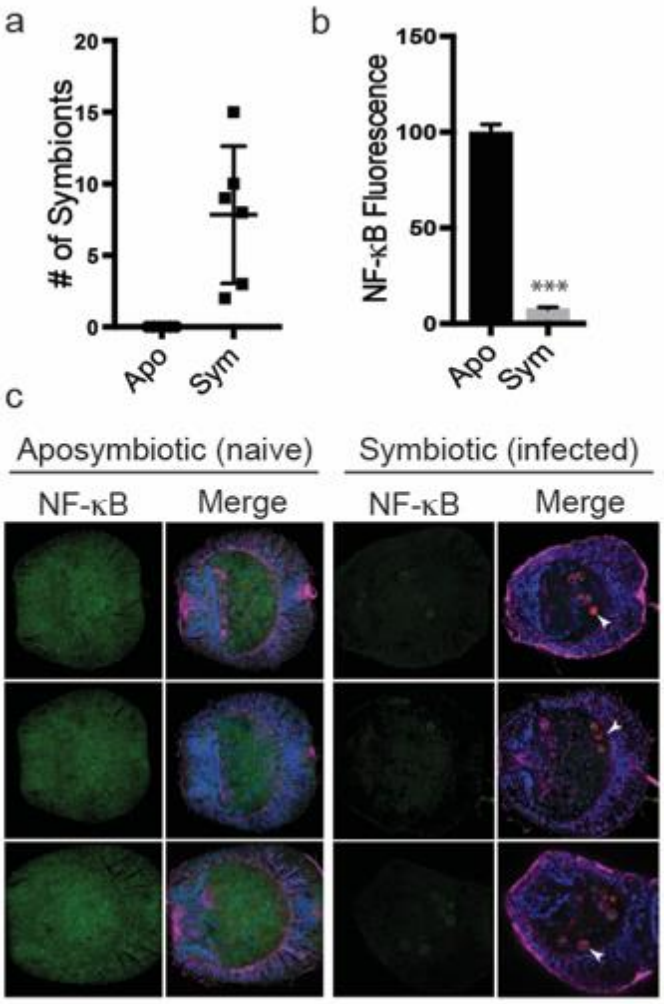

CHAPTER FOUR

INCREASED NF-κB EXPRESSION IS CORRELATED WITH RESISTANCE TO PATHOGEN INFECTION IN THE SEA ANEMONE AIPTASIA AND RESILIENCE TO THERMAL STRESS IN THE CORAL *POCILLOPORA DAMICORNIS*

4.1 Introduction

Previous studies have implicated host immunity as having a role in the establishment and disruption of cnidarian symbiosis (Mansfield and Gilmore, 2019; Palmer, 2018; Traylor-Knowles and Connelly, 2017). In this chapter, possible roles for transcription factor NF-κB in the establishment and/or loss of symbiosis in *Exaiptasia pallida* (Aiptasia) and loss of symbiosis in the coral *Pocillopora damicornis* are investigated. Specifically, the abilities of native and non-native Symbiodiniaceae species to affect NF-κB expression during the establishment of symbiosis in Aiptasia larvae are compared. In addition, because of reports of a role for transforming growth factor β in immune suppression in mammals (Denney et al. 2017) and cnidarians (Berthelier et al. 2017, Detournay et al. 2012), the effect of treatment of Aiptasia larvae with transforming growth factor β on NF-κB expression was determined. Given the results in Chapter Three showing that aposymbiotic Aiptasia have increased NF-κB levels and activity and that NF-κB has a conserved role in immunity across many phyla, we tested the hypothesis that aposymbiotic (high NF-κB) Aiptasia would have increased survival following *Serratia marcescens* infection as compared to symbiotic (low NF-κB) Aiptasia. Furthermore, NF-

κB levels were assessed in three *P. damicornis* colonies of which one demonstrated decreased thermal bleaching in a common garden heat stress experiment when compared to two isolates that bleached more readily. Finally, bioinformatic analyses were undertaken to identify putative NF-κB target genes in Aiptasia. Overall, the experiments in this chapter suggest that modulation of NF-κB is important for symbiosis establishment, pathogen resistance, and sensitivity to bleaching.

4.2 The symbiont *Breviolum minutum* downregulates NF-κB expression in Aiptasia larvae, whereas non-establishing Symbiodiniaceae, *Symbiodinium* sp. and *Effrenium voratum*, do not

To determine whether Symbiodiniaceae with differing abilities to establish symbiosis with Aiptasia also have different effects on host NF-κB expression, we incubated Aiptasia larvae with three Symbiodiniaceae species: the natural symbiotic partner *B. minutum* (formerly clade B01) and two non-establishing Symbiodiniaceae species, *Symbiodinium* sp. (formerly clade A03) and *Effrenium voratum* (formerly clade E01) (Hambleton et al. 2014, Wolfowicz et al. 2016). For these experiments naïve aposymbiotic larvae (strain CC7xPLFU) at five days post-fertilization (dpf) were inoculated with Symbiodiniaceae for five days. Larvae were then fixed, and NF-κB expression levels were quantified by immunohistochemistry of stained larvae and the number of Symbiodiniaceae cells in the gastric cavity were manually counted by scanning the Z-plane.

We found that 97.3% of larvae took up *B. minutum* into the gastric cavity whereas 57.5% and 3% of larvae took up *E. voratum* and *Symbiodinium* sp., respectively (Figure 4.1a). No Symbiodiniaceae were detected in control naïve aposymbiotic larvae (Figure 4.1a). These results demonstrate that Aiptasia larvae establish symbiosis with *B. minutum* more efficiently than *Symbiodinium* sp. ($n=29$, $p<0.0001$) and *E. voratum* ($n=29$, $p=0.001$; Figure 4.1a). Furthermore, larvae that took up *B. minutum* contained 6.4 algal cells per larva whereas larvae that took up *E. voratum* contained 2.4 algal cells per larva ($n=19$, $p=0.007$; Figure 4.1b). *Symbiodinium* sp. were rarely observed in larvae. Together, these results demonstrate that Aiptasia larvae take up *B. minutum* more efficiently and in higher cell numbers than they take up *Symbiodinium* sp. and *E. voratum*.

NF-κB expression in fixed and stained larvae was measured by corrected total cell fluorescence (CTCF) following immunofluorescent staining for NF-κB. As compared to aposymbiotic larvae, NF-κB expression was decreased by 56% in larvae that took up preferred *B. minutum* cells into their gastric cavity ($n=13$, $p<0.0001$), whereas larvae that took up non-preferred *E. voratum* cells showed no significant difference in NF-κB staining as compared to aposymbiotic controls (Figure 4.1c-d). NF-κB expression was not significantly different in larvae incubated with *Symbiodinium* sp., which is poorly taken up by Aiptasia larvae, as compared to non-infected aposymbiotic larvae (Figure 4.1b-c).

We next compared symbiont cell density and NF-κB expression levels in larvae that took up *B. minutum* or *E. voratum*. That is, Symbiodiniaceae cell counts and NF-κB

CTCF levels were plotted and analyzed by linear regression. This analysis showed that there is not a statistically significant correlation between Symbiodiniaceae cell number in the gastric cavity and NF-κB fluorescence levels for *B. minutum* (n=13, R^2=0.24, p=0.087; Figure 4.1e) or *E. voratum* (n=13, R^2=0.17, p=0.16) but for a given number of Symbiodiniaceae cells, larvae that took up *B. minutum* had lower NF-κB fluorescence levels than larvae with the same number of *E. voratum* cells (Figure 4.1e).

4.3 Treatment of aposymbiotic Aiptasia larvae with human TGFβ1 results in decreased NF-κB mRNA and protein expression

Previous data have suggested a role for the transforming growth factor β (TGFβ) cytokine in suppressing immunity in Aiptasia (Detournay et al. 2012) and in promoting the onset of symbiosis in larvae of the coral *Fungia scutaria* (Berthelier et al. 2017). Therefore, we hypothesized that the immune-suppressing activity of TGFβ might be due to effects on NF-κB. To determine whether TGFβ can affect NF-κB expression in Aiptasia, naïve aposymbiotic larvae were incubated with human TGFβ1 overnight, and then NF-κB mRNA and protein expression were quantified by qPCR and immunohistochemistry CTCF of individual larvae, respectively. Treatment with human TGFβ1 reduced NF-κB mRNA by 64% in treated larvae as compared to control untreated larvae ($p<0.05$; Figure 4.2a). Similarly, human TGFβ1 treatment reduced NF-κB protein staining by 31% (n=40, $p<0.0001$; Figure 4.2b-c). These results demonstrate that incubation with human TGFβ1 decreases NF-κB mRNA and protein levels in Aiptasia.

4.4 Aiptasia with high NF-κB expression show increased survival following pathogen infection as compared to anemones with low NF-κB expression

Given that NF-κB plays an important role in innate immunity in many metazoans (Gilmore and Wolenski 2012), we hypothesized that NF-κB also has an immunity role in Aiptasia. To test this hypothesis, we first compared NF-κB DNA-binding activity in lysates of symbiotic and aposymbiotic Aiptasia (strain CC7) using an electrophoretic mobility shift assay (EMSA). Consistent with our previous results using strain H2 anemones (Mansfield et al. 2017), long-term aposymbiotic CC7 anemones had 3.2-fold more NF-κB DNA-binding activity than symbiotic CC7 anemones (NF-κB-DNA complex band depicted by arrow) (Figure 4.3a-b).

To compare the immunocompetence of symbiotic (low NF-κB) and aposymbiotic (high NF-κB) Aiptasia, adult anemones of four different strains (H2, VW9, CC7, and wild [purchased from Carolina Biologicals]) were challenged with. *S. marcescens*, a bacterial pathogen that has been shown to cause white pox disease in wild coral (Sutherland et al. 2011) and lethality in Aiptasia (Krediet et al. 2014). In our experiments, anemones were incubated with ~1.90 x10^8 *S. marcescens* cells/ml in 32 ppt artificial seawater (ASW) for seven days. Anemones were then switched to fresh ASW (i.e., in the absence of bacteria) to allow recovery. Anemone survival at the end of two weeks in fresh ASW was assessed visually, by observing the presence of extended tentacles and anemone movement after touching with a plastic Pasteur pipette (Figure 4.3c). All infected anemones were compared to non-infected Aiptasia controls. Each anemone strain demonstrated a trend of increased survival of aposymbiotic infected anemones as

compared to symbiotic anemones (Figure 4.3d, left). When the results from infections of all anemone strains were summed, 95% of aposymbiotic Aiptasia survived bacterial infection, whereas only ~17% of symbiotic Aiptasia survived ($n=18$, $p<0.0001$; Figure 4.3d, right). This experiment shows that aposymbiotic Aiptasia are more likely to survive *S. marcescens* bacterial infection as compared to symbiotic anemones. These results also demonstrate a correlation between increased NF-κB levels and an increased ability to survive pathogen challenge, which suggests that NF-κB directs immune programs that make Aiptasia more resistant to bacterial challenge.

Due to conflicting reports of the role that host nutrition plays in immunity to pathogens, we were interested in determining whether nutritional state affects the ability of aposymbiotic Aiptasia to survive pathogen infection. For these experiments, aposymbiotic H2 Aiptasia were starved (of *Artemia* brine shrimp) for two weeks prior to assaying them for susceptibility to *S. marcescens*-induced lethality. One hundred percent of fed aposymbiotic anemones survived bacterial infection, whereas only 16.5% of starved aposymbiotic anemones survived ($n=6$, $p=0.037$; Figure 4.3e).

Taken together, the results in this section show a correlation between NF-κB expression and susceptibility to pathogen-induced disease. High NF-κB levels, in the absence of symbiosis, are correlated with increased survivability, as compared to symbiotic Aiptasia with low NF-κB levels.

4.5 High NF-κB expression is correlated with hosting *Durusdinium* symbionts and is associated with increased resistance to temperature-induced bleaching in the coral *Pocillopora damicornis*

Because of the associations described above between NF-κB levels and various physiological states in Aiptasia, we next determined whether NF-κB expression levels vary with bleaching outcomes in a coral. For these experiments, three *Pocillopora damicornis* genotypes (1, 2, and 3) were induced to bleach by increasing their temperature in the lab from 28 °C to 32 °C. The extent of bleaching was determined by comparing the color intensity of control and heat-treated coral tissue at the beginning and end of the experiment (Figure 4.4a-b). We found that these three isolates differed in their susceptibility to bleaching. Namely, heat-treated *P. damicornis* isolate 3 showed significantly less bleaching than isolates 1 and 2 (Figure 4.a-b).

In an effort to understand the molecular basis for the observed differences in bleaching among these three coral isolates (i.e., 1 and 2 vs 3), we first determined the composition of Symbiodiniaceae in each *P. damicornis* genotype using metabarcoding of the ITS2 locus. Heat-sensitive isolates 1 and 2 hosted mostly *Cladocopium* species, whereas heat-resistant isolate 3 hosted primarily *Durusdinium* species (Figure 4.4c). These results suggest that hosting *Durusdinium* is correlated with increased resistance to bleaching in *P. damicornis*, a finding that is consistent with a previous report in the coral *Acropora hyacinthus* (Barshis et al. 2015, Berkelmans and van Oppen 2006, Jones et al. 2008).

NF-κB expression was also quantified for control, non-heated *P. damicornis* isolates 1, 2, and 3. Non-heated control *P. damicornis* fragments were collected at the end of both experimental trials, and lysates were prepared and subjected to NF-κB Western blotting, using our custom-made Aiptasia NF-κB antiserum that cross-reacts with NF-κB from *P. damicornis* (Figure 4.4d). NF-κB band intensities were normalized to α-tubulin levels on the same blots. The bleaching resistant isolate 3 (n=6) showed approximately 30-fold more NF-κB as compared to isolates 1 (n=5, $p=0.015$) and 2 (n=6, $p<0.005$; Figure 4.4e-f). Thus, high NF-κB expression is correlated with bleaching resistance among these three *P. damicornis* isolates.

Because *P. damicornis* isolate 3 had high NF-κB levels and also hosted *Durusdinium* species of Symbiodiniaceae, it raised the possibility that the presence of *Durusdinium* was correlated with increased NF-κB expression. Because we could not compare NF-κB in identical *P. damicornis* genotypes infected with different Symbiodiniaceae, we compared NF-κB expression levels from genetically identical Aiptasia adults (strain CC7) that were stably infected with *Durusdinium, B. minutum,* or non-infected aposymbiotic anemones. We found that adult Aiptasia colonized with *Durusdinium* had NF-κB levels similar to aposymbiotic controls. However, Aiptasia hosting *B. minutum* have reduced NF-κB expression as compared to aposymbiotic Aiptasia, which is consistent with our results above (Figure 4.4a-b) and our previously reported results (Mansfield et al. 2017). This result indicates that, in Aiptasia, hosting *Durusdinium* does not reduce NF-κB expression levels whereas hosting *B. minutum* does (Figure 4.4g). Thus, the increased NF-κB expression levels in *P. damicornis* genotypes 3

vs. genotypes 1 and 2 may be due to the genera of symbiont being hosted by *P. damicornis* and not due to inherent differences in NF-κB expression among the genotypes.

4.6 Putative NF-κB binding sites are significantly enriched in upregulated inflammation genes in aposymbiotic Aiptasia

The data above suggest a role for NF-κB activity in pathogen protection in Aiptasia and bleaching resistance in *P. damicornis*. Although increased NF-κB expression and activity are correlated with resistance to mortality after bacterial infection and resistance to heat-induced bleached in these cnidarians, how NF-κB might be affecting these processes is not known. Given that NF-κB is a transcription factor that can activate reporter gene expression and is constitutively located in the nucleus of cells in both symbiotic and aposymbiotic anemones (Mansfield et al. 2017), it is likely that NF-κB regulates transcription to carry out its biological effects. Therefore, we sought to identify genes that may be direct targets of NF-κB in Aiptasia. Related to these studies, we have shown that Aiptasia NF-κB and human NF-κB proteins have highly similar DNA target site preferences (Mansfield et al. 2017). To identify predicted target genes of Aiptasia NF-κB, we analyzed regions of the genome that were one kb upstream of the transcription start site (to estimate probable promoter regions) of a subset of genes dysregulated (up- and down-regulated) in aposymbiotic Aiptasia as compared to symbiotic Aiptasia housing *Symbiodinium* sp. symbionts (Lehnert et al. 2014). These dysregulated genes are predicted to be involved in either oxidative stress response, inflammation or apoptosis

from a published RNA-seq dataset (Lehnert et al. 2014). Their putative promoter sequences were scanned for predicted NF-κB DNA-binding sites (Appendix I) using the top 950 sequences identified to bind bacterially expressed Aiptasia NF-κB in our previously published protein binding microarray (PBM) experiments (Mansfield et al. 2017) (Appendix II). The percentage of these sequences with putative NF-κB binding sites was quantified for upregulated and downregulated genes in each category. This analysis showed that 100% of upregulated inflammation gene promoters (n=6) contain predicted NF-κB binding sites, whereas only 20% of downregulated gene promoters (n=5) contain NF-κB sites ($p=0.015$; Figure 4.5) suggesting that NF-κB turns on transcription of these inflammation genes in aposymbiotic Aiptasia. The percentage of promoter sequences with predicted NF-κB binding sites was not significantly different between up- and downregulated genes involved in oxidative stress response and in apoptosis. However, there was a trend for oxidative stress response genes to have NF-κB binding sites in the promoters of upregulated genes as compared to downregulated, whereas apoptosis genes showed a trend for NF-κB binding sites in downregulated gene promoter regions as compared to upregulated. This result demonstrates that in Aiptasia, putative NF-κB DNA-binding sites are significantly more abundant in promoter regions of upregulated inflammation genes as compared to downregulated genes and a similar trend was observed in the promoter regions upstream of oxidative stress response genes. However, this correlation was not observed in apoptosis genes (Figure 4.5).

4.7 Chapter 4 summary

Immunity plays a role in regulating many symbiotic partnerships (Burns et al. 2017, Chu and Mazmanian 2013, McFall-Ngai et al. 2013, Nyholm and Graf 2012, Zientz et al. 2005). To investigate a similar role for immunity in the Cnidarian-Symbiodiniaceae mutualism, transcription factor NF-κB was characterized in two symbiotic cnidarians. Overall, this chapter demonstrates the specificity of host-Symbiodiniaceae interactions and NF-κB downregulation in Aiptasia and implicates TGFβ signaling as playing a role in suppressing NF-κB expression during the establishment of symbiosis. Our work demonstrates a positive correlation between high NF-κB expression and resistance to pathogen-induced disease in Aiptasia as well as resistance to heat stress in the coral *P. damicornis* hosting *Durusdinium* symbionts.

Figure 4.1 The symbiont *Breviolum minutum* downregulates NF-κB expression in Aiptasia larvae, whereas two non-establishing Symbiodiniaceae, *Symbiodinium* sp. and *Effrenium voratum*, do not

(a) NF-κB protein levels were measured by immunohistochemistry of whole larvae incubated with either *B. minutum, Symbiodinium* sp., *E. voratum*, or non-treated. (Larvae incubations with symbionts was performed by Phillip A. Cleves, Stanford University.) The percentage of larvae with Symbiodiniaceae cells in the gastric cavity were visually counted over three experimental trials by scanning through the Z-plane using confocal imaging. Each data point is an experimental trial. Total n=29. (b) The number of Symbiodiniaceae cells in larvae with either *B. minutum* or *E. voratum* in the gastric cavity were counted as above and then averaged. n=19. (c). Aiptasia NF-κB fluorescence in larvae was quantified using Corrected Total Cell Fluorescence (CTCF) of confocal images measured using ImageJ. Values represent the averages of 13 larvae for each group and are relative to the CTCF value of aposymbiotic larvae (100). n=13 for each group.*= $p<0.0001$. (d) Representative immunofluorescence images of larvae from each infection group. Panels show merged green, NF-κB; red, Symbiodiniaceae; white, α-tubulin. (e) Linear regression analysis was used to correlate the number of Symbiodiniaceae cells with NF-κB CTCF values for *B. minutum* uptake (n=13, $R^2=0.24$, p=0.087) and *E. voratum* uptake (n=13, $R^2=0.17$, p=0.16) in larvae.

Figure 4.1 The symbiont *Breviolum minutum* downregulates NF-κB expression in Aiptasia larvae, whereas two non-establishing Symbiodiniaceae species, *Symbiodinium* sp. and *Effrenium voratum*, do not

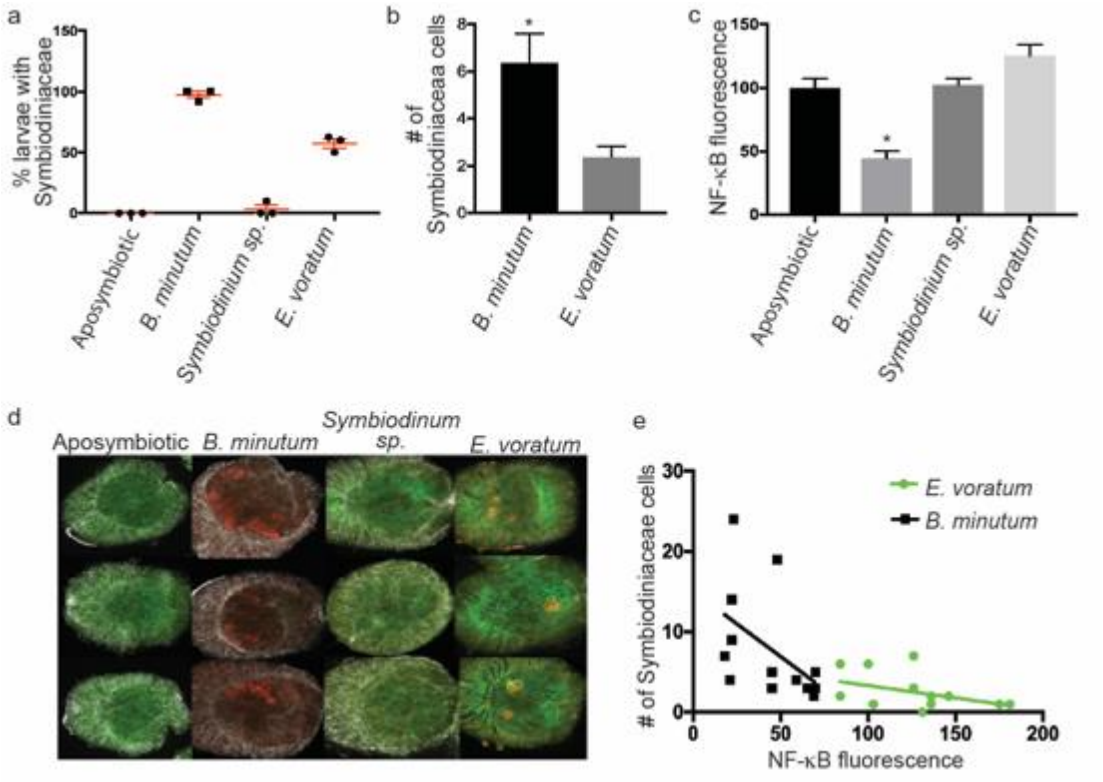

Figure 4.2 Treatment of aposymbiotic Aiptasia larvae with human TGFβ1 ligand results in decreased NF-κB RNA and protein expression

(a) Aposymbiotic Aiptasia larvae were incubated with 200 ng/ml human TGFβ1 in artificial sea water 18 h at room temperature. NF-κB transcript levels were measured by qPCR of cDNA from control and TGFβ-treated larvae. RNA was extracted from 200 pooled larvae per group. cDNA levels were measured for NF-κB and the L10 housekeeping. Each data point is an experimental trial. Statistical significance was determined by unpaired t-test. (b) Control and TGFβ-treated larvae were fixed and NF-κB protein staining levels were measured via immunohistochemistry. NF-κB fluorescence was quantified using Corrected Total Cell Fluorescence (CTCF) of confocal images taken at the same exposure and measured using ImageJ. Values are relative to the CTCF value of control larvae (100). Statistical significance was determined by unpaired t-test ($n=40$, $p<0.0001$). (c) Representative immunofluorescence images of control and TGFβ-treated larvae. Green, NF-κB. Merge of green, NF-κB; yellow, α-tubulin; blue, DAPI.

Figure 4.2 Treatment of aposymbiotic Aiptasia larvae with human TGFβ1 ligand results in decreased NF-κB RNA and protein expression

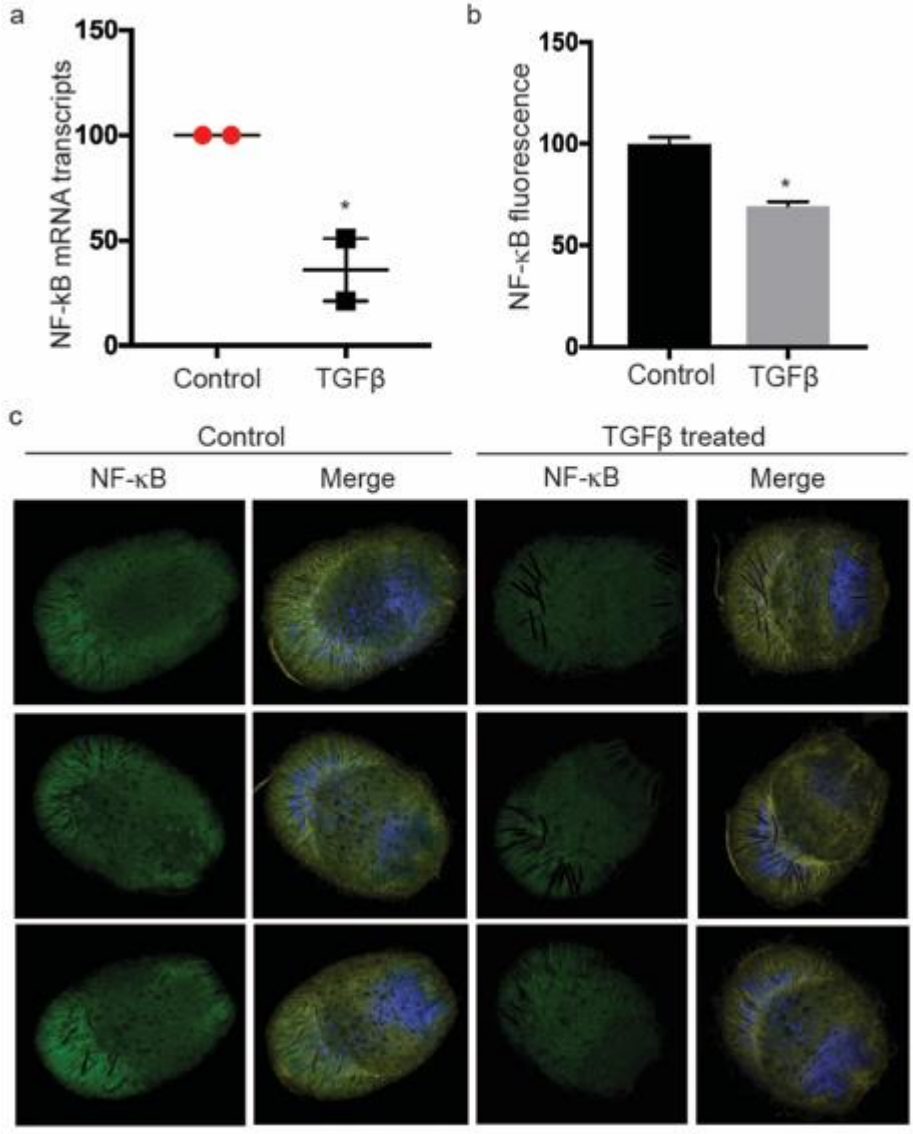

Figure 4.3 Aiptasia with high NF-κB expression show increased survival following pathogen infection as compared to anemones with low NF-κB expression

(a) NF-κB DNA-binding activity was measured by EMSA using lysates of symbiotic (sym) and aposymbiotic (apo) adult CC7 Aiptasia. Anemones had been maintained aposymbiotic for over three years at the time of the experiment. Each lane was loaded with equal amounts of protein for all biological replicates, n=3. The NF-κB DNA-binding complex is designated by the arrow. (b) The bands corresponding to NF-κB DNA-binding bands were quantified using ImageJ. Values were averaged per group and were normalized to symbiotic controls (1.0). (c) Anemones were incubated with *Serratia marcescens* for one week and were then allowed to recover in ASW for two weeks at which time viability was assessed. Representative images of control, non-infected anemones (left), infected anemones after the two-week recovery period (right), an anemone that did not survive infection (top, right) and an anemone that did survive (bottom, right). (d) The chart (left) indicates the number of anemones that survived *S. marcescens* infection in the indicated Aiptasia strains (H2, VW9, CC7, Wild [Carolina Biologicals]). The summary graph (right) combines the experimental trials from the chart on the left. Each data point is an individual experimental trial using three anemone replicates. Statistical significance was determined using unpaired t-test ($n=18$, $p<0.0001$). (e) Aposymbiotic H2 anemones were starved of *Artemia* for two weeks and infected with *S. marcescens* as in (c). Survivability was quantified as in (d) and compared to fed aposymbiotic anemones. Each data point is an experimental trial with n=3 anemones. Statistical significance was determined using an unpaired t-test ($n=6$, $p<0.037$).

Figure 4.3 Aiptasia with high NF-κB expression show increased survival following pathogen infection as compared to anemones with low NF-κB expression

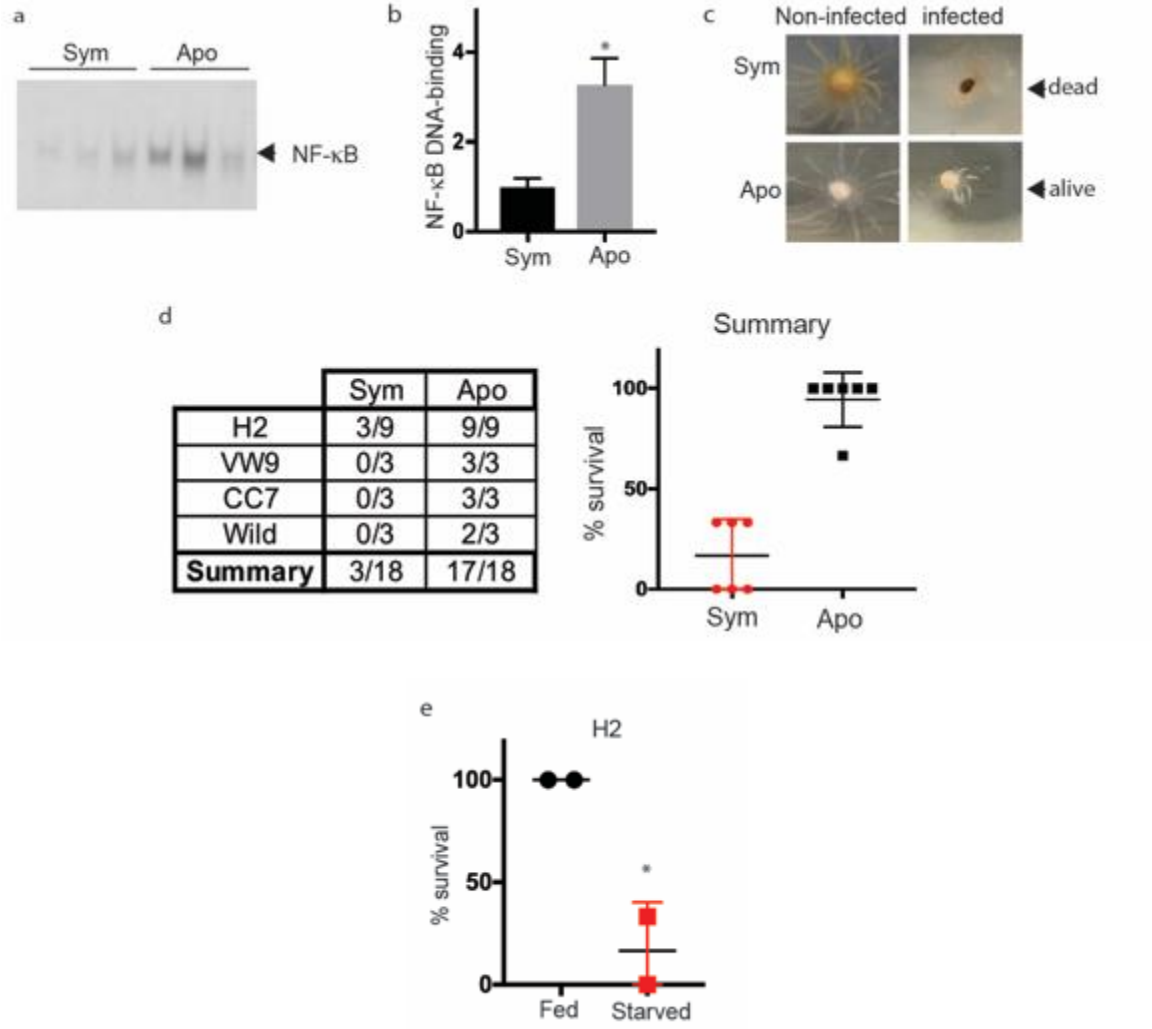

	Sym	Apo
H2	3/9	9/9
VW9	0/3	3/3
CC7	0/3	3/3
Wild	0/3	2/3
Summary	3/18	17/18

Figure 4.4 High NF-κB expression is correlated with hosting *Durusdinium* symbionts and is correlated with increased resistance to temperature-induced bleaching in the coral *Pocillopora damicornis*

(a) Three independent colonies of *P. damicornis* (1, 2, 3) kept in common garden conditions were fragmented and randomly assigned to six tanks such that each colony isolate was represented once in each of three replicate tanks per treatment. For each experimental trial, six fragments were obtained from each of three genotypes for a total of 18 fragments (n=9 per treatment group). Coral fragments were acclimated to tank conditions for two days at 28 °C. Target temperature for thermal stress treatment (32 °C) was achieved after two days of ramping at 2 °C per day. Heat treatment lasted for five days (trial 1) or seven days (trial 2) until fragments in heat stress treatments started to present bleached phenotypes. Representative images of control and heat treated coral at the end of trial 1. (b) Quantification of bleaching outcome among genotypes 1-3 as determined by colorimetric assay. Y-axis represents arbitrary units of final color intensity. (Color analysis was performed by Nicola Kriefall.) (c) Algal symbionts were genotyped via metabarcoding of ITS2. (Metabarcoding was performed by Nicola Kriefall and Dr. Sarah Davies). (d) A symbiotic branch of *P. damicornis* and a symbiotic Aiptasia anemone were lysed and subjected to anti-NF-κB Western blotting to detect full length and processed NF-κB bands. (e) Control samples were lysed and samples were subjected to anti-NF-κB Western blotting. The representative image shows NF-κB (top) and corresponding α-tubulin (bottom) levels control temperature coral from Trial 1. (f) NF-κB bands were quantified in ImageJ and intensities were normalized to α-tubulin band

intensity values. Values are the averages of three biological replicates from each of two experimental trials (n=6 except for genotype 1 which had n=5 due to an NF-κB band below detection limits in one sample). Values are relative to genotype 2 (the lowest expressing genotype, i.e., 1.0), and statistical significance was determined using an unpaired t-test (genotype 1, no significant difference; genotype 3, p=0.005). (g) Extracts from adult CC7 Aiptasia stably hosting Symbiodiniaceae *B. minutum* (B), *Durusdinium sp*. (D), and no symbiont (Apo) were subjected to anti-NF-κB Western blotting as in (e). Lanes represent extracts from individual anemones. All lanes were ran on the same blot, non-applicable lanes were cropped from the image.

Figure 4.4 High NF-κB expression is correlated with hosting *Durusdinium* symbionts and is correlated with increased resistance to temperature-induced bleaching in the coral *Pocillopora damicornis*

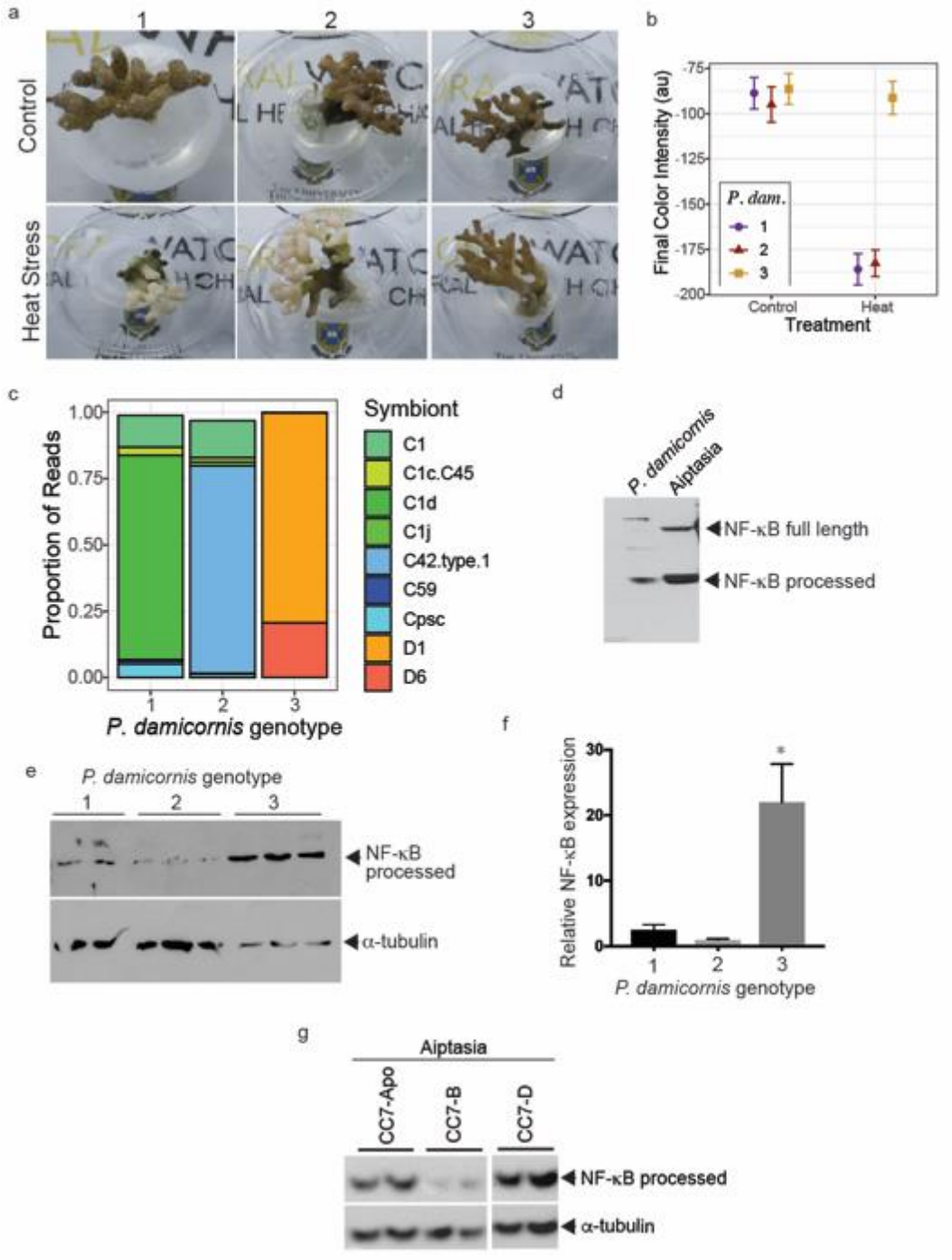

Figure 4.5. Putative NF-κB binding sites are enriched in genes upregulated in aposymbiotic Aiptasia

One kb promoter regions of a subset of dysregulated genes predicted to be involved in oxidative stress response, immunity, and apoptosis were compiled from a published RNA-seq dataset (Lehnert et al. 2014) (Appendix II). Promoter regions were scanned for predicted NF-κB DNA-binding sites using the top 25% of sequences (950 sites) (Appendix I) assayed to bind purified Aiptasia NF-κB in a previously published protein binding microarray (PBM) dataset (Mansfield et al. 2017). The percentage of genes with putative NF-κB binding sites was quantified for upregulated and downregulated immune-related genes in aposymbiotic Aiptasia. Statistical significance was determined by a two-tailed Fisher's exact test. The number of genes analyzed in each group is displayed within the graph bars. (Promoter scan performed by Dr. Trevor Siggers).

Figure 4.5. Putative NF-κB binding sites are significantly enriched in upregulated inflammation and oxidative stress response genes in aposymbiotic Aiptasia

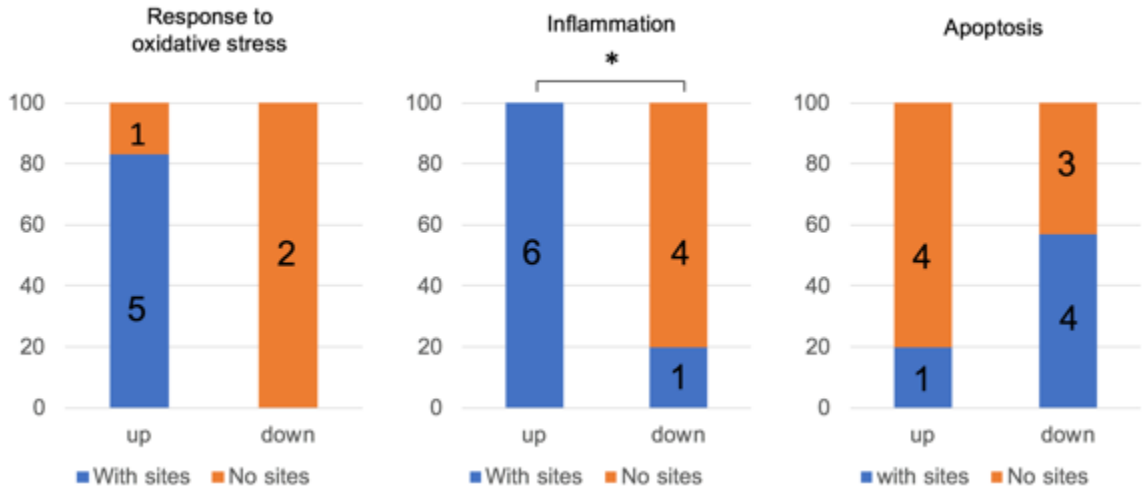

CHAPTER FIVE

DISCUSSION

5.1 Summary

The research described in this thesis characterizes transcription factor NF-κB in a sea anemone model of coral bleaching, Aiptasia. Our work demonstrates that NF-κB expression is downregulated by symbiosis and that reduced NF-κB expression is associated with decreased immunity and bleaching resistance in cnidarians. Overall, the results in Chapter Three show that basal NF-κB proteins have DNA-binding specificities and overall structures that are more similar to human NF-κB proteins than to human Rel proteins. Our results suggest that a form of non-canonical NF-κB processing is present in the sea anemone Aiptasia. We show that the Aiptasia NF-κB protein undergoes processing in human cells when human or Aiptasia IKK proteins are overexpressed. Additionally, we correlate NF-κB transcription factor expression and activity with symbiotic status in Aiptasia, demonstrating that NF-κB expression is suppressed by the establishment of symbiosis and is increased by loss of symbiosis. The results of Chapter Four focus on the molecular mechanism of NF-κB downregulation during the establishment of symbiosis, and the implications of reduced NF-κB levels for cnidarian biology. It is shown that NF-κB downregulation is specific to symbiosis onset with Symbiodiniaceae species *Breviolum minutum* and that human TGFß1 lowers NF-κB expression. Additionally we correlated high NF-κB expression with increased survivability to pathogen infection in Aiptasia and increased resistance to heat-induced bleaching in the coral *Pocillopora damicornis*.

5.2 Characterization of the Aiptasia NF-κB protein and processing events

Our results suggest that a form of non-canonical NF-κB processing is present in the sea anemone Aiptasia. We show that basal NF-κB proteins have DNA-binding specificities and overall structures that are more similar to human NF-κB proteins than to human Rel proteins. Moreover, the Aiptasia NF-κB protein undergoes processing in human cells when human or Aiptasia IKK proteins are overexpressed.

Mammals and arthropods have five and two or three Rel/NF-κB proteins, respectively, whereas many basal metazoan or pre-metazoans have a single NF-κB-like protein (Finnerty and Gilmore 2015, Gilmore and Wolenski 2012). Our PBM-based DNA-binding analyses also indicate that invertebrate NF-κB-like proteins (from *Capsaspora*, sponge, anemones, and *Drosophila*) are more similar to human NF-κB p50 and p52 proteins than to c-Rel and p65 proteins (Figure 3.2). Thus, it is almost certain that NF-κB proteins arose first during evolution and later expanded and diversified into the Rel family, consistent with earlier predictions (Huguet et al. 1997).

Our PBM analyses demonstrate that NF-κB DNA-binding site recognition is highly conserved across a great evolutionary distance. That is, there is little difference between the DNA-binding site profiles of human NF-κB p50 and either sponge or anemone NF-κB proteins. Nevertheless, there were two surprising results from our PBM analyses. First, the DNA-binding profile of the *Drosophila* Relish protein is clearly less similar to human p50 than are the DNA-binding profiles of NF-κB proteins of sponges and anemones. Thus, it appears that Relish has diverged more from the ancestral NF-κB protein than have human NF-κBs, suggesting that evolutionary pressure has had more of

an effect on the DNA-binding site specificity of Relish than on NF-κB proteins of sponges and cnidarians. Second, the DNA-binding profiles of the S and C polymorphic NF-κB proteins of *Nematostella* are as different from each other as each is from human p50. This result and the presence of both the S and C NF-κB alleles in natural breeding populations of *Nematostella* (Sullivan et al. 2009, Wolenski et al. 2011a) suggest that a considerable amount of intraspecies flexibility in κB-site binding affinity and preference can still support normal biological activities, at least in *Nematostella*. Nevertheless, as we have previously shown, the S allele appears to be the derived allele and the Nv-NF-κB-S protein has at least two compensating amino acid changes within the RHD that keep its DNA-binding activity within a proper range of κB-site binding (Wolenski et al 2011). Overall, these results suggest that along the main evolutionary branch from anemones to humans there has not been much diversification in NF-κB DNA-binding site preference, and thus differences in biological processes that are controlled by NF-κB proteins presumably arose due to mutations in target gene promoters that created NF-κB binding sites. For example, the derived biological processes (cnidocyte development and dorsal-ventral polarity) that are controlled by *Nematostella* and *Drosophila* NF-κB proteins (Minakhina and Steward 2006, Wolenski et al. 2013) likely came about due to the acquisition of NF-κB binding sites in the regulatory regions of genes required for cnidocyte and embryonic polarity development, respectively.

In the vertebrate non-canonical pathway, the inactive, cytoplasmic NF-κB complex is a p100-RelB heterodimer. The active p52/RelB heterodimer is generated by activation of the upstream kinase NIK that phosphorylates IKKα which then

phosphorylates C-terminal residues of p100 to induce proteasomal processing of p100 to p52. As we show in this thesis, Ap-NF-κB has three C-terminal Ser residues that are similar to those in human p100 (Figure 3.1b) and can be phosphorylated by human and Aiptasia IKKs (Figure 3.5c and 3.6a). Moreover, overexpression of human NIK (and consequent activation of IKKα), human IKKβ, or Ap-IKK in human 293 cells can induce processing of Ap-NF-κB (Figure 3.5d and 3.6b) to essentially the same extent as IKK-mediated phosphorylation has been shown to induce processing of human p100 (Qing et al. 2005, Senftleben et al. 2001). Of note, human IKKβ (required for canonical NF-κB signaling in mammals) induced phosphorylation and processing of Ap-NF-κB to a greater extent than did human IKKα (required for non-canonical NF-κB signaling in mammals) (Figure 3.6b). Furthermore, there is a single IKKα/β homolog in Aiptasia (and other basal animals) (Figure 3.4), suggesting that basal IKKs and their NF-κB substrates have properties that they share with both canonical and non-canonical signaling proteins of mammals. Furthermore, Ap-NF-κB has a glycine-rich region (GRR) between the RHD and the ANK repeat domain, and a similar GRR acts as a stop signal for the proteasome-mediated C-terminal processing of human p100 (Rape and Jentsch 2002). However, there are certain non-canonical pathway proteins that are not found in Aiptasia: namely, there are no known RelB-like proteins (or any Rel-like protein) in Aiptasia (Baumgarten et al. 2015) nor any other basal organism, and we have not been able to identify a NIK-like protein in Aiptasia or any basal organism.

Our results and others suggest that there has been co-evolution of the IKKs and their NF-κB/IκB substrates. For example, the nematode *C. elegans* has neither IKKs nor

NF-κB/IκB proteins. The sponge *Amphimedon queenslandica* has an NF-κB protein without any obvious C-terminal IKK phosphorylation sites (Figure 3.3), and *Amphimedon* lacks an IKKα/β ortholog (Figure 3.4). Moreover, the Relish protein of *Drosophila* lacks a GRR and C-terminal IKK phosphorylation sites, and the single *Drosophila* IKKα/β homolog does not appear to be involved in NF-κB processing or signaling (Minakhina and Steward 2006).

The truncated Ap-NF-κB protein (Δ427) enters the nucleus, binds DNA efficiently, and has intrinsic transactivation activity (Figure 3.1d, 3.5a-b). Thus, the Aiptasia NF-κB pathway appears to consist of a p100-like homodimer and an upstream IKK-like kinase, and activation of the Ap-IKK-like kinase presumably leads to phosphorylation of the Ap-NF-κB C terminus and proteolytic processing. Nevertheless, even though we can promote processing of Ap-NF-κB by overexpression of Ap-IKK in human cells in culture, the vast majority of Ap-NF-κB isolated from Aiptasia is in the processed form (Figure 3.7) and in the nucleus of cells (Figure 3.8g), regardless of whether the anemones harbor Symbiodiniaceae or have been rendered aposymbiotic by heat or menthol treatment. Whether Ap-NF-κB is always constitutively processed *in vivo* in anemones or there are factors or conditions that regulate Ap-NF-κB's processing is not clear at this time. In mammals, there are cases where the non-canonical NF-κB p100 is constitutively processed in animal tissues: for example, the majority of mouse NF-κB p100 is in its processed form when analyzed in extracts taken directly from liver, lymph nodes, and bone marrow but is primarily in its non-processed form when overexpressed in cells in culture (Senftleben et al. 2001).

5.3 NF-κB expression and symbiosis in Aiptasia

In terms of biological significance, the results presented in this thesis correlate NF-κB transcription factor expression and activity with symbiotic status in Aiptasia. That is, NF-κB expression is suppressed by the establishment of symbiosis and its expression is increased by loss of symbiosis. Specifically, in laboratory-spawned, naïve Aiptasia larvae, the introduction of *B. minutum* leads to the downregulation of NF-κB protein staining (Figure 3.10b and 3.10c). Conversely, when loss of symbiosis is induced by heat or menthol treatment in adult Aiptasia, NF-κB protein levels and DNA-binding activity increase, but only after *B. minutum* is cleared from the animals (Figure 3.8c, e-f, and 3.9a-b). In other published studies, NF-κB mRNA was found to be substantially upregulated in the threatened Caribbean coral *Acropora palmata* following one day of thermal stress (DeSalvo et al. 2010). A simple interpretation of these collective results is that at least certain species of Symbiodiniaceae down-regulate NF-κB expression in Aiptasia. Based on such results, we propose that NF-κB controls an immune pathway that must be suppressed for the establishment of symbiosis by certain species of Symbiodiniaceae in Aiptasia. Consistent with this proposal, symbiotic Aiptasia (i.e., with reduced NF-κB) have a reduced capacity to respond to immune elicitors as compared to aposymbiotic (i.e., high NF-κB) anemones (Detournay and Weis 2011). In addition, RNA-seq data comparing aposymbiotic and symbiotic adult Aiptasia show that symbiosis is associated with down-regulation of a gene set involved in inflammation in humans (Lehnert et al. 2014). In at least two symbiotic corals, *Orbicella faveolata* and *Acropora*

palmata, increased levels of NF-κB transcripts have been found in bleached animals (Anderson et al. 2016, DeSalvo et al. 2010).

It is important to note that the increase in Ap-NF-κB protein and activity that is seen with loss of symbiosis is not analogous to the rapid activation of NF-κB that occurs in many vertebrate and insect systems, i.e., wherein cytoplasmic NF-κB is rapidly freed from IκB inhibition to enter the nucleus. That is, the increases in Ap-NF-κB expression and activity following loss of symbiosis appear to be due to a corresponding increase in the total number of cells with nuclear Ap-NF-κB that arise following menthol or heat treatment. Thus, loss of symbiosis appears to result in increased transcription of Ap-NF-κB in a subset of gastrodermal cells, which occurs only after a significant loss of symbiosis has taken place. The resultant increase in expression of Ap-NF-κB protein that occurs after loss of symbiosis is maintained for over two months in the absence of *B. minutum* (Figure 3.9c).

5.4 The molecular mechanism of NF-κB downregulation during symbiosis onset

In Chapter Three it is shown that the presence of the *B. minutum* symbiont in Aiptasia larvae and adults results in reduced NF-κB expression (Mansfield et al. 2017). In Chapter Four, we show that incubation of Aiptasia larvae with Symbiodiniaceae *Symbiodinium* sp. or *E voratum*, which cannot establish symbiosis with Aiptasia, does not reduce NF-κB expression (Figure 4.1c-d). The inability of *Symbiodinium* sp. or *E voratum* to populate Aiptasia is correlated with their reduced uptake of Symbiodiniaceae cells as compared to

B. minutum (Figure 4.1a-b), which is consistent with previous data demonstrating Aiptasia's preference for *B. minutum* (Hambleton et al. 2014, Wolfowicz et al. 2016). Whether the inability of non-native Symbiodiniaceae species to establish residency in Aiptasia is also, at least in part, due to their inability to downregulate NF-κB is not clear. However, as we show by linear regression (Figure 4.1e) that, for the same number of symbionts, larvae with *B. minutum* have lower NF-κB expression than larvae with *E. voratum*, suggesting that NF-κB expression levels are correlated with the specific Symbiodiniaceae species that is being taken up and not simply symbiont cell number. That being said, it is clear that reduced NF-κB expression is not required for the establishment of symbiosis by all Symbiodiniaceae species, given that Aiptasia adults harboring *Durusdinium* sp. (clade D) do not show reduced NF-κB levels as compared to aposymbiotic anemones (Figure 4.1g).

How the presence of *B. minutum* in Aiptasia larvae and adults leads to reduced NF-κB expression is not known. However, our finding that incubation of aposymbiotic larvae with the ligand TGFβ reduced levels of NF-κB staining suggests that *B. minutum* could reduce NF-κB by affecting a host factor(s), including TGFβ. Consistent with this hypothesis, TGFβ has previously been shown to have the ability to promote symbiosis in cnidarians (Berthelier at al. 2017, Detournay et al. 2012). TGFβ comprises a superfamily of cytokines that induce anti-inflammatory and anti-immunity responses in vertebrate systems (Chen and Ten Dijke 2016, Denney et al. 2017, Ndungu et al. 2005, Simmons et al. 2006, Travis and Sheppard 2013). The predicted Aiptasia TGFβ homologue is 51% identical and 70% similar to human TGFβ1, and Detournay et al. (2012) have shown that

treatment with human TGFβ1 results in a decrease in nitric oxide production, a commonly used marker of immune activity levels (Coleman 2001), suggesting that TGFβ activation helps to suppress host immune activity. Moreover, in the coral *Fungia scutaria,* blocking endogenous host TGFβ signaling with a human anti-TGFβ antibody results in a decrease in the uptake of *B. minutum* (Berthelier et al. 2017). Taken together, these results are consistent with a model wherein a symbiont-induced host factor, such as TGFβ, leads to suppression of host immunity by reducing the expression and immunity-promoting activity of NF-κB. This suppression of NF-κB and immunity facilitates the efficient establishment and maintenance of symbiosis in Aiptasia larvae by certain species of Symbiodiniaceae, including *B. minutum*. It will be interesting to determine whether other species of Symbiodiniaceae that can populate Aiptasia or corals can reduce NF-κB levels. Additionally, since Aiptasia settlement has not yet been achieved in the lab, identifying the molecular mechanisms of symbiosis establishment post-settlement, perhaps in coral recruits, may provide additional insights by modeling a more ecologically relevant timepoint of symbiosis uptake.

5.5 The implications of NF-κB expression levels for cnidarian biology

A major goal of the experiments described in Chapter Four was to determine the biological significance of NF-κB expression in Aiptasia. Although NF-κB has well-documented roles in immune- and stress-related processes in triploblasts (Dev et al. 2011) this is the first study to provide experimental evidence for immune- and thermal stress-related roles for NF-κB in more basal, symbiotic cnidarians. We hypothesized that

although decreased NF-κB expression during the onset of symbiosis may be important for efficient colonization of symbionts in cnidarian hosts, dampening NF-κB may have negative consequences on host immune competency to pathogens. Therefore, we proposed that the symbiotic state in Aiptasia (low NF-κB) would be associated with low immunity and the inability to survive pathogen infection. Our results demonstrated that long-term aposymbiotic anemones have higher NF-κB DNA-binding activity as compared to symbiotic anemones (Figure 4.3a-b). This result is consistent with our results in Chapter Three showing increased NF-κB levels in H2 anemones after bleaching (Mansfield et al. 2017). After infection of Aiptasia with the bacterial pathogen *S. marcescens*, approximately 95% of aposymbiotic anemones (high NF-κB) survived whereas only 17% of symbiotic anemones (low NF-κB) survived (Figure 4.3d) demonstrating that NF-κB expression is positively correlated with reduced susceptibility to pathogen-induced disease in Aiptasia. These findings suggest that the levels of NF-κB expression can predict pathogen-induced disease survivability, with high NF-κB expression being more conducive to survival following infection. Furthermore, these results suggest a trade-off of symbiosis in cnidarians whereby immunity is lowered by certain symbiotic partnerships, but also results in a decreased ability to resist pathogen-induced disease.

NF-κB's correlation with disease survivability begins to untangle the complex interaction of immunity and symbiosis. For example, reports on the association of bleaching and disease have been confounding. The association of bleaching with an increased frequency of coral disease outbreaks is well-documented (Brown and

Rodriguez-Lanetty 2009, Maynard et al. 2015, Miller et al. 2009). Coral disease outbreaks are often correlated with high temperature, such as in black band (Sato et al. 2009), yellow band (Cervino et al. 2004), and white band syndromes (Heron et al. 2010). Pathogen abundance and coral disease prevalence are projected to increase as climate models predict a warming planet, which may lead to disease being a major future driver of coral decline (Maynard et al. 2015). Therefore, understanding the correlation between loss of symbiosis and bleaching is an important goal. In contrast to previously published literature, it has been recently reported from field studies that bleached corals are associated with lower disease prevalence than their non-bleached counterparts (Merselis et al. 2018). This correlation is consistent with our findings that aposymbiotic anemones (high NF-κB) survive pathogen infection better than symbiotic anemones, and suggests that aposymbiotic corals may resist disease better due to the loss of immune-suppressing symbionts. Due to the discrepancies in the correlation between disease and bleaching we aimed to understand how host nutrition may play a role in immunity to disease and NF-κB expression levels.

We have also shown that starving aposymbiotic anemones of *Artemia* for two weeks reduces survivability to *S. marcesens* infection (Figure 4.3), showing that high nutritional status is positively correlated with immune competency in Aiptasia. Together, results from Figure 4.3 show that under normal conditions, well-fed aposymbiotic anemones (high NF-κB) have increased resistance to disease as compared to symbiotic anemones (low NF-κB), possibly due to immunosuppression by symbiosis. However, when aposymbiotic Aiptasia are starved, anemones are less likely to survive pathogen

infection (Figure 4.3e). In the case of corals, one hypothesis is that long-term bleached corals, which are nutrient poor due to loss of symbionts or lack of heterotrophic food in tropical oligotrophic waters, would not be to mount an immune response and survive infection as compared to bleached corals that are less nutrient poor. The importance of feeding for immunocompetence has been demonstrated in honeybees, whereby an increased and more diverse pollen diet was correlated with increased immunocompetence (Alaux et al. 2010). In addition, feeding, i.e. heterotrophy, was demonstrated to mitigate coral stressors such as loss of symbiosis during heat stress in the facultatively symbiotic coral *Oculina arbuscula* (Aichelman et al. 2016), ocean acidification and temperature stress in *Acropora cervicornis* (Towle et al. 2015), tissue cover of coral colonies in *Astrangia poculata* (Burmester et al. 2018), and during bleaching recovery in *Montipora capitata* (Grottoli et al. 2006). Therefore, coral feeding is correlated with increased fitness to many of the environmental stressors associated with climate change.

We have also found that three isolates of *P. damicornis* exhibited differential bleaching susceptibilities in response to increased temperature, harbored different Symbiodiniaceae genera, and had different basal NF-κB levels (Figure 4.4a-f). The most thermoresistant isolate (3) had increased NF-κB levels and hosted *Durusdinium* species as compared to the two thermosensitive isolates (1, 2) that had lower NF-κB levels and hosted primarily *Cladocopium* species (Figure 4.4c). Of note, these samples were isolated from distinct colonies and are likely to represent different genotypes (Sarah Davies, personal communication). Therefore, differences in the bleaching susceptibilities of these three *P. damicornis* isolates could be due to 1) intrinsic genetic differences among the

three isolates, 2) differences in symbiont communities, or 3) a combination of genetic and symbiont-induced differences.

Others have found that hosting *Durusdinium* (formerly clade D) is associated with increased thermotolerance in corals (Barshis et al. 2013, Silverstein et al. 2017, Stat and Gates 2011). Whether host factors such as increased NF-κB levels (or other factors) also contribute to the bleaching resistance in isolate 3 is not clear at this time. However, we find it interesting that *Durusdinium* (unlike *B. minutum*) does not reduce NF-κB levels during symbiosis in Aiptasia (Figure 4.4g), which is consistent with the higher levels of NF-κB in *P. damicornis* isolate 3. Therefore, cnidarians that host *Durusdinium* may be more thermotolerant due to their hosting of this symbiont subtype, due to effects of *Durusdinium* on host physiology (e.g., by maintaining high NF-κB levels), or due to a combination of both host and symbiont effects. Relevant to these possibilities, *Durusdinium* do not appear to be inherently more thermal resistant than other Symbiodiniaceae genera when grown *in vitro* (Chakravarti and van Oppen 2018), and Barshis et al. (2013) have found that higher basal expression of certain host protective genes, i.e. "frontloaded genes", is associated with protection against bleaching in the coral *Acropora hyacinthus*. Thus, NF-κB could be a host-expressed frontloading factor that contributes to the thermotolerance of cnidarians that host *Durusdinium* species of symbionts. Of note, a recent study found that Aiptasia hosting *Durusdinium trenchii* have reduced glucose abundance as compared to Aiptasia hosting *B. minutum* (Matthews et al. 2018). Therefore, although *Durusdinium trenchii* confers a heat-resistant phenotype, this

partnership may lead to reduced growth rates of cnidarian hosts due to reduced carbon transfer by *Durusdinium* symbionts.

Our results indicate that NF-κB is associated with increased survivability to pathogens in Aiptasia and increased resistance to bleaching in *P. damicornis*. Based on RNA-seq experiments in Aiptasia (Lehnert et al. 2014), we found that putative NF-κB binding sites were significantly enriched in putative (1 kbp upstream) promoter regions of upregulated inflammation genes, as compared to downregulated inflammation genes in aposymbiotic Aiptasia (Figure 4.5), suggesting that NF-κB is a transcriptional activator of inflammation- or immune-related genes in aposymbiotic Aiptasia. Thus, one proposal is that NF-κB increases immunity by activating inflammatory genes to mitigate pathogen infection. Of note, increased levels of NF-κB transcripts in aposymbiotic Aiptasia larvae were not observed in Lehnert et al. (2014), and we have not empirically characterized NF-κB protein expression in adult CC7 aposymbiotic Aiptasia vs symbiotic Aiptasia hosting *Symbiodinium* sp. as studied by Lehnert et al. (2014). Future studies could be aimed at directly characterizing NF-κB target genes in Aiptasia through chromatin immunoprecipitation (ChIP) sequencing.

5.6 Conclusions and future directions

Immunity plays a role in regulating many symbiotic partnerships (Burns et al. 2017, Chu and Mazmanian 2013, McFall-Ngai et al. 2013, Nyholm and Graf 2012, Zientz et al. 2005). To investigate a similar role for immunity in the cnidarian-Symbiodiniaceae mutualism we have characterized transcription factor NF-κB in Aiptasia. Chapter Three

shows that there is a correlation between NF-κB transcription factor expression and activity with symbiotic status in Aiptasia, i.e., NF-κB expression is suppressed by the establishment of symbiosis and is increased by loss of symbiosis. Thus, Aiptasia joins a growing list of hosts that have symbiotic partners that downregulate NF-κB, and hence immunity, as a means to facilitate the establishment and maintenance of symbiosis. Others include Drosophila-gut microbiota (Chu and Mazmanian 2013), salamander-algae (Burns et al. 2017), honeybee-deformed wing virus (Nazzi et al. 2012, Di Prisco et al. 2016), and bobtail squid-*V. fischeri* (Chun et al. 2008).

The association between increased NF-κB expression/activity and loss of symbiosis in Aiptasia is especially noteworthy given that Aiptasia is a laboratory model for the pervasive climate change-induced coral bleaching that is occurring globally. In Chapter Four, the regulation of NF-κB and its possible roles in immunity and thermal tolerance in cnidarians are investigated. Our work demonstrates a positive correlation between NF-κB expression and resistance to pathogen-induced disease in Aiptasia as well as resistance to heat stress in the coral *P. damicornis*. Although NF-κB has well-documented roles in immune- and stress-related processes in triploblasts (Dev et al. 2011, Gilmore and Wolenski 2012); this is the first study to provide experimental evidence for immune- and thermal stress-related roles for NF-κB in thermosensitive cnidarians. From these findings, we propose that NF-κB can be used as a marker for immune competency to bacterial infection. Such studies may provide rationale for genetically modifying NF-κB expression in cnidarians with the goal of directly attributing changes in NF-κB expression with observed phenotypes.

Other important questions include the following:

1. Is NF-κB constitutively processed in Aiptasia, or is there a currently unknown signaling event that induces proteasomal processing? If so, in what state is Aiptasia NF-κB not processed? In many vertebrate and insect systems, NF-κB is rapidly activated i.e., cytoplasmic NF-κB is freed from IκB inhibition to enter the nucleus. However the vast majority of Ap-NF-κB isolated from Aiptasia is in the processed form (Figure 3.7) and in the nucleus of cells (Figure 3.8g). It is unclear whether Ap-NF-κB is constitutively processed or if there is a specific state (perhaps in a sterile environment) or a particular cell type where Ap-NF-κB is not processed. For example, the majority of mouse NF-κB p100 is processed in extracts when taken directly from liver, lymph nodes, and bone marrow (Senftleben et al. 2001).
2. How does the uptake of *B. minutum* result in NF-κB downregulation in Aiptasia while the other non-native Symbiodiniaceae species are not able to do so? Is there a *B. minutum* specific factor encoded by or induced by the algae that causes downregulation of NF-κB? In Chapter Four we show that *B. minutum* uptake is more efficient in Aiptasia larvae as compared to non-native Symbiodiniaceae (Figure 4.1a-b). How the presence of *B. minutum* in Aiptasia larvae and adults leads to reduced NF-κB expression is not known. However, our finding that incubation of aposymbiotic larvae with the ligand TGFβ reduced levels of NF-κB staining suggests that *B. minutum* could reduce NF-κB by affecting a host factor such as TGFβ. Similarly, in vertebrates, TGFβ is

a pathway commonly targeted by microbes to reduce host immunity (Denney et al. 2017, Ndungu et al. 2005, Simmons et al. 2006).

3. What is the effect of overexpressing/knocking down NF-κB during pathogen infection and during heat stress in Aiptasia? Does NF-κB overexpression mitigate symbiont loss/pathogen infection? Does NF-κB knockdown exacerbate symbiont loss/pathogen infection? Chapter Four demonstrates a positive correlation between high NF-κB expression and resistance to pathogen-induced disease in Aiptasia as well as resistance to heat stress in the coral *P. damicornis*. Therefore, our results would predict that overexpressing NF-κB will result in increased resistance to heat stress and pathogen infection in cnidarians. In contrast, knocking down NF-κB would be expected to cause increased susceptibility to pathogen-induced disease and symbiont loss during heat stress.
4. How does NF-κB activity mitigate pathogen infection/bleaching in cnidarians? What are the target genes NF-κB activates to increase fitness? NF-κB is an evolutionarily conserved transcription factor that activates transcription of many target genes involved in immunity and inflammatory processes (Dev et al. 2011, Gilmore and Wolenski 2012, Lawrence 2009). Based on our work, one hypothesis is that NF-κB increases immunity in cnidarians by activating inflammatory genes, which can then act to mitigate pathogen infection and increase resistance to bleaching by activating oxidative stress response genes.

Information about altered gene expression during environmental stress has aided in identifying possibly important pathways involved in bleaching; however, the characterization of how the protein products of these transcripts function and interact will be necessary to determine the importance of any given altered transcript. That is, although there is an abundance of transcriptomic information describing gene changes during and after bleaching, there is a lack of functional characterization of changes in the proteins encoded by these altered transcripts. Often this is because antibodies, such as the one we have prepared against Ap-NF-κB, are not available for relevant protein studies.

Although immunity is one of the most commonly dysregulated cellular pathways that has been associated with bleaching based on the identification of immunity homologs in cnidarians, there is essentially no information on the roles of the numerous genes identified in RNA-seq analyses that do not have identifiable homologues in mammals. Therefore, an increase in the molecular, cellular, and biochemical characterization of putative bleaching genes/proteins, both novel and conserved, will be necessary to gain a clearer understanding of the molecular mechanisms of bleaching and the role of immunity in processes such as symbiont uptake, maintenance, and expulsion. Moving forward, it will be necessary to develop more robust genetic and genomic tools, such that one can experimentally alter the expression of genes, e.g., NF-κB, to assess their roles in symbiosis/dysbiosis. Recent advances in the genetic modification of corals (Cleves et al. 2018) may lead to a better understanding of immune pathways involved in bleaching resistance or susceptibility. Moreover, the identification of genetic or epigenetic differences in immunity genes and pathways between individual corals that

show different susceptibility to bleaching will be valuable. Nevertheless, given the extensive diversity in genomes among cnidarians (Voolstra et al. 2017), as well as differences in their resident Symbiodiniaceae (LaJeunesse et al. 2018), it is likely that there are several different mechanisms by which cnidarian-symbiont mutualisms modulate immunity for symbiosis/dysbiosis. Lastly, information on the relationship between immunity and cnidarian-dinoflagellate symbiosis could also aid in coral conservation efforts.

APPENDIX I

List of Aiptasia NF-κB DNA-binding sequences (n=950) used for promoter analysis in Figure 4.5.

Binding site	Reverse Complement	Z-score
GGGAATCCCC	GGGGATTCCC	14.73699803
GGGGATCCCC	GGGGATCCCC	14.62360417
GGGATTCCCC	GGGGAATCCC	13.91822948
GGGAACCCCC	GGGGGTTCCC	12.95731457
GGGGAACCCC	GGGGTTCCCC	12.47794337
AAAAACCCCC	GGGGGTTTTT	12.07011279
GGGATCCCCC	GGGGGATCCC	12.04118885
GGGAATTCCC	GGGAATTCCC	12.004766
AAAAATCCCC	GGGGATTTTT	11.71928058
GGAATTCCCC	GGGGAATTCC	11.68490631
GGGACTCCCC	GGGGAGTCCC	11.31806798
GGATTCCCCC	GGGGGAATCC	11.31421223
GAAATCCCCC	GGGGGATTTC	11.15539177
GGAAACCCCC	GGGGGTTTCC	11.1516023
AAAATCCCCC	GGGGGATTTT	11.07330019
GGAATCCCCC	GGGGGATTCC	10.91096833
GGGAGTCCCC	GGGGACTCCC	10.89790453
GAAAACCCCC	GGGGGTTTTC	10.76197307
GGAAATCCCC	GGGGATTTCC	10.7573128
GGGAAACCCC	GGGGTTTCCC	10.57660978
AAAACCCCCC	GGGGGGTTTT	10.50861987
GGGGATTTTA	TAAAATCCCC	10.42413218
AAAACCCCCT	AGGGGGTTTT	10.41933869
AAAATCCCCT	AGGGGATTTT	10.40313271
GAAAATCCCC	GGGGATTTTC	10.3924121
AAAATTCCCC	GGGGAATTTT	10.38571457
AAATCCCCCC	GGGGGGATTT	10.38285816
AGGGGATTCC	GGAATCCCCT	10.35029575
AGGGGAATTC	GAATTCCCCT	10.27973872
GGGGAAACCC	GGGTTTCCCC	10.23806301
AAATTTCCCC	GGGGAAATTT	10.17386899
AAATTCCCCT	AGGGGAATTT	10.08928869
GAATTCCCCC	GGGGGAATTC	10.08642439
GGACTTCCCC	GGGGAAGTCC	10.08183013
AAATCCCCCT	AGGGGGATTT	10.07823879
AAATTCCCCC	GGGGGAATTT	10.06710502
GGATTTCCCC	GGGGAAATCC	10.02230333
GGGGAATTTA	TAAATTCCCC	9.905217688
GAAATTCCCC	GGGGAATTTC	9.886985204
CGGGGAATCC	GGATTCCCCG	9.865365216
CAAAATCCCC	GGGGATTTTG	9.851662122
GGGGAATACC	GGTATTCCCC	9.83602273

AGAATCCCCC	GGGGGATTCT	9.831448894
AGGAATCCCC	GGGGATTCCT	9.790094764
AAAATCCCCG	CGGGGATTTT	9.770663069
CGGGGATTCC	GGAATCCCCG	9.765032667
AGAATTCCCC	GGGGAATTCT	9.76044391
CAAAACCCCC	GGGGGTTTTG	9.756102408
GGGAAATCCC	GGGATTTCCC	9.753024647
AGGATTCCCC	GGGGAATCCT	9.704572637
AGGGGATTTC	GAAATCCCCT	9.686793004
AGGGGAATCC	GGATTCCCCT	9.67310507
AAAACCCCCG	CGGGGGTTTT	9.665985196
GGGGGTTTTA	TAAAACCCCC	9.65367517
GGGGACCCCC	GGGGGTCCCC	9.651371205
AAAATCCCCA	TGGGGATTTT	9.626285812
CGGGGAATTC	GAATTCCCCG	9.624689343
AGAAATCCCC	GGGGATTTCT	9.621502318
GGATTCCCCA	TGGGGAATCC	9.564263131
GAGAATCCCC	GGGGATTCTC	9.535709903
AGAAACCCCC	GGGGGTTTCT	9.533511375
AATTCCCCCG	CGGGGGAATT	9.515500933
AAAACCCCCA	TGGGGGTTTT	9.508668791
GAAACCCCCC	GGGGGGTTTC	9.472590531
AAAAGTCCCC	GGGGACTTTT	9.451037312
GGGGAATTCA	TGAATTCCCC	9.450319783
CAAATTCCCC	GGGGAATTTG	9.435007902
GGGAAGCCCC	GGGGCTTCCC	9.415791236
AGGGGGTTTC	GAAACCCCCT	9.414303042
AAATTCCCCG	CGGGGAATTT	9.405600706
GGGGAAAACC	GGTTTTCCCC	9.380958943
GGGGATTTCA	TGAAATCCCC	9.356753222
AATTCCCCCT	AGGGGGAATT	9.34170637
GGGAAGTCCC	GGGACTTCCC	9.306084316
AAACTCCCCC	GGGGGAGTTT	9.305637211
AAAACTCCCC	GGGGAGTTTT	9.291050094
GGGGATTACC	GGTAATCCCC	9.274570363
CGGGGATTTC	GAAATCCCCG	9.248310517
GAATCCCCCC	GGGGGGATTC	9.223914436
AGGGGATCCC	GGGATCCCCT	9.216736592
GGGGATTCCA	TGGAATCCCC	9.188140047
GAATTTCCCC	GGGGAAATTC	9.177514834
AAAAAACCCC	GGGGTTTTTT	9.168412063
GGGCTTCCCC	GGGGAAGCCC	9.167188881
AGGGGGTTCC	GGAACCCCCT	9.164215511
CGGGGGTTCC	GGAACCCCCG	9.10700375
AAATCCCCCA	TGGGGGATTT	9.095341859
AATTTCCCCC	GGGGGAAATT	9.032870375
AGGGGGATTC	GAATCCCCCT	9.029037228
AAATACCCCC	GGGGGTATTT	9.01918724
AAATCCCCCG	CGGGGGATTT	9.017865611
GGAACTCCCC	GGGGAGTTCC	8.985429597
GGAACCCCCC	GGGGGGTTCC	8.979981241

GAAAGTCCCC	GGGGACTTTC	8.976272966
CGGGGGATTC	GAATCCCCCG	8.948692133
CGGAATCCCC	GGGGATTCCG	8.930899048
AATCCCCCCC	GGGGGGGATT	8.929543299
CGAAATCCCC	GGGGATTTCG	8.927444601
CGAATTCCCC	GGGGAATTCG	8.927326349
GGGGATTTAC	GTAAATCCCC	8.921247092
GGGGAATCAC	GTGATTCCCC	8.918876316
GGGGGACCCC	GGGGTCCCCC	8.917960746
GGGGGATTTA	TAAATCCCCC	8.908190375
GGGGATTCTA	TAGAATCCCC	8.896810464
GGGAATACCC	GGGTATTCCC	8.886187703
GGGGAAATTA	TAATTTCCCC	8.87827649
GGGGAATCCA	TGGATTCCCC	8.875432673
ATAATCCCCC	GGGGGATTAT	8.841766249
AAGTTCCCCC	GGGGGAACTT	8.840452207
GAATTCCCCA	TGGGGAATTC	8.826879934
GGACTCCCCC	GGGGGAGTCC	8.817165215
AAATATCCCC	GGGGATATTT	8.804224954
AAATTCCCCA	TGGGGAATTT	8.802305091
AATTTCCCCT	AGGGGAAATT	8.798079489
AAAAAGTCCC	GGGACTTTTT	8.797379708
AATATCCCCC	GGGGGATATT	8.785568548
AGATTTCCCC	GGGGAAATCT	8.775462251
AAACCCCCCT	AGGGGGGTTT	8.764564221
GGGGGATTAC	GTAATCCCCC	8.760334884
AATAATCCCC	GGGGATTATT	8.757123328
CGGATTCCCC	GGGGAATCCG	8.743524852
GGGGAATTAC	GTAATTCCCC	8.729592544
CGGGGATCCC	GGGATCCCCG	8.724579416
AAACCCCCCC	GGGGGGGTTT	8.723994674
GATTTCCCCC	GGGGGAAATC	8.721246415
AAACTTCCCC	GGGGAAGTTT	8.713460536
AAGAATCCCC	GGGGATTCTT	8.712245894
AAAGTCCCCT	AGGGGACTTT	8.688536072
GAAACTCCCC	GGGGAGTTTC	8.686367501
AGATTCCCCC	GGGGGAATCT	8.662989374
GGGGGAACCC	GGGTTCCCCC	8.644258803
GAAATCCCCA	TGGGGATTTC	8.630155035
GGAAGTCCCC	GGGGACTTCC	8.62876002
GGAATCCCCA	TGGGGATTCC	8.607369846
AATTCCCCCA	TGGGGGAATT	8.60191933
AAAGTCCCCC	GGGGGACTTT	8.577439155
CGAAACCCCC	GGGGGTTTCG	8.573705084
AAACCCCCCA	TGGGGGGTTT	8.558542047
GGGGGATTCA	TGAATCCCCC	8.537134766
CGGGGGAATA	TATTCCCCCG	8.530709798
AAATCTCCCC	GGGGAGATTT	8.525355173
ATAATTCCCC	GGGGAATTAT	8.517713426
AATTCCCCCC	GGGGGGAATT	8.504842792
GATTCCCCCC	GGGGGGAATC	8.502737551

AGGGGGAATC	GATTCCCCCT	8.474160401
GGGGAGCCCC	GGGGCTCCCC	8.445682388
GGGAATTACC	GGTAATTCCC	8.441657166
AAACCCCCCG	CGGGGGGTTT	8.428847095
AGGAACCCCC	GGGGGTTCCT	8.428541438
GAGATTCCCC	GGGGAATCTC	8.416353229
GGAGTTCCCC	GGGGAACTCC	8.411858633
GGGGGAAAAC	GTTTTCCCCC	8.395923918
ATATTCCCCC	GGGGGAATAT	8.390934373
CAAATCCCCC	GGGGGATTTG	8.387432467
AGGGGAAATC	GATTTCCCCT	8.379742502
AATCTCCCCC	GGGGGAGATT	8.369514554
AGGGGGATTA	TAATCCCCCT	8.362469892
GGGGATACCC	GGGTATCCCC	8.356506285
AAAGTTCCCC	GGGGAACTTT	8.352873526
AATTTCCCCG	CGGGGAAATT	8.331623022
AGGGGGATCC	GGATCCCCCT	8.33078466
GGGAACTCCC	GGGAGTTCCC	8.327612803
GGGAGCCCCC	GGGGGCTCCC	8.324017262
AAAGTCCCCG	CGGGGACTTT	8.322154439
GGAGTCCCCC	GGGGGACTCC	8.320459887
AAAGATCCCC	GGGGATCTTT	8.31575941
AAACTCCCCT	AGGGGAGTTT	8.307410054
GGGACCCCCC	GGGGGGTCCC	8.29402962
CAATTTCCCC	GGGGAAATTG	8.291395608
GGGGGGATTA	TAATCCCCCC	8.278598187
GGATCCCCCC	GGGGGGATCC	8.27437332
GGGGGTTACC	GGTAACCCCC	8.273114231
GGGGAATCTA	TAGATTCCCC	8.256601112
AATCCCCCCG	CGGGGGGATT	8.255557353
GGGGGTTTCA	TGAAACCCCC	8.253703465
AATATTCCCC	GGGGAATATT	8.252179254
GGGGAGTTTA	TAAACTCCCC	8.250362645
AGGGATCCCC	GGGGATCCCT	8.248091339
GGGGGAAACC	GGTTTCCCCC	8.244686243
GGAAAACCCC	GGGGTTTTCC	8.201722307
ATTCCCCCCC	GGGGGGGAAT	8.176964351
AGTATTCCCC	GGGGAATACT	8.165040316
GATCCCCCCC	GGGGGGGATC	8.16386195
GGGGGAATAC	GTATTCCCCC	8.154839915
AATCCCCCCT	AGGGGGGATT	8.142888832
CAGAATCCCC	GGGGATTCTG	8.132339213
CAATCCCCCC	GGGGGGATTG	8.131170508
AAGATTCCCC	GGGGAATCTT	8.127458399
AAAAACCCCT	AGGGGTTTTT	8.103944577
GATAATCCCC	GGGGATTATC	8.098314137
GGATATCCCC	GGGGATATCC	8.098004507
ATATTTCCCC	GGGGAAATAT	8.089697333
AGTTTCCCCC	GGGGGAAACT	8.06592531
CGAATCCCCC	GGGGGATTCG	8.058888364
AATATCCCCT	AGGGGATATT	8.054956184

AACTCCCCCT	AGGGGGAGTT	8.054634733
AGGGGAATAC	GTATTCCCCT	8.041699056
AGGTTCCCCC	GGGGGAACCT	8.032954843
AGTTTTCCCC	GGGGAAAACT	8.027040939
GGGGGAATCA	TGATTCCCCC	8.01679481
AATACCCCCT	AGGGGGTATT	8.014785244
GGGATTACCC	GGGTAATCCC	8.013989102
AGGATCCCCC	GGGGGATCCT	8.012637342
GATTCCCCCA	TGGGGGAATC	8.008014631
GGGGTTTTTA	TAAAAACCCC	8.00545933
AAGAACCCCC	GGGGGTTCTT	8.0028188
GATTTTCCCC	GGGGAAAATC	8.001908224
GGGGGAATTA	TAATTCCCCC	7.994624228
GGGGATATTA	TAATATCCCC	7.989492415
GGGGATTATA	TATAATCCCC	7.986892325
GAAAAACCCC	GGGGTTTTTC	7.981545195
GAAGTTCCCC	GGGGAACTTC	7.974743908
AAGTTTCCCC	GGGGAAACTT	7.96268573
GGGGAATATA	TATATTCCCC	7.961793614
CAATTCCCCC	GGGGGAATTG	7.952608277
GAAGTCCCCC	GGGGGACTTC	7.94800048
AATTTTCCCC	GGGGAAAATT	7.947104748
AAAAAGCCCC	GGGGCTTTTT	7.943386035
AGAATCCCCT	AGGGGATTCT	7.943018846
AAAAGCCCCC	GGGGGCTTTT	7.940964782
CATAATCCCC	GGGGATTATG	7.925460311
GAAAAGTCCC	GGGACTTTTC	7.922430886
AAAGTCCCCA	TGGGGACTTT	7.922066949
AGGGGACTTC	GAAGTCCCCT	7.919154897
GGGGGATACC	GGTATCCCCC	7.917323954
GGGGAAATCA	TGATTTCCCC	7.915704904
GAACTCCCCC	GGGGGAGTTC	7.907244624
GGATCTCCCC	GGGGAGATCC	7.906707113
AGGGAATTCC	GGAATTCCCT	7.901342639
ACAATTCCCC	GGGGAATTGT	7.893811242
AATCCCCCCA	TGGGGGGATT	7.890904103
ATTTCCCCCC	GGGGGGAAAT	7.888334223
ACAATCCCCC	GGGGGATTGT	7.887423828
GAGAACCCCC	GGGGGTTCTC	7.885657048
GAATACCCCC	GGGGGTATTC	7.885519199
GGAGATCCCC	GGGGATCTCC	7.869716466
GGGGAAATAC	GTATTTCCCC	7.867179941
AATACCCCCC	GGGGGGTATT	7.865609931
GGGGGTTTAC	GTAAACCCCC	7.864284616
GGGGACTTTA	TAAAGTCCCC	7.859875881
GGGGGGGGAA	TTCCCCCCCC	7.856076881
AATTTCCCCA	TGGGGAAATT	7.855500492
AAGATCCCCC	GGGGGATCTT	7.855466955
ATTTCCCCCG	CGGGGGAAAT	7.854550936
GCAATCCCCC	GGGGGATTGC	7.851470962
AGGGGAATTA	TAATTCCCCT	7.821924988

CGATTTCCCC	GGGGAAATCG	7.816988904
GAATCTCCCC	GGGGAGATTC	7.813360264
GAATATCCCC	GGGGATATTC	7.800897797
GGGGGTTCCA	TGGAACCCCC	7.790753289
AGGGGATTTA	TAAATCCCCT	7.786889452
GGGGGTACCC	GGGTACCCCC	7.786561927
ATAAATCCCC	GGGGATTTAT	7.775875592
CAAAGTCCCC	GGGGACTTTG	7.770404589
CGGGGAAATC	GATTTCCCCG	7.760971807
ATAAACCCCC	GGGGGTTTAT	7.759250619
GGGACTTTTA	TAAAAGTCCC	7.755450903
AACTTCCCCC	GGGGGAAGTT	7.753202503
TAATCCCCCA	TGGGGGATTA	7.752247814
GGGGTACCCC	GGGGTACCCC	7.749414938
CGGGAATTCC	GGAATTCCCG	7.73064319
AGAAGTCCCC	GGGGACTTCT	7.724206425
GATATTCCCC	GGGGAATATC	7.711431242
AGGGGGGGGA	TCCCCCCCCT	7.705673259
ATCCCCCCCA	TGGGGGGGAT	7.704798558
AAACTCCCCG	CGGGGAGTTT	7.701719319
GGGCATCCCC	GGGGATGCCC	7.698961354
GGATACCCCC	GGGGGTATCC	7.695600209
GGAAAGTCCC	GGGACTTTCC	7.690205505
AGGAGTCCCC	GGGGACTCCT	7.69020123
AGGGGGAAAT	ATTTCCCCCT	7.68834808
AGGGGTTTTC	GAAAACCCCT	7.677723676
ATTTTCCCCC	GGGGGAAAAT	7.677505359
CAGATTCCCC	GGGGAATCTG	7.646004722
GGGGGGAAAC	GTTTCCCCCC	7.641165288
GAGTTCCCCC	GGGGGAACTC	7.639447615
GAAACCCCCA	TGGGGGTTTC	7.610575788
AGGGGGAATA	TATTCCCCCT	7.606784546
ACTTTCCCCC	GGGGGAAAGT	7.597425435
AGGGGGAAAC	GTTTCCCCCT	7.594090895
AGATTCCCCT	AGGGGAATCT	7.5917821
CGGGGGATTA	TAATCCCCCG	7.59102966
GGGGAACCAC	GTGGTTCCCC	7.585983567
GGGGGTATTA	TAATACCCCC	7.580555619
AACTCCCCCC	GGGGGGAGTT	7.577327073
GGGGACTACC	GGTAGTCCCC	7.562949385
AAGTCCCCCC	GGGGGGACTT	7.559911635
AGAAAGTCCC	GGGACTTTCT	7.555424628
CGGGTTCCCC	GGGGAACCCG	7.553824188
ACATTCCCCC	GGGGGAATGT	7.54999885
AGAGTCCCCC	GGGGGACTCT	7.54497616
ATCTCCCCCC	GGGGGGAGAT	7.543315041
CAGAACCCCC	GGGGGTTCTG	7.529578811
ATTTCCCCCA	TGGGGGAAAT	7.524520063
GGGGGGAACC	GGTTCCCCCC	7.517571906
GGGGAGTACC	GGTACTCCCC	7.516278447
CGGAACCCCC	GGGGGTTCCG	7.512466723

AGGGGAAAAC	GTTTTCCCCT	7.508120538
CGGGGAAACC	GGTTTCCCCG	7.508079052
GGAACCCCCA	TGGGGGTTCC	7.496914116
ATCCCCCCCC	GGGGGGGGAT	7.488267058
CATATTCCCC	GGGGAATATG	7.485395156
GGGGAACCCA	TGGGTTCCCC	7.484898166
AAAAGTCCCT	AGGGACTTTT	7.478292225
GGGGATTCAC	GTGAATCCCC	7.473707102
AACAATCCCC	GGGGATTGTT	7.456062447
AAATAGTCCC	GGGACTATTT	7.446729336
CAAGTTCCCC	GGGGAACTTG	7.444138163
AAAATACCCC	GGGGTATTTT	7.438964453
GGGGGGGACC	GGTCCCCCCC	7.433380091
ACAAATCCCC	GGGGATTTGT	7.432644338
GGGGGATCCA	TGGATCCCCC	7.420819493
GGGAGATCCC	GGGATCTCCC	7.4087904
GGGGATCCAC	GTGGATCCCC	7.40666494
AGGTTTCCCC	GGGGAAACCT	7.403851535
GGGGGAACCA	TGGTTCCCCC	7.40377859
GGGGAACTTA	TAAGTTCCCC	7.403018164
AGAACCCCCT	AGGGGGTTCT	7.399248183
AAAAACCCCG	CGGGGTTTTT	7.398173267
GATTTCCCCA	TGGGGAAATC	7.397164579
ATATTCCCCA	TGGGGAATAT	7.397011939
CAATACCCCC	GGGGGTATTG	7.392705898
GAAAAGCCCC	GGGGCTTTTC	7.379470978
GGGACGTCCC	GGGACGTCCC	7.368590737
AGTTCCCCCC	GGGGGGAACT	7.365571525
AGTAATCCCC	GGGGATTACT	7.356536346
GGACCCCCCC	GGGGGGGTCC	7.3490579
CGGGATCCCC	GGGGATCCCG	7.346759452
ATATCCCCCC	GGGGGGATAT	7.343565514
AGGGGGGAAT	ATTCCCCCCT	7.338668779
AAAAGTCCCG	CGGGACTTTT	7.337797805
CCCCCCCCCG	CGGGGGGGGG	7.334341985
GGGAAAACCC	GGGTTTTCCC	7.331653897
AAAAGCCCCT	AGGGGCTTTT	7.33092935
GAACTTCCCC	GGGGAAGTTC	7.325016965
GGGGATCTTA	TAAGATCCCC	7.324347632
CGGGGATTTA	TAAATCCCCG	7.318269906
AGGGGGTTTA	TAAACCCCCT	7.309722939
GGGGGAAATA	TATTTCCCCC	7.301118147
AACCCCCCCC	GGGGGGGGTT	7.288154271
GACTTCCCCC	GGGGGAAGTC	7.276507997
ATTCCCCCCG	CGGGGGGAAT	7.276272395
AGGGGAAAAT	ATTTTCCCCT	7.275399491
GGCAATCCCC	GGGGATTGCC	7.273363862
AACTTTCCCC	GGGGAAAGTT	7.268945297
CGGGGAAAAC	GTTTTCCCCG	7.266245429
GGGATCCCCA	TGGGGATCCC	7.26431097
GAGATCCCCC	GGGGGATCTC	7.260166465

GGGGATCACC	GGTGATCCCC	7.258891691
CAAACTCCCC	GGGGAGTTTG	7.257229925
CGGGGGAAAC	GTTTCCCCCG	7.24613117
GATATCCCCC	GGGGGATATC	7.245464603
GGGGGGAAAA	TTTTCCCCCC	7.23428958
CAAAAACCCC	GGGGTTTTTG	7.230956088
CGGGGAATTA	TAATTCCCCG	7.229245981
CAAAAGTCCC	GGGACTTTTG	7.207026215
GCATTCCCCC	GGGGGAATGC	7.202545858
GATAACCCCC	GGGGGTTATC	7.197958966
AGGGGGGGAT	ATCCCCCCCT	7.191117047
AGAGTTCCCC	GGGGAACTCT	7.179774974
GGGGGGTTTA	TAAACCCCCC	7.173372644
CAATATCCCC	GGGGATATTG	7.163177996
GAAGATCCCC	GGGGATCTTC	7.155673052
GGGGATCCCA	TGGGATCCCC	7.15430739
AATAACCCCC	GGGGGTTATT	7.151258898
AGGGACTTTC	GAAAGTCCCT	7.14376165
GGGGAAGTAC	GTACTTCCCC	7.141999714
CGTATTCCCC	GGGGAATACG	7.141438918
GAACCCCCCC	GGGGGGGTTC	7.137697051
GGGGAAGTTA	TAACTTCCCC	7.136702591
AGTTCCCCCA	TGGGGGAACT	7.13514224
AAACTCCCCA	TGGGGAGTTT	7.131956775
CGTTTTCCCC	GGGGAAAACG	7.130806429
GGGGGTTCTA	TAGAACCCCC	7.116830071
AATAGTCCCC	GGGGACTATT	7.114056283
GGGGGAGAAA	TTTCTCCCCC	7.104976258
GGGGGGAATA	TATTCCCCCC	7.104525208
AGATACCCCC	GGGGGTATCT	7.10411077
GGGGCCCCCC	GGGGGGCCCC	7.09174619
GGGCTCCCCC	GGGGGAGCCC	7.084127385
GAGTTTCCCC	GGGGAAACTC	7.080204054
GGACGTCCCC	GGGGACGTCC	7.079218919
GGGGGAATAA	TTATTCCCCC	7.075716059
GGGGGGTTAC	GTAACCCCCC	7.065674952
GGGGGGGGAC	GTCCCCCCCC	7.06070058
CGGGGAGTCC	GGACTCCCCG	7.059747708
GGGGATTTAA	TTAAATCCCC	7.050581798
GACATTCCCC	GGGGAATGTC	7.033769614
CGGTTTCCCC	GGGGAAACCG	7.03219025
GCAATTCCCC	GGGGAATTGC	7.031190296
GGGGCGCCCC	GGGGCGCCCC	7.027669892
GGAAAGCCCC	GGGGCTTTCC	7.026505344
ACTTCCCCCC	GGGGGGAAGT	7.025966917
ATTCCCCCCA	TGGGGGGAAT	7.008286196
AAGTCCCCCT	AGGGGGACTT	7.002156565
ATTTTTCCCC	GGGGAAAAAT	6.998260122
AGGGGGAGAT	ATCTCCCCCT	6.989593927
ATTTTCCCCG	CGGGGAAAAT	6.989352558
GATCTCCCCC	GGGGGAGATC	6.982542648

GGGGAATACA	TGTATTCCCC	6.981241806
GGGGAAAATA	TATTTTCCCC	6.980496055
CGGGGGGGAA	TTCCCCCCCG	6.979624767
AGAAAACCCC	GGGGTTTTCT	6.976531557
GGGGAATTAA	TTAATTCCCC	6.974130115
CCAAATCCCC	GGGGATTTGG	6.967491817
GGGATGCCCC	GGGGCATCCC	6.95922042
ATGTTCCCCC	GGGGGAACAT	6.951934087
CAGTTCCCCC	GGGGGAACTG	6.943866866
AGGGGTTTCC	GGAAACCCCT	6.934402206
GGGGAACTAC	GTAGTTCCCC	6.924049992
GGGGCTTTTA	TAAAAGCCCC	6.916326122
GGGGGAACTA	TAGTTCCCCC	6.914600688
GTTTCCCCCA	TGGGGGAAAC	6.914270545
CATTCCCCCC	GGGGGGAATG	6.914048101
GGGGATTGTA	TACAATCCCC	6.913303456
CGTTTCCCCC	GGGGGAAACG	6.908536651
CTAAATCCCC	GGGGATTTAG	6.906776825
GGCATTCCCC	GGGGAATGCC	6.899801895
GGGAACCACC	GGTGGTTCCC	6.895095566
AACTCCCCCG	CGGGGGAGTT	6.894231909
AACTTCCCCT	AGGGGAAGTT	6.88362383
GGGGGTTTAA	TTAAACCCCC	6.879482217
GGGGAAATAA	TTATTTCCCC	6.877516478
TGGGGGGGAA	TTCCCCCCCA	6.873731856
CGGGGGAAAA	TTTTCCCCCG	6.863922573
AGGGGGAAAA	TTTTCCCCCT	6.854623085
ATTCCCCTGA	TCAGGGGAAT	6.84073505
GGGGAACACC	GGTGTTCCCC	6.836265287
AAAAATTCCC	GGGAATTTTT	6.836182579
CATTTCCCCC	GGGGGAAATG	6.835390904
GGGGAGATTA	TAATCTCCCC	6.834842596
AGGAATTCCC	GGGAATTCCT	6.827368379
AATATCCCCA	TGGGGATATT	6.823594488
GGGGAAACTA	TAGTTTCCCC	6.820140916
AACATTCCCC	GGGGAATGTT	6.814336038
AGGGGGGGAC	GTCCCCCCCT	6.810575317
AACTTCCCCG	CGGGGAAGTT	6.809785994
AAATGTCCCC	GGGGACATTT	6.809757549
AATTACCCCC	GGGGGTAATT	6.798333755
AATACCCCCA	TGGGGGTATT	6.793407014
GGGGGGGAAA	TTTCCCCCCC	6.792810863
GGGGGGATAC	GTATCCCCCC	6.781951695
AAGTCCCCCG	CGGGGGACTT	6.780978946
TAAATCCCCA	TGGGGATTTA	6.778152822
GGGGGTTATA	TATAACCCCC	6.774097548
GGAATTTCCC	GGGAAATTCC	6.770373751
CAACTTCCCC	GGGGAAGTTG	6.769218661
AACCCCCCCG	CGGGGGGGTT	6.763259716
CATTTTCCCC	GGGGAAAATG	6.757465933
ATTATCCCCC	GGGGGATAAT	6.740252046

ACAAACCCCC	GGGGGTTTGT	6.739370119
AAGTACCCCC	GGGGGTACTT	6.737758993
AGGGGGATAC	GTATCCCCCT	6.737252166
GCAAATCCCC	GGGGATTTGC	6.734815627
AGGGAATCCC	GGGATTCCCT	6.728672163
CTAAACCCCC	GGGGGTTTAG	6.721729108
GGGTTCCCCA	TGGGGAACCC	6.721585399
TAATTCCCCA	TGGGGAATTA	6.710174311
AGGGGAGTCC	GGACTCCCCT	6.707444501
CGGGGAACTC	GAGTTCCCCG	6.706098464
AGGAAACCCC	GGGGTTTCCT	6.703204121
GGGGGAGTTA	TAACTCCCCC	6.702073476
GGGGACTTCA	TGAAGTCCCC	6.700484077
ATACCCCCCC	GGGGGGGTAT	6.697664683
TCCCCCCCCA	TGGGGGGGGA	6.690018316
AAATAACCCC	GGGGTTATTT	6.689953406
AGTATCCCCC	GGGGGATACT	6.689729821
CGGGGTTTTC	GAAAACCCCG	6.679392821
AGAACCCCCG	CGGGGGTTCT	6.678863244
GGGAAGTACC	GGTACTTCCC	6.672973082
ATTATTCCCC	GGGGAATAAT	6.672110647
AGTCTCCCCC	GGGGGAGACT	6.671990188
AGGGGGTATC	GATACCCCCT	6.664855985
GGGGGAAAAA	TTTTTCCCCC	6.662897852
CAAACCCCCC	GGGGGGTTTG	6.661503734
GGGATACCCC	GGGGTATCCC	6.658442143
CACAATCCCC	GGGGATTGTG	6.644033766
CAGTTTCCCC	GGGGAAACTG	6.642484244
ACTCCCCCCC	GGGGGGGAGT	6.640576567
CGGGAATCCC	GGGATTCCCG	6.637657403
GGGGAAAACA	TGTTTTCCCC	6.624008444
AGGGGAAAAA	TTTTTCCCCT	6.621730677
AGGGGGGGAA	TTCCCCCCCT	6.618087405
ATATCCCCCA	TGGGGGATAT	6.616050564
GGGATATCCC	GGGATATCCC	6.615475795
GGAAGCCCCC	GGGGGCTTCC	6.61500043
ATACTCCCCC	GGGGGAGTAT	6.606281495
ATATACCCCC	GGGGGTATAT	6.605978003
AGCATTCCCC	GGGGAATGCT	6.605164592
GACAATCCCC	GGGGATTGTC	6.6033821
GGGGAAACCA	TGGTTTCCCC	6.596525492
GGGGGATAAC	GTTATCCCCC	6.596501185
GGAATACCCC	GGGGTATTCC	6.59424521
AACATCCCCC	GGGGGATGTT	6.593437969
GGGACGCCCC	GGGGCGTCCC	6.586354311
GGTTTCCCCA	TGGGGAAACC	6.585758061
GGGGACTCCA	TGGAGTCCCC	6.581636707
GAAATACCCC	GGGGTATTTC	6.575101251
GGGGGAACAC	GTGTTCCCCC	6.571964493
GGGCCCCCCC	GGGGGGGCCC	6.567946194
AGTCCCCCCC	GGGGGGGACT	6.567738887

GAAAGCCCCC	GGGGGCTTTC	6.562974332
AAGAGTCCCC	GGGGACTCTT	6.56192006
TATTCCCCCA	TGGGGGAATA	6.560948648
GGGGAACTCA	TGAGTTCCCC	6.559132444
GGGGAAAGTA	TACTTTCCCC	6.558163154
GATACCCCCC	GGGGGGTATC	6.549715649
GGGGGGGAAC	GTTCCCCCCC	6.548019273
CCTTTCCCCC	GGGGGAAAGG	6.533231314
ATCTCCCCCA	TGGGGGAGAT	6.53221988
CTTTTCCCCC	GGGGGAAAAG	6.529824286
AAAAACCCCA	TGGGGTTTTT	6.527129047
CACATTCCCC	GGGGAATGTG	6.524531008
GGGGGAGTAC	GTACTCCCCC	6.521086156
GGGGATTACA	TGTAATCCCC	6.518169813
AAAAGCCCCG	CGGGGCTTTT	6.51636162
GGACTTTCCC	GGGAAAGTCC	6.500082836
GGGCGTCCCC	GGGGACGCCC	6.498855998
GTAATCCCCA	TGGGGATTAC	6.497628983
CATATCCCCC	GGGGGATATG	6.496507547
GGGGAATAAC	GTTATTCCCC	6.49591234
ATCCCCCCCG	CGGGGGGGAT	6.494721799
GTTTTCCCCA	TGGGGAAAAC	6.494544679
AGAGATCCCC	GGGGATCTCT	6.494438898
GGCTTTCCCC	GGGGAAAGCC	6.492187655
AACCCCCCCT	AGGGGGGGTT	6.489076759
GGGGGACTAC	GTAGTCCCCC	6.486215897
CCGTTCCCCC	GGGGGAACGG	6.483560982
ATTCTCCCCC	GGGGGAGAAT	6.476417165
CGGGACCCCC	GGGGGTCCCG	6.468065656
GGGGAGACCC	GGGTCTCCCC	6.465558109
GGGGGTTACA	TGTAACCCCC	6.459434215
AGGGGGGAAC	GTTCCCCCCT	6.455859082
AAATAATCCC	GGGATTATTT	6.455676208
CGAAAACCCC	GGGGTTTTCG	6.452299749
GGGGGATATA	TATATCCCCC	6.446020321
AGACTTCCCC	GGGGAAGTCT	6.445218674
AAAAACTCCC	GGGAGTTTTT	6.440496328
AGCAATCCCC	GGGGATTGCT	6.438631913
CTAATCCCCC	GGGGGATTAG	6.438101978
AAAAAATCCC	GGGATTTTTT	6.436720029
ATAGTTCCCC	GGGGAACTAT	6.429747421
GGGGAAAAAC	GTTTTTCCCC	6.410077355
AAACATCCCC	GGGGATGTTT	6.409185341
GGAATTCCCA	TGGGAATTCC	6.404982422
GGGGGGAACA	TGTTCCCCCC	6.404077442
GGGGAAACAC	GTGTTTCCCC	6.402548204
CGGGATTCCC	GGGAATCCCG	6.399446611
AACATCCCCT	AGGGGATGTT	6.396296602
GGCCTTCCCC	GGGGAAGGCC	6.393439186
AAACACCCCC	GGGGGTGTTT	6.390296911
AAAGACCCCC	GGGGGTCTTT	6.383011928

GGGGGGGGGA	TCCCCCCCCC	6.373218191
AATGTCCCCC	GGGGGACATT	6.371266575
GTATTCCCCA	TGGGGAATAC	6.365970996
GGGAAAGCCC	GGGCTTTCCC	6.3650069
CAGAGTCCCC	GGGGACTCTG	6.362031502
GTTCCCCCCA	TGGGGGGAAC	6.360957005
TGGGGGGAAA	TTTCCCCCCA	6.358812602
GAAAACCCCA	TGGGGTTTTC	6.355279906
AGACTCCCCC	GGGGGAGTCT	6.353184096
AACCCCCCCA	TGGGGGGGTT	6.349889278
GGACACCCCC	GGGGGTGTCC	6.348542964
GGGGAGAACC	GGTTCTCCCC	6.347108829
CTATTTCCCC	GGGGAAATAG	6.346695814
AACTTCCCCA	TGGGGAAGTT	6.340946557
GGGGATTTGA	TCAAATCCCC	6.33969653
CATCTCCCCC	GGGGGAGATG	6.33765952
GGGGGGACCC	GGGTCCCCCC	6.337000456
AGGGAATTTC	GAAATTCCCT	6.335877675
ATAACCCCCC	GGGGGGTTAT	6.331184449
CGGAGTCCCC	GGGGACTCCG	6.326114759
CGTTCCCCCC	GGGGGGAACG	6.321561754
CGTCCCCCCC	GGGGGGGACG	6.321333286
CACTTTCCCC	GGGGAAAGTG	6.317900513
GCGATTCCCC	GGGGAATCGC	6.313305408
CGGGGGGAAA	TTTCCCCCCG	6.312853049
ACATTTCCCC	GGGGAAATGT	6.30887628
GGGGGATCTA	TAGATCCCCC	6.305989318
GGAAATTCCC	GGGAATTTCC	6.305033488
AAAGCCCCCT	AGGGGGCTTT	6.299293728
AAATACCCCG	CGGGGTATTT	6.294464396
AATCTTCCCC	GGGGAAGATT	6.291408767
AGGGATTCCC	GGGAATCCCT	6.283544224
GGGAGACCCC	GGGGTCTCCC	6.278393039
GGGACTTTCA	TGAAAGTCCC	6.277694034
GGCATCCCCC	GGGGGATGCC	6.27680316
GGGGTTACCC	GGGTAACCCC	6.275907144
CGGGGGGGGA	TCCCCCCCCG	6.271367564
CGAAAGTCCC	GGGACTTTCG	6.258945812
GGGGAATAAA	TTTATTCCCC	6.254966509
CCAAACCCCC	GGGGGTTTGG	6.254819747
AAATATTCCC	GGGAATATTT	6.253238106
GGGGGATTAA	TTAATCCCCC	6.252357321
ACGAATCCCC	GGGGATTCGT	6.251473913
GGACATCCCC	GGGGATGTCC	6.250484083
CCCATTCCCC	GGGGAATGGG	6.248633222
CAAAAGCCCC	GGGGCTTTTG	6.247617736
GGGGAAAAAA	TTTTTTCCCC	6.241570423
ACTTTTCCCC	GGGGAAAAGT	6.240761931
ACAACCCCCC	GGGGGGTTGT	6.238079923
ATTTTCCCCA	TGGGGAAAAT	6.237136709
CCTTTTCCCC	GGGGAAAAGG	6.236520522

AAACGTCCCC	GGGGACGTTT	6.232360719
GGGGGGGATA	TATCCCCCCC	6.213013736
ATTTACCCCC	GGGGGTAAAT	6.212444114
GGAGTCCCCA	TGGGGACTCC	6.209394465
AAATACCCCT	AGGGGTATTT	6.195995098
GGGAATCACC	GGTGATTCCC	6.195905919
AGTTTCCCCA	TGGGGAAACT	6.19383415
GACTTTCCCC	GGGGAAAGTC	6.184381191
GGGGGAATGA	TCATTCCCCC	6.171003633
AAAAATACCC	GGGTATTTTT	6.168846545
GGGACTACCC	GGGTAGTCCC	6.16472253
AGGGGGGAAA	TTTCCCCCCT	6.163850427
GGGGAGTCCA	TGGACTCCCC	6.157433498
AAAAATCCCT	AGGGATTTTT	6.155383051
GGGGGGGTTA	TAACCCCCCC	6.153132365
GGACGCCCCC	GGGGGCGTCC	6.152679084
GGGGATAACC	GGTTATCCCC	6.140954506
GGGCACCCCC	GGGGGTGCCC	6.138225421
CTTTTTCCCC	GGGGAAAAAG	6.122634379
GGGAATTTTA	TAAAATTCCC	6.118642152
GGGGGAAACA	TGTTTCCCCC	6.113199626
AAGACCCCCC	GGGGGGTCTT	6.111099876
GGGACACCCC	GGGGTGTCCC	6.107519326
GGGGAACCTA	TAGGTTCCCC	6.106574386
GGGGGTTTGA	TCAAACCCCC	6.106280841
AATACTCCCC	GGGGAGTATT	6.101982077
CGCATCCCCC	GGGGGATGCG	6.097621853
CATCCCCCCC	GGGGGGGATG	6.096583007
AAGTATCCCC	GGGGATACTT	6.095567237
GGATGTCCCC	GGGGACATCC	6.094961327
GGGGGTAACC	GGTTACCCCC	6.072450189
GGGCCTCCCC	GGGGAGGCCC	6.072173561
GGGGGGAGTA	TACTCCCCCC	6.068056679
AAGGTCCCCC	GGGGGACCTT	6.065710302
GGGCGCCCCC	GGGGGCGCCC	6.065350657
AGGGACTTCC	GGAAGTCCCT	6.062755067
GGGGAAGATA	TATCTTCCCC	6.060958652
CGGGGTTTCC	GGAAACCCCG	6.058827828
GATGTCCCCC	GGGGGACATC	6.054357318
CCGTTTCCCC	GGGGAAACGG	6.053206934
GGAAATACCC	GGGTATTTCC	6.048761983
GAACATCCCC	GGGGATGTTC	6.046664403
AAAATTCCCT	AGGGAATTTT	6.045264
GGGGGAGAAC	GTTCTCCCCC	6.043492419
AGTAACCCCC	GGGGGTTACT	6.035293723
GAAAATTCCC	GGGAATTTTC	6.033912221
AATTATCCCC	GGGGATAATT	6.028420349
GACCTCCCCC	GGGGGAGGTC	6.02742239
GGGGAATGTA	TACATTCCCC	6.019993793
CGGAATTCCC	GGGAATTCCG	6.012392068
AGGGGGGTAT	ATACCCCCCT	6.003720251

GGGAAATACC	GGTATTTCCC	6.003639456
GGGGGGAGAA	TTCTCCCCCC	6.002383134
AAGAAACCCC	GGGGTTTCTT	5.995942217
CAGTCCCCCC	GGGGGGACTG	5.982896801
GGGGAAGTCA	TGACTTCCCC	5.978166581
GAGTCCCCCC	GGGGGGACTC	5.974220976
AAGCCCCCCC	GGGGGGGCTT	5.973608968
GGGGACTTAC	GTAAGTCCCC	5.971435201
AAAATTCCCG	CGGGAATTTT	5.968250714
AAAGCCCCCC	GGGGGGCTTT	5.963960106
AAACCTCCCC	GGGGAGGTTT	5.961713152
ATTACCCCCC	GGGGGGTAAT	5.961173585
GGCAACCCCC	GGGGGTTGCC	5.960120545
GGGGAGTTCA	TGAACTCCCC	5.948754082
TATTTCCCCA	TGGGGAAATA	5.946621177
ACGATTCCCC	GGGGAATCGT	5.942177874
GGGGGTTCAC	GTGAACCCCC	5.938916749
CGGGGGGGAC	GTCCCCCCCG	5.936571222
GGGGGAGCAC	GTGCTCCCCC	5.931320988
CAAAATTCCC	GGGAATTTTG	5.929585964
AGAATTTCCC	GGGAAATTCT	5.923471124
GGACTCCCCA	TGGGGAGTCC	5.905880586
GGGGAAGACC	GGTCTTCCCC	5.905529933
GAGTATCCCC	GGGGATACTC	5.896494968
CGGGACTTCC	GGAAGTCCCG	5.888990627
AGGGGGATAT	ATATCCCCCT	5.886578431
GGGGACACCC	GGGTGTCCCC	5.886530867
AGGGGGTCCC	GGGACCCCCT	5.885082684
GGGGAAGCAC	GTGCTTCCCC	5.875369784
GGGGGGAGAC	GTCTCCCCCC	5.875001993
GGGGGAAGAC	GTCTTCCCCC	5.867499831
CCGAACCCCC	GGGGGTTCGG	5.864490752
GGGAAATTTA	TAAATTTCCC	5.863555496
CAAAAATCCC	GGGATTTTTG	5.863189843
GAAAATACCC	GGGTATTTTC	5.855971616
CTTTCCCCCC	GGGGGGAAAG	5.843808974
AGGGGGGAGA	TCTCCCCCCT	5.84337873
GAAATTTCCC	GGGAAATTTC	5.842276462
CAACTCCCCC	GGGGGAGTTG	5.841240466
AGAAATTCCC	GGGAATTTCT	5.836000109
AGGTACCCCC	GGGGGTACCT	5.834266785
GTCCCCCCCA	TGGGGGGGAC	5.832719256
GGGGGGTAAC	GTTACCCCCC	5.82696806
ACTATCCCCC	GGGGGATAGT	5.826249553
GGGTATTTTA	TAAAATACCC	5.819434015
GGGGAATGCA	TGCATTCCCC	5.819106412
GGGGGTATAC	GTATACCCCC	5.814622576
GGGGAATGAC	GTCATTCCCC	5.814526639
AGGGGGGTTA	TAACCCCCCT	5.812335788
GGGGGAAAGA	TCTTTCCCCC	5.806653469
GGATAGTCCC	GGGACTATCC	5.802472632

AAAGCCCCCA	TGGGGGCTTT	5.80201894
GGGGGAGATA	TATCTCCCCC	5.801490491
GGGGGAACAA	TTGTTCCCCC	5.799977024
GGGGGGTACC	GGTACCCCCC	5.799242883
GGGGGGATAA	TTATCCCCCC	5.79875164
ACCCCCCCCG	CGGGGGGGGT	5.796692916
ACCTCCCCCC	GGGGGGAGGT	5.793821619
AGGGGGGATA	TATCCCCCCT	5.792972063
TAAACCCCCA	TGGGGGTTTA	5.784260555
AGGGATTTTC	GAAAATCCCT	5.78226787
AGGGAGTCCC	GGGACTCCCT	5.781863926
AAGAAGTCCC	GGGACTTCTT	5.781687362
AGGGGGAGAA	TTCTCCCCCT	5.776458331
ACTCTCCCCC	GGGGGAGAGT	5.77563381
GGGGATTGCA	TGCAATCCCC	5.774220158
AGGGACCCCC	GGGGGTCCCT	5.774096988
ATCTTCCCCC	GGGGGAAGAT	5.765910203
AGGAAGTCCC	GGGACTTCCT	5.757280901
CCATTTCCCC	GGGGAAATGG	5.753349492
GGGGTATTTA	TAAATACCCC	5.753107913
GGGGTTTCCA	TGGAAACCCC	5.752887801
GGGGAAATGA	TCATTTCCCC	5.751140128
GGATTTTCCC	GGGAAAATCC	5.746241506
GGGGACATTA	TAATGTCCCC	5.742810253
AGGGAAATTC	GAATTTCCCT	5.741103515
AAATCTTCCC	GGGAAGATTT	5.740840082
GGGAAAAACC	GGTTTTTCCC	5.735868277
GGCTTCCCCC	GGGGGAAGCC	5.735679996
ATAAAACCCC	GGGGTTTTAT	5.734130551
GAAAGTCCCA	TGGGACTTTC	5.732849895
CTCCCCCCCC	GGGGGGGGAG	5.731550208
CCTATTCCCC	GGGGAATAGG	5.726265996
ACCCCCCCCC	GGGGGGGGGT	5.714657736
AAAATACCCT	AGGGTATTTT	5.702868892
GGCCCCCCCC	GGGGGGGGCC	5.701154114
GAGAAGTCCC	GGGACTTCTC	5.699368757
GATAATTCCC	GGGAATTATC	5.699320134
GGGAGTACCC	GGGTACTCCC	5.698396241
AGGGGGGATG	CATCCCCCCT	5.69418072
CTTCCCCCCC	GGGGGGGAAG	5.692929173
GGGGGAGTAA	TTACTCCCCC	5.684295776
AAATGCCCCC	GGGGGCATTT	5.677506235
GGGGGAGTCA	TGACTCCCCC	5.674036277
GGGGGGGACA	TGTCCCCCCC	5.670947067
GCACCCCCCC	GGGGGGGTGC	5.667750992
TGGGGGAAAA	TTTTCCCCCA	5.667124648
AACAACCCCC	GGGGGTTGTT	5.664401821
ACCATTCCCC	GGGGAATGGT	5.662559892
GAAGACCCCC	GGGGGTCTTC	5.66094279
CAGAAACCCC	GGGGTTTCTG	5.658160979
GGGATTTTTA	TAAAAATCCC	5.655052415

GGGGTTTACC	GGTAAACCCC	5.653504497
GGGGAAACAA	TTGTTTCCCC	5.649041112
GGAAACTCCC	GGGAGTTTCC	5.647883454
AATTCTCCCC	GGGGAGAATT	5.647850842
CCAACCCCCC	GGGGGGTTGG	5.645472521
GGGGGACACC	GGTGTCCCCC	5.642198863
ACATCCCCCC	GGGGGGATGT	5.641358493
TCAGGGGAAA	TTTCCCCTGA	5.621827105
GGAAAATCCC	GGGATTTTCC	5.621581758
AGTCCCCCCA	TGGGGGGACT	5.619787786
AGGGGGTACC	GGTACCCCCT	5.617813434
GGACCTCCCC	GGGGAGGTCC	5.616987016
AAAATTTCCC	GGGAAATTTT	5.61130901
CCCGTTCCCC	GGGGAACGGG	5.607533397
GGCGTCCCCC	GGGGGACGCC	5.606509352
ATACTTCCCC	GGGGAAGTAT	5.605326767
GAATATTCCC	GGGAATATTC	5.599168114
GGGGGGGAGA	TCTCCCCCCC	5.596191016
GAACACCCCC	GGGGGTGTTC	5.584940258
AATGTTCCCC	GGGGAACATT	5.58273597
GGGAATGCCC	GGGCATTCCC	5.580988562
GGGGATTCGA	TCGAATCCCC	5.580566721
AACAGTCCCC	GGGGACTGTT	5.579481889
AAAAATCCCG	CGGGATTTTT	5.570041293
GGGGATGTTA	TAACATCCCC	5.566993613
AGTACCCCCC	GGGGGGTACT	5.565451526
AGAAAATCCC	GGGATTTTCT	5.561128349
AAGAATTCCC	GGGAATTCTT	5.560842805
CAACCCCCCC	GGGGGGGTTG	5.55161511
AGGGGTCCCC	GGGGACCCCT	5.550237927
GGGGGATCAC	GTGATCCCCC	5.549286687
GACATCCCCC	GGGGGATGTC	5.540159279
GGGGGATACA	TGTATCCCCC	5.539614295
GGCAGTCCCC	GGGGACTGCC	5.535718571
ACCCCCCCCA	TGGGGGGGGT	5.531071653
CGGGACTCCC	GGGAGTCCCG	5.530691413
ATCCTCCCCC	GGGGGAGGAT	5.522197716
GGGAGGCCCC	GGGGCCTCCC	5.520401953
GGGACATCCC	GGGATGTCCC	5.511966999
ATATAGTCCC	GGGACTATAT	5.510688329
AAATTTTCCC	GGGAAAATTT	5.504601653
ATCTTTCCCC	GGGGAAAGAT	5.49992939
ATAACCCCCA	TGGGGGTTAT	5.499597534
GGGGAAAGCA	TGCTTTCCCC	5.490521783
GGGAAACACC	GGTGTTTCCC	5.489466928
GGGGATTAAC	GTTAATCCCC	5.479740042
GGGACCTCCC	GGGAGGTCCC	5.474707391
GGGAAAATTA	TAATTTTCCC	5.46945251
GGGACTTCTA	TAGAAGTCCC	5.469125012
GATACTCCCC	GGGGAGTATC	5.467354089
GGGGAATCAA	TTGATTCCCC	5.464102734

GGGGGGACTA	TAGTCCCCCC	5.462377983
GGGGAAAAGA	TCTTTTCCCC	5.461222399
AGGGATTTCC	GGAAATCCCT	5.460038874
CAAATACCCC	GGGGTATTTG	5.458980229
AAAAAAACCC	GGGTTTTTTT	5.45756016
CGGGAATTTC	GAAATTCCCG	5.456973722
GGGAATTCCA	TGGAATTCCC	5.45677916
GGGGAGTTAC	GTAACTCCCC	5.456462292
CGGGGCCCCC	GGGGGCCCCG	5.453203987
ATAAAGTCCC	GGGACTTTAT	5.45074553
AACTACCCCC	GGGGGTAGTT	5.449118219
GGGGGAAGTA	TACTTCCCCC	5.444022861
CACTCCCCCC	GGGGGGAGTG	5.43862641
GCACTCCCCC	GGGGGAGTGC	5.41838009
GAAAAATCCC	GGGATTTTTC	5.417718342
GGGGATAATA	TATTATCCCC	5.406457954
GGGGGTATAA	TTATACCCCC	5.400089093
AGGGAACCCC	GGGGTTCCCT	5.400013545
GGGGACTATA	TATAGTCCCC	5.39667194
AAAACTCCCT	AGGGAGTTTT	5.391763502
GGGGGCACCC	GGGTGCCCCC	5.388749273
GGGGTTTTAC	GTAAAACCCC	5.388309376
ACTCCCCCCA	TGGGGGGAGT	5.388267346
AAAGAGTCCC	GGGACTCTTT	5.387978737
AAGTGTCCCC	GGGGACACTT	5.384766948
AAGTCTCCCC	GGGGAGACTT	5.382501712
GGAAACCCCA	TGGGGTTTCC	5.382210103
CGGGAGTCCC	GGGACTCCCG	5.378429496
ACGTTTCCCC	GGGGAAACGT	5.378334118
CTATTCCCCC	GGGGGAATAG	5.374290777
GAATAACCCC	GGGGTTATTC	5.3740887
CGCAACCCCC	GGGGGTTGCG	5.372716132
GGGGGTTAAC	GTTAACCCCC	5.362438689
GGGAATCCCA	TGGGATTCCC	5.35731077
GGGGTTTCTA	TAGAAACCCC	5.356098623
GATTATCCCC	GGGGATAATC	5.350581308
AGCGTTCCCC	GGGGAACGCT	5.349843894
AGGGAAATCC	GGATTTCCCT	5.348439253
CCCCCCCCCC	GGGGGGGGGG	5.34787339
AGGGGAATAA	TTATTCCCCT	5.343663428
GGGGGGTATA	TATACCCCCC	5.342798649
CAGTACCCCC	GGGGGTACTG	5.342130991
GGGAGTTTTA	TAAAACTCCC	5.330360893
ATTCCCCAGG	CCTGGGGAAT	5.325255921
ACCTTTCCCC	GGGGAAAGGT	5.325007508
CGGAAACCCC	GGGGTTTCCG	5.324795787
AAATAGCCCC	GGGGCTATTT	5.324050486
GAGAATTCCC	GGGAATTCTC	5.323827448
ACACTCCCCC	GGGGGAGTGT	5.318808949
ACACCCCCCC	GGGGGGGTGT	5.317037505
GGGGGGTACA	TGTACCCCCC	5.312410798

CGGAAGTCCC	GGGACTTCCG	5.308777195
GGGGAACGCA	TGCGTTCCCC	5.308024831
GGGGATCTAC	GTAGATCCCC	5.305852218
CGCCCCCCCC	GGGGGGGGCG	5.303619619
GGAGACCCCC	GGGGGTCTCC	5.30010966
AAAACTTCCC	GGGAAGTTTT	5.298331482
GCTTCCCCCC	GGGGGGAAGC	5.29639715
AGGGTATTCC	GGAATACCCT	5.292660348
GGGACTCCCA	TGGGAGTCCC	5.292521497
GGGGGTTGCA	TGCAACCCCC	5.290673707
CTGTTTCCCC	GGGGAAACAG	5.280353274
AGGGGGTAAA	TTTACCCCCT	5.278539736
GGCGTTCCCC	GGGGAACGCC	5.263255458
ATTTATCCCC	GGGGATAAAT	5.26297679
ATGTCCCCCC	GGGGGGACAT	5.259893776
AACGTTCCCC	GGGGAACGTT	5.257540946
GCTCCCCCCC	GGGGGGGAGC	5.257307619
GGGGGATAAA	TTTATCCCCC	5.248829522
AGCCCCCCCC	GGGGGGGGCT	5.24742233
GGGATTTTCA	TGAAAATCCC	5.233323318
GACAACCCCC	GGGGGTTGTC	5.228213962
AGCAACCCCC	GGGGGTTGCT	5.22747442
GGGATTCACC	GGTGAATCCC	5.219163722
GGAGGTCCCC	GGGGACCTCC	5.218206141
GCATCCCCCC	GGGGGGATGC	5.212232404
ATGCCCCCCC	GGGGGGGCAT	5.204628334
GGGGGAGGAA	TTCCTCCCCC	5.204087175
GATTCTCCCC	GGGGAGAATC	5.202847248
GGGGAATGGA	TCCATTCCCC	5.202646781
GGGGATATAC	GTATATCCCC	5.200389769
GGGGGACAAC	GTTGTCCCCC	5.193901817
GGAATGCCCC	GGGGCATTCC	5.193239561
ACCAATCCCC	GGGGATTGGT	5.191229542
CGGACTCCCC	GGGGAGTCCG	5.184220866
GGGGGAACGA	TCGTTCCCCC	5.17852475
AAAATCCCTA	TAGGGATTTT	5.175189717
GGGGAGATAA	TTATCTCCCC	5.174138092
AAATTCCCTC	GAGGGAATTT	5.17283631
AAGCTTCCCC	GGGGAAGCTT	5.170174652
GGTATCCCCA	TGGGGATACC	5.16890389
GGGGCACCCC	GGGGTGCCCC	5.167382752
GGGACTTTAC	GTAAAGTCCC	5.167218832
GGGGGCTTTA	TAAAGCCCCC	5.163997313
CACAACCCCC	GGGGGTTGTG	5.158814434
GAGAAACCCC	GGGGTTTCTC	5.158218531
ATCGTCCCCC	GGGGGACGAT	5.151444759
GGGGAACAAC	GTTGTTCCCC	5.150877153
ACGTCCCCCC	GGGGGGACGT	5.150491043
GACCCCCCCC	GGGGGGGGTC	5.148182667
AATATTCCCT	AGGGAATATT	5.144388767
AGGGGGGGGG	CCCCCCCCCT	5.139701713

GGCACCCCCC	GGGGGGTGCC	5.135427751
AACTCTCCCC	GGGGAGAGTT	5.132289451
AATGCCCCCC	GGGGGGCATT	5.131122759
AGGGGGGGGC	GCCCCCCCCT	5.12567704
GGGGACTCAC	GTGAGTCCCC	5.119606079
CTCCCCCCCA	TGGGGGGGAG	5.110711523
CGGGATTTTC	GAAAATCCCG	5.109197306
GGGGGAAGAA	TTCTTCCCCC	5.107969521
AAATTTCCCT	AGGGAAATTT	5.107717572
AAATACTCCC	GGGAGTATTT	5.104033043
CGGGAAATTC	GAATTTCCCG	5.098700394
GGGACTTACC	GGTAAGTCCC	5.098184341
GGGGAACATA	TATGTTCCCC	5.09667659
ACGCCCCCCC	GGGGGGGCGT	5.093358595
CAGAATTCCC	GGGAATTCTG	5.093080103
GGGAATATTA	TAATATTCCC	5.062620146
GGGGGACTAA	TTAGTCCCCC	5.062340645
GGCGATCCCC	GGGGATCGCC	5.0535608
GGGGGAGTGA	TCACTCCCCC	5.053114866
GGGGATATAA	TTATATCCCC	5.053039084
AAAGTTTCCC	GGGAAACTTT	5.049380343
CGGGGGGTAC	GTACCCCCCG	5.048835041
GAGCTCCCCC	GGGGGAGCTC	5.048056394
AAAATTCCCA	TGGGAATTTT	5.041891776
GGGGGGGTAC	GTACCCCCCC	5.039489486
GCAACCCCCC	GGGGGGTTGC	5.038307065
AAATTCCCTT	AAGGGAATTT	5.037293848
CGGGAACCCC	GGGGTTCCCG	5.036543347
GGGAATTCTA	TAGAATTCCC	5.035649667
GGGAACACCC	GGGTGTTCCC	5.034717921
CAACACCCCC	GGGGGTGTTG	5.032941771
CGGGAAATCC	GGATTTCCCG	5.032240557
AGAGACCCCC	GGGGGTCTCT	5.032223026
TGGGGAAAAA	TTTTTCCCCA	5.025856849
GGAGCCCCCC	GGGGGGCTCC	5.020799678
GGGACTTCCA	TGGAAGTCCC	5.018321179
GGGGGGGGTA	TACCCCCCCC	5.015355981
GGGGGGACGA	TCGTCCCCCC	5.013203881
CCCCTCCCCG	CGGGGAGGGG	5.01260061
AATAGCCCCC	GGGGGCTATT	5.010195885
GGGAATTTCA	TGAAATTCCC	5.000332619

As determined by PBM analysis fin Mansfield et al. (2017), these sites represent the top 25% most preferred binding sites for Aiptasia NF-κB. Sequences are listed by z-score.

APPENDIX II

One kb promoter regions of genes predicted to be involved in inflammation and oxidative stress response that were identified to be dysregulated in aposymbiotic adult Aiptasia in Lehnert et al. 2014 and the results of the promoter scan for each promoter.

Gene	Promoter region analyzed	Sites Identified
Upregulated genes		
Catalase	CACGGGATGTGTCAAGTGACGTTTACCACAGGAACCCCAAATC TCGCTTCAGGTTCATAAGAATCAAATTCCTTCTTCCTTGATTATTT TCACAATGTTGAAGTTTTTTTTCCTCAGATGTTTATATTCATCCATT TACTCATTAAGATAGTTGATTTCTTCCTTCTATCTCTATAAATTTGT TCTTTCTTTTATTTACCCGACCATAGRGACAGGGATCCCGAAAC GAAAACAGGTGTAACCAACAAAACTCATTCATCATTTCATTTCAT TATTAATTCGACCATTAACTAGAATTATAATCTTTATTTTTCCAAAA TATTACTAGCATCGGATCACTAGCCCCCATTCCCAAGTACCACG GACTGACCGCAGAGAGACCAGAGAGTTG**AGGGGAATCTC**CAC GAGGTTCAAGTCTCGCTACTGCGACGAATGTCTCGCTACGTGA ATGCATCCATTTTTTATTTTTTTATTGCACGCAACTTTTCAGTATTT TATTCCTGGAGATTGATTGACTTTTTGATTTATTGTTTGCTAACTC ATATCCGTTTGATCTACGGTTTTGACCCGCTTTTAGACGTCCATA TAAGCTCATATGTACATACGTAGAATTTCTCGTTTCAGCAACCAC TATCTGAAAATGCAGTATCATGATGACAAACCTCTAAATGGTGA CGTCACAAGTGACGTCACGGTTACGACCCACCTATGACATCACA GTTATGCGTCATACACATATTCACTTGACATCATTGCTCACAATTT CAGGATAAAATTGGTTTGAAAATATTCAGTACAAATGACATATTA TTAATGACACGTCCACTACGCTTTTATAATCGAGCCTTTATTCGC ATCTTTAATTAAATTTTCATTTGAAAATTAAATAACTGTCAATGTTA TGACTAATGTTCTATACAAAATCTCTCTAATAAATATGAAATTTCC TATTTTAGGAACTGAATAAGACTTTTATAAATAATATAAACTCATT TATTTAC	AGGGGAATCT: 7.5917821 GGGGAATCTC: 8.416353229
ADAM9	TTCCCATTTTTCAATCCTTAATTTAAAACTCAATTTTAAGAGCTCA ATGAAGAAATATATCCCGCGTTCCGCAATGATCTGCCTTTTGAAT ATGAGAATGTTTTWCATCAAATGAAAAACTTAAATGATTTTATTG ATATCTTAGTCTGAAAGATGAGGATCCTTCTGCTAATATTACTTT GCTGCTTCACTTTCAATGAAATTCGAGGTAAGATCAAAAAGTAG CAAATTACAATTCATAAAATATATAACTTTAGCTTATTTTCAAATA GAGCAATTTTATTTAATCCGTGAAATAAAAACTAAATAGTTCTTA ACAATCAGTCACTATTTTGTACTTAAATAGATGATAGCACTCAAG CGAATCAACTTATAGTTCAATACTCAGGAGACATAATTAAATACC CAAGAATCAAGTAATTTCATTTTTTTTCTTTTTTATTTATATCACA GTACAAATGAAATAAAGAATGAATGACTTAAATTGATTCTTGGG TATTTAATGTCTCCTGGGTATTGAACTATAATTTGATCCCCTGAAT GCTATCATCTATTTAGTATAAAATAGTGACTTATTGTTAAGAACTA TTTAGTTTCTATTTCACGGATTAAATAAAATTGCTCTATCAAAAAT GTGTTCTTTCTGAGAGTTTCTTTCGGCTGCAGCTTATCTTCTTTAG CGTGGCGACGCGACCATACCAGRAAAATGCTTCATGATGTTTG ACCAGGAATTGACTGACGTCAAACAAATAAAGTTCTACACCAAG CACCGGTTAAAATAATGCCATCGGTTTTGATCGACAGCAAAGCC ATTGTTTAGGCTGTTTTCTTTTATATTTATTTATTTTTTTWTGCTATT TATCGCGGTGCATCATTTAGGCATTCTTTACAAGCTCCTATCTTG CTTCTCTTGCTTACTACTTACTGGATTAGATATTGTGATCATAGGT GGTATACAGCAATATACGGAAATTATGATCTTTTTTTTGCTCGCA TTTCAAGTATACACCTAATTACGAAAAAGTTGTCC	NO

Transient receptor potential cation channel	ATCAAAATCTCTTTTCTTCCGACGGAATATGCTAGGTTTAAAATA AACTTGACGCGAATACAACGGGAARATCTCCTTTTTGCAAAAAC TTCAAGGAAATCTAGTGTAATTTTGCGTCATTTTCAATTGAAACTT CGTATTTAAGACTTGCATACTTGACCAAAAACGTCAAGTCAATCA TTAAAAGTAGTTTTCCTAACGTGAGAAGTTGTTTTTGTTTTGTAAA GCTTGACCGTTCAGAGGAAATGGCCAGASCAAGTGGTGTGAAA TAATCATAGTTAAAAATACTAGGGGACACTCGATGATAATGACA TTTTATACACCTCATAATAACTACCATCATAATGAATATTCATAAA TCATTAAAAGTCATAAAATTAAAATAATGAGAGAAAGATGAATC ATTATGAGCTCTTAAGAACGAAAATGCGACAAATTATTCTCAAAT ATCTGATTTCTATTGATTTCCAGAGATATTGTCCAAGCAAGAAAC CATGCTAAATTCATAGCATATGTTATCACCGGCACCTTGTAATGC TTTTCTCGCCGCTGGAGGCCAAAAATATAATTAAATGACTTATTA GAAAGGACAGAGAACACCTGGAAGAAATGAATGCCGTGGAAT ATTATTTATAAAAACATTATTTTGGAGAAATCAAATGCTTTCGGTT ATGAACTGAYTTTCTATCATTTCCTATTCGAATCGACCATGAGTT GATTTAGTATTTCGTATCACACGAAATCCTAACTATACCGAGCAC TTTATSACCTCATTATGTCGAACCGAGCTCTTGGATGTCGCTGTA CCTTTTTATTACAATTGTACTTTGCATTTTGTGTGGACCCCACTAT ATCGACCAAGGTATGAAATAATTATATAGAACGACCACATATAA CAGTGCCGGATCCAGGATTTTTCAAA**GGGGGGTTCC**TCTTTGTT TTCGCATTTTCCTAAAACGAACTTTTTTACTGTGCCTCTCGAACTG TAGCAAATTTAGTGTGAATATATT	GGGGGGTTCC: 8.979981241 GGGGGTTCCT: 8.428541438
Peroxidasin-related protein 1	TAACTTCTAAATTAGCTTGTTTGCACTTCTGAGGGTTTCTTAATAC AATCTCGTACCCAGCGCCACTGTCCCTCTTACTCACAGGCTCGC AACGAAAATCAGGGGCTCTGGAAATATCAAACACCGGAAGCCA GAATCAGGCTATTTCACCCATGCGCAGTAAAAACCCGATCTAAC GGCTTTATTTTACTCAAGAAAATCGGCTTAATGAAAGCCTTCGAA GTCAGAAA**AGGGATTTTTT**AGACCTTAGATGATAAATCTATCTTC TTCGAAGCTAGTCGATATCTATTATGATCAGATCGTAGCAGACA GTGACGGTTAGTGATTATCATGGCGTGACAGTTCGTCGCCTCG CTGTATTCCATTTTATACTTAATTGATCATATTACTCTCAAATGCC CACTTCATAGACTTAATAAATGCTTTTAAAGGAAGAATTGAAGGT GAGGTAGCGAAATACAGAATGATTTGAGTGTTTTTCTCGGTGAT ATTTTCACTTCCGGCGGCAAGTTGTTTATTTTATGAGCCAATCAG AGAGCGATAAATTTTCGAAATTTCCAGAGCATCTGTTTTTCGTCG AGCCTGTGAGCCTGCGAGTAAGAGGGACAGTGGTTCTGGGTA CGAGATTGTTCTTAATACTGCATGACCTGTCACGCATCCAGTCA CGTGATCCACAAAACCACATGGCCGGCTTGCAGCTTTCAACAG CCATTGCATCGAAGACTGCAAGAAAGCAGTCTCAAAATTTCCTC CCACCCTTCCCTCTACTCAGGTTTCCATCACTACTACTTTTTTCAA AGTTCTTTTCTTCCCAATGTGTATCACTGAATTACATTTCTACAAA TGAGCGTCTAATATAGGCATATTTTTTTTTCTTGCTGCTTACTTTC AAAAACGCATCAAATCTTAGTCGCGAACTGGGCACGGTAAGTT CCACATAGTGGTTCTATGAATGACTTTTGGTTTCTGGTTTTGATA TTACTCAATCTCGTGATTTTCAGTTCAGCAAC	AGGGATTTTT: 6.155383051 GGGATTTTTT: 6.436720029

Dual oxidase 2	GTTTTTTTTATAAAACACTTCAGCACCGCAACAATAATAAAGTAA TACAACAATATATCAAGTGAATATACCCACAAAACCTTTGGTCGA ATAGTGTTAATGAAATAACTCTGGTTAAGTTTCCATCAGTTTTTCA ATAAGATTATTCGGCAATTCCATTGGGCTAAACCTTCAAATATCT AAAGAGAACAAAGCTACGACAGTAGTATACACTATGTCATCAAG TCTATGCAAATGGTAAGTAACAATAGAATGACGTCAAAATGCAA TCAATACCCCTTCGGAAGACCAATAAACATGCACAGGAAGCCCT CGGAAGCGATCGACAGAACATATAACTTTAGTACGAGCGACCG CCGAAATTTCTCGCAACCAATGTGAATCAACCATCATTGCGGAT TTACGAAAATTTCTCGTGGATCGTGAAAATTCACTGCTGTGAAA GTTAACGACGTGCGTTTGCGTTGGCGAGTATATTCAAAGTTCTA TTAGTATTCTAAAAGTTTTAGGTCTTTCTTTCAGAAGAAATTGCTC TGAGCTCACTGGTTTCCATGAACAACAAAACACAAACAAAACTC TAAGAAACAATGGCTAGTTCCTAGTTAGAACTTCAATTTTTCATA ATAGTGACTAATATTAAACTATTATTTAGATTTTATTTCATGGAGA TATTGTTCGCACTTCATTATTACATTCATTTATATTCATTTACATTC ATTTGTATTTTAATAAAAAGTGCTTTGTCACCATTGCTATTAGCAA TATAAAACAACAACAAAATACATAGTGTATCTCGGCGGTGCGAC AGAAGTGGCAAAATGTAAACGCTGATTGAGTCTAAATATTTGTA TTCCACAGATTTACTAAACGCTATTTATCCGCTTCACTTATATTTA AATCGTAGTAGGCACATGCGCTCATTGGGTCTCTACCACTGATT GTTTATTACAATGCCTGCGATAGGTCTATTGGATGTACAG**CGGA** **TTCCCCA**AACAATAAT	CGGATTCCCC: 8.743524852 GGATTCCCCA: 9.564263131
Allene oxide synthase-lipoxygenase	GTCTGTTGCTTCTAGACACAATGGATCTCTATTTCCTAGTCAACT GTTCAGAGCTGCCTGTTCACCGTCCGTTTTCTGCTTGTGGTGTG TTTTCACAGGTCATACATACCCTATTTAGTTCTTTTTTCACTAAAT GTACAATTAAAGAGTAACTATCCCTACTTTTGTGACGATTCTCTTT TTTAGGTTTCCGAAAAATGCAGGAAAGTTAGAATACAAGTAATA TGCACACGACAGCCAGTACTAGTATAGTTAATACAAAATTTATAA ATTTATAGCAAAGATTTTATTTCTAGTTATCTACCATGGACTTATA ATATGACGAACGTGATGTAGCCTGATTGGAACTCTAAGTGTTGT CATGACAATTGCATGGGAAAGTTGAAATAGGCATCACTGTGTA GAGCAAAGACTTTAGCAAAAGAATGACAGAGATTTTTAAAGCTT GGGGGTCGAATAGATTTACGTTAAGGATAGCATTCGATCGCCA ATCGCGCGCGATTTAAGTAATCAGCCTAATAGAGTCTTTTGGGA GAAGAAAGAGAACCGGCCCCTAAACGGTAAATATGGACTTCTT GCGCTAGATATTCAGCTACTTGGTTGAAATAGAATTGTCGTTGTT TATTCATCAAGAGTGCAAAGCTGTTACTGTGATAAACTGCTTGTT ATCCATTTTGTACTCTGGGTGAAGCTTTACCCAGCATGCATAGC AAGGCGGAAGCACGACCGTAAAAGGTTTTCGCTGGTGACCGTA GTATCAGACACGCATGACAGAACAAGGTTGACTGTGAATTCCCT ATGTCTTCTTATCTTGTTGTCATTTTCAACTTTTAACGGAAATACA TTAACAGTTTGTAAGAAATATTATTTGACGTCTATATTCCTCTTGG TTGGATTTCATATCGAAGTCGACTTGACTGACATTTTTGTCGGTG GCTCACACAGTGTAAGTGAAATATTTACTTATAAAATAATCTCAA AA**TTATTTCCCC**TTGTGT	TTATTTCCCC: 6.877516478

Transmembrane protease serine 6	CCGATAGTGTGGTACACAAATGGCGATTCCTTCCATCCAAACGG GAGCGTTTTACAAACAAACCACCAGCCACTCCACTCAAAGCCAA AGAAACATCAGCAAGACTCTTGGAGCAAAACATGATCATAACCC GATTTGTGATCACATTTGGTTATGTAAGAATCCTAGCTTTACCAC GTATCTTGGGACGTCAACCAACTTATCCAACGTGAACGGGCTGT CCCGCATCCAAAGGTTAAGGAACCTAGCATCTAGACACAATCTA TGTTTTGACGGTTCCACTGTCAACGGAAGCACAAGGAATGGCG GCTCACTTATACTCACTTTTCTCCAAACCGCAATGTCTCCTTGCG ATACCCTCTTTAGTATCGTGTCTGTCACAAATGTCGAGAATTTCT TACACGAGGCATGGTTCTGCCATACTTTGGCAGGTGGGAGATC CGAGTCATAGCGGACTCCTTTGAAGGAACCAGAGAAATACTGC TGAAAATCCAGTACATTGACACCCTCTCTTAGCCACCTCTCTTAG CCACCCTCTCTGTTGCAAAATGACTTCCCATAGAGACAAGTCAA CATGGAGCCCTCCGGCCACAAATTCCTCTGGATCACGGAGGTG CAAAGTAGACAACTGAGGGACGCTTTRWTTTGACAGAATTTCC TCTACCAAAAAAAATAGT**ACCTCCCCCC**TGGACAGGGATCCCATC CATAGAAACCCATGATATCTTTCCAGCTCGAGGTTCTTCTATTAA CAATAGTTTACGATCAAACTCACGATCAGCGAACTCCCATTGAG GGGTTTTAAAACTGGGGTAGTCCTCTATTCGACGTCTTTTACTCT AAACATAAAAACAAACAAAGAAAGGTAAAGGGAGAAGACGATA AACCGATCTCATCATACAGGAATGAAAGTTTAAGG**AGTACCCC** **CC**ACATGATGGGATCCCTGACCAGGAGGGAGCAACTACCACG CCCACGCGAGAGTGAGACGCACCACAGACCGCCCAGTTGAGA GGCG	ACCTCCCCCC: 5.793821619 AGTACCCCCC: 5.565451526
Mannan-binding lectin serine protease 1	GTCGCAGTAGAACGGTAGTTATGACGTGGGTGAATGACACGG CTGATTGACAGCTCTTGATGGCTGTGACAGRAAGCACTTGAATG GTTTTCAATCTGACATGCAGGGCTGTGAATGGCTGCAAATCAGT CCATCAAGMGGGTCACTATGATTGATRTCCGCTACACTGCGTTC AATGAATTATAACTGTTTACTTCAAGCTATGTCTAACGTGTCGAC GGGATTTCCATAAGGTCAAGAGCAACTTCTAAAGCAAATAGATC AACTGAATTTATCTTGTATTTATGGAAAGTTTGTATTCAAGAAAG GAAATGGAATTCAAAGAATTTCAAAAATCAACAGCGAAGTGCA GTTAACAGCACGCAGCCGTCTAGCGAAATACACGAAATCTTGAT GTGTTGAAGTATCCTTGGACGTGAGCCCAGCGCATAACGCAAG GACATTATATAAATTACGTAACGCATTCGCGAGCGCCAAAAAGA AAAATAGCGCTTGCGAGAGAGCCAGGCGTGCAATAAAAGGAA CTTTAAAATTACGTATTGGATACGTGCGCGAAAACTCGACGTTTT CATTATTTGGTAAGCTAGTGCGTATAACGCAAGTACGTAGGATT GAGTCAAACAAACAAACGTAAGAAAGTGTTAATTACGTAACGCA AGTGCATATGGCAAACGTGTATTGCA**AGGGACTTTCT**TRCGTCA CAAATGCGCATAATCTCAACACATCCAAAGTAATGAAGGTTTTAT TAATAAGTACCACTTGCGCGTAACTCAGACGTATAAACGTAAGA GGCGATTAATTACGCTACGCATGCTCGTCATCCCTAAGAGATGT AAAAGGAGCATTTTTCGTTACGTTCAGCTGCTGTTTTTCTTAAGT CAGACATGTAACGTAAGAAACTTTTATATCGTCACACAATAGCG CTACTCTGGGTACCAGAGTTTGGAATGTTAGACTTTGGAAAGAG CATACGCGAATGTGTAACGTATTTACTCTTAAAACTC	AGGGACTTTC: 7.14376165 GGGACTTTCT: 7.555424628

Plasminogen	TGTAGAAAAAGCAATTATTCTTGTTTGCTAAATTAATGTTTTTCTT AAAAAGTCGATAAATTTAAGGAATTATACCGAAGCAAAATAACA AACAACGTCAACAACACAATCCACTTTGTTAGTGAAATTCAGTTT CATGTGCGTTTTCTGCCTTAACTCAAAGATTTCCAGAAGAACTCA TCAACAAAGTAAGTGGAGGCAAAATTTTAATTAAATGTTTGTCA GTCAAAATTTCAGTGTATTATTGAACACTC**GGGAGTTTTT**TTAAC TTGAATAGGAACTATATAGATCTTGACAGGTGACCCTCACCTTCT ATGACCCGCTAGCACTTGGTTAACTTGCAAAGGAACGCGGGAA AAGCTGAACTCAGGAGATAATTATGCCGCTAAAACGTCGAGTA AAATTCACAATAAACCATTTAGACACCACTTTTTTATGTCCCGAC GTTTTAAATACCTGGTGCATCTGCAAAAAGCTAAAAAATCTTCTT ACAATTACTCAATGAACCATACTATCATATATTAACAGTTTAAATT AAAGGCAACCACCATCATGACTTAGATGACACATAAATTTGTCA TGACCTGTTTTTCGACAACTAATATCAATTCAAGACAAAAGCTAA ATTCAGTCAGATTCAGCTGATCTCGTCGTGTGCTGTGACGTGAA GGTAAGAAACCTAATTTTGAACACACATAAAATTCACTGTGCAT GTAGTACTAATTTGTACAAATTTGTCTAAAAGCCTTATAAAAAGA GCAAACTTACTAAATCCGTGAAAAGAGAATTGTACAAAAATTAC CAAATTTGCGAATCCCTTTGTTCTCTATTGTCACATTAACACTATT TAGCAGTAAATAGTAAAGTCATTTTCATCCGTCTGTGAAATAGG AATTGTACTATTAAATA**CTATTTCCCCCT**ATTAGCTCCCAATAGTT TAACTTATGTCATGCGACAAATTATTTAGGCAAACACGGTTTTGA GTTTGCATTTTGGTAGCCTACTACACC	GGGAGTTTTT: 6.440496328 CTATTTCCCC: 6.346695814 TATTTCCCCC: 7.301118147 ATTTCCCCCT: 7.68834808
Ephrin type A receptor 3	ATTGGTCAATGATCAGGTTTCAAACCTGAGACCTTTGCTAGGGT CATACACCTTAAGTAACAATGCGCTTAAGAACTAGGGAACTCTC TATTGTTCTGCGGCATTGCAACTTTTGCACGTACGAATGTCTTGG TTTTCACAATGATTATGTATCAACCTATGGGTAACACATTTTTGAA ATAAAATGTTGAAAAACTCTATTTTGAAACAAACTTTCTTTTGTAT TAAAAGCTCTTATCCAATCATAAGCACTCAAAACAATAGCCAAAA GATGATTCTACTTTGC**TATGTTCCCC**ACGTAGAATTGCATTAATA TTGAAGCTAAAGAAAGCTTTAATGAAAGTGAAAACAGACATCAA ATAAAATATTAGAAACTGCGCTAACTTGTGAAATTATAGCAGATT TTCATGTTTTAACCAATGGGATGTATGGATTATACAATGCACAAT TAGCACCTTCTTGCATTCCTTTGCCGTTTGCTTCCCTAGTTCTTAC TCGGGGCATTACTTAATATCTATTCTAGAACTCAATAATTTATGA GCTATTAGTCCAATGAGCATCGAACTATTGGCTCACATGATGGG CCTTTATATCCCGATAAAGCACTGATGTTTTATTAATCAGTTCTAT ATCAGATATATAGAACCGATGTTTTATTAATCAGTTCTATATCATA TATAAAGAACTGATGTTCAAGGTCATCAGCGCTTTATCGCAACC CAACACTAGCAAAGGTCTCAGTTTTAATGTCGCATYAYAKRCCTT TGCTAGGTTTTAAATCAGTTTGAATCAATGTGCAGACATGCAGT ATAGCATAGACYAGCCGTTCTTACGTGTGGGATCAAAATTCTTTC AAATTGTGGCAAATGCACATGCTCAGTAGAAGTTTAATATGCAT TATCACTGTTTTCGCATTTTTTAGCTTTTTTTCTAAAATGATAACGA TTTCTGGATGTTAAAATTCTAGAAGTAGTATAAAGAACTCAAGA GTGTATTTTATCGGGACTAAAGA	TATGTTCCCC: 5.09667659

Phospholipase A2	ATTGGTCAATGATCAGGTTTCAAACCTGAGACCTTTGCTAGGGT CATACACCTTAAGTAACAATGCGCTTAAGAACTAGGGAACTCTC TATTGTTCTGCGGCATTGCAACTTTTGCACGTACGAATGTCTTGG TTTTCACAATGATTATGTATCAACCTATGGGTAACACATTTTTGAA ATAAAATGTTGAAAAACTCTATTTTGAAACAAACTTTCTTTTGTAT TAAAAGCTCTTATCCAATCATAAGCACTCAAAACAATAGCCAAAA GATGATTCTACTTTGC**TATGTTCCCC**ACGTAGAATTGCATTAATA TTGAAGCTAAAGAAAGCTTTAATGAAAGTGAAAACAGACATCAA ATAAAATATTAGAAACTGCGCTAACTTGTGAAATTATAGCAGATT TTCATGTTTTAACCAATGGGATGTATGGATTATACAATGCACAAT TAGCACCTTCTTGCATTCCTTTGCCGTTTGCTTCCCTAGTTCTTAC TCGGGGCATTACTTAATATCTATTCTAGAACTCAATAATTTATGA GCTATTAGTCCAATGAGCATCGAACTATTGGCTCACATGATGGG CCTTTATATCCCGATAAAGCACTGATGTTTTATTAATCAGTTCTAT ATCAGATATATAGAACCGATGTTTTATTAATCAGTTCTATATCATA TATAAAGAACTGATGTTCAAGGTCATCAGCGCTTTATCGCAACC CAACACTAGCAAAGGTCTCAGTTTTAATGTCGCATYAYAKRCCTT TGCTAGGTTTTAAATCAGTTTGAATCAATGTGCAGACATGCAGT ATAGCATAGACYAGCCGTTCTTACGTGTGGGATCAAAATTCTTTC AAATTGTGGCAAATGCACATGCTCAGTAGAAGTTTAATATGCAT TATCACTGTTTTCGCATTTTTTAGCTTTTTTTCTAAAA TGATAACGATTTCTGGATGTTAAAATTCTAGAAGTAGTATAAAGA ACTCAAGAGTGTATTTTATCGGGACTAAAGA	TATGTTCCCC: 5.09667659
Arachidonate 5-lipoxygenase	TGCCAATTATCAACGGGTGAAATGATATGACGTCAT**GGGGGGT** **TGTG**GCATAACCGCATACAAAGAATAAGTGTCAAGCTTTCAAAA TTCACGTACAACCCAGCCATAAGGTTACAGCTTTTACTTAATTGC GGCTTCAAAGATCGATTAACTTCTTAGTTGACTTTCTAAACCAAC CATAATCTTTAAGAATTATCAAAAATATGAAAGAATTTTATGTATA TTTAGATAAACAATGTAATTTATTGATTTTACTATTCGGCTTTGCA TTTAAGTAATAGCTTCATTCAATTCTCTGTTTTAWTATTGTAC TATTCATAACTAACAATGAGGTGAATTTGAAGGCTTTTGCATCAT GATTGGTGAAGTCTTGAATTTTTAGTTTGCGTGAATGGACATGC AAGACAGACTCAGTCGTCGCGTGCTTTCACTTTTTTTCGCCTTGT AAAATATTTTCAGTTTTAGTATTAACCGGAACAAGCTGTCATTCC CATCGTAGCAAAATCAAAGTGAAGTGTTKTCATTCCGAAGAAGA ATTTCAGTTTAATCTCCTTTTTATTTATTTATTTATTTTTCTTTTTTTT CTATTGTAGTCCCATTGTAGTCCCATATTTTTAAAACTATAAACAG TAAATTCATAGATATTTATAAAAAGTGAATTTACAAGCTATGTTAA TATTAAATTCGAGTGATTTGCATTTAGAAATAACCTGCGTAGTTG CTGCGCATGCGTACCAAATTATACCTCTTCTCGYCATTTCTTATGT TTTTATGGCTTTCTTCAAATAATTTAACGTTGAATCGTGTATTATA GAGCAAATGAGCTTATATAGAAGCAAAACTGTTAATAAAAAAAC GCTTTTTTATCTTTAACTATATCCCACATGTTTGAATATTTTTGGC GCATGTATGSCTCAGTTCCTCGCTYTCAGTTTCTTTGCCTTAAACT AATGAGTAAGGAAAATAACGATCTGGGTGACGCCAGATCCTTA CGATAAGTTT	GGGGGGTTGT: 6.238079923 GGGGGTTGTG: 5.158814434

Transcription factor E2F3	TAGTTACCTAGGATCAATCAGTGAGTCACATACTAGGTGAATCCGTAC AAGAAAAAAAAAAGATTTMATCAAATTTCATTGATGCTATTTCATCAATA TCTTTTATAAGATTTGATGGATGTGACTTACACTGTAACACTAGTACAC CAGCATCTACAGGTTATACTTTCAATTCCATATGTGTGTGAAAATGTTTT CTTTGAACTGTGCTTTTACATTGGCTTATAATTTGCAGAAATATTCATAA ATTTAAACAWTTTTTATTGACAGTTCCCTTGTTTTAATGCCACTTGTAGT ATCTTATATCTACTAGTAAAGTCTCTGTGTACTTCTTGTTCCACATGTAT ATGAATCATATTACATGGATATAATRTTACAATTTATAATCAACCAATCA CATTACTATGTACATTACTACATTCCTCCCCTTTCAGAAATAATCATATA CATTATTAATAATAATTAATTTTTTKGAATATAAATTTAGCCATTCATGAA ATATTAATTCACAATAATTTTTGATTTCAAAATTTTAGTTCAACAGTAACT TATCAGTGTTCTTAGAGTAAATGTTTTCTTTCAATGTTCATCAGTTATCT GTGAATCCTCTAAGGTAGGTATCAAAGGTAGACSTCCTCTGTCTTTGT GACCTTCTGAGTGGTTGTGGAAGTGCTGGTTCTTTGATGGAGTGGCA ATTCCTCTGGTAGGTCTGGTAGTTGCAGTAGCTTGAGCATATGTTGGT GCGATTGCTAGCATATCTGGTGGTGTAGGGTTGTCTTCAGCCTGCTCT TTCAGTCCCAATTTCAAGGCTTTGATTTTTGACGCATCTCTACAAATGG TCTTTCCATCACTTAGACGTCTTGCAATGATGGATGATCCCTTGATAAT TGTGGCTATGTATATGCTTGGTTCATACACAKTGTCTACAACTACTGCA TCACCTTCTTGCATGTTGTGGGTTGAYGCACTGTATCTTTTTTCGTGGT ATTGCTTACACCTTTCT	NO
Receptor-binding cancer antigen expressed on SiSo cells	TAATAACGACATTTTCTCGTGCTCTCTTTTGTGTTTGGTCAGGTCTTTGC GCAAGAGAATCTGTTGTTAAATAAAGCAGCGGTTTTGCGCTATTCGAA ACTGGAGTATTGATCTTAAAATGTCAAGAGTAAATAATTTCTCCATGTG ATTTATAAGTAGAAATTATTTACTATGTCTAGTTGCACACAAAACAAAC GGAATAACAAGATGGCAAGCTGAATAATATCCTGGATAATTGACCCAA CACAATGTACAYGCAGCACAATGTTAAGAATCACATTCATTGAGAGAA ATTTAGAGTAAACATCTGAGTTTCAAATTTCAAATTTATTGTAAAACAG GGCTCGAAATAATGGCTGGTCAAAGGACAATGTCCTTCCAAATTCGCT AGATGACCAGCCAAATCAGGTTTTGAAAGCACAAATTGACCTGAGAC ATTTTTAGACAAATAAAAAAAACAAGCAATTCTCAATTGGCTAAATAAA TCTTTTACAAGCCATTTTAAAAAATGCTTGCCGTTCTTTCTGAATACAAA AACCTATGAATTTATAAAAGAAAATAATAGTATAATACAGTTTTTATCCA CGACATGACCTGACAAAAATGAATTATCTTTTCAATGTATTATTTTAACT ATAGATATTCAAAGACTTTTCGTTAATGTTGAAAAACGAATAGACCACA AGCCAATTAGTCTCCTCGCAGCCGTTCTTAGTGGTGGGCTCCCTGTCC CCAGCCTCACTAAGAATGGCTGCGAGGAGACTGGAAGCTAATGTCCA ATTGCAGAAAATGTATTAATGTGACAGGGTCACTTTCGTGACCAATGT CAGTAATTTTTGGATTACATAATTAAGCATTTGTTTTGTAGTTAAAACTG TTTTACTGCAAATCTAAGATATGATTTAGTCAAAAGGGCTTATTTTGTTR CTGTCACGATATCTTGGGATTAGAACCTGAGTCATGCAATACTCATGT GATGTAATTTCCTGTCACATCAACAAGCAGATAAT	NO

Tumor protein p73	TATATGCGTTCGCGAAGCTTTGAACATTCTAAGCAGATATGGATAAAT ATGCTACACTTAACTAGACCGTGCAATTTCAATCAATAGTGCTTTAGCA GGTAGATATATCTATGAAATATTACATTCTTCAACCGCGGCAGCTACTG CATGCCAAAAGGCTAGTACGTTCTGAAGAACACCGTGAGAGTGCCGG AATTTACGGTCATTTTGCACCAAAAATCTCTCGCACATCAATCATAGAG ACACTGAGTCTAAGAAAGCTAGACTAGATGCGTAGAAATGTGGAAAA CAGCTGAAATTTAGGTGAAATTCTTACCACAAAAAGACGCGCAATCTT CACACCGCACCGTTCTGCATCAACACTTTGACAGTTTTCGCACACGTG AATATGCAAATTTCACATGCAAAAACACAACTCTAGGGGAGTAGGGT GGTATATGCATTGGACAAAAAGTGAAAATGGGAGAAAAAAAATTGTA AGAATAATTGTAGTAATATTTCTGAGAGAAATATTTTTATGATGGGCTA CAAAATATTTCAACCATTTGGGGGAAAATAACTCAGAAATTGTAATTTA ACTGAATCCTTTATTTTGTATTTTTATTCTTTTAATCAAAATGTATTTCAAT ATGAATTTATGATTTAGCACATGCCAAGTGAGTTTCAATAATCAAGTCC AAATTGGACAAAACAGTTATTCAATTCATTTATTTAAAAAACATAACAG CAAACTTTAAACCACAGGCAGCCCAAGCTAAGCATTTAACTAGCAGAT TATAGCGATATCTATAAATGTAAATACGAAATTTTTGAAAGAAAAAATA AGTAAAAAAAAATTTGTCTTACCTTATGATGTGGTCTTAGTTATGAATTTA GTCGTAATTTTGCCGTTTTTCTTTGATATCTCCCGGCCTTTACTTATATC ACTGAAAGGCAGGACAGACCGGCTCGAAAAAATTCAAACTCATTCCTT TATTAGCTAGTTATACTACTTACTCGTTTCCAGTTTTC	TGGGGGAAAA: 5.667124648 GGGGGAAAAT: 7.677505359 GGGGAAAATA: 6.980496055
paired box protein Pax-3	TTTCTTTCTCGTCTTTGTGGAGTGCGTCGGACATGCGGAAATAACACA TGACCTCATTTAAATGGAATCTTCCTCAGGACCAAGTAGTACGTTTTTA AGCATGATTGAGTATCAGTAAGCTTTCCAATGCCAGTTTTCAAGTATGT AATTAAGTGTTCATTTATTGCCGGGCATTTTTAAACCTTTCGAAAAATGT AATGAGGTATTGAAACATGAGATTCGTGTTTGATATAATTGCTTTCGAA ATTATTCGTAAAGAATTMATGGTCGGAGAAATTCAAAGCAAAAGTTG GCATGATCTTATTTGAGAAGYGACTTTCTGGATTTTAGGTGAGGTACA CTATTGGTACACTCCTATGAAATTAAAAAAAAAAATCGCGAAAAAAACA CAAGTCAGTTCATTTATCGTGCTACTAAACTTGCTTTTGTTTACTTTGTA CTATATTGCTMTTCATAATTAACTGCACTTTATTTGAGGATGAAAGCGA AGTTTATTAGTTTGTCTTTAACTTACACAGAGTCACTTTCTAGCGAGTTG AATATAAATTGATTCACAGGTAACTGGACTTTGACCTTGAAATGCTTTC TGGAAGTTCTTATAGAACTTAGCCTCTTATAACTTAGACTTTTGAACATA TTTTTGAATGTTGTTTTTAAACAACATCAAATTCGCACGATTTCCTCTTA GAAGGCGGTATGTATAGCTATTTATTATTGTAAGCTATACCTCTATAAA TTGCTAAATTGTATATTTGTAAAGTCTTATATATAAAAATATATAAAATTT ATCTATTGTAGTTGAGATAAACTATGTTGTGTATCTAAAATTGAAAATG CATGCCAACAAAGAGTGCTAGAAATTAAAGTAACAATAGACTCTGATG ACCTGATGATAGCAAAAACATTTAAGAACAAAACCCACATAGAATTTC ATCTTTCACATTTTTAACAATTATAGCCAAATCAAAAGTAATTTAGATTC CCATATATCTTATATATGAACTT	NO

Apoptosis-inducing factor 1	TAGCAATTTAACAATTCAATACTTTAACTTTCGTGGTGTCTTGTCGAATT ATCAAATACGTCGCGATGGCGACGTTTTGTAACGCAATACATTTCCGC GTATAGTTGATGAGAAACATTCACTTCATGCTATTTTATTCTTCTTTCCA TTAGTTCTTTACATCTCTTCCCTTCTTTTTATATCCATTTTTCCGTATATTC TTCATTTTCTTATAACATGATGATTAATGGTCACTTTTGGATATCTCCTAT TATATAGGGCTGCAACATGGGAGTATTCAGTATCCGTTACGGAATGCA AGACAAGCCCCAAGACTAAAACATGAAGACCTGTCACATGAACTAGA AATATCATTAACATTACAGCGTTTTGGAAAACTTAAGTTAAAGTCAACA ATATCCGCGTATACAAAAAAATAAGGGTGCAATCAGTACTGTGTGGTT TAAAAACCCATTTTATAAAACGGCAAGAAGAGAAAAATATTTCGTCAAT ATGTTATTGAATTGAATGTTGACCATTAGTTGAATATCAGACTAGTGTA TACATCGATATTCCTAATTTTACAGAATTTTTCCAAAACACTGTATACAG AATTTGCACTAAATGTAATCAAGACACAGATATAAATAATTGATATCTA TTTGAATATTTTATATGTTTATCGCTGAAATTGCATGTAAATGGCACTAG AAATAAAAAGCGAAAAAAGTACCAATAGATTGATTATTTGCCTTGTACC TGACTATATGATAGTCTTTACTCCGACGAAGGATTAACGTCCGAAACG TCAGTAAGTTATTCCACATACTTTTTTACGGTGTTAAATTTATCTTTTTAC ATAATTATATGATAGTCTCCTTCGCAGCGCCCTTTTATCGGACAAAGAA GGGTGGGCTGCGAAGGAGACTGCAATAGATACATCACCTCATTAAAA AAAATCGTTTAAGTCATTGGGCTACCTGTGCTTTTATGTGAGCCAGTG ATTTTCGAGTAACA	NO

Downregulated genes		
Soluble guanylate cyclase 88E	ATAACTTGGAGATCTTATAAGAGGTTTATTCGCCGTGCGTGCGC GGTTGGTTGCACAGGAGCAGGTGTTAGATGGCATACAGTGTGT TTCAAAAGGTTTACCGCTGAAGGCGGAAGCATTACGAAATGAA AAGTGTCGCCGGGCATTACGAAATCAGTAGTGTCGTATTCCGG TGACTCTAAAACGAAGCTGCCCTAGAATCAGCTTTTTTTGCTATA TTTTTGTTTGAAAAAAGCAAAAAAAAAAGTGCATTAAATACATAT TTCTCATGTTGTGTAAATATTTAAAGTTTCTTTTGTTCTTCTGTCCT CCACCAGTATTTAAACCAGGAATTTTACGGAGACCAGTTTCGCT TTATTAAGCATTTTCAATCTGTATTTTTTGTAAAATTCATGGTTTAA ATGCTTGTGAAAGACAGAAGAACAAAAGAAACTTTAGATATTTA CACAACATGAGATTTTTTTCAAGGTCTTTCGAAATCAAAATAAGA AACATTTCAAATAAAACTACCAAATGTTATAGTCACGCAAATGCC TAAATACTAGATAATTTTAAATTTCAATCTAGTAAAAGAATTTTAA AATTCATTTTTCAATCATTTTCTTAGCCAAATTTCCTCCGAGTTATA ACTTTAGCTCGAGTGAATTGTAATGTGAAAGGAAATATGCTAAT GAGAGTTGACAGACTTTAATTTCCATTGTTTTTTTTGTTGGTATTC GAATATTGCACTCTAAATTCCCATTCACACCGGTGAATTTTGTTG TTATTTCTTATGCGATTTCTCAGGCGAATATCAAAAATACATAATA GATTTTGTCTTATCCTTGTGAAGAGAAGTTTACTTAGCTTATCTCT ATACTGAACACAATTTTGCAAGTAAATTATTTAACATTATAGGAT CAAACTGATCGCAAAATCGCCGTTAAATACGCCAGTGTAAAAAC GGGCCTTAAATGTTTATTGAGTGATCTTTCTCAAGTTTATATTACT AGAACTTAGAAGGAC	NO

Peroxidasin-like protein 2	TASAAGCGTTACGTTTTTCCTACGGAACTGGAAGTCTCMTACGTAATA ACGTAATGATGACTAATGATMTTATCTAAGATTAGTGAGTAGGGATTA GCTATACGACACGTTTCCTACGTGAACCATAATTATCTAACTAAATAAT GTTGAGGGAAAGTAAGAGCGTTTTAAAACTAACACTTCATCATCAGTA TCATAATAATATATCCGGCAAGATTCGCTAGACTAGACTTTTTTGGTTC TTATCGTATCTTTGATTGTCTTATTTTAATGATACTTAAATTTGAAAGATG CAATTTCTCTGAGAGTTTTCTTCTCTTGCTACAAAGCTGGTATCTATTTC CTACGATTGATAAACCCACTCGAGTTTACAGCAATTCAGCAACTCTAAT AGACAATATCCTCACAAATAACCCTGTTCCTGGGATRTGTAGTAGAAA TATTGTTTCGAGCGCTATTCCCAGTTTCTTTATTGAGACTAATACCCTCC AAATAACAGTCTTACATAGATTCTGTATCACAATTAATGTATGACATAAT CAATGACAGTGCTCCTAGGAACTTAAAATCGCTTTTTACTAGTACCAAA GAGATTCATTATTATGAAACCAGATCTTCTATACAAAAAATAATCTTTAT ACGAGATTTTCCAGATTAAATCTACAAAGAGATTCCTTTTCTCGAGTGG GCGTAAGATTGTGGAATCAAATCCCAGTTTCTTTGAAATGATCACTGTT GAAATTTCGCTTCAAAAAAGAAGTTCGACTAAGTTTATTTGACTATTTA AGAAAAAAATGGTTACTATTGTTAAATCTCAAAATTATTTAAGTAATAGT TCAAACAAAATATAGTAATAATATCTAATAATAAGATGCTTTACCTCAAA TTATTATTATTTTTCTWTTTTCTTTCTTTCTTTCCCGYATATATCTATCAAG TATTTATCAAGTATATATTTTCCTCATACTCTTCTATTGTCATTGCTCAAC TGTAAAATATTTTTAAG	NO
Ficolin 2	TCATTGATAGATAATCATTCTCTTCCGTATTGATATTGGAGCTCCACTAT TAGGTATTACCTAATTTTTATATTATATATATAGTTTTATTGAATAGAATT GTTGATGGTTGTACCATAAAATGAAGGACTAACCTGGGCATTTGCTTG GATTGCATTTCCTTGATTCTTTGTCGTTTCCAGTGCAATTTTCACCACCA TTGGCTGGCGCAGGATTTGTACATGTTCTTGATCGTGATTGGTCGCCT CCACCACACGTGACTGAACAACGTTCCCAAGATGTCCAGGTTGACCA ATTTCCATGGACTAATGTGACGTTAATAAAAATCGAAAATCGATCAAAA ATTAGCGTACAAAACTATGTGTATTATTTAGACTATTTAATGTACACTGC ACATGAGAGAGAGTTGTCAACTAAAACAGACTTTCAAGCAATTCTTTTA TGCTTCAATACCCTTTTCGCAGTTTTCTCCACCAAATCCCTTGTTGCATT CGCAGTGAGAATGCTGCCTGTTCTCCTGCAAAACGCACTTGCCGCCAT TACGACAGGGCGTTTCTTGGCATGGATTCTATAAAGACAAATACGGAA GTCGTTAGATTATGACTCAAAATACATGCATGTATTATTTGTTAGAATAT AAACACGGTAGACTTAGGTAATCTCTGGAAATAGAGTCGTGAATAATT TTAAGTTTAGAGCAAAATCACAACAAGCGACATTTCCCTGAAGCATGT TGCATTGGCACCTTGACATTCACTCAGTTTAAACTACAGGATAGCAATT TATACCTGGCATTTTACGAACATAGCTACTAACAGTAGCTATTTTAACC TGTATTTATAGAATCGTGCGAACCAGAAGTTGAATTTTAGATATACGC GCGGTATCCATAACAACGGTCTCTTTGTAAACACTTTGCATGCTGATG AAGTTATTATAGAAGAACGAAACGTCTAAATAACTTCATTATATAATCA ACCCAGAGACAAAGGATTTTTAAAGTGTTTAAA	NO

Discodin, CUB, and LCCL domain containing 2	CGAGCATTTAATGAGTTTAAGTTTTGGGCGTCAAATTATAAGGAAATT GCTATCTTGCCCTCTAATAGTGGTAGCGTTGGTCTGTACTTGGAGCAT TTAATTGAAGACAAYTGCGYGTATTCAAAACTTGAGTCGGCTTTTTATG GTATTCAGTGGGCGCATAATATCTATGGTCATGCTAGCCCTTGCCAGT CGGGTCTCGTCAAACACATTCTTGAAGCAGGCAAGCGTAAGTTGCGT AAATCGACTGTAAAGAAAGAACCGGTTACTTATCGTATGATATCGGAA CTRTGCTCCAAGTTTGCTGTTCCAAGTGCCAATCTGGCCGACCTAAGA TTAGCAGCGATCTGTGTTACARCCTTTAATGGGTTTCTACGTTATAACG AACTTTCCAGCCTCCGGTGCTGCGATGTGAAATTCTGCAHGAGACAG CCTGATAATTTTGTTGAACTTTACATTGWCCAAAGTAAAACTGATATTT ACAGGGATGGTGCTAAAGTGCTGCTTGCCGCATCTCATGACCATTGTT GTCCTTTTACCATACTTAMTAGATATGTACATGCTGGAAGTCTTAATCT TTTTTCTGAGGAACCATTTTTTCGCAGTTTATATTTTGTCAAATCGTCTA ATAGCTATAAGCTTAGATCTAGTGGGATGAGCTACACTCGTACGAGA GAAATTGTTTTGTCTGCCTTTGARAGYATCGGCTATGAYAAAAAGCAGT TTGGTTTGCATAGTTTGAGAAGTGGGGGTGCGACAGCCGCAGCAAAC GCCGGTATCAACGATCGATTATTCAAGAGACACGGCAGGTGGAAGTC TGAAACCGCAAAGGACGGTTATGTCAAAGATAGCATAGATTCCCTACT TTCTGTTTCACGTAGTTTGGCTAAGTGTGAATGAAAAAAAAAGAAGAA GTTAAATGTGTTTAGAATTAGTTTCAAGCACAGCAAAAGCAAATTCATA TATATTTTCCAAATGGCTTTCTTTATCGTCGAA	NO
Hepatocyte nuclear factor 4	TTAACCAAATAAGAAAAAAAACATATAAGATTGATTCAAGTGTGCAGT GCAAATGAAGAAAAGTCTAGTGAATTCTTGTTAGGTAGTAAGATCCTG TTTGTCTTGTCGGCTTTATAAAAACGGTCAGCAAGCGCTCTGCGCGCA ACAAGAGTTGTTTTTGATGCTAATGCACTAAGTGACTTTTTTATTAGCTA AATTTCTCGCTATTCACCATTTGCTCACGTCCTTTGGTCTTTAAAGTAAA TAAGCACTTATGCAATCTTTTCTTTCTTTTTGTTTTTTTACTTTGTTTATAT ATTTATATAATGGCTTTGCCTTTTCGAAAATAATCTAAAAGTGTCTTTTA GGAGCCGCATTGCGACGGAATAGATTGAACGATGGAAAGTGATGCA AGCAAAATTGCATACATAATAAAATGCTATTTTAATAGAAATACTATAC ACTTGTTCAAAATTATATGCCGAGGCAACAATGATCACGAGAAAAACC TAACGGGAATAAAGTACAAATATTCCATAGGCCGTGCCAACTCCCAGA TCAACCTTGGATGGCATTCCTCGTTCTTTATTTGTACAATTTGTCATTTT ATTGGAATATTTATATACTTTTCATTGATTTGTTATTAATATGAAGTGCCT GTAAAATGGTTTTGAATGAAAATAACAAAAGTACGCATTTAAAAATAAA AATTAAGTTTTCATCACCTCAAAACTCA**AAAAACCCCG**AAATGTCACG TGTGCGAACATTTTCGAAAAGGCTATAGTTATGTTTTCTTCGTTTTATAT CTAAAAACTGCACTGATTCTTCAAAATTAGTTAGGATATCGTGATTATT GATTATCTTTCATCTTGAGAATCTTTAAAAATGTTTATTAAATCAATTATA AAGTTGACAAAATTGGTTATTTTTGGCGAGGCTTTGTTTACAAGACGAT GACGTGTTGTCGTATAGCGCTCGTGGCTCCCTCGAGTCACATGACTAT CGCACAGTTATCRCGGCA	AAAAAACCCC: 9.168412063 AAAAACCCCG: 7.398173267

Adenosine receptor A2B	TCCCTTTTTCGGACGACTAACGCCTGTCGTAAACCCATGCTACCAAGA AGTGCACCCTTTGACGTCGCCGGTTTTTCCAACCAATCAGATGCCAGA ATTGAACCATTTGCCATCAATACCCACAATGCATCGCAGCGTGACAGA TCCTGAACTAGTTCGTTACTTAATGCTTCAAAATGGCGCTATGAAAGAA CCAATGAAACCATACCAATGGTACAACCATGATACATATGAAAGAAGT GCATATCCCGCGGGATGGGACCCGTATCTCGGGTCGAGGGGATTCTT ATCACCATCGCAGGTTTATAAAGAGGGTAAGAACGCTCAGGAAGGTT TCAATGGTACGCGATACAAATGTGGGTTGTGCGGAGCATCATTCTCTC TCCAGAGACTTTTAAACCGACACATGAAGACCCATTCGTTCTACAAGC GATATCACTGTCAGTTTTGTGGCAAAGGATAAAAAAAAATCGTATGTCA AAAAAATGGTTCGAGAAAACTTCATTCGTTTTCGGAAGAACGATGAGA AAATTAGTCAGCTTGRCAGCTATTGTTAAACTTTAATCACATTCTCACAA TTTTTAGATTTATACGCAGGTCTGARTTGTAAAATCATGTACTGGCTAC ATGATTGTTCTGCCAGATGTATGAGTAAATTTTCCACTAAAATTGCAAT TTTCTTATTGAATAATTAAAAAAAAAAACTCAATGCAGGAACATAATTTA TCCCTCAAACCATACATTGCTTTTTTTATGATATTTTAACTATAATATTAC TAAAAATAGTTTCAAAAACRCAAAGAAGTAATCGACCACGATTATAGT GCCGGATATAAAAAATGTCACTATTTGGTAAAAGAGAATTGAAAAGCA GAATCTCCATCCTGTTTTTCTGCACGAAACTTTAGTGTGCAGTCACTGT ATACAGTCTGAGATCTTCAGAAGACACACCATGTCCCCTACCYCTAATA GCACAGTGACTTGTTTCATTGCAACAGTAATC	NO
Scavenger receptor Class B member 1	AATAACGTATTTTGTACTGACGAGAACGACTATCAGACRAAATATGCA AAAAACCTAAAAGAAACAAGCTCTGGTGACACACAGTAGAAAGATAA TTTAGAGGATATTTCGCTGTACTTTAATGCTTGCGGGGTTGTATATAAC TTATAGCCAGTTTRCAACCTGAGTGTCAATCGATAGTGTTTTGCCACAG GGAATAAAATTCAAGAACAAAAATTAAAGAACTGCTTGGCTAGCTCCA CTATAGAGAAGGAAAATGAAGCAYAGAGAATCTTGGCAGTTGTAGCT AAATGACGTCATTGTGCAAATAACCTATTATTTCTTTAATCTCAGAACCA GAGAGCATAAACAGAGGGCATACTGTCGTTTATGTAGCTTATCAGTGT GTTTATGAATTTATAAACGAGACTAACGGAAGCGATAGTTTCTTGAAA ACGGCGGAAAAAACACCATATTAAAAAATATCAATGGTGTAAATGGG GTCTGAAAATCTTGCGTCATAAAACTATACTAAGGTTCTTGTCCATGTA TGTTGAGATTTTTAAGCATCCAATCTAAAATGATAAAAAGCATGTTAGA TGACAGTGTGTTTCATAAAGCAGYGAACTTCCATAGTTGCAGTCATATA TACCTTGGTTTCTTAGCCTTGGTATATTCAAAATAATTAAACAGCGTAG TACAGTCATTGCCATTTCTCGTTTTCGATTTTCTCTTGCTAAGTCCAACC TGTTTACAACGACTAAATCCGGCGCATCCTACTAAGAAAAAAAGACTG GTTATTCCATATATATTTAAGTGTCTTGATTCCATTTCAAATTATTTTAGT TTATAGACCATTGGTTGCATTTTGTGTAGTCGAGGAAATGACTATAAAT TTCGCTTTTATCTCGTTATTACTTACTAGATGATATGGGCTTCCATTGGA TGTGCTTCTTGACAATCTAGAGGAACAAAACCGATAKACGGCACTTAT TAAAAGAGGGAAAGGATTTAATAAAATCACT	NO

TNF receptor-associated factor 3	GACACAGCGGTTACAGAGGTTTACGTCATCAGCAGTGTTTGACGTCTA TATAACACGTGTACGAGCACTTTGCACCGTCATTAAGTCCTTTGCAAAA AAGCGAAAGTTATATTTGAGGTAAGTATCAATTAAAATCGAGTTTTAAA ATTTTAAGTTTATCAAAAGCAACTTTCATTTGTTTAACCGATATCAAAAC AAAAAAATTTCAATTTTTATTTTACAGTGTCTGCTTTTCAGTAAGTTTTTA ACTATTTTCAGTCAACAAAAAATATATACTTATAATATTATTTCATGAACT ATGAAGTTATCGATAATACAAGGAATATTGAGAATTGTCAGCATTCGA CAACTTACAAGTTTGTGATTATAGTCCGATGTCCAAAAGCCACAGTTCT CCACATCTTGCGTTACATGTCTTGCAACAGTATATTTCGACACAAATCG AAAGATGCCCAAATATGTCCTGAAGCTCGATGGAGCATACTAGATTAT CAATTGCAATTTAACAAAAGCATTCCATTTTCTGTGCTTCTAGTGCACG CAAAGAGATGATGTCAAAAATATAATGACTAACATAACTTGAAAGAAC GAAGCGAGACGAAGCCATCCATGTGTGTGAACCTAAATAACACACGG TTCAAATTTAAGAAGTAGTGTTTAACTTGACTGTTGGCTTCGATTGTAC TGTACCCTGGTTCCAGAGGCTTCGTTCTCTGTATCTCAGTTTTATTTCCT TATGTCAACTTACCAAGAAGGGAAATCGGAGATTATAGATCTCCAAAA ATGACGGTAGTTTAACCAATCAAGTTTATTTTCTTACCCACATTGTTGAT TGTACTTTGTTTCGAAAGTGCAATACGATATAGTACTGGAAACTTGATG TCATATTTTCAGTCTTATTTCTATGAAGCCACCAACCATTTATTCCACTCT TTAGGACCAATTTAATTTTTGAATATGCTAAGGCTATAATTTCTGCCGC CTTTAGAACTATTTCTTCTTTCAG	NO
Kruppel-like factor 11	CCGAATATTTTTCGTTCTTGCATATGCTTCGTTTTTGTTTTTGGAATTATT ATAATAATTCAGTGTAATAATGTTATTAGCTTCGGCTTTTTCACATGTTG TCCAGAGAGTCTGAATACATGCTCAATACTGAATGCATTTGACTATGA CAGTAATTGGGTTGACGCTAGACTTGACCTGCTGTTTATTCTTTAAGCG AAGCTTCATGTATATTTAGTGGATTTGTTGTTTTAAAGGATCTTGCTCG CGTTAATCCATAGCAGTCACTTTTTATGCAAGGGAACCTGACCCCAAA TTACGGCCACCGTGTAATAAAAAATACCTTGTTGGGGCGTGGCTCATG TCAGTAAGGTTGGTCTTTAATTTGACTTTTATTTTGCAGAGTATGTTTAA AATAATGCATCTGCAGCCCTATCGGTATACTATTCTCRCTTTTCTTTGAT CGTTGAAGCTCACTTGGGTAAAACTGGGTGGGGTCAGTTATGGACAG CCGACGCCCATAAAACACCTTGGTTTCATCATCCATGAAAGTCTTGTCA TTACCTTAGAAAAGATGGCTTCTAGCAGGTTAGGAAACGCCTTTAAAA ACACTTATTTTCTAGTTGACCAGCGTTTTCTCATCAGAAATGTCATAAA GGGAATTTTTTCTCAAGTTTATTATGATTTATTTTTTAATTTTTTAATTTTT GGATTTTTGTTGTTTTTTTCTAGTAAGCCATTCGTATATTAACGTTTTTAA AAAGAGAAAATCACGTGCTTCAGAGAGTCACATGCACGTGTTTTCTAT TTTTGTATGTCAACACAGAGTAGGTACAAAGGTCATTTCTTATTTTGCT GTTCCACATGGTTGAGGGTTTCTCCATGAAGTGTTCACATGTATGCTTC ATGCTGATTGGCTAAACTTATGTGTATTGAATTCTCATTGGTCAAGCCC ACACTTACGCCCCCTTTCCTGCATGATCATGGCTACTGATCTAAGTTCA ACTTTCAAAACGACCA	AAGGGAATTT: 5.037293848 AGGGAATTTT: 6.045264 GGGAATTTTT: 6.836182579

Growth arrest and DNA damage-inducible protein	CCTTGTACATTTTATGGTGCAATTGGAACTCACGTGACAGTAGCAAAC TGACCAGGGGTAGGGACATATACTTTTCTAATAAATGCAAAATATAAA GCTTTTTTTACACATGAAACCATTTTAATCCTCTTGGGAGATTAACTACA ACAATTCTTAGTTTTTGTAGATAATTTGTATAATTTTTATTTTTCTCTGCTT GATAATTTAATCTTAAAAATAAAGACCCCTACCCGTTCCCCAAGAGGA ACGCATGAATGCGGAACCAGGCAGGAAATTGGGCGCGAGTTCTTTC GGGGGTTTCCCTGTGACGTCAATTGTGACACGTGGCTTTGACAGACG ACGTAAGGCAAGATCAAGCAAGACTTTCATCAACTAAATTATTCATTCT TGTGTCTTTACTTTTTAAGGTAAGCTTTCTGTAGAAAAAGGCATTTTGG AGAATTCACTAATAAATGGGAACTGATTCAAAGGGATTAAAAAAAATA AATACATGATTACAACGTATGAAAGAATGAGTGAATTACAAGCAAGAA AAATGAATAAATCGATTAATTTGGAATTAGGGATATTTACATGTATGAA AAGGGAAATAACCAAAATAATAGATACAAAAAATAACTTTATAGAAAA TTATAAAAAAAAATCTGATGTGGATTAAGAGAGACTTTAGAGAATACAA GAGTATATAAATCAGCTTTGAAATTGATAAACAAACAAACAAATAAATA AATAAAACAAACTGTCAATCAACCCAAATTTTAGTGCTACATCTTTATTC TAATATGCATAATTATTACTGACAGCTGTCATTTAACAGATTTACAGTAT TCAAAGGTTGGATAACTTCACTTACATTACCACCATTTGTGATTATYGTA TTGCTACCAGTTAAAGACTGGAGGCATTTTTACACTGTACATTTGTGAA AAATCTTGCTGGTAATAATAAATTGTGCAAATGGCAAATCATTCAAATG TTAAATGTCTCTAAAGGAATTTAAA	CCCGTTCCCC: 5.607533397 GGGGGTTTCC: 11.1516023 GGGGTTTCCC: 10.57660978
Ribonucleoside-diphosphate reductase	CCATTCATTCCTTATTGAATTCATAAATGCAAGATGCAAATCATTCCAGT ATTCRACTTCAATCCTMAACYGTTTTGTCTTATYTTGGAGATTTTCATCC CACAGATCTTTGAGAGGAGAAACAAAGTCAGCAATWAGGAGAGGTA GTGGATTRTCTTTGATATCAACRGATGCATTGGATYGACAAGTGTTGC CAATACACTCTAAGCTGTCTTCATAACTTGCGTCAATTATAACCCATTTT GYGTTAAGATCTGTTGTTCCTTGTGACACTGGTTCACAATGTTTGACTT CTAATTCTACTTTAAAAGCTTGACCTTCATGCTGTAATTCTAAAAACCTC TGATTACCTACAGACATGACTTTATCAAAAAGAAAATGYTCGGGACCA TGCAAAAGAAGTGAAAGATCTTGTGCATGTTTTTTATCGTATTTGGCAG TTAGTATAACCTGTGAGAGTTTCATAGGTAACATGTCGATATCTACTAT ATGACCTGTTCTAAGACCATGCCTTGATAAGTCGTCTTCCCATAATATC AAGTGTAAATATCTCTCCCCGTTTTCTTCACATGTAGCACCACCTTCAA GGCTCTTGATCTCCTCAGGTGTAAAATGTCTGCAACGAACATTAAGGT TATGATTTCTAAAACCATCTGAGCAGTTCGGATCAAGTTTGACTTCTAA GGATATAAAATTATCTTTGCTAAATTCATTTTCCTGGGACGGCAATACT GCATTATAATCTAGGAAGTCGTCTCCATACTTAGAGCCAAAAGAAATT GAAGAAACGCCGTAGATCTTAGCTAACACCATCACGAAAACTGTCCAC AAAAACACTTCAGGCTGACCGCCATTTTGGATAATTTATGCGTCAAATT GTTTAAAAGGCCTGGTGATGAGCTCGCACCAGTCTTTTTCCATTTATTG CATAATTATTTAAAACCAACATGCATTTGTAATTTGTCATTTCCACGTGT TTTTCATGTTTTGCAGTATTTCT	NO

Organic cation transporter	ACAAGACGAAAACTCACCAGATAAATCGAAAATGAAAATGACAACTG CTAATACATTAGAATTATCATAAACAAATACACAACCAAAGTACAAAAG AAAACATAGTTAAGTAATTATGCCAATGACATAACCTAGTAAAATAACA AAGCCTTCTTCAACTTTAGGACATGTACGTCTAAGTGGTGCTATACGTA CTTGTTTAGGGTTCGAAGCAGGTCTTTCGTTAACTTGAGAAGCCTGTG CCTGAAGGCTGTAGTTAAGATTAAAGTTTATTCCCTGAAATGAAAGTA AACGGATCTAATAAATTGAACTTTTTGGATCACACTGACAAGAGTTGA GTCGAGAAAGATGACCTACTTCTCTCGCTATTACACGGCCAGTTTTTG CAGCTCTGCTTGGATGGTGGTACATAGTATAGACACTTCAGTTCTCTAT GTTATAAATATATATTTTATCCATACTTTATCCATTATTGCAATTATTATT GCACCAAAATGTGGATAACTGTTATGATCATTGAAACAAACGTCGACG TATTTCGGACGCCATCTTGAATTTGCCGCTGGACTCGTTGCCTGGCAG CCACTCGGAAGTCCCGGATGGATGAACAAATCTGAACAACATTGAAA ACAAAACAAAACAAACATAAATTAAGCAAAACATTGAAGAACGAAACA AAATTCAAAAGAAAAACAAATAAAACAAAAACAAACAAACACAAAAGT AAACGAAATGAAATAAAACAACAATTCGAACTCCCTATTACCCCCACCT GAATTGTAAAATAATAATGCACGAATCATTTTTTCGATTTCTTACATGGA TATAGGTATAGATTATATTATTTTATAGTTTTATTGTGCTCAGGACACCC ATTGATAACAGATGCACATGCAACTGAAGGGACCACCCTGTATATTCT TCTTCTTATAATCTGTAATCTCATGATGACGTTGCCAAGTTTCGTGACCT AAATGGCCCCGTCACATGCCCCAGAA	CGGAAGTCCC: 5.308777195 GGAAGTCCCG: 5.888990627
TNF receptor superfamily member 2	AACTTTTAAAAAGAAAAATAATGAACATTCTGTTGCTTCACAAGCACTA TATGGATAATTGTTCTCAATGGCTTTTTTGTGATGATTCTGCAAATTATT GTAGCATTYCAAAAGAAACTCCACACAAAGTTTTATGACTTTAGATTCA AAGTGATTTGAAGGTTTGAACTACAAAAATAGTGTAGTGTTTTGGTTTG CATAAATTTCAGGTACCTTGATATTATTATCAATGGATATTGCTTCAGTT GATAATCATTTAGATTTTGATAAAAGTCTGACAAAAAAAAAATATGTTTTT TGAAAACTAAAATTTAAAGATTAAACTATTATGAAATGTATTTAGTATTG TCATTTATTTCAATGGTGTATGCATACACGCTATTTAGATTGTTATAGTA ACCACTTGTTAATAAATTAAATAGTTGAATTAAATTTCTATTCTCTTTTTT TTATCATACAGACTGATCTGCATGTAGGCAGTCAACGTGTTCTAACGT GTTRAATTGTGAAGGGTGCCAAATAAATTCCCCCTTCCCTCTCAAGAG TCACATGGCTCACATGATTTGCGCGACTACACGGAAACGCGCTGTAC ACTCTTCTTTATTGAGTTAACTTTTTTACTGTTCATTGATAATGCGGGAT TGGTTTACAATATGTTGTCATATCTTTTGTATTTTGACAGCGGGGGAGC CATTAACCCCGCAGTTCTACACAAAGAACAGCCTGGAAACGTTTTTGA GACGGCATTAACGTTTTTGTTTTAGTTTACGTTCTTAGTGATGATTCAG CATCACTGGAGATGTGCCCCAGCACAACATGGCGCATTTTATCATGTT GAGTAGCGTTCTCTGATTGGATGGATATATTTAGTTAGGGGAATCCCC AATTACGCTGTCCATCTGGGTAATTCCGACATGGAATTTATAAAATACC GCTATAGTATAACACTATCACAA	TAAATTCCCC: 9.905217688 AAATTCCCCC: 10.06710502 AATTCCCCCT: 9.34170637 AGGGGAATCC: 9.67310507 GGGGAATCCC: 13.91822948 GGGAATCCCC: 14.73699803 GGAATCCCCA: 8.607369846

NF-κB binding site sequences (and the associated PBM z-score [based on Mansfield et al. 2017]) for the indicated promoter regions are listed in the right column. NO; indicates that no NF-κB binding site sequences were found. NF-κB binding site sequences are indicated in the promoter sequence (red). Some of the indicated NF-κB sites are overlapping.

REFERENCES

Adams, J. C. and J. Lawler (2004). The thrombospondins. *International Journal of Biochemistry and Cell Biology* **36**: 961-968.

Aichelman, E., J. E. Townsend, T. A. Courtney, J. H. Baumann, S. W. Davies, and K. D. Castillo (2016). Heterotrophy mitigates the response of the temperate coral *Oculina arbuscula* to temperature stress. *Ecology and Evolution* **6**: 6758-6769.

Ainsworth, T. D., E. Kramasky-Winter, Y. Loya, O. Hoegh-Guldberg, and M. Fine (2007). Coral disease diagnostics: what's between a plague and a band? *Applied and Environmental Microbiology* **73**: 981-992.

Alaux, C., F. Ducloz, D. Crauser, and Y. Le Conte (2010). Diet effects on honeybee immunocompetence. *Biology Letters* **6**: 562-565.

Altschul, S. F., T. L. Madden, A. A. Schäffer, J. Zhang, Z. Zhang, W. Miller, W. and D.J. Lipman (1997). Gapped BLAST and PSI-BLAST: a new generation of protein database search programs. *Nucleic Acids Research* **25**: 3389-3402.

Anderson, D. A., M. E. Walz, E. Weil, P. Tonellato, and M. C. Smith (2016). RNA-Seq of the Caribbean reef-building coral *Orbicella faveolata* (Scleractinia-Merulinidae) under bleaching and disease stress expands models of coral innate immunity. *PeerJ* **4**: e1616.

Areschoug, T. and S. Gordon (2009). Scavenger receptors: role in innate immunity and microbial pathogenesis. *Cellular Microbiology* **8**: 1160-1169.

Ashton-Rickardt, P. G. (2012). An emerging role for serine protease inhibitors in T lymphocyte immunity and beyond. *ISRN Immunology* **2012**: 354365.

Barshis, D. J., J. T. Ladner, T. A. Oliver, F. O. Seneca, N. Traylor-Knowles, N. and S. R. Palumbi (2013). Genomic basis for coral resilience to climate change. *Proceedings of the National Academy of Sciences USA* **110**: 1387-1392.

Baumgarten, S., O. Simakov, L. Y. Esherick, Y.J. Liew, E. M. Lehnert, C. T. Michell, Y. Li, E. A. Hambleton, A. Guse, M. E. Oates, J. Gough, V. M. Weis, M., Aranda, J. R., Pringle, and C. R. Voolstra (2015). The genome of *Aiptasia*, a sea anemone model for coral symbiosis. *Proceedings of the National Academy of Sciences USA* **112**: 11893-11898.

Bay, R. A., N. H. Rose, C. A. Logan, and S. R. Palumbi (2017). Genomic models predict successful coral adaptation if future ocean warming rates are reduced. *Science Advances* **3**: e1701413.

Berger. M. F., A. A. Philippakis, A. M. Qureshi, F. S. He, E. W. Estep 3rd, and M. L. Bulyk (2006). Compact, universal DNA microarrays to comprehensively determine transcription-factor binding site specificities. *Nature Biotechnology* **24**: 1429-1435.

Berthelier, J., C. E. Schnitzler, E. M. Wood-Charlson, A. Z. Poole, V. M., Weis, V. M. and O. Detournay (2017). Implication of the host TGFβ pathway in the onset of symbiosis between larvae of the coral *Fungia scutaria* and the dinoflagellate *Symbiodinium* sp (clade C1f). *Coral Reefs* **36**: 1263-1268.

Berkelmans, R. and M. J. J. van Oppen (2006). The role of zooxanthellae in the thermal tolerance of corals: a 'nugget of hope' for coral reefs in an era of climate change. *Proceedings of the Royal Society of London B: Biological Sciences* **273**: 2305-2312.

Beutler, B. and E. M. Y. Moresco (2008). The forward genetic dissection of afferent innate immunity. *Current Topics in Microbiology and Immunology* **321**: 3-26.

Bieri, T., M. Onishi, T. Xiang, A. R. Grossman, and J. R. Pringle (2016). Relative contributions of various cellular mechanisms to loss of algae during cnidarian bleaching. *PLoS One* **11**: e0152693.

Bordenstein, S. R. and K. R Theis (2015). Host biology in light of the microbiome: ten principles of holobionts and hologenomes. *PLoS Biology* **13**: e1002226.

Bouchard, J. N. and H. Yamasaki (2008). Heat stress stimulates nitric oxide production in Symbiodinium microadriaticum: a possible linkage between nitric oxide and the coral bleaching phenomenon. *Plant & Cell Physiology* **49**: 641-652.

Brandt, M. E. and J. W. McManus (2009). Disease incidence is related to bleaching extent in reef-building corals. *Ecology* **90**: 2859-2867.

Brennan, J. J., J. L. Messerschmidt, L. M. Williams, B. J., Matthews, M. Reynoso, and T. D. Gilmore (2017). Sea anemone model has a single Toll-like receptor that can function in pathoden detection, NF-κB signal transduction, and development. *Proceedings of the National Academy of Sciences USA* **114**: e10122-e10131.

Brown, T. and M. Rodriguez-Lanetty (2015). Defending against pathogens – immunological priming and its molecular basis in a sea anemone, cnidarian. *Scientific Reports* **5**: 17425.

Burmester, E. M., A. Breef-Pilz, N. F. Lawrence, L. Kaufman, J. R. Finnerty, and R. D. Rotjan (2018). The impact of autotrophic versus heterotrophic nutritional pathways on colony health and would recovery in corals. *Ecology and Evolution* **8**: 10805-1-816.

Burns, J. A., H. Zhang, E. Hill, E. Kim, and R. Kerney (2017). Transcriptome analysis illuminates the nature of the intracellular interaction in a vertebrate-algal symbiosis. *eLife* **6**: e22054.

Cao, Y., M. K. Halane, W. Gassmann, and G. Stacey (2017). The role of plant innate immunity in the legume-rhizobium symbiosis. *Annual Review of Plant Biology* **68**: 535-561.

Catanese, M. T., R. Graziani, T. von Hahn, M. Moreau, T. Huby, G. Paonessa, C. Santini, A. Luzzago, C. M. Rice, R. Cortese, A. Vitelli, and A. Nicosia (2007). High-avidity monoclonal antibodies against the human scavenger class B type I receptor efficiently block hepatitis C virus infection in the presence of high-density lipoprotein. *Journal of Virology* **15**: 8063-8071.

Cerenius, L. and K. Soderhall (2004). The prophenoloxidase-activating system in invertebrates. *Immunological Reviews* **198**: 116-126.

Cervino, J. M., R. L. Hayes, S. W. Polson, S. C. Polson, T. J. Goreau, R. J. Martinez, G. and W. Smith (2004). Relationship of Vibro species infection and elevated temperatures to yellow blotch/band disease in Caribbean corals. *Applied and Environmental Microbiology* **70**: 6855-6864.

Chakravarti, L. J. and M. J. H., van Oppen (2018). Experimental evolution in coral photyosymbionts as a tool ot increase thermal tolerance. *Frontiers in Marine Science* **2018**: 00227

Chen, M. C., Y. M. Cheng, P. J. Sung, C. E. Kuo, and L. S. Fang (2003). Molecular identification of Rab7 (ApRab7) in *Aiptasia pulchella* and its exclusion from phagosomes harboring zooxanthellae. *Biochemical and Biophysical Research Communications* **308**: 586-595.

Chen, W. and P. Ten Dijke (2016). Immunoregulation by members of the TGFβ superfamily. *Nature Reviews. Immunology* **16**: 723-740.

Chen, Y., L. He, Y. Peng, X. Shi, J. Chen, J. Zhong, X. Chen, G. Cheng, and H. Deng (2015). The hepatitis C virus protein NS3 suppresses TNF-α-stimulated activation of NF-κB by targeting LUBAC. *Science Signaling* **8**: ra118.

Chu, H. and S. K. Mazmanian (2013). Innate immune recognition of the microbiota promotes host-microbial symbiosis. *Nature Immunology* **7**: 668-675.

Chun, C. K., J. V. Troll, I. Koroleva, B. Brown, L. Manzella, E. Snir, H. Almabrazi, T. E. Scheetz, M. F. Bonaldo, T. L. Casavant, M. B. Soares, E. G. Ruby, and M. J. McFall-Ngai (2008). Effects of colonization, luminescence, and autoinduced on host

transcription during development of the squid-vibrio association. *Proceedings of the National Academy of Sciences USA* **105**: 11323-11328.

Clark, R. I., K. J. Woodcock, F. Geissmann, C. Trouillet, and M. S. Dionne (2011). Multiple TGF-β superfamily signals modulate the adult Drosophila immune response. *Current Biology* **21**: 1672-1677.

Cleves, P. A., M. E. Strader, L. K. Bay, J. R. Pringle, and M. V. Matz (2018). CRISPR/Cas9-mediated genome editing in a reef-building coral. *Proceedings of the National Academy of Sciences USA* **115**: 5235-5240.

Coffroth, M. A., D. M. Poland E. L. Petrou D. A. Brazeau D. A. and J. C. Holmberg (2010). Environmental symbiont acquisition may not be the solution to warming seas for reef-building corals. *PLoS ONE* **5**: e13258.

Coleman, J. W. (2001). Nitric oxide in immunity and inflammation. *International Immunopharmacology* **1**: 1397-1406.

Coles, S. L. and B. E. Brown (2003). Coral bleaching--capacity for acclimatization and adaptation. *Advances in Marine Biology* **46**: 183-223.

Courtois, G. and T. D. Gilmore (2006). Mutations in the NF-κB signaling pathway: implications for human disease. *Oncogene* **25**: 6831-6843.

Crawford, S. E., V. Stellmach, J. E. Murphy-Ullrich, S. M. Ribeiro, J. Lawler, R. O. Hynes, G. P. Boivin, and N. Bouck (1998). Thrombospondin-1 is a major activator of TGF-beta1 in vivo. *Cell* **93**: 1159-1170.

Davy, S. K., D. Allemand, and V. M. Weis (2012) Cell biology of cnidarian-dinoflagellate symbiosis. *Microbiology and Molecular Biology Reviews* **76**: 229-261.

Degnan, B. M., M. Vervoot, C. Larroux, and G. S. Richards (2009). Early evolution of metazoan transcription factors. *Current Opinion in Genetics and Development* **19**: 591-599.

Denney, L., W. Branchett, L. G. Gregory, R. A. Oliver, and C. M. Lloyd (2017). Epithelial-derived TGF-β1 acts as a pro-viral factor in the lung during influenza A infection. *Mucosal Immunology* **11**: 523-535.

DeSalvo, M. K., S. Sunagawa, C. R. Voolstra, and M. Medina (2010). Transcriptomic responses to heat stress and bleaching in the elkhorn coral Acropora palmata. *Marine Ecology Progress Series* **402**: 97-113.

DeSalvo, M. K., C. R. Voolstra, S. Sunagawa, J. A. Schwarz, J. H. Stillman, M. A. Coffroth, A. M. Szmant, and M. Medina (2008). Differential gene expression during

thermal stress and bleaching in the Caribbean coral *Montastraea faveolata*. *Molecular Ecology* **17**: 3952-3971.

Detournay, O., C. E. Schnitzler, A. Poole, A. and V. M Weis (2012). Regulation of cnidarian-dinoflagellate mutualisms: Evidence that activation of a host TGFβ innate immune pathway promotes tolerance of the symbiont. *Developmental and Comparative Immunology* **38**: 525-537.

Denney, L., W. Branchett, L. G. Gregory, R. A., Oliver, and C. M. Lloyd (2017). Epithelial-derived TGF-β1 acts as a pro-viral factor in the lung during influenza A infection. *Mucosal Immunology* **11**: 523-535.

Dev, A., S. Iyer, B. Razani, and G. Cheng (2011). NF-κB and innate immunity. *Current Topics in Microbiology and Immunology* **349**: 115-143.

Di Prisco, G., D. Annoscia, M Margiotta, R. Ferrara, P. Varricchio, V. Zanni, E. Caprio, F. Nazzi, and F. Pennacchio (2016). A mutualistic symbiosis between a parasitic mite and a pathogenic virus undermines honey bee immunity and health. *Proceedings of the National Academy of Sciences USA* **113**: 3203-3208.

Dixon, G. B., S. W. Davies, G. V. Aglyamova, E. Meyer, L. K. Bay, and M. V. Matz (2015). Genomic determinants of coral heat tolerance across latitudes. *Science* **6242**: 1460-1462.

Doerre, S. and R. B. Corley (1999). Constitutive nuclear translocation of NF-κB in B cells in the absence of IκB degradation. *Journal of Immunology* **163**: 269-277.

Dudley, A. M., J. Aach, M. A. Steffen, and G. M. Church (2002). Measuring absolute expression with microarrays with a calibrated reference sample and an extended signal intensity range. *Proceedings of the National Academy of Sciences USA* **99**: 7554-7559.

Dunkelberger, J. R. and W. C. Song (2010). Complement and its role in innate and adaptive immune responses. *Cell Research* **20**: 34-50.

Dunn, S. R., C. E. Schnitzler, and V. M. Weis (2007). Apoptosis and autophagy as mechanisms of dinoflagellate symbiont release during cnidarian bleaching: every which way you lose. *Proceedings of the Royal Society B: Biological Sciences* **274**: 3079-3085.

Dunn, S. R. and V. W. Weis (2009). Apoptosis as a post-phagocytic winnowing mechanism in a coral-dinoflagellate mutualism. *Environmental Microbiology* **11**: 268-276.

Finnerty, J. R. and T. D. Gilmore (2015). Methods for analyzing the evolutionary relationship of NF-κB proteins using free, web-driver bioinformatics and phylogenetic tools. *Methods in Molecular Biology* **1280**: 631-646.

Franchi, L., N. Warner, K. Viani, and G. Nunez (2009). Function of Nod-like receptors in microbial recognition and host defense. *Immunological Reviews* **227**: 106-128.

Fuess, L. E., C. J. H, Pinzón, E. Weil, E. and L. D. Mydlarz (2016). Associations between transcriptional changes and protein phenotypes provide insights into immune regulation in corals. *Developmental and Comparative Immunology* **62**: 17-28.

Fujise, L., H. Yamashita, G. Suzuki, K. Sasaki, L. M. Liao, and K. Koike (2014). Moderate thermal stress causes active and immediate expulsion of photosynthetically damaged zooxanthellae (*Symbiodinium*) from corals. *PLoS ONE* **9**: e114321.

Ganot, P., A. Moya, V. Magnone, D. Allemand, P. Furla, and C. Sabourault (2011). Adaptations to endosymbiosis in a cnidarian-dinoflagellate association: differential gene expression and specific gene duplications. *PLoS Genetics* **7**: e1002187.

Gauthier, M. and B. M. Degnan (2008). The transcription factor NF-κB in the demosponge *Amphimedon queenslandica*: insights on the evolutionary origin of the Rel homology domain. *Developmental Genes and Evolution* **218**: 23–32.

Gerdol, M., P. Venier, P. Edomi, and A. Pallavicini (2017). Diversity and evolution of TIR-domain-containing proteins in bivalves and Metazoa: New insights from comparative genomics. *Developmental and Comparative Immunology* **70**: 145-164.

Gilmore, T. D (2006) Introduction to NF-κB: pathways, players, perspectives. *Oncogene* **25**: 6680-6684.

Gilmore, T. D. and F. S.Wolenski (2012). NF-κB: where did it come from and why? *Immunological Reviews* **246**: 14-35.

Grawunder, D. E. A. Hambleton, M. Bucher, I. Wolfowicz, N., Bechtoldt, and A. Guse (2015). Induction of gametogenesis in the cnidarian endosymbiosis model *Aiptasia* sp. *Scientific Reports* **5**: 15677.

Green, E. A., S. W. Davies, M. V. Matz, and M. Medina (2014) Quantifying cryptic *Symbiodinium* diversity within *Orbicella faveolata* and *Orbicella franksi* at the Flower Garden Banks, Gulf of Mexico. *PeerJ* **2**: e386.

Grottoli, A. G., L. J. Rodrigues, and J. E. Palardy (2006). Heterotrophic plasticity and resilience in bleached corals. *Nature* **440**: 1186–1189.

Hamada, M., E. Shoguchi, C. Shinzato, T. Kawashima, D. J. Miller, and N. Satoh (2013). The complex NOD-like receptor repertoire of the coral *Acropora digitifera* includes novel domain combinations. *Molecular Biology and Evolution* **30**: 167-176.

Hambleton, E. A., A. Guse, and J. R. Pringle (2014). Similar specificities of symbiont uptake by adults and larvae in an anemone model system for coral biology. *Journal of Experimental Biology* **217**: 1613-1619.

Hawkins, T. D., B. J. Bradley, and S. K. Davy (2013). Nitric oxide mediates coral bleaching through an apoptotic-like cell death pathway: evidence from a model sea anemone-dinoflagellate symbiosis. *FASEB Journal* **27**: 4790-4798.

Hayden, M. S. and S. Ghosh (2008). Shared principles in NF-κB signaling. *Cell* **132**: 344-362.

Hirsch, A. M. (1999). Role of lectins (and rhizobial exopolysaccharides) in legume nodulation. *Current Opinion in Plant Biology* **2**: 320-326.

Hoegh-Guldberg, O., P. J. Mumby, A. J. Hooten, R. S. Stenech, P. Greenfield, E. Gomez, C. D. Harvell, P. F. Sale, A. J. Edwards, K. Caldeira, N. Knowlton, C. M. Eakin, R. Iglesias-Prieto, N. Muthiga, R. H. Bradbury, A. Dubi, and M. E. Hatziolos (2007). Coral reefs under rapid climate change and ocean acidification. *Science* **5857**: 1737-1742.

Hoegh-Guldberg, O. (1999). Climate change, coral bleaching and the future of the world's coral reefs. *Marine and Freshwater Research* **50**: 839-866.

Hong, M. C., Y. S. Huang, P. C. Song, W. W. Lin, L. S. Fang, and M. C. Chen (2009). Cloning and characterization of ApRab4, a recycling Rab protein of *Aiptasia pulchella*, and its implication in the symbiosome biogenesis. *Marine Biotechnology NY* **11**: 771-785.

Hughes, T. P., J. T. Kerry, A. H. Baird, S. R. Connolly, A. Dietzel, C. M. Eakin, S. F. Heron, A. S. Hoey, M. O. Hoogenboom, G. Liu, M. J. McWilliam, R. J. Pears, M. S. Pratchett, W. J. Skirving, J. S. Stella, G. and Torda (2018). Global warming transforms coral reef assemblages. *Nature* **556**: 492-496.

Huguet, C., P. Crepieux, and V. Laudet (1997) Rel/NF-kB transcription factors and IkB inhibitors: evoluation from a unique common ancestor. *Oncogene* **15**: 2965-2974.

Hutagalung, A. H. and P. J. Novick (2011). Role of Rab GTPases in membrane traffic and cell physiology. *Physiological Reviews* **91**: 119-149.

Jimbo, M., T. Yanohara, K. Koike, K. Koike, R. Sakai, K. Muramoto, H. Kamiya (2000). The D-galactose-binding lectin of the octocoral *Sinularia lochmodes*: characterization

and possible relationship to the symbiotic dinoflagellates. *Comparative Biochemisty and Physiology – Part B Biochemistry and Molecular Biology* **125**: 227-236.

Jones, A. M., R. Berkelmans, M. J. H. van Oppen, J. C. Mieog, and W. Sinclair (2008). A community change in the algal endosymbionts of a scleractinian coral following a natural bleaching event: field evidence of acclimatization. *Proceedings of the Royal Society of London B: Biological Sciences* **275**: 1359-1365.

Kaniewska, P., P. R. Campbell, D. I. Kline, M. Rodriguez-Lanetty, D. J. Miller, S. Dove, and O. Hoegh-Guldberg (2012). Major cellular and physiological impacts of ocean acidification on a reef building coral. *PLoS ONE* **7**: e34659.

Kemper, C., J. P. Atkinson, and D. E. Hourcade (2010). Properdin: emerging roles of a pattern-recognition molecule. *Annual Review of Immunology* **28**: 131-155.

Kim, C. H., D. Paik, F. Rus, and N. Silverman (2014). The caspase-8 homolog Dredd cleaves Imd and Relish but is not inhibited by p35. *Journal of Biological Chemistry* **289**: 20092-20101.

Kim, D. W., G. Lenzen, A. L. Page, P. Legrain, P. J. Sansonetti, and C. Parsot (2005). The Shigella flexneri effector OspG interferes with innate immune responses by targeting ubiquitin-conjugating enzymes. *Proceedings of the National Academy of Sciences of the United States of America* **102**: 14046–14051.

Koike, K., M. Jimbo, R. Sakai, M. Kaeriyama, K. Muramoto, T. Ogata, T. Maruyama, and H. Kamiya (2004). Octocoral chemical signaling selects and controls dinoflagellate symbionts. *Biological Bulletin* **207**: 80-86.

Krediet, C. J., J. L. Meyer, N. Gimbrone, R. Yanong, I. Berzins, A. Alaely, H. Castro, K. B. Ritchie, V. J. Paul and M. Teplitski (2014). Interactions between the tropical sea anemone *Aiptasia pallida* and *Serratia marcescens*, an opportunistic pathogen of corals. *Environmental Microbiology Reports* **3**: 287-292.

Kuballa, P., W. M. Nolte, A. B. Castoreno, and R. J. Xavier (2012). Autophagy and the immune system. *Annual Review of Immunology* **30**: 611-646.

Kvennefors, E. C., W. Leggat, O. Hoegh-Guldberg, B. M. Degnan, and A. C. Barnes (2008). An ancient and variable mannose-binding lectin from the coral *Acropora millepora* binds both pathogens and symbionts. *Developmental and Comparative Immunology* **32**: 1582-1592.

Kvennefors, E. C. E., W. Leggat, C. C. Kerr, T. D. Ainsworth, O. Hoegh-Guldberg, and A. C. Barnes (2010). Analysis of evolutionarily conserved innate immune components in coral links immunity and symbiosis. *Developmental and Comparative Immunology* **34**: 1219-1229.

Kvitt, H., H. Rosenfeld, K. Zandbank, and D. Tchernov (2011). Regulation of apoptotic pathways by *Stylophora pistillata* (Anthozoa, Pocilloporidae) to survive thermal stress and bleaching. *PLoS ONE* **6**: e28665.

LaJeunesse, T. C. (2005). "Species" radiations of symbiotic dinoflagellates in the Atlantic and Indo-Pacific since the Mioene-Pliocene transition. *Molecular Biology and Evolution* **3**: 570-581.

Lajeunesse, T.C., J.E. Parkinson, P.W. Gabrielson, H.J. Jeong, J.D. Reimer, C.R. Voolstra, and S.R. Santos. (2018). Systematic revision of Symbiodiniaceae highlights the antiquity and diversity of coral endosymbionts. *Current Biology* 28: 2570-2580.

Lawrence, T. (2009). The nuclear factor NF-κB pathway in inflammation. *Cold Spring Harbor Perspectives in Biology* **1**: a001651.

Lehnert, E. M., M. E. Mouchka, M. S. Burriesci, N. D. Gallo, J. A. Schwarz, and J. R. Pringle (2014). Extensive differences in gene expression between symbiotic and aposymbiotic cnidarians. *G3 (Bethesda)* **4**: 277-295.

Li, B., F. Lu, X. Wei, and R. Zhao (2008). Fucoidan: structure and bioactivity. *Molecules* **13**: 1671-1695.

Li, S., L. Zhang, Q. Yao, L. Li, N. Dong, J. Rong, W. Gao, X. Ding, L. Sun, X. Chen, S. Chen, and F. Shao (2013). Pathogen blocks host death receptor signalling by arginine GlcNAcylation of death domains. *Nature* **501**: 242–246.

Lin, K. L., J. T. Wang, and L. S. Fang (2000). Participation of glycoproteins on zooxanthellal cell walls in the establishment of a symbiotic relationship with the sea anemone, *Aiptasia pulchella*. *Zoological Studies* **39**: 172-178.

Livak, K. G. and T. D. Schmittgen (2001). Analysis of relative gene expression data using real-time quantitiative PCR and the 2(-Delta Delta C(T)) method. *Methods* **25**: 402-408.

Logan, D. D. K. A. C. LaFlamme, V. M. Weis, and S. K. (2010). Flow-cytometric characterization of the cell-surface glycans of symbiotic dinoflagellates (*Symbiodinium* Spp.). *Journal of Phycology* **46**: 525-533.

Logan, M. R., S. O. Odemuyiwa, and R. Moqbel and (2003). Understanding exocytosis in immune and inflammatory cells: The molecular basis of mediator secretion. *Journal of Allergy and Clinical Immunology* **111**: 923-932.

Mansfield, K. M. and T. D. Gilmore (2019). Innate immunity and cnidarian-*Symbiodiniaceae* mutualism. *Developmental and Comparative Immunology* **90**: 199-209.

Mansfield, K. M., N. M. Carter, L. Nguyen, P. A. Cleves, A., Alshanbayeva, L. M. Williams, C. Crowder, A. R. Penvose., J. R. Finnerty, V. M. Weis, T. W. Siggers, and T. D. Gilmore (2017). Transcription factor NF-κB is modulated by symbiotic status in a sea anemone model of cnidarian bleaching. *Scientific Reports* **7**: 16025.

Matthers, J. L., C. A. Oakley, A. Lutz, K. E. Hillyer, U. Roessner, A. R. Grossman, V. M. Weis, and S. K. Davy (2018). Partner switching and metabolic flux in a model cnidarian-dinoflagellate symbiosis. *Proceedings of the Royal Society B: Biological Sciences* **285**: 20182336.

Matthews, J. L., C. M. Crowder, C. A. Oakley, A. Lutz, U. Roessner, E. Meyer, A. R. Grossman, V. M. Weis, and S. K. Davy (2017). Optimal nutrient exchange and immune responses operate in partner specificity in the cnidarian-dinoflagellate symbiosis. *Proceedings of the National Academy of Sciences USA* **114**: 13194-13199.

Maynard, J., R. van Hooidonk, C. M. Eakin, M. Puotinen, M. Garren, G. Williams, S. F. Heron, J. Lamb, E. Weil, B. Willis, and C. D. Harvell (2015). Projections of climate conditions that increase coral disease susceptibility and pathogen abundance and virulence. *Nature Climate Change* **5**: 688-694.

McFall-Ngai, M., M. G. Hadfield, T. C. Bosch, H. V. Carey, T. Domazet-Loso, A. E. Douglas, N. Dubilier, G. Eberl, T. Fukami, S. F. Gilbert, U. Hentschel, N. King, S. Kjelleberg, A. H. Knoll, N. Kremer, S. K. Mazmanian, J. L., Metcalf, K. Nealson, N. E. Pierce, J. F. Rawls, A. Reid, E. G. Ruby, M. Rumpho, J. G. Sanders, D. Tautz, and J. J. Wernegreen (2013). Animals in a bacterial world, a new imperative for the life sciences. *Proceedings of the National Academy of Sciences USA* **110**: 3229-3236.

Meints, R. H. and R. L. Pardy (1980). Quantitative demonstration of cell surface involvement in a plant-animal symbiosis: lectin inhibition of reassociation. *Journal of Cell Science* **43**: 239-251.

Menzel, L. P. and C. H. Bigger (2015). Identification of unstimulated constitutive immunocytes, by enzyme histochemistry, in the coenenchyme of the octocoral *Swiftia exserta. Biological Bulletin* **229**: 199-208.

Merselis, D. G., D. Lirman, and M. Rodriguez-Lanetty (2018). Symbiotic immuno-suppression: is disease susceptibility the price of bleaching resistance? *PeerJ* **6**: e4494.

Miller, J., E. Muller, C. Rogers, R. Waara, A. Atkinson, K. R. T. Whelan, M. Patterson, and B. Witcher (2009). Coral disease following massive bleaching in 2005 causes 60% decline in coral cover on reefs in the US Virgin Islands. *Coral Reefs* **28**: 925.

Minakhina, S. and R. Steward (2006). Nuclear factor-kappa B pathways in *Drosophila*. *Oncogene* **25**: 6749-6757.

Mohamed, A. R., V. Cumbo, S. Haruu, C. Shinzato, C. X. Chan, M. A. Ragan, D. G. Bourne, B. L. Willis, E. E. Ball, N. Satoh, D. J. Miller (2016). The transcriptomic response of the coral *Acropora digitifera* to a competent *Symbiodinium* strain: the symbiosome as an arrested early phagosome. *Molecular Ecol*ogy **25**: 3127-3141.

Muscatine, L. and J. W. Porter (1977). Reef corals: mutualistic symbioses adapted to nutrient-poor environments. *BioScience* **27**: 454-460.

Mydlarz, L. D., C. S. Couch, E. Weil, G. Smith and C. D. Harvell (2009). Immune defenses of healthy, bleached and diseased *Montastraea faveolata* during a natural bleaching event. *Diseases of Aquatic Organisms* **87**: 67-78.

Nagata, S. and M. Tanaka (2017). Programmed cell death and the immune system. *Nature Reviews Immunology* **17**: 333-340.

Nazzi, F., S. P. Brown, D. Annosia, F. Del Piccolo, G. Di Prisco, P. Varricchio, G. Della Vedova, F. Cattonaro, E. Caprio, and F. Pennacchio (2012). Synergistic parasite-pathogen interactions mediated by host immunity can drive the collapse of honeybee colonies. *PLoS Pathogens* **8**: e1002735.

Ndungu, F. M., B. C. Urban, K. Marsh, and J. Langhorne (2005). Regulation of immune response by *Plasmodium*-infected red blood cells. *Parasite Immunol*ogy **27**: 373-384.

Neubauer, E. F., A. Z. Poole, P. Neubauer, O. Detournay, K. Tan, S. K. Davy and V. M. Weis (2017). A diverse host thrombospondin-type-1 repeat protein repertoire promotes symbiont colonization during establishment of cnidarian-dinoflagellate symbiosis. *eLife* **6**: e24494.

Neubauer, E. F., A. Z. Poole, V. M. Weis, and S. K. Davy (2016). The scavenger receptor repertoire in six cnidarian species and its putative role in cnidarian-dinoflagellate symbiosis. *PeerJ* **4**: e2692.

Newton, H. J., J. S. Pearson, L. Badea, M. Kelly, M. Lucas, G. Holloway, K. M. Wagstaff, M. A. Dunstone, J. Sloan, J. C. Whisstock, J. B. Kaper, R. M. Robins-Brown, D. A. Jans, G. Frankel, A. D. Phillips, B. S. Coulson, and E. L. Hartland (2010). The type III effectors NleE and NleB from enteropathogenic E. coli and OspZ from Shigella block nuclear translocation of NF-κB p65. *PLoS Pathogens* **6**: e1000898.

Nyholm, S. V. and J. Graf (2012). Knowing your friends: invertebrate innate immunity fosters beneficial bacterial symbioses. *Nature Reviews Microbiology* **10**: 815-827.

Nyholm, S. V. and M. J. McFall-Ngai (2004). The winnowing: establishing the squid-*vibrio* symbiosis. *Nature Reviews Microbiology* **2**: 632-642.

Ocampo, I. D., A. Zarate-Potes, V. Pizarro, C. A. Rojas, N. E. Vera, and L. F. Cadavid (2015). The immunotranscriptome of the Caribbean reef-building coral *Pseudodiploria strigosa*. *Immunogenetics* **67**: 515-530.

Palmer, C. V. (2018). Immunity and the coral crisis. *Communications Biology* **1**: 91.

Palmer, C. V., J. C. Bythell and B. L. Willis (2011). A comparative study of phenoloxidase activity in diseased and bleached colonies of the coral *Acropora millepora*. *Developmental and Comparative Immunology* **35**: 1096-1099.

Palumbi, S. R., D. J. Barshis, N. Traylor-Knowles, and R. A. Bay (2014). Mechanisms of reef coral resistance to future climate change. *Science* **344**: 895-898.

Parkinson, J. E., T. R. Tivey, P. E. Mandelare, D. A. Adpressa, S. Loesgen, V. M. Weis (2018). Subtle differences in symbiont cell surface glycan profiles do not explain species-specific colonization rates in a model cnidarian-algal symbiosis. *Frontiers in Microbiology* **9**: 842.

Paxton, C. W., S. K. Davy, and V. M. Weis (2013). Stress and death of cnidarian host cells play a role in cnidarian bleaching. *Journal of Experimental Biology* **216**: 2813-2820.

Pearson, J. S., C. Giogha, S. Y. Ong, C. L. Kennedy, M. Kelly, K. S. Robinson, T. W. Lung, A. Mansell, P. Riedmaier, C. V. Oates, A. Zaid, S. Mühlen, V., Crepin, O. Marches, C. S. Ang, N. A. Williamson, L. A. O'Reilly, A. Bankovacki, U. Nachbur, G. Infusini, A. I. Webb, J. Silke, A. Strasser, G. Frankel and E. L. Hartland (2013). A type III effector antagonizes death receptor signalling during bacterial gut infection. *Nature* **501**: 247–251.

Perez, S. and V. Weis (2006). Nitric oxide and cnidarian bleaching: an eviction notice mediates breakdown of a symbiosis. *Journal of Experimental Biology* **209**: 2804-2810.

Pernice, M., S. R. Dunn, T. Miard, S. Dufour, S. Dove, and O. Hoegh-Guldberg (2011). Regulation of apoptotic mediators reveals dynamic responses to thermal stress in the reef building coral *Acropora millepora*. *PLoS ONE* **6**: e16095.

Pinzón, J. H., B. Kamel, C. A. Burge, C. D. Harvell, M. Medina, E. Weil, and L. D. Mydlarz (2015). Whole transcriptome analysis reveals changes in expression of immune-related genes during and after bleaching in a reef-building coral. *Royal Society Open Science* **2**: 140214.

Poole, A. Z., S. A. Kitchen, and V. M. Weis (2016). The role of complement in cnidarian-dinoflagellate symbiosis and immune challenge in the sea anemone *Aiptasia pallida*. *Frontiers in Microbiology* **7**: 519.

Poole, A. Z. and V. M. Weis (2014). TIR-domain-containing protein repertoire of nine anthozoan species reveals coral-specific expansions and uncharacterized proteins. *Developmental and Comparative Immunology* **46**: 480-488.

Porter, S., I. M. Clark, L. Kevorkian, D. R. Edwards (2005). The ADAMTS metalloproteinases. *Biochemical Journal* **386**: 15-27.

Prashar, A., L. Schnettger, E. M. Bernard, and M. G. Gutierrez (2017). Rab GTPases in immunity and inflammation. *Frontiers in Cellular and Infection Microbiology* **7**: 435.

Qing, G., Z. Qu, and G. Xiao (2005). Regulation of NF-κB2 p100 processing by its *cis*-acting domain. *Journal of Biological Chemistry* **280**: 18-27.

Quistad, S. D., Y. W. Lim, G. G. Z. Silva, C. E. Nelson, A. F. Haas, L. W. Kelly, R. A. Edwards, and F. L. Rohwer (2016). Using viromes to predict novel immune proteins in non-model organisms. *Proceedings of the Royal Society B: Biological Sciences* **283**: 20161200.

Rape, M. and S. Jentsch (2002). Taking a bite: proteasomal protein processing. *Nature Cell Biology* **4**: E113-E116.

Richier, S., M. Rodriguez-Lanetty, C. E. Schnitzler, and V. M. Weis (2008). Response of the symbiotic cnidarian *Anthopleura elegantissima* transcriptome to temperature and UV increase. *Comparative Biochemistry and Physiology. Part D, Genomics & Proteomics* **3**: 283-289.

Rodrigues, C. D., M. Hannus, Prudêncio, C. Martin, L. A. Gonçalves, S. Portugal, S., Epiphanio, A. Akinc, P. Hadwiger, K. Jahn-Hofmann, I. Röhl, G. J. van Gemert, J. F. Franetich, A. J. Luty, R. Sauerwein, D. Mazier, V. Koteliansky, H. P. Vornlocher, C. J. Echeverri, and M. M. Mota (2008). Host scavenger receptor SR-B1 plays a dual role in the establishment of malaria parasite liver infection. *Cell Host & Microbe* **4**, 271-282.

Rodriguez-Lanetty, M., D. A. Krupp, and V. M. Weis (2004). Distinct ITS types of *Symbiodinium* in Clade C correlate with cnidarian/dinoflagellate specificity during onset of symbiosis. *Marine Ecology Progress Series* **275**: 97-102.

Rodriguez-Lanetty, M., W. S. Phillips, and V. M. Weis (2006a). Transcriptome analysis of a cnidarian-dinoflagellate mutualism reveals complex modulation of host gene expression. *BMC Genomics* **7**: 23.

Rodriguez-Lanetty, M., E. M. Wood-Charlson, L. L. Hollingsworth, D. A. Krupp, and V. M. Weis (2006b). Temporal and spatial infection dynamics indicate recognition

events in the early hours of a dinoflagellate/coral symbiosis. *Marine Biology* **149**: 713-719.

Rodriguez-Lanetty, M., S. Harii, O. Hoegh-Guldberg (2009). Early molecular responses of coral larvae to hyperthermal stres. *Molecular Ecology* **24**: 5101-5114.

Rosales, C., and E. Uribe-Querol (2017). Phagocytosis: a fundamental process in immunity. *BioMed Research International* **2017**: 9042851.

Rosenstiel, P., E. E. R. Phillip, S. Schreiber, and T. C. G. Bosch (2009). Evolution and function of innate immune receptors – insights from marine invertebrates. *Journal of Innate Immunity* **1**: 291-300.

Rosental, B., Z. Kozhekbaeva, N. Fernhoff, J. M. Tsai, and N. Traylor-Knowles (2017). Coral cell separation and isolation by fluorescence-activated cell sorting (FACS). *BMC Cell Biology* **18**: 30.

Ryu, J. H., E. M. Ha, and W. J. Lee (2010). Innate immunity and gut-microbe mutualism in *Drosophila*. *Developmental and Comparative Immunology* **34**: 369-376.

Ryu, J. H., S. H. Kim, H. Y. Lee, J. Y. Bai, Y. D. Nam, J. W. Bae, D. G. Lee, S. C. Shin, E. M. Ha, and W. J. Lee (2008). Innate immune homeostasis by the homeobox gene caudal and commensal-gut mutualism in Drosophila. *Science* **319**: 777-782.

Safavi-Hemami, H., N. D. Young, J. Doyle, L. Llewellyn, and A. Klueter (2010). Characterisation of nitric oxide synthase in three cnidarian-dinoflagellate symbioses. *PLoS ONE* **5**: e10379.

Sato, Y., D. G., Bourne, and B. L. Willis (2009). Dynamics of seasonal outbreaks of black band disease in an assemblage of Montipora species at Pelorus Island (Great Barrier Reef, Australia). *Proceedings of the Royal Society B: Biological Sciences* **276**: 2795-2803.

Schwarz, R. S., L. Hodes-Villamar, K. A Fitzpatrick, M. G. Fain, A. L. Hughes, and L. F. Cadavid (2007). A gene family of putative immune recognition molecules in the hydroid *Hydractinia*. *Immunogenetics* **59**: 233-246.

Sebé-Pedrós, A., B. Saudemont, E. Chomsky, F. Plessier, M. P. Mailhé, J. Renno, Y. Loe-Mie, A. Lifshitz, Z. Mukamel, S. Schmutz, S. Novault, P. R. H. Steinmetz, F. Spitz, A. Tanay, H. Marlow (2018). Cnidarian cell type diversity and regulation revealed by whole-organism single-cell RNA-seq. *Cell* **173**: 1520-1534.

Sedger, L. M. and M. F. McDermott (2014). TNF and TNF-receptors: from mediators of cell death and inflammation to therapeutic giants - past, present and future. *Cytokine and Growth Factor Reviews* **25**: 453-472.

Seneca, F. O. and S. R. Palumbi (2015). The role of transcriptome resilience in resistance of corals to bleaching. *Molecular Ecology* **24**: 1467-1484.

Senftleben, U., Y. Cao, G. Xiao, F. R. Greten, G. Krahn, G. Bonizzi, Y. Chen, Y. Hu, A. Fong, S. C. Sun, and M. Karin (2001). Activation by IKKα of a second, evolutionary conserved, NF-κB signaling pathway. *Science* **293**: 1495-1499.

Shinzato, C., E. Shoguchi, T. Kawashima, M. Hamada, K. Hisata, M. Tanaka, M. Fujie, M. Fujiwara, R. Koyanagi, T. Ikuta, A. Fujiyama, D. J. Miller, and N. Satoh (2011). Using the *Acropora digitifera* genome to understand coral responses to environmental change. *Nature* **476**: 320-323.

Siggers, T., A. B. Chang, A. Teixeira, D. Wong, K. J. Williams, B. Ahmed, J. Ragoussis, I. A. Udalova, S. T. Smale and M. L. Bulyk (2011) Principles of dimer-specific gene regulation revealed by a comprehensive characterization of NF-κB family DNA binding. *Nature Immunology* **13**: 95-102.

Silverstein, R. N., R. Cunning, and A. C, Baker (2017). Tenacious Symbiodinium in clade D remain in reef corals at both high and low temparatures despite impairment. *Journal of Experimental Biology* **220**: 1192-1196.

Simmons, K. J., P. N. Nde, Y. Y. Kleshchenko, M. F. Lima, and F. Villalta (2006). Stable RNA interference of host thrombospondin-1 blocks *Trypanosoma cruzi* infection. *FEBS Letters* **580**: 2365-2370.

Stat, M. and R. D. Gates (2011). Clade D Symbiodinium in scleractinian corals: a "nugget" of hope, a selfish opportunist, an ominous sign, or all of the above? *Journal of Marine Biology* **2011**: 730715.

Sullivan, J.C., F. S. Wolenski, A. M. Reitzel, C. E. French, N. Traylor-Knowles, T. D. Gilmore, and J. R. Finnerty (2009). Two alleles of NF-κB in the sea anemone *Nematostella vectensis* are widely dispersed in nature and encode proteins with distinct activities. *PLoS ONE* **4**: e7311.

Sun, S. C. (2012) The noncanonical NF-κB pathway. *Immunological Reviews* **246**: 125-40.

Sutherland, K. P., S. Shaban, J. L. Joyner, J. W. Porter and E. K. Lipp (2011). Human pathogen shown to cause disease in the threatened elkhorn coral *Acropora palmata*. *PLoS ONE* **8**: e23468.

Tchernov, D., H. Kvitt, L. Haramaty, T. S. Bibby, M. Y. Gorbunov, H. Rosenfeld, and P. G. Falkowski (2011). Apoptosis and the selective survival of host animals following thermal bleaching in zooxanthellate corals. *Proceedings of the National Academy of Sciences of the United States of America* **108**: 9905-9909.

Thomas, D. D., L. A. Ridnour, J. S. Isenberg, W. Flores-Santana, C. H. Switzer, S. Donzelli, P. Hussain, C. Vecoli, N. Paolocci, S. Ambs, C. A. Colton, C. C. Harris, D.

Towle, E. K., I. C. Enochs, and C. Langdon (2015). Threatened Caribbean coral is able to mitigate the adverse effects of ocean acidification on calcification by increasing feeding rate. *PLoS One* **10**:e0139398.

Roberts, D. and D. A. Wink (2008). The chemical biology of nitric oxide: implications in cellular signaling. *Free Radical Biology and Medicine* **45**: 18-31.

Trapido-Rosenthal, H., S. Zielke, R. Owen, L. Buxton, B. Boeing, R. Bhagooli, and J. Archer (2005). Increased zooxanthellae nitric oxide synthase activity is associated with coral bleaching. *Biological Bulletin* **208**: 3-6.

Trapido-Rosenthal, H. G., K. H. Sharp, T. S. Galloway, and C. E. Morrall (2001). Nitric oxide and cnidarian-dinoflagellate symbioses: pieces of a puzzle. *Integrative and Comparative Biology* **41**: 247-257.

Travis, M. A. and D. Sheppard (2014). TGF-beta activation and function in immunity. *Annual Review of Immunology* **32**: 51-82.

Traylor-Knowles, N., N. H. Rose, E. A. Sheets, and S. R. Palumbi (2017). Early transcriptional responses during heat stress in the coral *Acropora hyacinthus*. *Biological Bulletin* **232**: 91-100.

Tucker, R. P. (2004). The thrombospondin type 1 repeat superfamily. *Journal of Biochemistry and Cellular Biology* **6**: 969-974.

Uribe-Querol, E. and C. Rosales (2017). Control of phagocytosis by microbial pathogens. *Frontiers in Immunology* **8**: 1368.

van de Water, J., M. Chaib De Mares, G. B. Dixon, J. B. Raina, B. L. Willis, D. G. Bourne, and M. J. H. van Oppen (2018). Antimicrobial and stress responses to increased temperature and bacterial pathogen challenge in the holobiont of a reef-building coral. *Molecular Ecology* **27**: 1065-1080.

Vidal-Dupiol, J., M. Adjeroud, E. Roger, L. Foure, D. Duval, Y. Mone, C. Ferrier-Pages, E. Tambutte, S. Tambutte, D. Zoccola, D. Allemand, G. Mitta (2009). Coral bleaching under thermal stress: putative involvement of host/symbiont recognition mechanisms. *BMC Physiology* **9**: 14.

Vodovotz, Y, A. G. Geiser, L. Chesler, J. J. Letterio, A. J. Campbell, M. S. Lucia, M. B. Sporn, and A. B. Roberts (1996). Spontaneously increased production of nitric oxide

and aberrant expression of the inducible nitric oxide synthase *in vivo* in the transforming growth factor beta 1 null mouse. *Journal of Experimental Medicine* **183**: 2337–2342.

Voolstra, C. R., Y. Li, Y. J. Liew, S. Baumgarten, D. Zoccola, J. F. Flot, S. Tambutte, D. Allemand, and M. Aranda (2017). Comparative analysis of the genomes of *Stylophora pistillata* and *Acropora digitifera* provides evidence for extensive differences between species of corals. *Scientific Reports* **7**: 17583.

Weis, V. M. (2008). Cellular mechanisms of Cnidarian bleaching: stress causes the collapse of symbiosis. *Journal of Experimental Biology* **211**: 3059-3066.

Weis, V. M. (2010). The susceptibility and resilience of corals to thermal stress: adaptation, acclimatization or both? *Molecular Ecology* **19**: 1515-1517.

Weis, V. M., S. K. Davy, O. Hoegh-Guldberg, M. Rodriguez-Lanetty, and J. R. Pringle (2008). Cell biology in model systems as the key to understanding corals. *Trends in Ecology and Evolution* **23**: 369-376.

Weis, V. M., W. S. Reynolds, M. L. deBoer, and D. A. Krupp (2001). Host-symbiont specificity during onset of symbiosis between the dinoflagellate *Symbiodinium* spp. and planula larvae of the scleractinian coral *Fungia scutaria*. *Coral Reefs* **20**: 301-308.

Winters, G., R. Holzman, A. Blekhman, S. Beer, and Y. Loya (2009). Photographic assessment of coral chlorophyll contents: Implications for ecophysiological studies and coral monitoring. *Journal of Experimental Marine Biology and Ecology* **380**: 25-35.

Williams, L. M., L. E. Fuess, J. J. Brennan, K. M. Mansfield, E. Salas-Rodriguez, J. Welsh, J. Awtry, S. Banic, C. Chacko, A. Chezian, D. Dowers, F. Estrada, Y. H Hsieh, J. Kang, W. Li, Z. Malchiodi, J. Malinowski, S. Matuszak, T. T. McTigue, D. Mueller, B. Nguyen, M. Nguyen, P. Nguyen, S. Nguyen, N. Njoku, K. Patel, W. Pellegrini, T. Pliakas, D. Qadir, E. Ryan, A. Schiffer, A. Thiel, S. A. Yunes, K. E. Spilios, C. J., Pinzon, L. D. Mydlarz, and T. D. Gilmore (2018). A conserved Toll-like receptor-to-NF-κB signaling pathway in the endangered coral *Orbicella faveolata*. *Developmental and Comparative Immunology* **79**: 128-136.

Wolenski, F. S., C. A. Bradham, J. R. Finnerty, and T. D. Gilmore (2013). NF-κB is required for cnidocyte development in the sea anemone *Nematostella vectensis*. *Developmental Biology* **373**: 205-215.

Wolenski, F. S., S. Chandani, D. J. Stefanik, N. Jiang, E. Chu, J. R. Finnerty and T. D. Gilmore (2011a). Two polymorphic residues account for the differences in DNA binding and transcriptional activation by NF-κB proteins encoded by naturally

occurring alleles in *Nematostella vectensis*. *Journal of Molecular Evolution* **73**: 325-326.

Wolenski, F.S. M. R. Garbati, T. J. Lubinski, N. Traylor-Knowles, E. Dresselhaus, D. J. Stefanik, H. Goucher, J. R. Finnerty and T. D. Gilmore (2011b). Characterization of the core elements of the NF-κB signaling pathway of the sea anemone *Nematostella vectensis*. *Molecular and Cellular Biology* 31: 1076-1087.

Wolfowicz, I., S. Baumgarten, P. A. Voss, E. A. Hambleton, C. R. Voolstra, M. Hatta, and A. Guse (2016). *Aiptasia* sp. larvae as a model to reveal mechanisms of symbiont selection in cnidarians. *Scientific Reports* **6**: 32366.

Xiang, T., E. A. Hambleton, J. C. DeNofrio, J. R. Pringle, and A. R. Grossman (2013) Isolation of clonal axenic strains of the symbiotic dinoflagellate *Symbiodinium* and their growth and specificity. *Journal of Phycology* **49**: 447-458.

Yellowlees, D., T. A. Rees, and W. Leggat (2008). Metabolic interactions between algal symbionts and invertebrate hosts. *Plant, Cell & Environment* **31**: 679-694.

Yen, H., T. Ooka, A. Iguchi, T. Hayashi, N. Sugimoto and T. Tobe (2010). NleC, a type III secretion protease, compromises NF-κB activation by targeting p65/RelA. *PLoS Pathogens* **6**: e1001231.

Yu, J. W., S. Hoffman, A. M. Beal, A. Dykon, M. A. Ringenberg, A.C. Hughes, L. Dare, A. D., Anderson, J. Finger, V, Kasparcova, D. Rickard, S. B. Berger, J. Ramanjulu, J. G. Emery, P. J. Gough, J. Bertin, and K. P. Foley (2015). MALT1 protease activity is required for innate and adaptive immune responses. *PLoS ONE* **10**: e0127083.

Zhou, Y., N. Dong, L. Hu, and F. Shao (2013). The Shigella type three secretion system effector OspG directly and specifically binds to host ubiquitin for activation. *PLoS ONE* **8**: e57558.

Zientz, E., H. Feldhaar, S. Stoll and R. Gross (2005). Insights into the microbial world associated with ants. *Archives of Microbiology* **184**: 199-206.

CURRICULUM VITAE